

Electrosprayed coatings: from passive to active surfaces for bone implants

Ruggero Bosco

Colofon

Thesis Radboud University Nijmegen Medical Centre, Nijmegen, The Netherlands, with summary in English and Dutch

Electrosprayed coatings: from passive to active surfaces for bone implants

This research forms part of the Project **P2.04 BONE-IP** of the research program of the **BioMedical Materials** institute, co-funded by the **Dutch Ministry of Economic Affairs, Agriculture and Innovation**.

Cover Design:	Proefschriftmaken.nl Ruggero Bosco
Layout:	Ruggero Bosco
Printing:	Proefschriftmaken.nl Uitgeverij BOXPress
Publisher:	Uitgeverij BOXPress, Oisterwijk

ISBN:

Copyright Ruggero Bosco ©

All rights reserved. No parts of this publications may be reported or transmitted, in any form or by any means, without the permission of the author.

Electrosprayed coatings: from passive to active surfaces for bone implants

Doctoral Thesis

ter verkrijging van de graad van doctor

aan de Radboud Universiteit Nijmegen

op gezag van de rector magnificus prof. Mr. S.C.J.J. Kortmann,

volgens besluit van het college van decanen

in het openbaar te verdedigen op maandag 10 November 2014

om 14.30 uur precies

by

Ruggero Bosco

Geboren op 25 Februari 1983

te Milan, Italië

Promotor:

Prof. dr. J.A. Jansen

Copromotoren:

Dr. Ing. J.J.J.P. van den Beucken

Dr. S.C.G. Leeuwenburgh

Manuscriptcommissie:

Prof. dr. W.B. van den Berg

Dr. A.H.M.S.M. van Kuppevelt

Prof.dr. H. Weinans

Paranimfen:

Daniel Alves Cardoso

Shankar Mahadevan

Electrosprayed coatings: from passive to active surfaces for bone implants

Doctoral Thesis

To obtain the degree of doctor
from Radboud University Nijmegen
on the authority of the Rector Magnificus prof. dr. S.C.J.J. Kortmann,
according to the decision of the Council of Deans
to be defended in public on Monday, November 10, 2014

at 14.30 hours

by

Ruggero Bosco

Born in Milan, Italy
on February 25, 1983

Supervisor:

Prof. dr. J.A.Jansen

Co-supervisors:

Dr. Ing. J.J.J.P. van den Beucken

Dr. S.C.G. Leeuwenburgh

Doctoral Thesis Committee:

Prof. dr. W.B. van den Berg

Dr. A.H.M.S.M. van Kuppevelt

Prof.dr. H. Weinans

Ushers:

Daniel Alves Cardoso

Shankar Mahadevan

To Marta

CONTENTS

Chapter I | Page 11

Instructive coatings for biological guidance of bone implants

Chapter II | Page 39

Surface Engineering for Bone Implants: A Trend from Passive to Active Surfaces

Chapter III | Page 67

Electrostatic Spray Deposition of Biomimetic Nanocrystalline Apatite Coating on Titanium

Chapter IV | Page 87

Configurational effects of collagen/ALP coatings on enzyme immobilization and surface mineralization

Chapter V | Page 111

Nano-sized hydroxyapatite crystals functionalized with alendronate as bioactive components for bone implant coatings to decrease osteoclastic activity.

Chapter VI | Page 133

Synergistic effects of bisphosphonate and calcium phosphate nanoparticles on peri-implant bone response in osteoporotic rats

Chapter VII | Page 159

Electrospray deposition of strontium-substituted nano-hydroxyapatite to stimulate the response of osteoblastic cells to titanium implants.

Chapter VIII | Page 179

Summary, closing remarks and future perspectives

Samenvatting, afsluitende opmerkingen en toekomstperspectief

Acknowledgment | Page 201

List of publications | Page 205

Curriculum Vitae | Page 207

Chapter I

Instructive coatings for biological guidance of bone implants

Ruggero Bosco[#], Eva R Urquia Edreira[#], Joop GC Wolke, Sander CG Leeuwenburgh,

Jeroen JJP van den Beucken, John A Jansen*

Surface and Coatings Technology, 2013, 233: 91-98.

1. Introduction

Load-bearing bone implants for dental and orthopedic applications to replace hard tissue are generally made from bioinert materials, including titanium, stainless steel, cobalt-chromium, alloys or certain ceramics (e.g. alumina and zirconia). Extensive efforts have been dedicated to the optimization of the interaction with bone tissue at the implant interface via surface modifications to enhance the surface biocompatibility and osteoconductive properties of these implants. Still, implant failure remains a problem for especially clinical cases characterized by compromised local or systemic conditions (e.g. osteoporosis and diabetes).¹

Biomaterials research is evolving from the use of bioinert and biologically passive implants toward actively interacting implants that stimulate tissue regeneration. Currently, there is an increasing interest in biomaterials that are capable of activating protein adsorption processes and specific cellular responses. Surface physico-chemical properties need to be modified in order to transform passive inert implant surfaces into active ones able to instruct the biological environment toward regeneration of bone tissue (Figure 1). For instance, physical surface modifications in topography or macrostructural properties have been reported to concentrate more bone morphogenetic proteins (BMPs) and stimulate osteogenesis.^{2, 3} On the other hand, chemical surface modifications have been shown to play an essential role in bone tissue responses.⁴⁻¹⁰ For ceramic coatings, the liberation of certain ions from the implant surface into the surroundings increases local super-saturation of the biologic fluid causing precipitation of carbonated apatite that incorporates calcium, phosphate and other ions, as well as proteins, and other organic compounds.¹¹ Furthermore, the immobilization of biomolecules into the coating materials allows implants to deliver drugs and growth factors.¹² In addition, when referring to organic coatings, the use of organic compounds derived from the extracellular matrix

(ECM) of bone attempts to stimulate mineralization and/or adhesion of cells onto the bone implant surfaces.

This review aims to provide an overview of surface modifications for load-bearing bone implants. Special attention is devoted to the most recent developments of inorganic and organic coatings for bone implants that actively interact with bone tissue to aid skeletal repair and reconstruction.

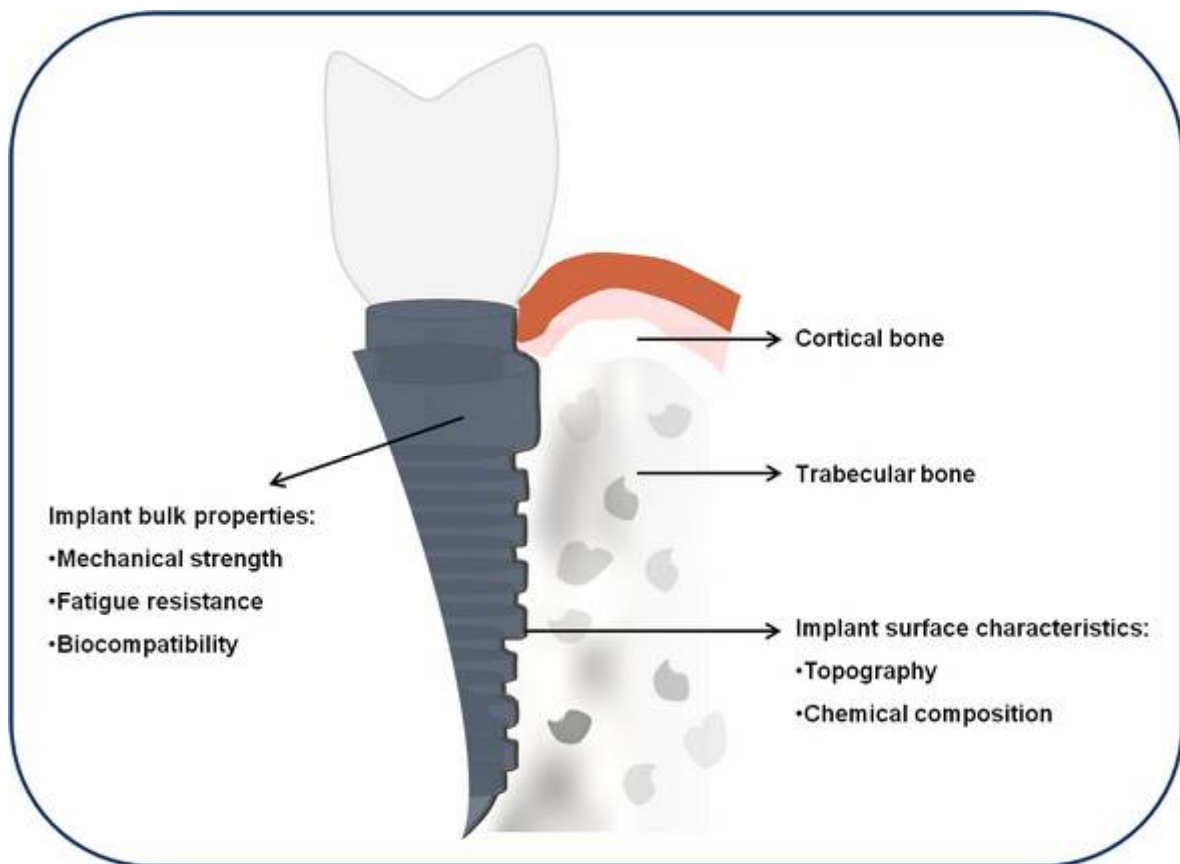


Figure 1. *Schematic overview of a bone implant.*

2. Inorganic coatings

Bone tissue is a composite that exhibits a rich hierarchical structure. The cells within bone tissue are embedded in an extracellular matrix made of organic and inorganic compounds, which permit bone tissue to remodel and adapt its structure in response to mechanical stress (Figure 2). More specifically, the strength of bone tissue is related to the orderly interspersed inorganic crystals within the organic compounds.^{13, 14} These crystals have an apatite structure (i.e. $\text{Ca}_{10}(\text{PO}_4)_6(\text{OH})_2$ for hydroxyapatite), in which calcium and phosphate are the most prominent elements. Synthetic inorganic materials have therefore been extensively explored to mimic the mineral part of bone tissue for bone implantology applications.

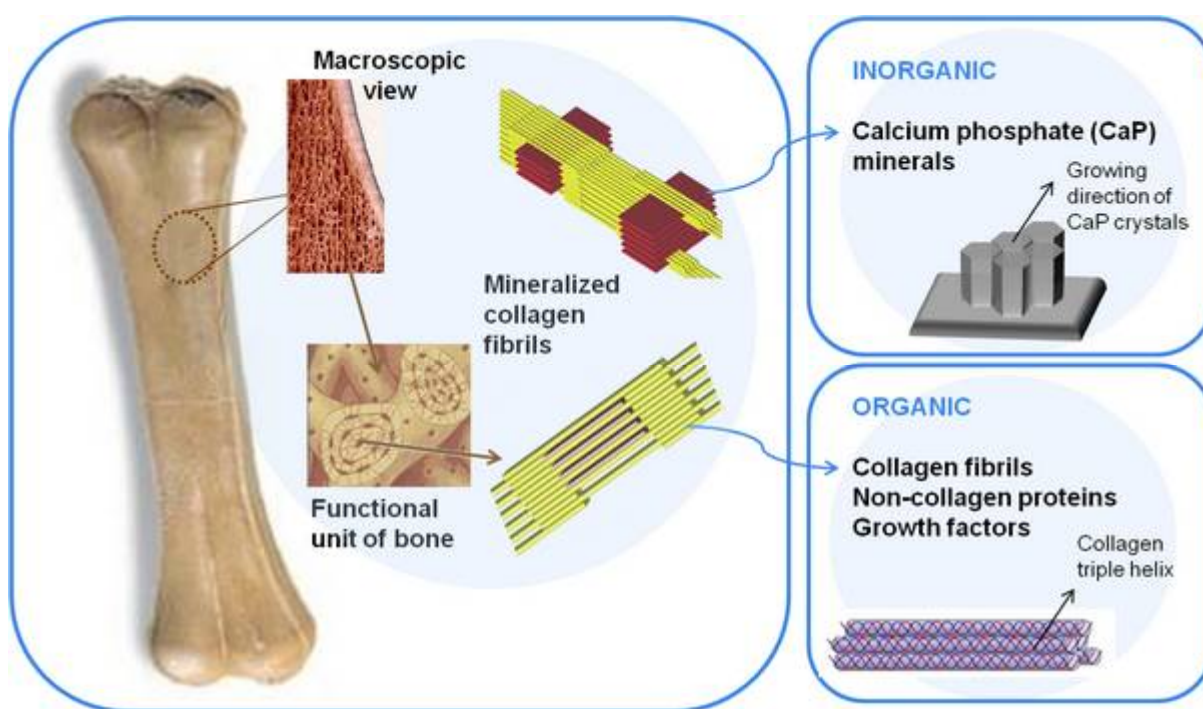


Figure 2. Hierarchical levels of bone structure.

2.1. Properties and bonding mechanism of CaP-based ceramics

Calcium phosphate (CaP) ceramics are synthetic materials that share common mineral phase properties with bone tissue and are biodegradable, bioactive and osteoconductive.¹⁵

CaP ceramic materials are characterized by their hardness, strength, low electrical conductivity, brittleness and inferior mechanical properties. Due to their inferior mechanical properties, the application of CaP ceramics as bulk materials under load-bearing conditions is limited. Used as implant surface coatings, these CaP ceramics provide a physical matrix at the implant surface suitable for interaction with bone tissue.

CaP ceramics bond to bone tissue through the release of ions from the implant surface inducing apatite nucleation, followed by the formation of a carbonated apatite layer on the biomaterial surface.¹⁶ This apatite layer at the surface is chemically and crystallographically equivalent to the bone tissue mineral phase. As such, this carbonated apatite layer creates an ideal environment for protein and cellular attachment and subsequent strongly bonded bone formation. Several parameters of CaP ceramics, either in bulk or coating form, have been demonstrated to alter protein binding, cell-material interactions and implant resorption rate. These inherent parameters include chemical composition, crystallinity, surface area, surface charge, surface topography and porosity, elasticity and fatigue of the implant surface.

2.1.1. Pure CaP-based coatings

CaP-based ceramic coatings were originally developed to improve bone-implant attachment and enhance surface reactivity, for example of dental implants and metallic prostheses, because of their favorable bioactivity and osteoconductivity. Surface properties of the implant material such as coatings roughness, chemical purity, and topography should be optimized to improve osseointegration. Bioactive materials, such as

CaP ceramics, several classes of bioglasses, calcium carbonates and calcium sulfates, evoke specific biological responses, stimulate bone tissue formation and directly bond to adjacent bone tissue.

There are several CaP phases, the most commonly used for bone ingrowth has been hydroxyapatite (HA; $\text{Ca}_{10}(\text{PO}_4)_6\text{OH}_2$), which has crystalline and molecular structure similarities to the inorganic phase of bones and teeth.¹⁷⁻¹⁹ Other structures include brushite (DCPD, $\text{CaHPO}_4 \cdot \text{H}_2\text{O}$), and tricalcium phosphate (α -TCP and β -TCP, $\text{Ca}_3(\text{PO}_4)_2$) have been used as bioactive coatings to modify the surface of bioinert metals or polymers.²⁰ At physiological pH (between 7.2-7.6), HA is the most stable CaP phase. The partial dissolution of the ceramic (i.e. release of ions) initiates the re-precipitation of biological apatite crystals and subsequent proteins and cells attachment to the implant surface. Amorphous CaP coatings have higher dissolution and re-precipitation rates than the crystalline CaP coatings and present faster bone formation²¹ and produce higher cell differentiation *in vitro* studies.^{21, 22} However, crystalline CaP coatings are preferred when long-term stability of the implant is desirable. The biological properties of these CaP-based ceramic coatings are related to their chemical composition, Ca/P ratio, crystallographic structures and solubility. Consequently, the release of ions and the interaction with body fluid, cells and tissue of CaP implant coatings differs related to specific CaP coating structure.^{23, 24}

2.1.2. Incorporation of active ions into CaP-based ceramic coatings

In an attempt to further increase the biological performance of CaP-based ceramic coatings, research focused on the incorporation of ions into the ceramic lattice. Ionic doping not only changes the chemical composition but also physicochemical properties, such as morphology and crystallinity. Numerous articles have claimed that silicon (Si)

substitution into the crystal structure of CaP ceramics, in particular HA, positively influences the biological response compared to pure CaP coatings.²⁵⁻²⁷ For example, Patel et al.²⁶ compared granules of pure HA and Si-substituted HA when implanted in a rabbit model; more bone ingrowth and bone-implant coverage were found with the incorporation of silicate ions into the HA structure. Similar results were obtained by Hing et al.²⁷ using porous HA and silicate-substituted HA scaffolds. The authors claimed that the presence of Si ions is responsible for an increased collagen deposition, cells differentiation, bone ingrowth and repair. However, a recent critical review on Si-substituted CaP coatings has shown that there is no experimental evidence that Si ions are released (at sufficiently high concentrations) from the CaP lattice *in vitro* or *in vivo* studies²⁵. The heterogeneity of studies based on Si-substituted CaP remain inconclusive regarding the cause for the positive biological responses: topographical effects or the release of Ca ions instead of the Si ions release. A major criticism is moved concerning the analysis of the effective principle through Si ions could enhance bone deposition or formation²⁵. The incorporation of magnesium (Mg) ions into HA in an *in vivo* study has shown that Mg-substituted HA enhances the osteoconductivity and resorption compared to commercial HA. Landi and Tampieri highlighted how Mg substituted hydroxylapatite (HA) has chemico-physical properties that increase solubility compared to synthetic HA that resemble more the characteristics of natural HA²⁸. Experiments substituting calcium by strontium (Sr) ions have been performed in several calcium phosphate ceramics, such as HA^{29, 30}, β -TCP³¹ and α -TCP³². Fielding et al. showed that the addition of silver (Ag) and Sr dopants to the HA coating enhanced cell proliferation and differentiation activity compared with pure HA coating.³³ Lithium (Li) incorporation into the CaP coating changes the coating morphology and interferes with the CaP crystallization. The presence of lithium has been demonstrated to enhance MG63 cell attachment and early

proliferation.³⁴ Lastly, zinc (Zn) incorporation has also been widely studied. *In vivo* studies demonstrated more bone apposition when using low concentrations of zinc (~0.3 wt.%), whereas long-term implantation studies with low concentrations of zinc or high concentrations of zinc (~0.6 wt.%) led to an increased resorption of bone.^{35, 36}

2.1.3. CaP-based ceramic coatings with entrapment of biomolecules

HA ceramics have been used as a delivery system for chemicals³⁷, antibiotics³⁸ and anticancer drugs.³⁹ A final approach toward inorganic surface modifications with enhanced biological performance involves the entrapment of biomolecules into a ceramic coating, enabling active release of drugs (e.g. anti-microbial coatings). By local delivery of antibiotic drugs from a coated implant, the occurrence of post-surgery infections can be reduced, enhancing the short and long term stability of a bone implant.¹² The use of CaP coatings as delivery vehicles for antimicrobial agents such as chlorhexidine has already reported its efficacy in an *in vitro* study by Campbell et al. In this study the incorporation of chlorhexidine within the hydroxyapatite (HA) coatings showed an initial rapid release followed by a period of slower sustained release. The *in vitro* evaluation results showed that a large “inhibition zone” was formed around the HA/chlorhexidine coating compared to HA coating.¹⁰ Moreover, for compromised situations such as osteoporosis, the incorporation of bisphosphonate drugs (e.g. alendronate) into the inner layers of CaP coatings has shown beneficial results on osteoblast cells differentiation.⁴⁰ CaP coatings used as local delivery of drugs or antimicrobial agents offers the possibility of improving efficacy (i.e. dosage near the affected site) and reduce the treatment duration.

A classification of the different instructive inorganic and organic coating materials and their interaction when implanted is shown in Figure 3.

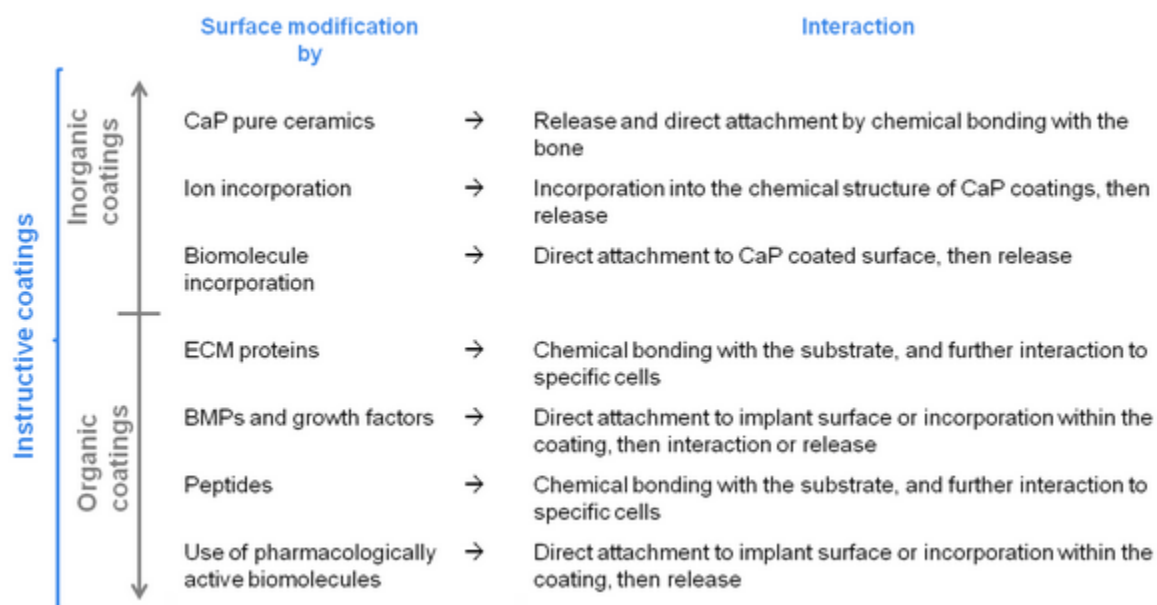


Figure 3. *Classification and interaction of instructive coatings.*

3. Organic coatings

The bone tissue extracellular matrix (ECM) is composed of a hierarchical and complex structure of inorganic and organic phases. The inorganic or crystalline phase of bone represents 50% of the total volume and 70% of the weight, and mainly consists of a stiff, carbonated and nano-sized apatite. The organic phase of bone tissue constitutes the remaining volume, which comprises collagen (40% in volume of the organic phase) and other proteins, such as proteoglycans, glycoproteins (alkaline phosphatase, osteonectin), bone sialoproteins and growth factors.

In the last decades, organic biomolecules derived from the ECM have been increasingly considered a fundamental source in the development of organic bone implant coatings.⁴¹ Bone implants surfaces can be enriched⁴²⁻⁴⁴ using organic biomolecules to obtain instructive medical devices able induce a biological response at the tissue-implant interface. Organic-based coatings involve immobilization of structural proteins, Bone Morphogenetic Proteins (BMPs) and growth factors and peptides to stimulate cell adhesion onto implant surfaces^{45, 46} and an approach on the use of pharmacologically active biomolecules.

3.1. Surface modifications by ECM proteins

Collagen is the main component of the bone tissue organic phase and it has a fundamental structural and functional role. The minimum element is the collagen fibril that is composed of a structured repetition of tropocollagen molecules (300 nm size) that are interconnected in a right-helix structure. Between tropocollagen molecules, there is a gap zone, in which the nano-sized hydroxyapatite crystals can start nucleation and mineralization. Moreover, the structural presence of collagen in the ECM is fundamental to obtain the mechanical properties of bone tissue.

Collagen has been used as a coating material to retain biomolecules at the implant surface and improve their activity. Collagen-based coatings are able to bind an important ECM protein called fibronectin, which plays a major role in the interaction between implant surfaces and the surrounding biological medium (e.g. cell adhesion, growth, migration and differentiation).⁴⁷ Different research groups have also tried to use collagen to increase proliferation or differentiation of osteoblasts and osteoprogenitor cells. Douglas et al. showed the positive effect of a layer of collagen promoting osteoblasts focal adhesion. Rammelt et al. showed a comparison between collagen and other biomolecules in an *in vivo* experiment on a rat model. Their analysis is not focus on the biochemical mechanism of action of these biomolecules but it remarks the efficacy of the coated samples in new bone formation⁴⁸⁻⁵⁰.

Osteoblasts (bone forming) and osteoclasts (bone resorbing) are the most important cell types in bone tissue. These cells maintain the balance between dissolved and deposited mineral phase. This balance between osteoclasts and osteoblasts is defined as *bone turn over* and it is controlled through several signaling pathways. The key element to regulate the *bone turn over* is to affect cell differentiation and proliferation. Lastly, *in vivo* experiments using collagen-coated bone implants have reported successful results, evidenced by an improved bone implant contact, bone density and bone formation.⁵¹⁻⁵³

3.2. Surface modifications by growth factors and biomolecules

Osteotropic biomolecules (e.g. growth factors, GFs) have been used to improve tissue response and bone formation. GFs are widely used to obtain cell differentiation in *in vitro* procedures. Several GFs, including bone morphogenetic protein (BMP), transforming growth factor-beta (TGF- β), fibroblast growth factor (FGF), platelet-derived growth factor (PDGF), and insulin-like growth factor (IGF), have shown an active role in bone

tissue formation also after their immobilization onto implants surface⁵⁴⁻⁵⁶. Stadlinger *et al.* investigated GFs that belong to the TGF- β superfamily (e.g. BMP-2, BMP-4, BMP-7 and TGF- β 1) and showed successful results in terms of bone to implant contact, bone density and osteoinduction in a pre-clinical study.⁵⁷

The synergistic effects of collagen and other biomolecules, such as GFs, bone sialoproteins or with hydroxyapatite, have shown potential as initiators of mineralization by deposition of calcium phosphate onto implant surfaces^{41, 58, 59}.

3.3. Surface modifications by peptides

The use of complete proteins as a coating material can introduce biological effects that can become an obstacle to bone cells recruitment or to bone initial contact. The immobilization of these biomolecules is often associated with their tendency to lose their 3D-conformation and hence impedes with their biological activity. As such, their adsorption to an implant surface often decreases the efficacy of immobilized proteins. The use of short peptide sequences derived from entire proteins as coating material can offer a solution to this problem.^{60, 61} The Arg-Gly-Asp RGD peptide sequence^{62, 63} has been widely used and presents a predominant binding site for cells via integrin receptors. Various other peptide sequences have been used similarly onto implanted materials. Bone implants surfaces enriched with a layer of these peptides demonstrated improved biological effects *in vitro* in terms of cells proliferation, mineralization and adhesion.⁶⁴⁻⁶⁶

3.4. Use of pharmacologically active biomolecules

An alternative selection of molecules for bone implant coatings is offered by pharmaceutical research. Especially for compromised health conditions (e.g. patients with osteoporosis, osteopenia or diabetes) pharmaceutical drugs can be used for surface

modifications in order to provide a localized therapy. Molecules with specific active properties, defined as active principles, represent the fundamental material in drugs composition. The use of active principles in reduced amounts and *in situ* (i.e. local administration instead of systemic administration) is a challenge for several medical fields. Adsorption of locally deliverable drugs onto bone implants can be obtained through immersion of implants in a solution that contains active principles prior to implantation. Anti-osteoporotic drugs, such as bisphosphonates⁶⁷ or antibiotics like chlorhexidine⁶⁸, are currently adopted to enhance the biological performance of implants used in compromised bone conditions⁶⁹. Bone implants can be coated with active biomolecules to become able to face lower bone density in osteoporotic patients or reduce fibrotic tissue formation in diabetic conditions. Bisphosphonates can be added as a coating material to reduce the number or the activity of osteoclasts in order to modify the balance between bone forming and bone resorbing cells.

Immobilization of active biomolecules onto bone implants is the most recent development in surface engineering to obtain instructive coatings.⁷⁰ A recent review on bisphosphonates (BPs) showed that BPs that have an affinity for CaP materials can be incorporated into CaP coatings by soaking the implants into BPs solution and achieve stronger primary fixation by the inhibition of osteoclast action.⁷¹

4. Coating deposition techniques

The most commonly used coating techniques are physical coating deposition methods, although there is a trend toward the utilization of wet-chemical deposition techniques (e.g. biomimetic and sol-gel deposition techniques) for inorganic and organic coatings (Table 1). The deposition of uniform and adherent coatings of any organic biomolecule requires a deposition technique that does not cause damage to the biomolecule. The major drawbacks of biomolecules used for surface modification include the sensitivity of these biomolecules to physicochemical conditions and hence the requirement of controlled settings during deposition. In fact, high temperatures or exposure to ion beams or plasmas can alter the organic structure of the biomolecules reducing their activity. Several wet-chemical deposition techniques that allow preservation of biomolecule activity have been explored in the past few decades.⁴⁶

	Deposition technique	Type of coating material	Coating thickness	Advantages	Disadvantages
Wet-chemical deposition	Biomimetic	osteocalcin, fibronectin and poly (L-lysine). BMP-2 incorporated into biomimetic CaP coatings	< 30 μm	Coating of complex geometries; co-deposition of biomolecules	Time consuming; requires controlled pH
	Sol-gel	Aluminosilicate, fluoridated hydroxyapatite (HA), Si-substituted HA and bioglass	< 1 μm	Coating of complex geometries; low processing temperature	Requires controlled atmosphere processing; expensive raw materials
	Electrospray	HA, Nano HA, ALP, biomolecules-HA composite collagen	0.1-5 μm	Co-deposition of biomolecules; control over coating composition and morphology	Low mechanical strength; line of sight technique
Physical deposition	RF magnetron sputtering	HA, Si-HA, carbonated HA, and Zn, Mg, and Al-doped CaPs	0.5-5 μm	Uniform and dense coating; strong adhesion	Line of sight technique; time consuming; low deposition rates
	Plasma spray	HA, Si-HA and antibacterial Ag-HA composite coatings	50-250 μm	High deposition rates	Non-uniform coating crystallinity; line of sight technique
	Pulsed laser	HA resistant to dissolution in SBF, Ag-HA, HA and fluorinated-HA, alendronate-doped HA	0.05-5 μm	Control over coating chemistry and morphology	Line of sight technique
	Ion beam dynamic mixing	Calcium phosphate (CaP)	0.05-1 μm	High adhesive strength	Line of sight technique; requires high sintering temperatures
	Ion beam assisted deposition	CaP	0.02-10 μm	Increased tensile bond strength	Line of sight technique

Table 1. Characteristics of deposition techniques.

4.1. Wet-chemical deposition techniques

Biomimetic deposition mimics the natural deposition of biological apatite and opened up a new way to develop biomaterials. It was introduced by Kokubo et al. in 1990 and the system originally involved simple immersion of (pre-treated) titanium substrates into a so-called simulated body fluid (SBF) to obtain deposition onto the surface of the substrates of a biologically active bone-like CaP layer.⁷² The deposition is performed under physiological conditions (37°C, pH 7.4, $p(\text{CO}_2)=0.05$ atmosphere and appropriate electrolyte concentrations)⁷³ and biomolecules can be dissolved in the liquid and hence be incorporated in the growing coating. Several reports have shown the cell and tissue response (i.e. differentiation of stem cells into osteoblasts that deposit bone matrix on the ceramic surface) by the incorporation of biomolecules in combination to CaP coatings using the biomimetic deposition technique.⁷⁴⁻⁷⁶ One of the main advantages of biomimetic deposition, in fact, is the possibility of co-precipitating ceramic (nano)particles with biomolecules (e.g. osteogenic agents).⁷⁷ Bone implants have been immersed in a suspension containing antibiotics⁷⁸ or active principles like bisphosphonates⁷⁹⁻⁸¹ to obtain adsorption of these bioactive biomolecules onto the implant surface. Each application showed different response according with the expected role of the active agent incorporated onto implants through biomimetic deposition.

The sol-gel coating technique involves the immersion of a substrate into a concentrated solution with a gel-like texture^{82, 83}. This technique provides a resourceful approach to synthesize inorganic polymer and organic-inorganic hybrid materials under mild conditions. Moreover, sol-gel technique includes inherent advantages such as single step manufacturing process, material homogeneity at the molecular level and chemical bonding between the substrate and the coating.⁸⁴

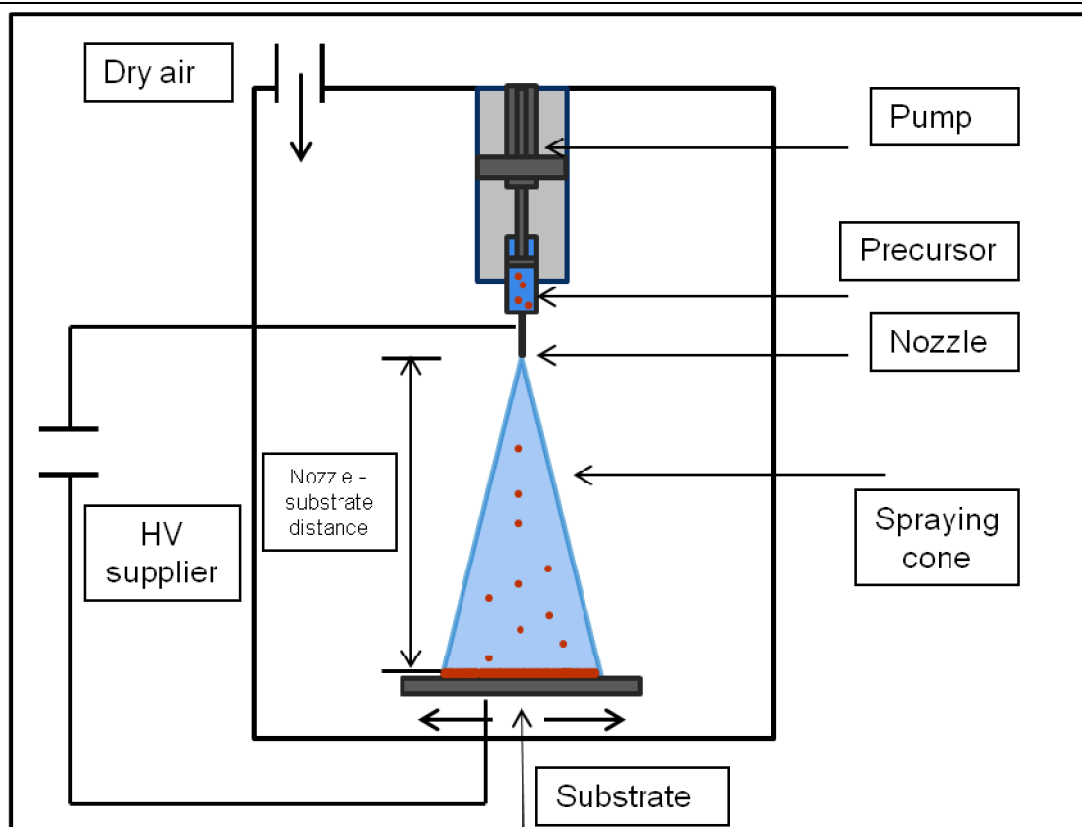


Figure 4. Schematic representation of electro spray deposition (ESD) apparatus

The electrospray deposition (ESD) technique is an electrochemical coating method with promising applicability for inorganic and organic coatings. ESD, schematically represented in Figure 4, shares the benefits of preserving biomolecules as the wet chemical deposition methods, such as biomimetic or sol-gel, and the deposition control of dry methods described for inorganic coating materials. ESD method is applicable to solutions or suspensions containing precursor materials that, under the influence of a high electrical field, creates an aerosol of similarly charged micron-sized droplets are^{85, 86}. ESD can be performed at ambient temperature and pressure but requires that precursors are particles or molecules that carry an electrical charge or that can be dispersed in electrolytic solutions. Also the targets, onto which the coating is applied, have to be

conductive. ESD allows for a strong control over physicochemical coating properties such as thickness or chemical composition.⁸⁷

Although dip coating⁸⁸, sol-gel and biomimetic coatings are suitable for coating a complex shape (e.g. porous, 3D, etc.), all these techniques suffer from weak adhesive strength.

4.2. Physical deposition techniques

Other physical coating techniques such as plasma-spraying, pulsed laser deposition, ion beam deposition and sputter deposition offer advantages over wet-chemical depositions with respect to interfacial strength and crystallinity.

Plasma-spraying was the first coating technique for biomedical applications; this technique is also very successful for applying CaP coatings on implants due to its high deposition rate. Plasma spraying produces coatings with desired chemistry and crystallinity, despite poor control of the thickness and surface morphology.⁸⁹ Pulsed laser is a technique that allows deposition of thin, dense, well adhering coatings with control chemistry and crystallinity.⁹⁰ Ion beam deposition technique (Figure 5 A) is a vacuum technique used to deposit coatings from precursor materials vaporized. Inherent properties and chemical composition of the coating may differ from that of the bulk material due to the high energy involved.⁹¹ Lastly, one of the most frequently applied techniques used to prepare CaP coatings by physical vapor deposition process is radio-frequency (RF) magnetron sputtering (Figure 5 B). This technique deposits thin coatings chemically bonded with the substrate which improves adhesion between the coatings and the substrate.⁹²

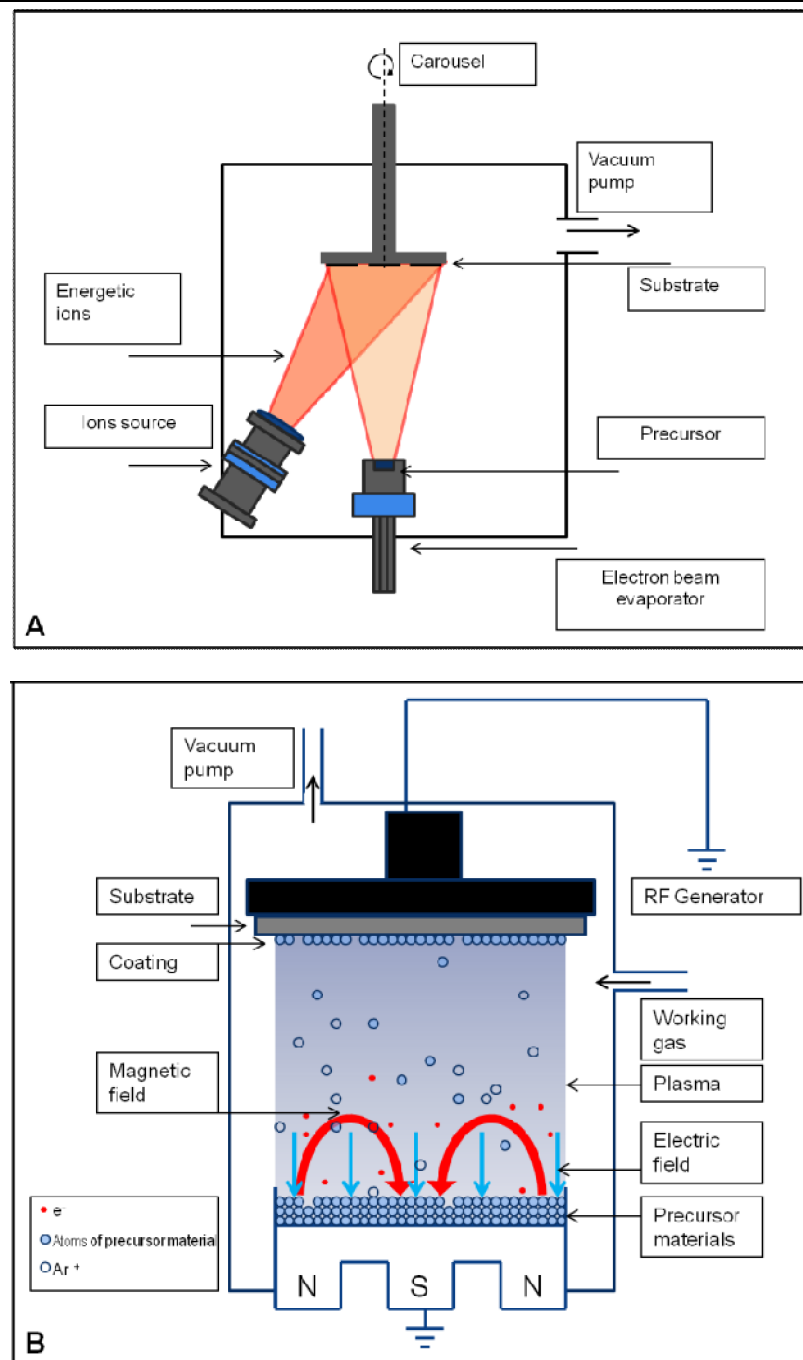


Figure 5. Schematic representation of physical deposition technique. (A) Ion beam deposition scheme. (B) Radio frequency magnetron sputtering apparatus.

5. Future perspectives

The science of surface modification has shown significant progress in clinical applications through the development of more active inorganic and organic coating materials on implant surfaces. However, many scientific and technological challenges remain in biomaterials research. Further research and full understanding of fundamental aspects of the field such as the process of bone formation, attachment of proteins and specific cells, cell adhesion, bone stimulation or induction by inorganic and organic coatings are essential.

The use of CaP as a bone implant surface coating is well established in the field of biomaterials research, although the validity and efficacy of efforts focused on substitution within the crystal lattice have yet to be thoroughly explored. CaP-based coatings employed as a local delivery system of antimicrobials or pharmaceuticals offer great potential for medical applications, but still more precise control on local release kinetics is required.

Deposition of coating materials can strongly modify implant surface characteristics. Different coatings are obtained by selecting precursor materials for deposition, but also the coating techniques have a strong role in the final surface modifications. A deposited layer of calcium phosphate can assume totally different nano-, micro- and macromorphology if biomimetic, electrospray or RF magnetron sputtering deposition technique is used (Figure 6 A-C).

Incorporation of organic compounds into coatings, such as proteins derived from ECM, BMPs and other growth factors, peptides or pharmacologically active biomolecules have shown to play an effective role in stimulating cell adhesion to implant surfaces. Nevertheless, optimization of coating degradation, immobilization of biomolecules and effective concentrations are needed to improve functionality and biological efficacy. A

representation of surfaces treated with biomolecules with two different methods is given in Figure 6 D and E.

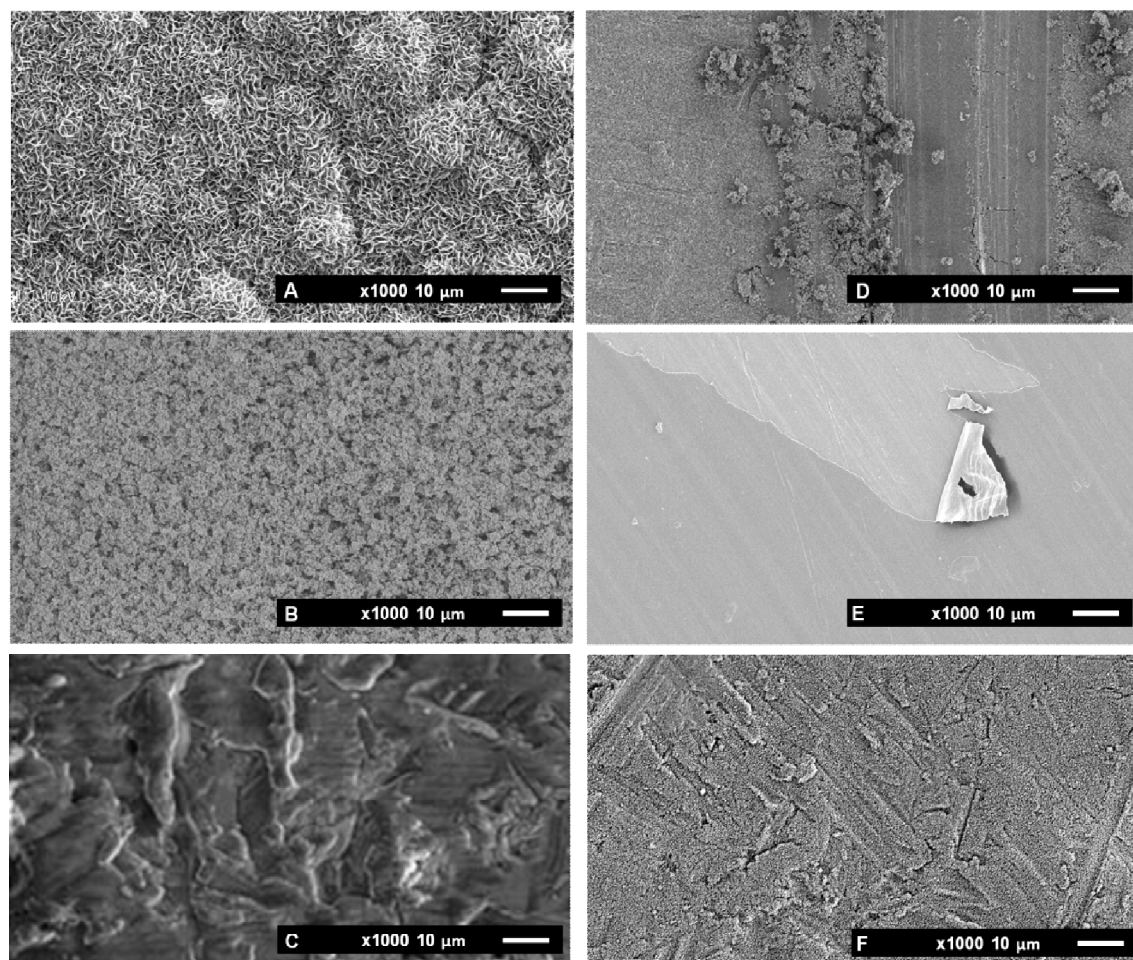


Figure 6. Overview of scanning electron microscopy images of surfaces of coated titanium sample substrates. Different coating techniques are considered and different precursor materials. Inorganic coating: (A) Calcium phosphate biomimetic deposition. (B) Calcium phosphate electrospray deposition (C) Calcium phosphate RF magnetron sputtering deposition. Organic coating: (D) Wet chemical deposition of biomolecules (Alkaline Phosphatase) (E) Collagen deposited with electro spray deposition. Composite coating: (F) Calcium phosphate and collagen electrospray deposition.

The heterogeneity of available biomaterials and deposition methods is leading to a continuous evolution of surface modifications that combine different techniques and materials to obtain solutions for specific needs, such as improved retention of deposited materials or to create composite coating layers (Figure 6 F).

Finally, initial research steps have been taken regarding the optimization of surface properties for bone implants to be used in compromised situations (e.g. osteoporosis and

diabetes research). More reactive surfaces, with direct tissue interaction, have been engineered to improve bone quality. Future research strategies should consider validating therapeutic safety and effectiveness of therapeutic coatings.

6. Objectives of this study

The principal objective of this thesis was to use Electrostatic Spray Deposition to fabricate novel coatings for bone implants, able to improve surface bioactivity. The main approach was to investigate the state-of-the-art and determine the materials and the methods that could be adopted to rapidly improve titanium-based implant performance for orthopedic applications.

The complexity and the heterogeneity of bone tissue served as an inspiration to explore the role of different compounds for bone implant surface modifications. Inorganic constituents of bone (such as hydroxyapatite), organic and extra-cellular compounds (i.e. alkaline phosphatase and collagen) and molecules able to trigger specific behavior in bone cells (osteoclast and osteoblast) were the tools used to design new bioactive coatings. ESD was adopted as the preferred coating method to exploit its versatility in terms of compounds that can be deposited. Regarding inorganic coatings, the described research focused on i) the possibility to deposit nano-sized hydroxyapatite crystals that resemble the natural bone inorganic phase, ii) the possibility of enrich nano crystals with bioactive drugs or bioinorganic substitution and iii) the role of nano crystals coating toward biological responses. Organic coatings were obtained using collagen and alkaline phosphatase to mimic the natural acellular mechanism to induce (surface) mineralization on samples. Biological response to the investigated coating was obtained with in vitro and in vivo experiments.

More specifically the research described in this thesis aimed to:

1. Investigate the current state-of-the-art for coatings using inorganic and/or organic and the methods adopted to deposit such coatings on metallic materials (Chapter II);
2. Evaluate the role of deposition parameters of ESD to obtain coatings based on nano-sized hydroxyapatite crystals inspired by natural bone inorganic phase (Chapter III);
3. Deposit biomolecules preserving their activity and the role of configurations in coating performances (Chapter IV);
4. Obtain a bioactive compound, based on hydroxyapatite, able to trigger specific cellular (osteoclast) responses and deposit it onto titanium using ESD to obtain local therapeutic efficacy (Chapter V);
5. Verify the efficacy of bisphosphonate and nano-sized hydroxyapatite, as single compounds or combined, as coatings for bone implants to be used in compromised (osteoporosis) and healthy conditions (Chapter VI).
6. Test the efficacy of bioinorganic based coatings obtaining strontium doped hydroxyapatite and test its impact on osteoblast behavior (Chapter VII).

References

1. Bornstein, M. M.; Cionca, N.; Mombelli, A., Systemic conditions and treatments as risks for implant therapy. *Int J Oral Maxillofac Implants* 2009, 24 Suppl, 12-27.
2. Ripamonti, U.; Roden, L. C.; Renton, L. F., Osteoinductive hydroxyapatite-coated titanium implants. *Biomaterials* 2012, 33, (15), 3813-3823.
3. Habibovic, P.; Gbureck, U.; Doillon, C. J.; Bassett, D. C.; van Blitterswijk, C. A.; Barralet, J. E., Osteoconduction and osteoinduction of low-temperature 3D printed bioceramic implants. *Biomaterials* 2008, 29, (7), 944-953.
4. Hing, K. A.; Revell, P. A.; Smith, N.; Buckland, T., Effect of silicon level on rate, quality and progression of bone healing within silicate-substituted porous hydroxyapatite scaffolds. *Biomaterials* 2006, 27, (29), 5014-5026.
5. Brook, I.; Freeman, C.; Grubb, S.; Cummins, N.; Curran, D.; Reidy, C.; Hampshire, S.; Towler, M., Biological evaluation of nano-hydroxyapatite–zirconia (HA–ZrO₂) composites and strontium–hydroxyapatite (Sr–HA) for load-bearing applications. *Journal of Biomaterials Applications* 2011.
6. Yang, F.; Dong, W.-j.; He, F.-m.; Wang, X.-x.; Zhao, S.-f.; Yang, G.-l., Osteoblast response to porous titanium surfaces coated with zinc-substituted hydroxyapatite. *Oral Surgery, Oral Medicine, Oral Pathology and Oral Radiology* 2012, 113, (3), 313-318.
7. Bigi, A.; Boanini, E.; Capuccini, C.; Fini, M.; Mihailescu, I. N.; Ristoscu, C.; Sima, F.; Torricelli, P., Biofunctional alendronate–Hydroxyapatite thin films deposited by Matrix Assisted Pulsed Laser Evaporation. *Biomaterials* 2009, 30, (31), 6168-6177.
8. Müller, L.; Conforto, E.; Caillard, D.; Müller, F. A., Biomimetic apatite coatings—Carbonate substitution and preferred growth orientation. *Biomolecular Engineering* 2007, 24, (5), 462-466.
9. Ferro, D.; Barinov, S. M.; Rau, J. V.; Teghil, R.; Latini, A., Calcium phosphate and fluorinated calcium phosphate coatings on titanium deposited by Nd:YAG laser at a high fluence. *Biomaterials* 2005, 26, (7), 805-812.
10. Campbell, A. A.; Song, L.; Li, X. S.; Nelson, B. J.; Bottoni, C.; Brooks, D. E.; DeJong, E. S., Development, characterization, and anti-microbial efficacy of hydroxyapatite-chlorhexidine coatings produced by surface-induced mineralization. *Journal of Biomedical Materials Research* 2000, 53, (4), 400-407.
11. LeGeros, R. Z., Calcium phosphate-based osteoinductive materials. *Chem Rev* 2008, 108, (11), 4742-53.
12. Bose, S.; Tarafder, S., Calcium phosphate ceramic systems in growth factor and drug delivery for bone tissue engineering: A review. *Acta Biomaterialia* 2012, 8, (4), 1401-1421.
13. Currey, J. D., Bone architecture and fracture. *Curr Osteoporos Rep* 2005, 3, (2), 52-6.
14. Currey, J. D., Bones: structure and mechanics. In Press, P. U., Ed. 2002.
15. LeGeros, R. Z., Calcium Phosphate-Based Osteoinductive Materials. *Chemical Reviews* 2008, 108, (11), 4742-4753.
16. Hench, L. L., Bioceramics. *Journal of the American Ceramic Society* 1998, 81, (7), 1705-1728.
17. Kamitakahara, M.; Ohtsuki, C.; Miyazaki, T., Coating of bone-like apatite for development of bioactive materials for bone reconstruction. *Biomed Mater* 2007, 2, (4), R17-23.
18. Voigt, J. D.; Mosier, M., Hydroxyapatite (HA) coating appears to be of benefit for implant durability of tibial components in primary total knee arthroplasty. *Acta Orthop* 2011, 82, (4), 448-59.
19. Kim, K. H.; Ramaswamy, N., Electrochemical surface modification of titanium in dentistry. *Dent Mater J* 2009, 28, (1), 20-36.
20. Leeuwenburgh, S. C.; Wolke, J. G.; Schoonman, J.; Jansen, J. A., Influence of precursor solution parameters on chemical properties of calcium phosphate coatings prepared using Electrostatic Spray Deposition (ESD). *Biomaterials* 2004, 25, (4), 641-9.

21. Wang, J.; Layrolle, P.; Stigter, M.; de Groot, K., Biomimetic and electrolytic calcium phosphate coatings on titanium alloy: physicochemical characteristics and cell attachment. *Biomaterials* 2004, 25, (4), 583-92.
22. Ehara, A.; Ogata, K.; Imazato, S.; Ebisu, S.; Nakano, T.; Umakoshi, Y., Effects of alpha-TCP and TetCP on MC3T3-E1 proliferation, differentiation and mineralization. *Biomaterials* 2003, 24, (5), 831-6.
23. Yao, Z. Q.; Ivanisenko, Y.; Diemant, T.; Caron, A.; Chuvilin, A.; Jiang, J. Z.; Valiev, R. Z.; Qi, M.; Fecht, H. J., Synthesis and properties of hydroxyapatite-containing porous titania coating on ultrafine-grained titanium by micro-arc oxidation. *Acta Biomaterialia* 2010, 6, (7), 2816-2825.
24. Pan, Y. K.; Chen, C. Z.; Wang, D. G.; Yu, X., Microstructure and biological properties of micro-arc oxidation coatings on ZK60 magnesium alloy. *Journal of Biomedical Materials Research Part B: Applied Biomaterials* 2012, n/a-n/a.
25. Bohner, M., Silicon-substituted calcium phosphates - a critical view. *Biomaterials* 2009, 30, (32), 6403-6.
26. Patel, N.; Best, S. M.; Bonfield, W.; Gibson, I. R.; Hing, K. A.; Damien, E.; Revell, P. A., A comparative study on the in vivo behavior of hydroxyapatite and silicon substituted hydroxyapatite granules. *J Mater Sci Mater Med* 2002, 13, (12), 1199-206.
27. Hing, K. A.; Revell, P. A.; Smith, N.; Buckland, T., Effect of silicon level on rate, quality and progression of bone healing within silicate-substituted porous hydroxyapatite scaffolds. *Biomaterials* 2006, 27, (29), 5014-26.
28. Landi, E.; Logroscino, G.; Proietti, L.; Tampieri, A.; Sandri, M.; Sprio, S., Biomimetic Mg-substituted hydroxyapatite: from synthesis to in vivo behaviour. *J Mater Sci Mater Med* 2008, 19, (1), 239-47.
29. Verberckmoes, S. C.; Behets, G. J.; Oste, L.; Bervoets, A. R.; Lamberts, L. V.; Drakopoulos, M.; Somogyi, A.; Cool, P.; Dorriné, W.; De Broe, M. E.; D'Haese, P. C., Effects of Strontium on the Physicochemical Characteristics of Hydroxyapatite. *Calcified Tissue International* 2004, 75, (5), 405-415.
30. Christoffersen, J.; Christoffersen, M. R.; Kolthoff, N.; Barenholdt, O., Effects of strontium ions on growth and dissolution of hydroxyapatite and on bone mineral detection. *Bone* 1997, 20, (1), 47-54.
31. Kannan, S.; Pina, S.; Ferreira, J. M. F., Formation of Strontium-Stabilized β -Tricalcium Phosphate from Calcium-Deficient Apatite. *Journal of the American Ceramic Society* 2006, 89, (10), 3277-3280.
32. Saint-Jean, S. J.; Camire, C. L.; Nevsten, P.; Hansen, S.; Ginebra, M. P., Study of the reactivity and in vitro bioactivity of Sr-substituted alpha-TCP cements. *J Mater Sci Mater Med* 2005, 16, (11), 993-1001.
33. Fielding, G. A.; Roy, M.; Bandyopadhyay, A.; Bose, S., Antibacterial and biological characteristics of silver containing and strontium doped plasma sprayed hydroxyapatite coatings. *Acta Biomater* 2012, 8, (8), 3144-52.
34. Wang, J.; de Groot, K.; van Blitterswijk, C.; de Boer, J., Electrolytic deposition of lithium into calcium phosphate coatings. *Dent Mater* 2009, 25, (3), 353-9.
35. Kawamura, H.; Ito, A.; Miyakawa, S.; Layrolle, P.; Ojima, K.; Ichinose, N.; Tateishi, T., Stimulatory effect of zinc-releasing calcium phosphate implant on bone formation in rabbit femora. *J Biomed Mater Res* 2000, 50, (2), 184-90.
36. Kawamura, H.; Ito, A.; Muramatsu, T.; Miyakawa, S.; Ochiai, N.; Tateishi, T., Long-term implantation of zinc-releasing calcium phosphate ceramics in rabbit femora. *J Biomed Mater Res* 2003, 65, (4), 468-74.
37. Bajpai, P. K.; Benghuzzi, H. A., Ceramic systems for long-term delivery of chemicals and biologicals. *J Biomed Mater Res* 1988, 22, (12), 1245-66.
38. Shinto, Y.; Uchida, A.; Korkusuz, F.; Araki, N.; Ono, K., Calcium hydroxyapatite ceramic used as a delivery system for antibiotics. *J Bone Joint Surg Br* 1992, 74, (4), 600-4.
39. Uchida, A.; Shinto, Y.; Araki, N.; Ono, K., Slow release of anticancer drugs from porous calcium hydroxyapatite ceramic. *J Orthop Res* 1992, 10, (3), 440-5.

40. Zhou, H.; Lawrence, J. G.; Touny, A. H.; Bhaduri, S. B., Biomimetic coating of bisphosphonate incorporated CDHA on Ti6Al4V. *J Mater Sci Mater Med* 2012, 23, (2), 365-74.
41. de Jonge, L. T.; Leeuwenburgh, S. C.; Wolke, J. G.; Jansen, J. A., Organic-inorganic surface modifications for titanium implant surfaces. *Pharm Res* 2008, 25, (10), 2357-69.
42. Sumner, D. R.; Turner, T. M.; Purchio, A. F.; Gombotz, W. R.; Urban, R. M.; Galante, J. O., Enhancement of bone ingrowth by transforming growth factor- β . *Journal of Bone and Joint Surgery - Series A* 1995, 77, (8), 1135-1147.
43. Puleo, D. A., Biochemical surface modification of Co-Cr-Mo. *Biomaterials* 1996, 17, (2), 217-222.
44. Endo, K., Chemical modification of metallic implant surfaces with biofunctional proteins (Part 1). Molecular structure and biological activity of a modified NiTi alloy surface. *Dental materials journal* 1995, 14, (2), 185-198.
45. Schliephake, H.; Scharnweber, D., Chemical and biological functionalization of titanium for dental implants. *Journal of Materials Chemistry* 2008, 18, (21).
46. Nijhuis, A. W. G.; Leeuwenburgh, S. C. G.; Jansen, J. A., Wet-Chemical Deposition of Functional Coatings for Bone Implantology. *Macromolecular Bioscience* 10, (11), 1316-1329.
47. Petrie, T. A.; García, A. J., Extracellular Matrix-derived Ligand for Selective Integrin Binding to Control Cell Function
Biological Interactions on Materials Surfaces. In Puleo, D. A.; Bizios, R., Eds. Springer US: 2009; pp 133-156.
48. Muller, R.; Abke, J.; Schnell, E.; Macionczyk, F.; Gbureck, U.; Mehrl, R.; Ruszczak, Z.; Kujat, R.; Englert, C.; Nerlich, M.; Angele, P., Surface engineering of stainless steel materials by covalent collagen immobilization to improve implant biocompatibility. *Biomaterials* 2005, 26, (34), 6962-6972.
49. Douglas, T.; Heinemann, S.; Hempel, U.; Mietrach, C.; Knieb, C.; Bierbaum, S.; Scharnweber, D.; Worch, H., Characterization of collagen II fibrils containing biglycan and their effect as a coating on osteoblast adhesion and proliferation. *Journal of Materials Science: Materials in Medicine* 2008, 19, (4), 1653-1660.
50. Rammelt, S.; Illert, T.; Bierbaum, S.; Scharnweber, D.; Zwipp, H.; Schneiders, W., Coating of titanium implants with collagen, RGD peptide and chondroitin sulfate. *Biomaterials* 2006, 27, (32), 5561-5571.
51. Schliephake, H.; Scharnweber, D.; Dard, M.; Sewing, A.; Aref, A.; Roessler, S., Functionalization of dental implant surfaces using adhesion molecules. *Journal of Biomedical Materials Research Part B: Applied Biomaterials* 2005, 73B, (1), 88-96.
52. Bernhardt, R.; van den Dolder, J.; Bierbaum, S.; Beutner, R.; Scharnweber, D.; Jansen, J.; Beckmann, F.; Worch, H., Osteoconductive modifications of Ti-implants in a goat defect model: characterization of bone growth with SR β -CT and histology. *Biomaterials* 2005, 26, (16), 3009-3019.
53. Alghamdi, H. S.; van Oirschot, B.; Bosco, R.; den Beucken, J. J. J. P.; Aldosari, A. A. F.; Anil, S.; Jansen, J. A., Biological response to titanium implants coated with nanocrystals calcium phosphate or type 1 collagen in a dog model. *Clinical Oral implants Research* 2012.
54. Solheim, E., Growth factors in bone. *Int Orthop* 1998, 22, (6), 410-6.
55. Hall, J.; Sorensen, R. G.; Wozney, J. M.; Wikesjo, U. M., Bone formation at rhBMP-2-coated titanium implants in the rat ectopic model. *J Clin Periodontol* 2007, 34, (5), 444-51.
56. Siebers, M. C.; Walboomers, X. F.; Leeuwenburgh, S. C.; Wolke, J. C.; Boerman, O. C.; Jansen, J. A., Transforming growth factor-beta1 release from a porous electrostatic spray deposition-derived calcium phosphate coating. *Tissue Eng* 2006, 12, (9), 2449-56.
57. Stadlinger, B.; Pilling, E.; Mai, R.; Bierbaum, S.; Bernhardt, R.; Scharnweber, D.; Eckelt, U., Effect of biological implant surface coatings on bone formation, applying collagen, proteoglycans, glycosaminoglycans and growth factors. *Journal of Materials Science: Materials in Medicine* 2008, 19, (3), 1043-1049.
58. de Jonge, L. T.; van den Beucken, J. J. J. P.; Leeuwenburgh, S. C. G.; Hamers, A. A. J.; Wolke, J. G. C.; Jansen, J. A., In vitro responses to electrosprayed alkaline phosphatase/calcium phosphate composite coatings. *Acta Biomaterialia* 2009, 5, (7), 2773-2782.

59. Stadlinger, B.; Pilling, E.; Mai, R.; Bierbaum, S.; Berhardt, R.; Scharnweber, D.; Eckelt, U., Effect of biological implant surface coatings on bone formation, applying collagen, proteoglycans, glycosaminoglycans and growth factors. *J Mater Sci Mater Med* 2008, 19, (3), 1043-9.
60. Shin, H.; Jo, S.; Mikos, A. G., Biomimetic materials for tissue engineering. *Biomaterials* 2003, 24, (24), 4353-64.
61. Morra, M., Biochemical modification of titanium surfaces: peptides and ECM proteins. *Eur Cell Mater* 2006, 12, 1-15.
62. Elmengaard, B.; Bechtold, J. E.; Soballe, K., In vivo effects of RGD-coated titanium implants inserted in two bone-gap models. *J Biomed Mater Res A* 2005, 75, (2), 249-55.
63. Schliephake, H.; Scharnweber, D.; Dard, M.; Sewing, A.; Aref, A.; Roessler, S., Functionalization of dental implant surfaces using adhesion molecules. *J Biomed Mater Res B Appl Biomater* 2005, 73, (1), 88-96.
64. Roessler, S.; Born, R.; Scharnweber, D.; Worch, H.; Sewing, A.; Dard, M., Biomimetic coatings functionalized with adhesion peptides for dental implants. *J Mater Sci Mater Med* 2001, 12, (10-12), 871-7.
65. LeBaron, R. G.; Athanasiou, K. A., Extracellular matrix cell adhesion peptides: functional applications in orthopedic materials. *Tissue Eng* 2000, 6, (2), 85-103.
66. Sreejalekshmi, K. G.; Nair, P. D., Biomimeticity in tissue engineering scaffolds through synthetic peptide modificationsâ€”Altering chemistry for enhanced biological response. In Wiley Online Library: Vol. 96, pp 477-491.
67. Bigi, A.; Boanini, E.; Capuccini, C.; Fini, M.; Mihailescu, I. N.; Ristoscu, C.; Sima, F.; Torricelli, P., Biofunctional alendronate-Hydroxyapatite thin films deposited by Matrix Assisted Pulsed Laser Evaporation. *Biomaterials* 2009, 30, (31), 6168-6177.
68. Barbour, M. E.; O'Sullivan, D. J.; Jagger, D. C., Chlorhexidine adsorption to anatase and rutile titanium dioxide. *Colloids and Surfaces A: Physicochemical and Engineering Aspects* 2007, 307, (1â€“3), 116-120.
69. Abtahi, J.; Tengvall, P.; Aspenberg, P., A bisphosphonate-coating improves the fixation of metal implants in human bone. A randomized trial of dental implants. *Bone* 2012, 50, (5), 1148-1151.
70. Bosco, R.; Van Den Beucken, J.; Leeuwenburgh, S.; Jansen, J., Surface Engineering for Bone Implants: A Trend from Passive to Active Surfaces. In 2012; Vol. 2, pp 95-119.
71. Cattalini, J. P.; Boccaccini, A. R.; Lucangioli, S.; Mourino, V., Bisphosphonate-Based Strategies for Bone Tissue Engineering and Orthopedic Implants. *Tissue Eng Part B Rev* 2012.
72. Kokubo, T.; Kushitani, H.; Sakka, S.; Kitsugi, T.; Yamamuro, T., Solutions able to reproduce in vivo surface-structure changes in bioactive glass-ceramic A-W. *J Biomed Mater Res* 1990, 24, (6), 721-34.
73. Kokubo, T.; Takadama, H., How useful is SBF in predicting in vivo bone bioactivity? *Biomaterials* 2006, 27, (15), 2907-2915.
74. Gandolfi, M. G.; Ciapetti, G.; Perut, F.; Taddei, P.; Modena, E.; Rossi, P. L.; Prati, C., Biomimetic calcium-silicate cements aged in simulated body solutions. Osteoblast response and analyses of apatite coating. *J Appl Biomater Biomech* 2009, 7, (3), 160-70.
75. Wu, G.; Liu, Y.; Iizuka, T.; Hunziker, E. B., Biomimetic coating of organic polymers with a protein-functionalized layer of calcium phosphate: the surface properties of the carrier influence neither the coating characteristics nor the incorporation mechanism or release kinetics of the protein. *Tissue Eng Part C Methods* 2010, 16, (6), 1255-65.
76. Pasinli, A.; Yuksel, M.; Celik, E.; Sener, S.; Tas, A. C., A new approach in biomimetic synthesis of calcium phosphate coatings using lactic acid-Na lactate buffered body fluid solution. *Acta Biomater* 2010, 6, (6), 2282-8.
77. Liu, Y.; Layrolle, P.; de Bruijn, J.; van Blitterswijk, C.; de Groot, K., Biomimetic coprecipitation of calcium phosphate and bovine serum albumin on titanium alloy. *Journal of Biomedical Materials Research* 2001, 57, (3), 327-335.
78. Jahoda, D.; Nyc, O.; Pokorny, D.; Landor, I.; Sosna, A., [Antibiotic treatment for prevention of infectious complications in joint replacement]. *Acta Chir Orthop Traumatol Cech* 2006, 73, (2), 108-14.

79. Denissen, H.; Van Beek, E.; Lowik, C.; Papapoulos, S.; Van Den Hooff, A., Ceramic hydroxyapatite implants for the release of bisphosphonate. *Bone and Mineral* 1994, 25, (2), 123-134.
80. Seshima, H.; Yoshinari, M.; Takemoto, S.; Hattori, M.; Kawada, E.; Inoue, T.; Oda, Y., Control of bisphosphonate release using hydroxyapatite granules. *Journal of Biomedical Materials Research - Part B Applied Biomaterials* 2006, 78, (2), 215-221.
81. Boanini, E.; Torricelli, P.; Gazzano, M.; Giardino, R.; Bigi, A., Alendronate-hydroxyapatite nanocomposites and their interaction with osteoclasts and osteoblast-like cells. *Biomaterials* 2008, 29, (7), 790-796.
82. Shadanbaz, S.; Dias, G. J., Calcium phosphate coatings on magnesium alloys for biomedical applications: A review. *Acta Biomaterialia* 2012, 8, (1), 20-30.
83. Ji, X.; Lou, W.; Wang, Q.; Ma, J.; Xu, H.; Bai, Q.; Liu, C.; Liu, J., Sol-gel-derived hydroxyapatite-carbon nanotube/titania coatings on titanium substrates. *Int J Mol Sci* 2012, 13, (4), 5242-53.
84. Bagheri, H.; Piri-Moghadam, H.; Ahdi, T., Role of precursors and coating polymers in sol-gel chemistry toward enhanced selectivity and efficiency in solid phase microextraction. *Analytica Chimica Acta* 2012, 742, (0), 45-53.
85. W, S., Corona spray pyrolysis: A new coating technique with an extremely enhanced deposition efficiency. *Thin Solid Films* 1984, 120, (4), 267-274.
86. Wilhelm, O.; Mädler, L.; Pratsinis, S. E., Electrospray evaporation and deposition. *Journal of Aerosol Science* 2003, 34, (7), 815-836.
87. de Jonge, L. T.; Leeuwenburgh, S. C. G.; van den Beucken, J. J. J. P.; Wolke, J. G. C.; Jansen, J. A., Electrosprayed Enzyme Coatings as Bioinspired Alternatives to Bioceramic Coatings for Orthopedic and Oral Implants. *Advanced Functional Materials* 2009, 19, (5), 755-762.
88. Aksakal, B.; Hanyaloglu, C., Bioceramic dip-coating on Ti-6Al-4V and 316L SS implant materials. *Journal of Materials Science: Materials in Medicine* 2008, 19, (5), 2097-2104.
89. Kurzweg, H.; Heimann, R. B.; Troczynski, T.; Wayman, M. L., Development of plasma-sprayed bioceramic coatings with bond coats based on titania and zirconia. *Biomaterials* 1998, 19, (16), 1507-11.
90. Cleries, L.; Fernandez-Pradas, J. M.; Morenza, J. L., Bone growth on and resorption of calcium phosphate coatings obtained by pulsed laser deposition. *J Biomed Mater Res* 2000, 49, (1), 43-52.
91. Choi, J. M.; Kim, H. E.; Lee, I. S., Ion-beam-assisted deposition (IBAD) of hydroxyapatite coating layer on Ti-based metal substrate. *Biomaterials* 2000, 21, (5), 469-73.
92. Wolke, J. G.; van Dijk, K.; Schaeken, H. G.; de Groot, K.; Jansen, J. A., Study of the surface characteristics of magnetron-sputter calcium phosphate coatings. *J Biomed Mater Res* 1994, 28, (12), 1477-84.

Chapter II

Surface Engineering for Bone Implants: A Trend from Passive to Active Surfaces

Ruggero Bosco, Jeroen Van Den Beucken, Sander Leeuwenburgh and John Jansen *

Coatings, 2012, 2.3: 95-119.

1. Introduction

The use of medical implants has expanded dramatically during the past decades owing to increased life-expectancy, changing lifestyles and improved implant technology. Problems related to orthopedic, oral and maxillofacial disorders annually affect millions of patients that need a long-term solution to regain a high quality of life. Diseases and problems caused by damaged or diseased bone tissue represent an annual cost that now exceeds 40 billion Euro worldwide[1]. Nevertheless, the rapid increase in the number of elderly people and the corresponding growth of the world population require that tissues and organs endure longer and are also able to perform in compromised health conditions[2].

The musculoskeletal system has structural, protective and mechanical functions. Consequently, in order to develop functional replacements for diseased/malfunctioning joints or bone-anchored elements (like teeth), extensive and multidisciplinary knowledge on bone healing is required. The emergence of modern biology has provided novel insights into the biological mechanisms that are responsible for bone healing which currently facilitates the development of artificial implants that interact optimally with bone tissue[3].

The present review provides an overview of the requirements for bone implants and the approaches that are currently investigated to increase their performance by means of surface modifications. Both physical and chemical surface modifications are being discussed to transform passive inert implants into smart implant surface that actively instruct the physiological environment towards regeneration of bone tissue.

2. Bone Implants

2.1. Implants: Interface between Living Tissue and Dead Matter

Bone is a natural and highly hierarchical structured organic-inorganic composite material made of collagen fibrils hardened with interspersed hydroxyapatite (HA) nanocrystals. Bone is one of the very few human tissues that contains an inorganic phase for mechanical reinforcement.

The skeletal system is responsible for the support, movement, and protection of the internal organs. During activities such as walking and chewing, heavy loads are transferred towards bone tissue which means that artificial implants need to be load-bearing. Cycles of chewing, for example, are estimated to be of the order of 1×10^5 cycles a year with an average force of 700 N[4,5]. The mechanical properties of bone tissue are maintained through a continuous remodeling process of bone formation and resorption (bone turnover) that is regulated by “Wolff’s Law”:

“Bone is deposited and reinforced at areas of greatest stress”[6].

The cells which are responsible for tissue remodeling are osteoblasts (bone-forming) and osteoclasts (bone-resorbing)[3]. Once a material is introduced into bone tissue, a foreign body response is initiated in the surrounding tissue. In more detail, this response consists of the following phases: injury, blood-material interactions, blood clot formation, inflammatory responses, granulation tissue development, and tissue remodeling. Bone tissue can be formed directly at the implant surface of certain bone-bonding materials without the formation of surrounding fibrous tissue capsules, whereas synthetic materials are generally encapsulated upon implantation in soft tissue. During a foreign body response, the local biological environment is different from the healthy tissue since this foreign body response results into elevated concentrations of reactive oxygen species, proteolytic enzymes, fibrotic proteins, giant cells and reduced pH values near the implant surface. As a result, this altered environment has a strong effect on implanted materials, which means that this initial biological response should be the starting point for design of novel implant surfaces with improved functionality[7].

2.2. Material Requirements for Load-Bearing Bone Implants

Metals are applied as biomaterials for bone substituting applications due to their superior mechanical performances. The elastic modulus of cortical bone ranges from 10 to 20GPa[4,8,9], which is considerably lower compared to values of metallic biomaterials that are conventionally used for load-bearing applications such as titanium and stainless steel which exhibit elastic moduli of about 118 GPa[10] and 206 GPa[11], respectively. Besides elasticity, fatigue properties are also crucial for optimal performance of permanent bone implants. The strong resistance to fatigue is an additional factor which has prompted the use metals in load bearing applications.

The transmission of load between the artificial implant and host tissue is crucial to ensure anchoring of bone implants in bone tissue. Load distribution at the interface between a load-bearing bone implant and natural tissue is strongly affected by the differences in elastic modulus and mechanical strength. A mismatch in stiffness between implants and bone tissue, for example, can cause severe bone resorption due to the reduction of stress from bone tissue. This phenomenon, known as stress shielding[4], can have severe consequences that compromise the success of bone implants. A material that can achieve a strong fixation between bone tissue and the implant surface can transfer the load and the stress from the implant to the surrounding bone tissue, thereby ensuring sufficient bone density and strength[12].

In addition to its mechanical performance, synthetic materials that are implanted in bone tissue need to be non-toxic, non-immunogenic, non-thrombogenic, and non-carcinogenic[13]. In that respect, titanium and its alloys have become preferred materials due to their high specific strength, low elastic modulus which matches with the elastic modulus of bone tissue, and most of all, their capacity to form a thin but very stable oxide layer (*i.e.*, passivation) on the surface which is responsible for its inertness[14].

Although bio-inertness can be considered as a beneficial property for load-bearing implant surfaces, the advent of regenerative medicine has resulted into a paradigm shift with respect to the concept of biocompatibility. As a result, the importance of surface modifications has increased considerably. In 1987, biocompatibility was defined as “the ability of a material to perform with an appropriate host response in a specific situation”[13]. During the following two decades, however, the concept of biocompatibility has shifted continuously resulting into changing design criteria for novel implant materials. As a consequence, surface properties of implants have gained importance since artificial implants are exposed to the surrounding tissue at the material surface. As a result, implants are currently designed from a bio-inspired rather than a technologically inspired perspective

2.3. From Passive to Active Bone Implant Surfaces

As described above, modifications of bone implant surfaces have received increasing research interest in order to orchestrate the physiological healing process and obtain biologically active materials that provide biological cues towards tissue regeneration. The ability to target and trigger specific responses and recruit the correct type of cells or stimulate them to perform optimally requires additional functionality of the bone implant surface. The deposition of coatings allows modifying the surface of a material to evoke preferred biological responses, including the reduction of non-specific protein adsorption and immobilization of compounds that encourage specific interactions with cells. Such coatings can be made of materials that degrade in a controllable manner over time without compromising the bulk properties of the device, thereby obtaining a modulated response that transforms a material from passive to active. Recently, Williams stressed the bioactive role of materials as described above by defining biocompatibility as [13,15] “the ability of a biomaterial to perform its desired function with respect to a medical therapy, without eliciting any undesirable local or systemic effects in the recipient or beneficiary of that therapy, but generating the most appropriate beneficial cellular or tissue response to that specific situation, and optimizing the clinically relevant performance of that therapy”.

In the current review, the term “passive” refers to implants that are not chemically or biologically reactive and present rather inert surfaces to the surrounding tissues, whereas the term “active” refers to implants that have been modified to deliberately interfere with the physiological environment by providing biological cues that trigger specific responses.

2.4. Surface Modifications for Bone Implants

Surfaces of bone implants represent the site of interaction with the surrounding living tissue and are therefore crucial to enhance the biological performance of implants [16,17]. Surface engineering aims to design implants of improved biological performance which

are able to modulate and control the response of living tissue. Generally, surface engineering includes modification of topographical (*i.e.*, roughness) and chemical (*i.e.*, coating) characteristics of a medical device. Topographical modifications of titanium and its alloys were aimed at increasing the roughness of implant surfaces, thus increasing the surface area of implants compared to larger smooth surfaces. The increased surface area increases cell attachment and augments the biomechanical interlocking between bone tissue and the implant. To this end, several techniques have been developed, including grit-blasting and acid etching. Grit-blasting is obtained by bombardment of implant surfaces by means of silica (also known as sand-blasting), hydroxyapatite, alumina or TiO₂ particles. Acid-etching treatments are generally performed using hydrofluoric, nitric, or sulphuric acid. A detailed analysis of topographical modification of implants and its relevance for commercial applications has been performed by Dohan Ehrenfest *etal.*[18]. Recently, the emergence of nanotechnology has expanded the scope of topographical modifications from the micro- to nanoscale, thereby affecting cells, biomolecules and ions at the nanoscale. Nanotechnology is the field that focuses on synthesis, characterization and application of materials with at least one dimension sized between 1 and 100 nm. Recently, this nanoscale dimension has received increasing interest in the field of surface engineering, e.g., by developing coatings of thickness below 100 nm or using nanoparticles or nanocrystals with dimensions smaller than 100 nm as components for nanostructured coatings[19].

Surface modifications based on the deposition of coatings retain the mechanical properties of titanium while the functionality of the implant surface can be upgraded by application of (bio)chemical compounds that act as cues towards improved bone regeneration. Upon successful immobilization of these compounds onto implant surfaces, the substrate is responsible for the load-bearing function of the implant whereas the coating should facilitate optimal integration into the surrounding tissues.

3.Surface Engineering: Coating Deposition

3.1. Biological Activity of Bone Implant Coatings

The biological response to implanted bone implants is time-dependent and should ultimately result into complete integration of the artificial implant within the native bone tissue. The initial inflammatory response that follows implant installation determines subsequent remodeling phases in the process of bone healing that lead to transfer of mechanical forces and the high degree of organization of functional bone tissue[20]. Biocompatibility and osteoconductivity of the implant are generally recognized as main success factors for satisfactory long-term performance endosseous implants[21].

Every bone implant is recognized by human tissues as a foreign body[13,22,23]. For this reason the main aim of coating development until two decades ago was to avoid or limit this foreign body response since an excessive foreign body response creates an

intermediate layer of collagenous fibrous tissue in between the material surface and the hosting tissue[22,23]. This fibrous capsule will ultimately result into loss of implant function and ultimately implant loosening. Coatings can be applied onto bone implants to avoid soft tissue formation and create a strongly integrated and interlocked transition between tissue and the implant surface, a phenomenon that is called osteointegration. According to the European Society of Biomaterials, during the consensus conference of 1987, a material can be defined bioactive if it is “one which has been designed to induce specific biological activity”. For materials implanted in bone tissue, bioactive materials correspond to implants that induce a direct bond between the implant surface and the surrounding bone tissue.

Summarizing, the primary aim of engineering bone implant surfaces is to positively modulate the interfacial response between the implant and host tissue. For this purpose, numerous surface engineering methods have been introduced in the last four decades to change surface topography and chemistry of endosseous dental implant. Junker *et al.* has systematically reviewed the efficacy of a wide variety of surface modifications including roughening of dental implants as well as applications of inorganic (calcium phosphate) or organic (adhesion peptides, growth factors) coatings. An overview of the most extensively used topography modifications of commercially available dental implants is reported in Table 1. The following sections will discuss current trends in surface engineering based on inorganic, organic and composite coatings.

Table 1. Overview of commercially available surface modifications (topography) for dental implants.

Name	Description
OsseoSpeed (Astra Tech AB, Mölndal, Sweden)	Titanium oxide blasting followed by chemical modification of the surface by hydrofluoric acid treatment
SLActive (ITI; Institute Straumann, Waldenburg, Switzerland)	Coarse grit-blasting with 0.25–0.5mm aluminum oxide grit at 5 bar followed by acid etching
TiUnite (Nobel Biocare Holding AG, Zürich, Switzerland)	Electrochemical anodization process
Nanotite (3i Implant Innovations, Palm Beach Gardens, FL, USA)	Sol-gel deposition
Friadent plus (Dentsply Friadent, Mannheim, Germany)	large grit blasting (354–500 μm) and acid etching in hydrochloric acid/sulfuric acid/hydrofluoric acid/oxalic acid
Ossean (intra-Lock, Boca-Raton, FL, USA)	is a grit-blasted/acid-etched/calcium phosphate impregnated surface

3.2. Trends in Material for Inorganic Coatings on Bone Implants

In bone tissue, the inorganic phase is mainly composed of carbonate-rich hydroxyapatite. Consequently, hydroxyapatite ceramics have always been an obvious candidate for deposition as coating onto bone implant surfaces. These hydroxyapatite coatings were shown to be bioactive and stimulate the formation of new bone tissue in numerous pre-clinical and clinical studies[24–28]. Chemical parameters such as the Ca/P ratio, phase composition and crystal structure have been evaluated and tested extensively to optimize the performance of CaP coatings. HA coatings showed a persistent significant improvement of the osteoconductivity of metallic implants[29–35].

During the past two decades, recent trends in research on calcium phosphate (CaP) coatings

mainly focused on modification of its chemical structure and addition of ionic dopants. Currently, several types of CaP-based coatings have been explored such as pure HA[36–44], Si-containing HA (Si-HA) [31,40,45–52], Sr-doped HA [53–56], Mg-substituted HA [47], bisphosphonate and HA [55,57], carbonated HA[32,47,58], fluorinated HA[44,59–61] and antibacterial Ag-containing HA (Ag-HA)[62–67].

3.3. Trends in Material for Organic Coatings on Bone Implants

Over the past two decades, organic compounds derived from the extracellular matrix (ECM) of bone issue are increasingly considered as source of inspiration for bioinspired design of organic bone implant coatings[68].

Different approaches can be used to upgrade a bone implant from a passive medical device to an instructive implant that can solicit a desired tissue response[69–73] using organic biomolecules. Organic surface modifications that are currently investigated involve immobilization of among others structural proteins, signaling molecules, enzymes or peptides onto biomaterial surfaces to target cell response at the tissue-implant interface[74,75].

A widely investigated approach aims at improving the adhesion of cells onto bone implant

surfaces. ECM biomolecules such as fibronectin, vitronectin, type I collagen, osteopontin, and bone sialoprotein[76] have been successfully immobilized onto bone implants. These proteins exerted biological effects upon immobilization onto surfaces, but the tendency of proteins to fold upon adsorption to an implant surface remains problematic and decreases the efficacy of immobilized proteins. However, short peptide sequences derived from entire proteins can overcome this problem[77]. Surface-immobilized peptide sequences can recruit or trigger specific cellular interactions[77,78]. The peptide sequence that has been investigated most extensively so far is the Arg-Gly-Asp (RGD) peptide sequence which is the predominant binding site for cells via integrin receptors RGD

sequence[79,80], but various other peptide sequences have been used similarly onto implanted materials[81–84].

Alternatively, osteotropic biomolecules such as growth factors (GFs) can be immobilized onto implant surfaces. Several GFs, including bone morphogenetic protein (BMP), transforming growth factor-beta (TGF- β), fibroblast growth factor (FGF), platelet-derived growth factor (PDGF), and insulin-like growth factor (IGF), have been shown to stimulate formation of bone tissue around implants upon immobilization onto their surface. Most emphasis, however, has been put on the immobilization of members of the TGF- β superfamily such as BMP-2, BMP-7 and TGF- β 1, which have shown promising results in enhancing bone formation around bone implants[85–87].

Besides targeting cellular behavior directly, organic biomolecules such as collagen can also improve mechanical properties of surface coatings while biomolecules such as osteopontin, osteonectin, bone sialoprotein, osteocalcin, or alkaline phosphatase have been investigated as initiators of mineralization by deposition of calcium phosphate onto implant surfaces. For example, immobilized alkaline phosphatase was shown to induce deposition of apatitic mineralization layers *in vitro* and new bone formation *in vivo*[68,88].

3.4. Trends in Materials for Composite and Combined Coatings on Bone Implants

Since bone is a composite tissue, deposition of composite coatings consisting of inorganic and organic constituents is an obvious next step towards design of implant coatings with improved bioactivity and efficacy.

For example, composite coatings composed of collagen and CaP minerals could combine the benefits of the mineral phase (in terms of osteoconduction) and the collagenous matrix (in terms of abundance of RGD-sequences) to affect cellular adhesion, subsequent proliferation, and differentiation phases[89,90]. In addition to the biological effects of collagen[91], CaP-collagen composite coatings showed an improved retention of CaP crystals onto implant surfaces[92,93].

Also growth factors have been co-deposited with calcium phosphate or collagen coatings onto implant surfaces[87,94–97]. In fact, GFs immobilized on titanium implants pre-coated with collagen showed increased osteogenic properties compared to GFs bound to untreated titanium surfaces[98,99]. This may be due to a sustained delivery profile or a higher stability of the growth factor[94,100,101].

Infections during or after surgery still remain a big threat that can compromise the short- and long-term stability of orthopedic implants[102,103]. Therefore, antibiotics have also been loaded into CaP coatings onto titanium implants[104]. The coated antibiotic-HA-composite exhibited a reduced infection rate compared with CaP coatings *in vivo*[105]. In order to reduce the risk of antibiotic resistance also non-antibiotic organic compounds with antimicrobial activity like chlorhexidine, chloroxylenol, and poly(hexamethylenebiguanide)[106–112] have been investigated as potential alternatives.

These organic molecules are commonly used for their broad spectrum of antimicrobial action and lower risk of drug resistance.

Composite coatings can also be prepared by incorporating antimicrobial elements such as silver ions into organic or inorganic coatings since bacterial resistance against silver is minimal[113].

Finally, bone implants are often applied in patients of compromised health. Post-menopausal osteoporosis, for example, reduces bone density resulting into higher prevalence of bone fractures. The use of a local active compound for the prevention or reduction of these osteoporotic fractures could improve the efficacy and fixation of bone implants into osteoporotic bone. Bisphosphonates (BPs) are a group of synthetic drugs with a structural backbone similar to inorganic pyrophosphate with a general structure of $\text{PO}_3\text{-C-PO}_3$. BPs have been used, for long times, for the treatment of skeletal metabolism disorders such as osteoporosis, Paget's disease, tumor-associated osteolysis and hypercalcemia[114–116]. BPs act by reducing osteoclasts (bone resorbing cells) activity but systemic delivery of BPs by oral administration or intravenous injection is associated with serious side-effects[117,118]. The affinity of BPs for HA has been used to develop new CaP-BP composite coating systems for the controlled release of BP from bone implants[119–121]. The reduced activity of bone resorbing cells induced an improved mechanical interlocking of the implant with the hosting bone tissue and correspondingly a faster recovery from surgery[122].

4. Coating Techniques

In order to improve surfaces properties, innovative coating compounds only are not sufficient. Techniques and technology used to deposit these substrates onto implants surfaces have witnessed a constant evolution during the past decades. Calcium phosphate are the largest group of materials used for coating deposition, for which several types of deposition techniques have been investigated including dip and immersion coating, electrophoretic deposition, laser deposition, thermal spraying (including plasma spraying and high-velocity oxy-fuel combustion spraying), biomimetic deposition and sol-gel deposition[123]. Characteristics of several commonly used coating techniques including their advantages, limitations and precursors used are summarized in Table 2.

4.1. Dry Deposition Techniques

Among all the coating techniques that have been investigated for deposition of CaP coatings, physical coating techniques are the ones that most often reached the commercial market. These physical coating techniques, such as plasma-spraying, radio frequency magnetron sputtering, pulsed laser deposition (PLD) and ion beam assisted deposition (IBAD) have been used to deposit several types of CaPs. The most widespread method to

deposit CaP coatings onto implants is the plasma-spraying technique mainly due to its high deposition rate and the possibility to cover large areas.

Table 2. Overview of characteristics of coating techniques.

Technique	Coating thickness	Advantage	Disadvantage	Precursor materials
Plasma spraying	50–250 μm	High deposition rates	Non-uniform coating crystallinity; line of sight technique	HA [36,124–128], Si-HA [40,49] and antibacterial Ag- HA composite coatings [66,67,129]
RF magnetron sputtering	0.5–5 μm	Uniform and dense coating; strong adhesion	Line of sight technique; time consuming; low deposition rates	HA [43], Si-HA [48,52], carbonated HA [32], and Zn, Mg, and Al-doped CaPs [130]
Plasma spraying	50–250 μm	High deposition rates	Non-uniform coating crystallinity; line of sight technique	HA [36,124–128], Si-HA [40,49] and antibacterial Ag- HA composite coatings [66,67,129]
Pulsed laser deposition	0.05–5 μm	Control over coating chemistry and morphology	Line of sight technique	HA resistant to dissolution in SBF [29], Ag-HA [131,132], HA [133–140] and fluorinated HA [60] alendronate-doped HA [57]
Ion beam dynamic mixing deposition	0.05–1 μm	High adhesive strength	Line of sight technique; requires high sintering temperatures	CaP coatings [141–147]
Ion beam assisted deposition	0.02–10 μm	increased tensile bond strength	Line of sight technique;	CaP [31,148–150]
Biomimetic deposition	<30 μm	Coating of complex geometries; co-deposition of biomolecules	Time consuming; requires controlled pH	osteocalcin [151], fibronectin [152] and poly(L-lysine) [153]. BMP-2 incorporated into biomimetic CaP coatings [154,155].
Sol-gel deposition	<1 μm	Coating of complex geometries; low processing temperature	Requires controlled atmosphere processing; expensive raw materials	aluminosilicate [156], fluoridated hydroxyapatite, [157] Si-substituted hydroxyapatite [158], and bioglass [159–161]
Electrophoretic deposition	0.1–2 mm	Uniform coating; coating of complex geometries; high deposition rates	Difficult to produce crack-free coatings; low adhesive strength	CaP-chitosan composite coatings successfully combined with CaSiO ₃ , heparin, and silica [162–164]
Electrospray deposition	0.1–5 μm	Co-deposition of biomolecules; control over coating composition and morphology	Low mechanical strength; Line of sight technique	HA [165,166], Nano HA [167], ALP [168], biomolecules-HA composite [88] collagen [169]

The plasma-spraying (PS) technique involves the introduction of precursor materials (feedstock) into the hot plasma jet (Figure 1) generated by a plasma torch[31,170], at atmospheric pressure (Atmospheric Plasma Spraying, APS), under vacuum (Vacuum Plasma Spraying, VPS) or under reduced pressure (Low Pressure Plasma Spraying, LPS)[171–179]. As a consequence, upon impingement of feedstock powders particles onto the implant surface, an adherent coating is formed due to partial or complete melting of the powder particles.

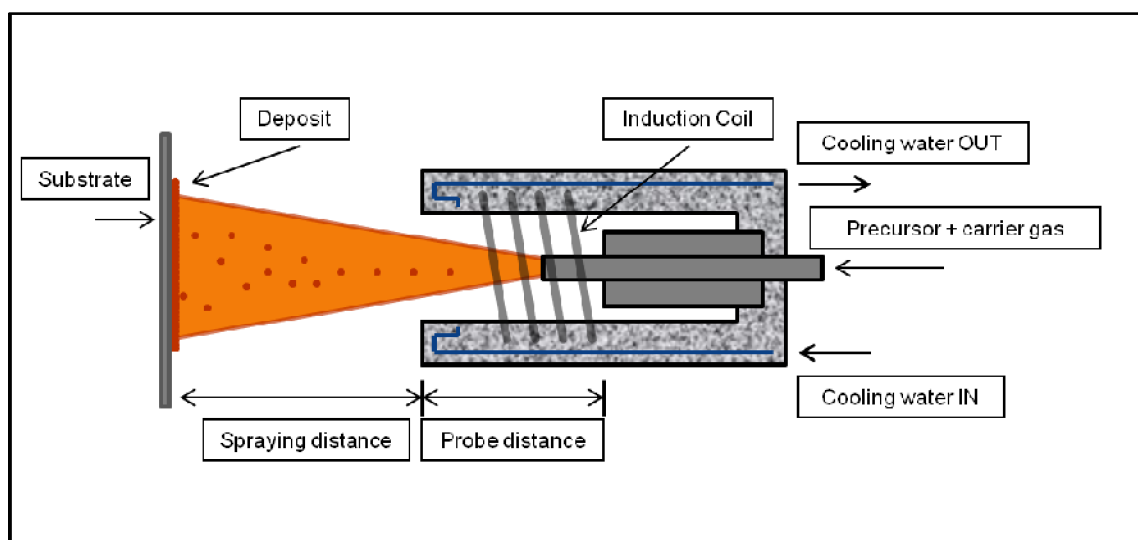


Figure 1. Schematic representation of a Radio Frequency (RF) plasma torch.

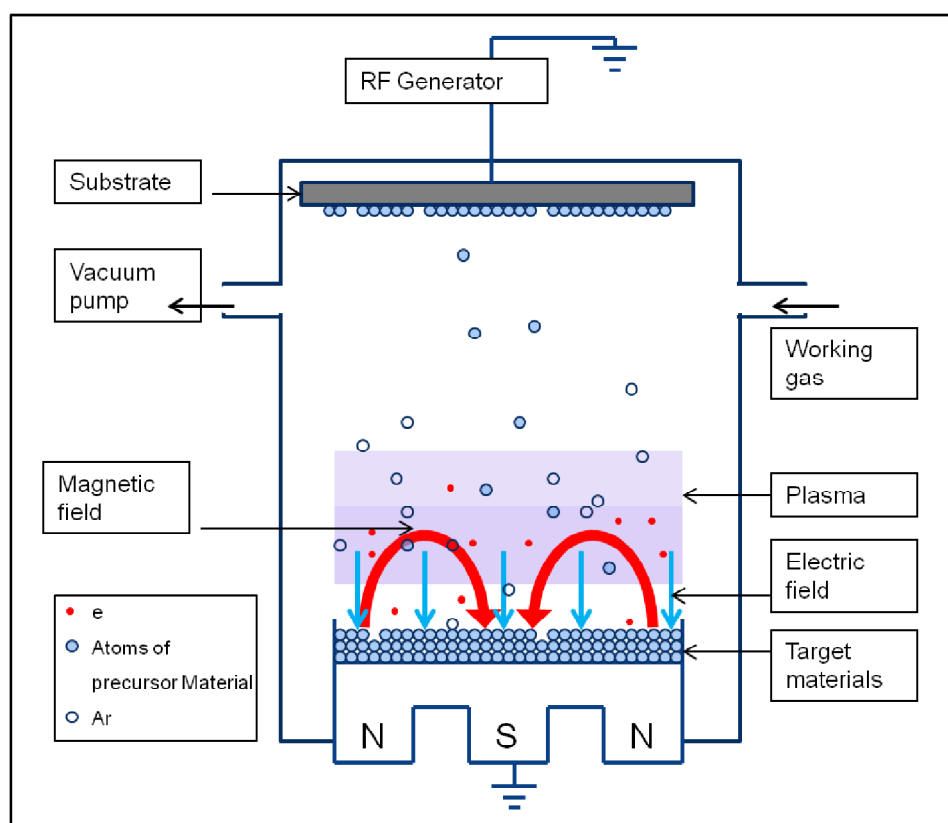


Figure 2. Schematic representation of RF magnetron sputtering.

Another physical technique that is often used to deposit strongly adherent HA onto implants is Radio Frequency (RF) magnetron sputtering (Figure 2)[180–184]. Sputtering is a process whereby atoms or molecules of some materials are ejected in a vacuum chamber, becoming precursors for coating, due to bombardment with high-energy ions[31,185].

Pulsed laser deposition (PLD) is a physical vapor deposition technique that was first described by Cotell[186] to deposit thin films of CaP[55,132,138,187–191]. The PLD system (Figure 3) is typically composed of a KrF laser source, an ultrahigh vacuum deposition chamber equipped with a rotating target and a fixed substrate holder plus pumping systems. The PLD process involves the irradiation of a solid target by a focused pulsed laser and this interaction creates compounds such as $\text{Ca}_4\text{P}_2\text{O}_9$, $\text{Ca}_3(\text{PO}_4)_2$, CaO , P_2O_5 , and H_2O [29]. This high energy plasma cloud is composed of electrons, atoms, ions, molecules, molecular clusters and, in some cases, droplets and target fragments. This plasma cloud expands, either in vacuum or in a gaseous environment, and deposits on a substrate, typically with a temperature in the range of 350–600 °C, producing a thin adherent film onto the target[192]. An alternative set-up called matrix assisted pulsed laser evaporation (MAPLE) was developed for delicate and accurate deposition of both organic and inorganic materials[133].

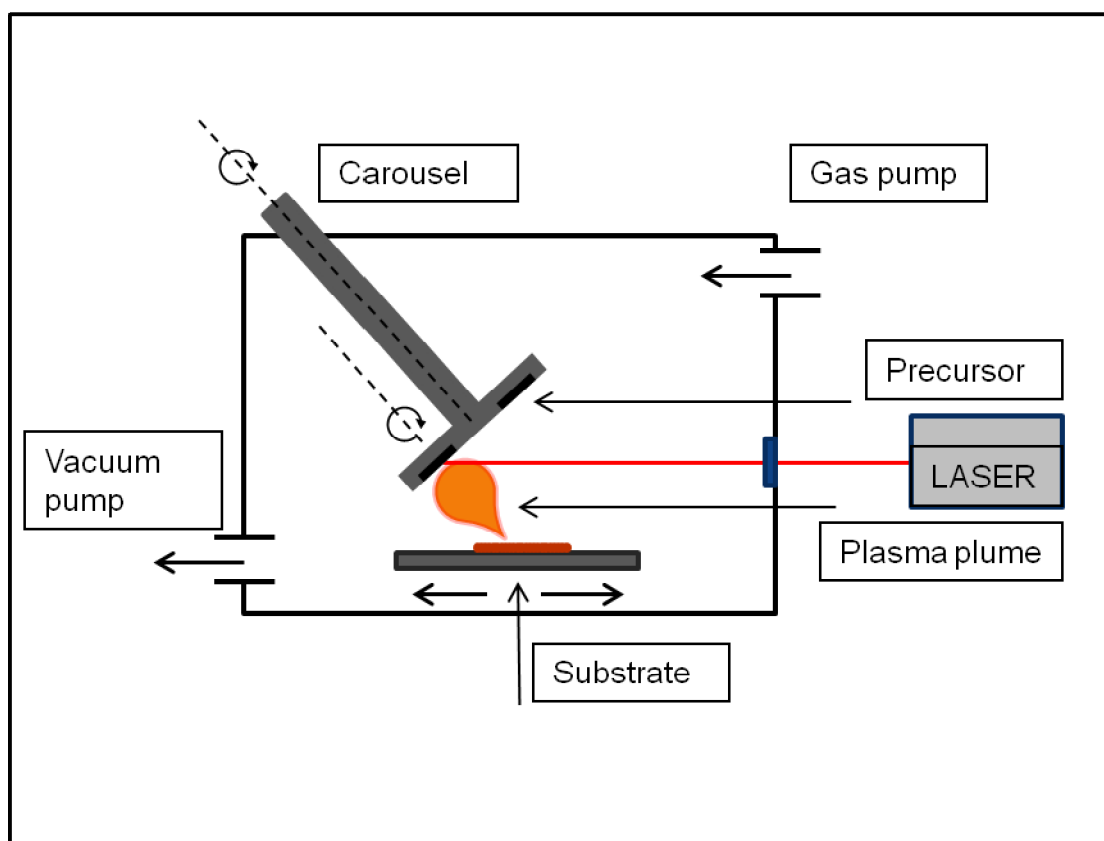


Figure 3. Schematic representation of the pulsed laser deposition (PLD) coating system.

Ion beam assisted deposition (IBAD) is a vacuum technique that has also been used to deposit very thin ceramic coating layers on metals, polymers or ceramics. A typical IBAD system consists of two main elements: electron or ion bombarded precursor materials that vaporize

forming an elemental cloud that covers the surface of a substrate[31,148–150] as well as an ion gun that irradiates the substrate with highly energetic gas ions that can be inert like Ar^+ or reactive like O^{2+} to induce adhesion of the precursors from the above-mentioned elemental cloud[149].

All these physical deposition techniques, however, are highly energetic to achieve a strong fixation of the coating on the surface. This energy (plasma, laser or ions bombardment) involves high temperature that can reach, in some cases, up to 2000 °C[193,194]. Increased temperature during deposition facilitates a firm fixation of the coating onto the surface but it limits the selection for materials that can be coated. Organic materials and biomolecules cannot be deposited using these physical techniques and crystallinity of precursor phases are affected by the thermal process which impedes deposition of biologically relevant CaPs such as carbonate-substituted apatites.

4.2. Wet Deposition Techniques

Wet chemical deposition methods such as biomimetic and sol-gel are alternatives to physical deposition techniques which allow for preservation of biomolecules activity. These techniques have strong advantages related to their simple experimental setup, mild chemical preparation conditions and the possibility to coat implants with a complex three-dimensional geometry (such as porous implants). Such implants cannot be coated using physical coating techniques due to their line-of-sight characteristics. In a recent review by Nijhuis *et al.*[75], an overview is given of current trends in wet chemical deposition of biomedical coatings for bone substitution.

The biomimetic deposition method was introduced for the first time by Kokubo *et al.* in 1990 and is formed under physiological conditions (37 °C, pH 7.4, $p(\text{CO}_2)$ = 0.05 atmosphere and appropriate electrolyte concentrations)[195]. The system involves simple immersion of (pretreated) Ti substrates into a so-called simulated body fluid (SBF) to obtain deposition of a biologically active bone-like CaP layer formed onto the surface of the substrates.

The sol-gel technique is based on colloidal suspensions of solid particles (1–500 nm in size) in a liquid solution (a sol). The sol can be applied onto the substrate via different methods like spin-coating, spraying, or dip-coating. The coating, still in gel form, is put on the target surface and after drying only the precursor materials, through the sol-gel transition, are left as a thin layer[196,197]

4.3. Electrochemical Deposition Techniques

In order to combine the advantage of physical deposition (in terms of quantity control) and wet chemical deposition (non-aggressive setting) electrochemical deposition methods have been advocated. These types of coating depositions can be performed at ambient temperature and pressure provided that precursors are particles or molecules that carry an electrical charge or that can be dispersed in electrolytic solutions. The substrates, onto which the coating is applied, also need to be conductive.

Electrophoretic deposition, for instance, is a technique based on migration of precursor particles suspended in liquid towards substrate surfaces under the influence of an externally applied electrical field. The medium used for electrophoretic deposition is made of organic solvents such as isopropanol or ethanol[198,199]. This technique is a submersion method and so it allows for coating of, e.g., porous implants.

Another promising electrochemical coating system is the electrospray deposition (ESD) technique. Using this technology solutions or suspensions containing precursor materials are sprayed onto substrates under the influence of a high electrical field that creates an aerosol of similarly charged micron-sized droplets[200,201]. ESD allows for a strong control over physicochemical coating properties such as thickness or chemical composition.

4.4. Clinical Performance

Over the past two decades, the application of treatments such as gritblasting and acid etching has become widely accepted as routine topographical treatment for oral implants, as evidenced by numerous commercial implant systems that are being marketed after, e.g., a combination of gritblasting and acid etching. An overview of surface modification of oral implants that are commercially available is shown in Table 1.

Regarding the application of additional coatings it should be stressed that despite extensive research efforts only a limited amount of techniques have made it to clinical trials and commercialization (mainly PS, RF magnetron sputtering and IBAD), whereas most of the other techniques (such as biomimetic deposition, electrospray deposition, *etc.*) are still in the pre-clinical phase. In most cases, adhesion, cost-effectiveness and high costs related to industrial upscaling were the determining factors that limited widespread use and market penetration of various novel surface engineering techniques so far.

5. Summary and Future Perspectives

Since the application of plasma-sprayed hydroxyapatite coatings onto metallic bone implants in the 1980s, the concept of bone implant coatings has shifted from passive protecting thin films to active and instructive immobilized layers. Nowadays, a plethora of coating techniques is being investigated to actively orchestrate a desired biological response at the interface between artificial implants and the surrounding living tissue. In view of the aging population and changing lifestyle, surgeons will be confronted with an increasing number of patients of compromised health that need implants of higher efficacy than currently available. To this end, bone implant surfaces will be increasingly enriched with biomolecules to accelerate the bone healing process. For this purpose, a wide variety of biomolecules such as growth factors, bioactive proteins, enzymes, and non-viral genes (DNAs, RNAs) is currently being evaluated pre-clinically.

For optimal therapeutic efficacy, the fate of these biomolecules needs to be controlled, *i.e.* efficient immobilization strategies need to be developed for covalent or non-covalent immobilization.

References

1. Zethraeus, N.; Borgström, F.; Ström, O.; Kanis, J.; Jönsson, B. Cost-effectiveness of the treatment and prevention of osteoporosis—A review of the literature and a reference model. *Osteoporos. Int.* 2007, *18*, 9–23.
2. Barrère, F.; Mahmood, T.A.; de Groot, K.; van Blitterswijk, C.A. Advanced biomaterials for skeletal tissue regeneration: Instructive and smart functions. *Mater. Sci. Eng. Rep.* 2008, *59*, 38–71.
3. Scholz, M.S.; Blanchfield, J.P.; Bloom, L.D.; Coburn, B.H.; Elkington, M.; Fuller, J.D.; Gilbert, M.E.; Muflahi, S.A.; Pernice, M.F.; Rae, S.I.; *et al.* The use of composite materials in modern orthopaedic medicine and prosthetic devices: A review. *Compos. Sci. Technol.* 2011, *71*, 1791–1803.
4. Ramakrishna, S.; Mayer, J.; Wintermantel, E.; Leong, K.W. Biomedical applications of polymer-composite materials: A review. *Compos. Sci. Technol.* 2001, *61*, 1189–1224.
5. Flanagan, D.; Ilies, H.; McCullough, P.; McQuoid, S. Measurement of the fatigue life of mini dental implants: A pilot study. *J. Oral Implantol.* 2008, *34*, 7–11.
6. Ahn, A.C.; Grodzinsky, A.J. Relevance of collagen piezoelectricity to “Wolff’s Law”: A critical review. *Med. Eng. Phys.* 2009, *31*, 733–741.
7. Anderson, J.M.; Rodriguez, A.; Chang, D.T. Foreign body reaction to biomaterials. *Semin. Immunol.* 2008, *20*, 86–100.
8. Turner, C.H.; Rho, J.; Takano, Y.; Tsui, T.Y.; Pharr, G.M. The elastic properties of trabecular and cortical bone tissues are similar: Results from two microscopic measurement techniques. *J. Biomech.* 1999, *32*, 437–441.
9. Stephani, G.; Quadbeck, P.; Andersen, O. New multifunctional lightweight materials based on cellular metals—Manufacturing, properties and applications. In *Proceedings of International Conference on Advanced Structural and Functional Materials Design*, Osaka, Japan, 10–12 November 2008; doi:10.1088/1742-6596/165/1/012061.
10. Matsuno, H.; Yokoyama, A.; Watari, F.; Uo, M.; Kawasaki, T. Biocompatibility and osteogenesis of refractory metal implants, titanium, hafnium, niobium, tantalum and rhenium. *Biomaterials* 2001, *22*, 1253–1262.
11. Mitsuo, N. Mechanical properties of biomedical titanium alloys. *Mater. Sci. Eng.* 1998, *243*, 231–236.
12. Frost, H.M. The Utah paradigm of skeletal physiology: An overview of its insights for bone, cartilage and collagenous tissue organs. *J. Bone Miner. Metab.* 2000, *18*, 305–316.
13. Williams, D.F. On the mechanisms of biocompatibility. *Biomaterials* 2008, *29*, 2941–2953.
14. Tengvall, P.; Ljunstrom, I. Physico-chemical considerations of titanium as a biomaterial. *Clin. Mater.* 1992, *9*, 115–134.
15. John, C.W. Predicting clinical biological responses to dental materials. *Dent. Mater.* 2012, *28*, 23–40.

16. Sun, L.; Berndt, C.C.; Gross, K.A.; Kucuk, A. Material fundamentals and clinical performance of plasma-sprayed hydroxyapatite coatings: A review. *J. Biomed. Mater. Res.* 2001, *58*, 570–592.
17. Moura, C.C.G.; Souza, M.A.; Dechichi, P.; Zanetta-Barbosa, D.; Teixeira, C.C.; Coelho, P.G. The effect of a nanothickness coating on rough titanium substrate in the osteogenic properties of human bone cells. *J. Biomed. Mater. Res.* 2010, *94*, 103–111.
18. Dohan Ehrenfest, D.M.; Coelho, P.G.; Kang, B.-S.; Sul, Y.-T.; Albrektsson, T. Classification of osseointegrated implant surfaces: Materials, chemistry and topography. *Trends Biotechnol.* 2010, *28*, 198–206.
19. Mendonça, G.; Mendonça, D.B.S.; Aragão, F.J.L.; Cooper, L.F. Advancing dental implant surface technology—From micron- to nanotopography. *Biomaterials* 2008, *29*, 3822–3835.
20. Lemons, J.E. Biomaterials, biomechanics, tissue healing, and immediate-function dental implants. *J. Oral Implantol.* 2004, *30*, 318–324.
21. Albrektsson, T.; Wennerberg, A. Oral implant surfaces: Part 1—Review focusing on topographic and chemical properties of different surfaces and *in vivo* responses to them. *Int. J. Prosthodont.* 2004, *17*, 536–543.
22. Ratner, B.D.; Bryant, S.J. Biomaterials: Where we have been and where we are going. *Annu. Rev. Biomed. Eng.* 2004, *6*, 41–75.
23. Anderson, J.M. Biological responses to materials. *Ann. Rev. Mater. Sci.* 2001, *31*, 81–110.
24. Yang, Y.; Kim, K.H.; Ong, J.L. A review on calcium phosphate coatings produced using a sputtering process an alternative to plasma spraying. *Biomaterials* 2005, *26*, 327–337.
25. Ong, J.L.; Chan, D.C. Hydroxyapatite and their use as coatings in dental implants: A review. *Crit. Rev. Biomed. Eng.* 2000, *28*, 667–707.
26. Junker, R.; Dimakis, A.; Thoneick, M.; Jansen, J.A. Effects of implant surface coatings and composition on bone integration: A systematic review. *Clin. Oral Implant. Res.* 2009, *20*, 185–206.
27. Wang, C.; Karlis, G.A.; Anderson, G.I.; Dunstan, C.R.; Carbone, A.; Berger, G.; Ploska, U.; Zreiqat, H. Bone growth is enhanced by novel bioceramic coatings on Ti alloy implants. *J. Biomed. Mater. Res. Part A* 2009, *90*, 419–428.
28. Palmquist, A.; Omar, O.M.; Esposito, M.; Lausmaa, J.; Thomsen, P. Titanium oral implants: Surface characteristics, interface biology and clinical outcome. *J. R. Soc. Interf.* 2010, *7*, S515–S527.
29. Dinda, G.P.; Shin, J.; Mazumder, J. Pulsed laser deposition of hydroxyapatite thin films on Ti-6Al-4V: Effect of heat treatment on structure and properties. *Acta Biomater.* 2009, *5*, 1821–1830.
30. Suchanek, W.; Yoshimura, M. Processing and properties of hydroxyapatite-based biomaterials for use as hard tissue replacement implants. *J. Mater. Res.* 1998, *13*, 94–117.

31. Paital, S.R.; Dahotre, N.B. Calcium phosphate coatings for bio-implant applications: Materials, performance factors, and methodologies. *Mater. Sci. Eng. Rep.* 2009, *66*, 1–70.
32. Sima, L.E.; Stan, G.E.; Morosanu, C.O.; Melinescu, A.; Ianculescu, A.; Melinte, R.; Neamtu, J.; Petrescu, S.M. Differentiation of mesenchymal stem cells onto highly adherent radio frequency-sputtered carbonated hydroxylapatite thin films. *J. Biomed. Mater. Res.* 2010, *95*, 1203–1214.
33. Saithna, A. The influence of hydroxyapatite coating of external fixator pins on pin loosening and pin track infection: A systematic review. *Injury* 2010, *41*, 128–132.
34. Barrere, F.; van der Valk, C.M.; Meijer, G.; Dalmeijer, R.A.; de Groot, K.; Layrolle, P. Osteointegration of biomimetic apatite coating applied onto dense and porous metal implants in femurs of goats. *J. Biomed. Mater. Res. Appl. Biomater.* 2003, *67*, 655–665.
35. Morris, H.F.; Ochi, S.; Spray, J.R.; Olson, J.W. Periodontal-type measurements associated with hydroxyapatite-coated and non-HA-coated implants: Uncovering to 36 months. *Ann. Periodontol.* 2000, *5*, 56–67.
36. Dudek, A. Investigations of microstructure and properties in bioceramic coatings used in medicine. *Arch. Metall. Mater.* 2011, *56*, 135–140.
37. Pichugin, V.F.; Surmenev, R.A.; Shesterikov, E.V.; Ryabtseva, M.A.; Eshenko, E.V.; Tverdokhlebov, S.I.; Prymak, O.; Epple, M. The preparation of calcium phosphate coatings on titanium and nickel-titanium by rf-magnetron-sputtered deposition: Composition, structure and micromechanical properties. *Surf. Coatings Technol.* 2008, *202*, 3913–3920.
38. Surmenev, R.A.; Ryabtseva, M.A.; Shesterikov, E.V.; Pichugin, V.F.; Peitsch, T.; Epple, M. The release of nickel from nickel-titanium (NiTi) is strongly reduced by a sub-micrometer thin layer of calcium phosphate deposited by rf-magnetron sputtering. *J. Mater. Sci. Mater. Med.* 2010, *21*, 1233–1239.
39. Cao, N.; Dong, J.; Wang, Q.; Ma, Q.; Wang, F.; Chen, H.; Xue, C.; Li, M. Plasma-sprayed hydroxyapatite coating on carbon/carbon composite scaffolds for bone tissue engineering and related tests *in vivo*. *J. Biomed. Mater. Res.* 2010, *92*, 1019–1027.
40. Tang, Q.; Brooks, R.; Rushton, N.; Best, S. Production and characterization of HA and SiHA coatings. *J. Mater. Sci. Mater. Med.* 2010, *21*, 173–181.
41. Cheng, G.J.; Ye, C. Experiment, thermal simulation, and characterizations on transmission laser coating of hydroxyapatite on metal implant. *J. Biomed. Mater. Res.* 2010, *92*, 70–79.
42. Carrado, A. Structural, microstructural, and residual stress investigations of plasma-sprayed hydroxyapatite on Ti-6Al-4 V. *ACS Appl. Mater. Interf.* 2010, *2*, 561–565.
43. Surmenev, R.A.; Surmeneva, M.A.; Evdokimov, K.E.; Pichugin, V.F.; Peitsch, T.; Epple, M. The influence of the deposition parameters on the properties of an rf-magnetron-deposited nanostructured calcium phosphate coating and a possible growth mechanism. *Surf. Coatings Technol.* 2011, *205*, 3600–3606.

44. Wolke, J.G.C.; de Blieck-Hogervorst, J.M.A.; Dhert, W.J.A.; Klein, C.P.A.T.; de Groot, K. Studies on the thermal spraying of apatite bioceramics. *J. Therm. Spray Technol.* 1992, *1*, 75–82.
45. Thian, E.S.; Huang, J.; Best, S.M.; Barber, Z.H.; Bonfield, W. Silicon-substituted hydroxyapatite thin films: Effect of annealing temperature on coating stability and bioactivity. *J. Biomed. Mater. Res.* 2006, *78*, 121–128.
46. Porter, A.E.; Rea, S.M.; Galtrey, M.; Best, S.M.; Barber, Z.H. Production of thin film silicon-doped hydroxyapatite via sputter deposition. *J. Mater. Sci.* 2004, *39*, 1895–1898.
47. Huang, T.; Xiao, Y.; Wang, S.; Huang, Y.; Liu, X.; Wu, F.; Gu, Z. Nanostructured Si, Mg, CO₃²⁻ substituted hydroxyapatite coatings deposited by liquid precursor plasma spraying: Synthesis and characterization. *J. Therm. Spray Technol.* 2011, *20*, 829–836.
48. Thian, E.S.; Huang, J.; Best, S.M.; Barber, Z.H.; Bonfield, W. Silicon-substituted hydroxyapatite: The next generation of bioactive coatings. *Mater. Sci. Eng.* 2007, *27*, 251–256.
49. Xiao, F.J.; Peng, L.; Zhang, Y.; Yun, L.J. Silicon-substituted hydroxyapatite composite coating by using vacuum-plasma spraying and its interaction with human serum albumin. *J. Mater. Sci. Mater. Med.* 2009, *20*, 1653–1658.
50. Gomes, P.S.; Botelho, C.; Lopes, M.A.; Santos, J.D.; Fernandes, M.H. Evaluation of human osteoblastic cell response to plasma-sprayed silicon-substituted hydroxyapatite coatings over titanium substrates. *J. Biomed. Mater. Res. Appl. Biomater.* 2010, *94*, 337–346.
51. Gomes, P.; Botelho, C.; Lopes, M.; Santos, J.; Fernandes, M. Effect of silicon-containing hydroxyapatite coating on human *in vitro* osteoblastic response. *Bone* 2009, *44* (supplement 2), s267.
52. Thian, E.S.; Best, S.M. *Thin Calcium Phosphate Coatings for Medical Implants*; Springer-Verlag New York, USA, 2009; p. 199.
53. Toft Vestermarck, M; Strontium in the bone-implant interface. *DanMed. Bull.*, 2011 May, *58*(5):B4286.
54. Xue, W.; Hosick, H.L.; Bandyopadhyay, A.; Bose, S.; Ding, C.; Luk, K.D.K.; Cheung, K.M.C.; Lu, W.W. Preparation and cell-materials interactions of plasma sprayed strontium-containing hydroxyapatite coating. *Surf. Coatings Technol.* 2007, *201*, 4685–4693.
55. Mihailescu, I.N.; Ristoscu, C.; Bigi, A.; Mayer, I. *Laser-Surface Interactions for New Materials Production*; Series: Springer series in Material Science, 2010; Vol. 130, p. 235–260.
56. Capuccini, C.; Torricelli, P.; Sima, F.; Boanini, E.; Ristoscu, C.; Bracci, B.; Socol, G.; Fini, M.; Mihailescu, I.N.; Bigi, A. Strontium-substituted hydroxyapatite coatings synthesized by pulsed-laser deposition: *In vitro* osteoblast and osteoclast response. *Acta Biomater.* 2008, *4*, 1885–1893.
57. Bigi, A.; Boanini, E.; Capuccini, C.; Fini, M.; Mihailescu, I.N.; Ristoscu, C.; Sima, F.; Torricelli, P. Biofunctional alendronate-Hydroxyapatite thin films deposited by Matrix Assisted Pulsed Laser Evaporation. *Biomaterials* 2009, *30*, 6168–6177.

58. Rau, J.V.; Generosi, A.; Laureti, S.; Komlev, V.S.; Ferro, D.; Cesaro, S.N.; Paci, B.; Albertini, V.R.; Agostinelli, E.; Barinov, S.M. Physicochemical investigation of pulsed laser deposited carbonated hydroxyapatite films on titanium. *ACS Appl. Mater. Interf.* 2009, *1*, 1813–1820.
59. Ding, L.; Zheng, Y.; Wan, Q.B.; Pei, X.B.; Chen, S.Y. Fluoridated hydroxyapatite/carbon nanotubes composite coating fabricated by radio frequency magnetron sputtering. *Mater. Sci. Forum* 2011, *675–677*, 869–871.
60. Rau, J.V.; Smirnov, V.V.; Laureti, S.; Generosi, A.; Varvaro, G.; Fosca, M.; Ferro, D.; Cesaro, S.N.; Albertini, V.R.; Barinov, S.M. Properties of pulsed laser deposited fluorinated hydroxyapatite films on titanium. *Mater. Res. Bull.* 2012 *45*, 1304–1310.
61. Yang, C.; Liu, F.; Ren, S.; Yang, G. Microstructure and magnetic properties of a two-phase alloy of α -Fe and metastable Fe₃B. *J. Magn. Magn. Mater.* 2009, *321*, 91–94.
62. Wang, G.; Zreiqat, H. Functional coatings or films for hard-tissue applications. *Materials* 2010, *3*, 3994–4050.
63. Bai, X.; More, K.; Rouleau, C.M.; Rabiei, A. Functionally graded hydroxyapatite coatings doped with antibacterial components. *Acta Biomater.* 2010, *6*, 2264–2273.
64. Simchi, A.; Tamjid, E.; Pishbin, F.; Boccaccini, A.R. Recent progress in inorganic and composite coatings with bactericidal capability for orthopaedic applications. *Nanomed. Nanotechnol. Biol. Med.* 2011, *7*, 22–39.
65. Feng, Q.L.; Kim, T.N.; Wu, J.; Park, E.S.; Kim, J.O.; Lim, D.Y.; Cui, F.Z. Antibacterial effects of Ag-HAp thin films on alumina substrates. *Thin Solid Films* 1998, *335*, 214–219.
66. Chen, Y.; Zheng, X.; Xie, Y.; Ji, H.; Ding, C.; Li, H.; Dai, K. Silver release from silver-containing hydroxyapatite coatings. *Surf. Coatings Technol.* 2010, *205*, 1892–1896.
67. Shimazaki, T.; Miyamoto, H.; Ando, Y.; Noda, I.; Yonekura, Y.; Kawano, S.; Miyazaki, M.; Mawatari, M.; Hotokebuchi, T. *In vivo* antibacterial and silver-releasing properties of novel thermal sprayed silver-containing hydroxyapatite coating. *J. Biomed. Mater. Res. Appl. Biomater.* 2010, *92*, 386–389.
68. de Jonge, L.T.; Leeuwenburgh, S.C.; Wolke, J.G.; Jansen, J.A. Organic-inorganic surface modifications for titanium implant surfaces. *Pharm. Res.* 2008, *25*, 2357–2369.
69. Lynch, S.E.; Buser, D.; Hernandez, R.A.; Weber, H.P.; Stich, H.; Fox, C.H.; Williams, R.C. Effects of the platelet-derived growth factor/insulin-like growth factor-I combination on bone regeneration around titanium dental implants. Results of a pilot study in beagle dogs. *J. Periodontol.* 1991, *62*, 710–716.
70. Sumner, D.R.; Turner, T.M.; Purchio, A.F.; Gombotz, W.R.; Urban, R.M.; Galante, J.O. Enhancement of bone ingrowth by transforming growth factor- β . *J. Bone Jt. Surg. Ser.* 1995, *77*, 1135–1147.
71. Puleo, D.A. Biochemical surface modification of Co-Cr-Mo. *Biomaterials* 1996, *17*, 217–222.

72. Endo, K. Chemical modification of metallic implant surfaces with biofunctional proteins (Part 1). Molecular structure and biological activity of a modified NiTi alloy surface. *Dent. Mater. J.* 1995, *14*, 185–198.
73. Nanci, A.; Wuest, J.D.; Peru, L.; Brunet, P.; Sharma, V.; Zalzal, S.; McKee, M.D. Chemical modification of titanium surfaces for covalent attachment of biological molecules. *Can. Assoc. Radiol. J.* 1998, *49*, 324–335.
74. Schliephake, H.; Scharnweber, D. Chemical and biological functionalization of titanium for dental implants. *J. Mater. Chem.* 2008, *18*, 2404–2414.
75. Nijhuis, A.W.G.; Leeuwenburgh, S.C.G.; Jansen, J.A. Wet-Chemical deposition of functional coatings for bone implantology. *Macromol. Biosci.* 2010, *10*, 1316–1329.
76. Pierschbacher, M.D.; Ruoslahti, E. Cell attachment activity of fibronectin can be duplicated by small synthetic fragments of the molecule. *Nature* 1984, *309*, 30–33.
77. Shin, H.; Jo, S.; Mikos, A.G. Biomimetic materials for tissue engineering. *Biomaterials* 2003, *24*, 4353–4364.
78. Morra, M. Biochemical modification of titanium surfaces: Peptides and ECM proteins. *Eur. Cell Mater.* 2006, *12*, 1–15.
79. Elmengaard, B.; Bechtold, J.E.; Soballe, K. *In vivo* effects of RGD-coated titanium implants inserted in two bone-gap models. *J. Biomed. Mater. Res.* 2005, *75*, 249–255.
80. Schliephake, H.; Scharnweber, D.; Dard, M.; Sewing, A.; Aref, A.; Roessler, S. Functionalization of dental implant surfaces using adhesion molecules. *J. Biomed. Mater. Res. Appl. Biomater.* 2005, *73*, 88–96.
81. Roessler, S.; Born, R.; Scharnweber, D.; Worch, H.; Sewing, A.; Dard, M. Biomimetic coatings functionalized with adhesion peptides for dental implants. *J. Mater. Sci. Mater. Med.* 2001, *12*, 871–877.
82. Massia, S.P.; Hubbell, J.A. An RGD spacing of 440 nm is sufficient for integrin alpha V beta 3-mediated fibroblast spreading and 140 nm for focal contact and stress fiber formation. *J. Cell Biol.* 1991, *114*, 1089–1100.
83. LeBaron, R.G.; Athanasiou, K.A. Extracellular matrix cell adhesion peptides: Functional applications in orthopedic materials. *Tissue Eng.* 2000, *6*, 85–103.
84. Sreejalekshmi, K.G.; Nair, P.D. Biomimeticity in tissue engineering scaffolds through synthetic peptide modifications Altering chemistry for enhanced biological response. *J. Biomed. Mater. Res. Part A* 2010, *96*, 477–491.
85. Solheim, E. Growth factors in bone. *Int. Orthop.* 1998, *22*, 410–416.
86. Hall, J.; Sorensen, R.G.; Wozney, J.M.; Wikesjo, U.M. Bone formation at rhBMP-2-coated titanium implants in the rat ectopic model. *J. Clin. Periodontol.* 2007, *34*, 444–451.
87. Siebers, M.C.; Walboomers, X.F.; Leeuwenburgh, S.C.; Wolke, J.C.; Boerman, O.C.; Jansen, J.A. Transforming growth factor-beta1 release from a porous electrostatic spray deposition-derived calcium phosphate coating. *Tissue Eng.* 2006, *12*, 2449–2456.
88. de Jonge, L.T.; van den Beucken, J.J.J.P.; Leeuwenburgh, S.C.G.; Hamers, A.A.J.; Wolke, J.G.C.; Jansen, J.A. *In vitro* responses to electrosprayed alkaline

- phosphatase/calcium phosphate composite coatings. *Acta Biomater.* 2009, 5, 2773–2782.
89. Anselme, K. Osteoblast adhesion on biomaterials. *Biomaterials* 2000, 21, 667–681.
 90. Morra, M.; Cassinelli, C.; Cascardo, G.; Cahalan, P.; Cahalan, L.; Fini, M.; Giardino, R. Surface engineering of titanium by collagen immobilization. Surface characterization and *in vitro* and *in vivo* studies. *Biomaterials* 2003, 24, 4639–4654.
 91. Schliephake, H.; Scharnweber, D.; Dard, M.; Robetaler, S.; Sewing, A.; Hutmacher, C. Biological performance of biomimetic calcium phosphate coating of titanium implants in the dog mandible. *J. Biomed. Mater. Res.* 2003, 64, 225–234.
 92. Wahl, D.A.; Czernuszka, J.T. Collagen-hydroxyapatite composites for hard tissue repair. *Eur. Cell Mater.* 2006, 11, 43–56.
 93. de Jonge, L.T.; Leeuwenburgh, S.C.; van den Beucken, J.J.; te Riet, J.; Daamen, W.F.; Wolke, J.G.; Scharnweber, D.; Jansen, J.A. The osteogenic effect of electrosprayed nanoscale collagen/calcium phosphate coatings on titanium. *Biomaterials* 2010, 31, 2461–2469.
 94. Fischer, U.; Hempel, U.; Becker, D.; Bierbaum, S.; Scharnweber, D.; Worch, H.; Wenzel, K.W. Transforming growth factor beta1 immobilized adsorptively on Ti6Al4V and collagen type I coated Ti6Al4V maintains its biological activity. *Biomaterials* 2003, 24, 2631–2641.
 95. Cole, B.J.; Bostrom, M.P.; Pritchard, T.L.; Sumner, D.R.; Tomin, E.; Lane, J.M.; Weiland, A.J. Use of bone morphogenetic protein 2 on ectopic porous coated implants in the rat. *Clin. Orthop. Relat. Res.* 1997, 15, 219–228.
 96. Herr, G.; Hartwig, C.H.; Boll, C.; Kusswetter, W. Ectopic bone formation by composites of BMP and metal implants in rats. *Acta Orthop. Scand.* 1996, 67, 606–610.
 97. Liu, Y.; Hunziker, E.B.; Layrolle, P.; de Bruijn, J.D.; de Groot, K. Bone morphogenetic protein 2 incorporated into biomimetic coatings retains its biological activity. *Tissue Eng.* 2004, 10, 101–108.
 98. Liu, Y.; Huse, R.O.; de Groot, K.; Buser, D.; Hunziker, E.B. Delivery mode and efficacy of BMP-2 in association with implants. *J. Dent. Res.* 2007, 86, 84–89.
 99. Liu, Y.; Hunziker, E.B.; Layrolle, P.; de Bruijn, J.D.; de Groot, K. Bone morphogenetic protein 2 incorporated into biomimetic coatings retains its biological activity. *Tissue Eng.* 2004, 10, 101–108.
 100. Uludag, H.; Gao, T.; Porter, T.J.; Friess, W.; Wozney, J.M. Delivery systems for BMPs: Factors contributing to protein retention at an application site. *J. Bone Jt. Surg. Am.* 2001, 83, S128–S135.
 101. Uludag, H.; D’Augusta, D.; Palmer, R.; Timony, G.; Wozney, J. Characterization of rhBMP-2 pharmacokinetics implanted with biomaterial carriers in the rat ectopic model. *J. Biomed. Mater. Res.* 1999, 46, 193–202.
 102. Ewald, A.; Hösel, D.; Patel, S.; Grover, L.M.; Barralet, J.E.; Gbureck, U. Silver-doped calcium phosphate cements with antimicrobial activity. *Acta Biomater.* 2011, 7, 4064–4070.

103. Zhao, L.; Chu, P.K.; Zhang, Y.; Wu, Z. Antibacterial coatings on titanium implants. *J. Biomed. Mater. Res. Appl. Biomater.* 2009, *91*, 470–480.
104. Jahoda, D.; Nyc, O.; Pokorný, D.; Landor, I.; Sosna, A. Antibiotic treatment for prevention of infectious complications in joint replacement. *Acta Chir. Orthop. Traumatol. Cech.* 2006, *73*, 108–114.
105. Alt, V.; Bitschnau, A.; Osterling, J.; Sewing, A.; Meyer, C.; Kraus, R.; Meissner, S.A.; Wenisch, S.; Domann, E.; Schnettler, R. The effects of combined gentamicin-hydroxyapatite coating for cementless joint prostheses on the reduction of infection rates in a rabbit infection prophylaxis model. *Biomaterials* 2006, *27*, 4627–4634.
106. Campbell, A.A.; Song, L.; Li, X.S.; Nelson, B.J.; Bottoni, C.; Brooks, D.E.; DeJong, E.S. Development, characterization, and anti-microbial efficacy of hydroxyapatite-chlorhexidine coatings produced by surface-induced mineralization. *J. Biomed. Mater. Res.* 2000, *53*, 400–407.
107. Morra, M.; Cassinelli, C.; Cascardo, G.; Carpi, A.; Fini, M.; Giavaresi, G.; Giardino, R. Adsorption of cationic antibacterial on collagen-coated titanium implant devices. *Biomed. Pharmacother.* 2004, *58*, 418–422.
108. Kim, W.-H.; Lee, S.-B.; Oh, K.-T.; Moon, S.-K.; Kim, K.-M.; Kim, K.-N. The release behavior of CHX from polymer-coated titanium surfaces. *Surf. Interf. Anal.* 2008, *40*, 202–204.
109. Harris, L.G.; Mead, L.; Muller-Oberlander, E.; Richards, R.G. Bacteria and cell cytocompatibility studies on coated medical grade titanium surfaces. *J. Biomed. Mater. Res.* 2006, *78*, 50–58.
110. Kozlovsky, A.; Artzi, Z.; Moses, O.; Kamin-Belsky, N.; Greenstein, R.B. Interaction of chlorhexidine with smooth and rough types of titanium surfaces. *J. Periodontol.* 2006, *77*, 1194–1200.
111. Barbour, M.E.; O'Sullivan, D.J.; Jagger, D.C. Chlorhexidine adsorption to anatase and rutile titanium dioxide. *Coll. Surf. Physicochem. Eng. Asp.* 2007, *307*, 116–120.
112. Darouiche, R.O.; Green, G.; Mansouri, M.D. Antimicrobial activity of antiseptic-coated orthopaedic devices. *Int. J. Antimicrob. Agents* 1998, *10*, 83–86.
113. Jonathan, P.; Nazhat, S.N.; Blaker, J.J.; Boccaccini, A.R. In *Vitro Attachment of Staphylococcus Epidermidis to Surgical Sutures with and without Ag-Containing Bioactive Glass Coating*; Sage: London, UK, 2004; Volume 19, p. 11.
114. Roy, M.; Bandyopadhyay, A.; Bose, S. *In vitro* antimicrobial and biological properties of laser assisted tricalcium phosphate coating on titanium for load bearing implant. *Mater. Sci. Eng.* 2009, *29*, 1965–1968.
115. Roelofs, A.J.; Thompson, K.; Gordon, S.; Rogers, M.J. Molecular mechanisms of action of bisphosphonates: Current status. *Clin. Cancer Res.* 2006, *12*, 6222s–6230s.
116. van beek, E.; Lowik, C.; van der Pluijm, G.; Papapoulos, S. The role of geranylgeranylation in bone resorption and its suppression by bisphosphonates in fetal bone explants in vitro: A clue to the mechanism of action of nitrogen-containing bisphosphonates. *J. Bone Miner. Res.* 1999, *14*, 722–729.

117. Wysowski, D.K. Reports of esophageal cancer with oral bisphosphonate use. *Mass. Med. Soc.* 2009, 360, 89–90.
118. Marx, R.E. Oral and intravenous bisphosphonate-induced osteonecrosis of the jaws. *J. Oral Maxillofac. Surg.* 2007, 65, 2397–2410.
119. Denissen, H.; van Beek, E.; Lowik, C.; Papapoulos, S.; van Den Hooff, A. Ceramic hydroxyapatite implants for the release of bisphosphonate. *Bone Miner.* 1994, 25, 123–134.
120. Seshima, H.; Yoshinari, M.; Takemoto, S.; Hattori, M.; Kawada, E.; Inoue, T.; Oda, Y. Control of bisphosphonate release using hydroxyapatite granules. *J. Biomed. Mater. Res. Appl. Biomater.* 2006, 78, 215–221.
121. Boanini, E.; Torricelli, P.; Gazzano, M.; Giardino, R.; Bigi, A. Alendronate-hydroxyapatite nanocomposites and their interaction with osteoclasts and osteoblast-like cells. *Biomaterials* 2008, 29, 790–796.
122. Peter, B.; Pioletti, D.P.; Laib, S.; Bujoli, B.; Pilet, P.; Janvier, P.; Guicheux, J.; Zambelli, P.Y.; Bouler, J.M.; Gauthier, O. Calcium phosphate drug delivery system: Influence of local zoledronate release on bone implant osteointegration. *Bone* 2005, 36, 52–60.
123. Yang, Y.; Kim, K.-H.; Ong, J.L. A review on calcium phosphate coatings produced using a sputtering process an alternative to plasma spraying. *Biomaterials* 2005, 26, 327–337.
124. Huang, Y.; Qu, Y.; Yang, B.; Li, W.; Zhang, B.; Zhang, X. *In vivo* biological responses of plasma sprayed hydroxyapatite coatings with an electric polarized treatment in alkaline solution. *Mater. Sci. Eng.* 2009, 29, 2411–2416.
125. Wu, G.M.; Hsiao, W.D.; Kung, S.F. Investigation of hydroxyapatite coated polyether ether ketone composites by gas plasma sprays. *Surf. Coatings Technol.* 2009, 203, 2755–2758.
126. Kozerski, S.; Pawlowski, L.; Jaworski, R.; Roudet, F.; Petit, F. Two zones microstructure of suspension plasma sprayed hydroxyapatite coatings. *Surf. Coatings Technol.* 2010, 204, 1380–1387.
127. d’Haese, R.; Pawlowski, L.; Bigan, M.; Jaworski, R.; Martel, M. Phase evolution of hydroxapatite coatings suspension plasma sprayed using variable parameters in simulated body fluid. *Surf. Coatings Technol.* 2010, 204, 1236–1246.
128. Cao, N.; Dong, J.; Wang, Q.; Ma, Q.; Xue, C.; Li, M. An experimental bone defect healing with hydroxyapatite coating plasma sprayed on carbon/carbon composite implants. *Surf. Coatings Technol.* 2010, 205, 1150–1156.
129. Noda, I.; Miyaji, F.; Ando, Y.; Miyamoto, H.; Shimazaki, T.; Yonekura, Y.; Miyazaki, M.; Mawatari, M.; Hotokebuchi, T. Development of novel thermal sprayed antibacterial coating and evaluation of release properties of silver ions. *J. Biomed. Mater. Res. Appl. Biomater.* 2009, 89, 456–465.

130. Hong, Z.; Mello, A.; Yoshida, T.; Luan, L.; Stern, P.H.; Rossi, A.; Ellis, D.E.; Ketterson, J.B. Osteoblast proliferation on hydroxyapatite coated substrates prepared by right angle magnetron sputtering. *J. Biomed. Mater. Res.* 2010, *93*, 878–885.
131. Jelinek, M.; Weiserova, M.; Kocourek, T.; Zezulova, M.; Strnad, J. Biomedical properties of laser prepared silver-doped hydroxyapatite. *Laser Phys.* 2011, *21*, 1265–1269.
132. Jelinek, M.; Kocourek, T.; Jurek, K.; Remsa, J.; Mikšovský, J.; Weiserova, M.; Strnad, J.; Luxbacher, T. Antibacterial properties of Ag-doped hydroxyapatite layers prepared by PLD method. *Appl. Phys. Mater. Sci. Proc.* 2010, *101*, 615–620.
133. Koch, C.F.; Johnson, S.; Kumar, D.; Jelinek, M.; Chrisey, D.B.; Doraiswamy, A.; Jin, C.; Narayan, R.J.; Mihailescu, I.N. Pulsed laser deposition of hydroxyapatite thin films. *Mater. Sci. Eng.* 2007, *27*, 484–494.
134. Vasanthan, A.; Kim, H.; Drukteinis, S.; Lacefield, W. Implant surface modification using laser guided coatings: *In vitro* comparison of mechanical properties. *J. Prosthodont.* 2008, *17*, 357–364.
135. Man, H.C.; Chiu, K.Y.; Cheng, F.T.; Wong, K.H. Adhesion study of pulsed laser deposited hydroxyapatite coating on laser surface nitrided titanium. *Thin Solid Films* 2009, *517*, 5496–5501.
136. Yang, S.; Xing, W.; Man, H.C. Pulsed laser deposition of hydroxyapatite film on laser gas nitriding NiTi substrate. *Appl. Surf. Sci.* 2009, *255*, 9889–9892.
137. Socol, G.; Macovei, A.M.; Miroiu, F.; Stefan, N.; Duta, L.; Dorcioman, G.; Mihailescu, I.N.; Petrescu, S.M.; Stan, G.E.; Marcov, D.A.; *et al.* Hydroxyapatite thin films synthesized by pulsed laser deposition and magnetron sputtering on PMMA substrates for medical applications. *Mater. Sci. Eng. Solid-State Mater. Adv. Technol.* 2010, *169*, 159–168.
138. Rajesh, P.; Muraleedharan, C.V.; Komath, M.; Varma, H. Pulsed laser deposition of hydroxyapatite on titanium substrate with titania interlayer. *J. Mater. Sci. Mater. Med.* 2011, *22*, 497–505.
139. Zeng, H.; Lacefield, W.R.; Mirov, S. Structural and morphological study of pulsed laser deposited calcium phosphate bioceramic coatings: Influence of deposition conditions, laser parameters, and target properties. *J. Biomed. Mater. Res.* 2000, *50*, 248–258.
140. Garcia-Sanz, F.J.; Mayor, M.B.; Arias, J.L.; Pou, J.; Lean, B.; Perez-Amor, M. Hydroxyapatite coatings: A comparative study between plasma-spray and pulsed laser deposition techniques. *J. Mater. Sci. Mater. Med.* 1997, *8*, 861–865.
141. Choi, J.M.; Kim, H.E.; Lee, I.S. Ion-beam-assisted deposition (IBAD) of hydroxyapatite coating layer on Ti-based metal substrate. *Biomaterials* 2000, *21*, 469–473.
142. Luo, Z.S.; Cui, F.Z.; Feng, Q.L.; Li, H.D.; Zhu, X.D.; Spector, M. *In vitro* and *in vivo* evaluation of degradability of hydroxyapatite coatings synthesized by ion beam-assisted deposition. *Surf. Coatings Technol.* 2000, *131*, 192–195.
143. Kim, T.N.; Feng, Q.L.; Luo, Z.S.; Cui, F.Z.; Kim, J.O. Highly adhesive hydroxyapatite coatings on alumina substrates prepared by ion-beam assisted deposition. *Surf. Coatings Technol.* 1998, *99*, 20–23.

144. Coelho, P.G.; Lemons, J.E. Physico/chemical characterization and *in vivo* evaluation of nanothickness bioceramic depositions on alumina-blasted/acid-etched Ti-6Al-4V implant surfaces. *J. Biomed. Mater. Res.* 2009, *90*, 351–361.
145. Rabiei, A.; Thomas, B.; Jin, C.; Narayan, R.; Cuomo, J.; Yang, Y.; Ong, J.L. A study on functionally graded HA coatings processed using ion beam assisted deposition with *in situ* heat treatment. *Surf. Coatings Technol.* 2006, *200*, 6111–6116.
146. Coelho, P.G.; Cardaropoli, G.; Suzuki, M.; Lemons, J.E. Histomorphometric evaluation of a nanothickness bioceramic deposition on endosseous implants: A study in dogs. *Clin. ImplantDent. Relat. Res.* 2009, *11*, 292–302.
147. Kim, H.; Choi, S.H.; Chung, S.M.; Li, L.H.; Lee, I.S. Enhanced bone forming ability of SLA-treated Ti coated with a calcium phosphate thin film formed by e-beam evaporation. *Biomed. Mater.* 2009, *5*, 044106.
148. Lee, I.S.; Whang, C.N.; Kim, H.E.; Park, J.C.; Song, J.H.; Kim, S.R. Various Ca/P ratios of thin calcium phosphate films. *Mater. Sci. Eng.* 2002, *22*, 15–20.
149. Rautray, T.R.; Narayanan, R.; Kwon, T.Y.; Kim, K.H. Surface modification of titanium and titanium alloys by ion implantation. *J. Biomed. Mater. Res. Appl. Biomater.* 2011, *93*, 581–591.
150. Yang, J.X.; Jiao, Y.P.; Cui, F.Z.; Lee, I.S.; Yin, Q.S.; Zhang, Y. Modification of degradation behavior of magnesium alloy by IBAD coating of calcium phosphate. *Surf. Coatings Technol.* 2008, *202*, 5733–5736.
151. Krout, A.; Wen, H.B.; Hippensteel, E.; Li, P. A hybrid coating of biomimetic apatite and osteocalcin. *J. Biomed. Mater. Res.* 2005, *73*, 377–387.
152. Chen, C.; Lee, I.-S.; Zhang, S.-M.; Yang, H.C. Biomimetic apatite formation on calcium phosphate-coated titanium in Dulbecco's phosphate-buffered saline solution containing CaCl_2 with and without fibronectin. *Acta Biomater.* 2010, *6*, 2274–2281.
153. Ryu, H.S.; Hong, S.-H. Hybrid coatings of poly(L-lysine) and apatite on micro-arc oxidized titania. *Mater. Lett.* 2009, *63*, 2107–2110.
154. Liu, Y.; de Groot, K.; Hunziker, E.B. BMP-2 liberated from biomimetic implant coatings induces and sustains direct ossification in an ectopic rat model. *Bone* 2005, *36*, 745–757.
155. Ishibe, T.; Goto, T.; Kodama, T.; Miyazaki, T.; Kobayashi, S.; Takahashi, T. Bone formation on apatite-coated titanium with incorporated BMP-2/heparin *in vivo*. *Oral Surg. Oral Med. Oral Pathol. Oral Radiol. Endod.* 2009, *108*, 867–875.
156. Leivo, J.; Meretoja, V.; Vippola, M.; Levanen, E.; Vallittu, P.; Mantyla, T.A. Sol-gel derived aluminosilicate coatings on alumina as substrate for osteoblasts. *Acta Biomater.* 2006, *2*, 659–668.
157. Cheng, K.; Weng, W.; Wang, H.; Zhang, S. *In vitro* behavior of osteoblast-like cells on fluoridated hydroxyapatite coatings. *Biomaterials* 2005, *26*, 6288–6295.
158. Balamurugan, A.; Rebelo, A.H.S.; Lemos, A.F.; Rocha, J.H.G.; Ventura, J.M.G.; Ferreira, J.M.F. Suitability evaluation of sol-gel derived Si-substituted hydroxyapatite

- for dental and maxillofacial applications through in vitro osteoblasts response. *Dent. Mater.* 2008, 24, 1374–1380.
159. Liu, J.; Miao, X. Sol-gel derived bioglass as a coating material for porous alumina scaffolds. *Ceram. Int.* 2004, 30, 1781–1785.
160. Fathi, M.H.; Doost Mohammadi, A. Preparation and characterization of sol-gel bioactive glass coating for improvement of biocompatibility of human body implant. *Mater. Sci. Eng.* 2008, 474, 128–133.
161. Mirhosseini, N.; Crouse, P.L.; Li, L.; Garrod, D. Combined laser/sol-gel synthesis of calcium silicate coating on Ti6Al4V substrates for improved cell integration. *Appl. Surf. Sci.* 2007, 253, 7998–8002.
162. Pang, X.; Casagrande, T.; Zhitomirsky, I. Electrophoretic deposition of hydroxyapatite-CaSiO₃-chitosan composite coatings. *J. Coll. Interf. Sci.* 2009, 330, 323–329.
163. Sun, F.; Pang, X.; Zhitomirsky, I. Electrophoretic deposition of composite hydroxyapatite-chitosan-heparin coatings. *J. Mater. Proc. Technol.* 2009, 209, 1597–1606.
164. Grandfield, K.; Zhitomirsky, I. Electrophoretic deposition of composite hydroxyapatite-silica-chitosan coatings. *Mater. Charact.* 2008, 59, 61–67.
165. Schouten, C.; Meijer, G.J.; van den Beucken, J.J.J.P.; Leeuwenburgh, S.C.G.; de Jonge, L.T.; Wolke, J.G.C.; Spauwen, P.H.M.; Jansen, J.A. *In vivo* bone response and mechanical evaluation of electrosprayed CaP nanoparticle coatings using the iliac crest of goats as an implantation model. *Acta Biomater.* 2010, 6, 2227–2236.
166. Leeuwenburgh, S.C.G.; Wolke, J.G.C.; Siebers, M.C.; Schoonman, J.; Jansen, J.A. *In vitro* and *in vivo* reactivity of porous, electrosprayed calcium phosphate coatings. *Biomaterials* 2006, 27, 3368–3378.
167. Iafisco, M.; Bosco, R.; Leeuwenburgh, S.C.G.; van den Beucken, J.J.J.P.; Jansen, J.A.; Prat, M.; Roveri, N. Electrostatic spray deposition of biomimetic nanocrystalline apatite coatings onto titanium. *Adv. Eng. Mater.* 2012, 14, B13–B20.
168. de Jonge, L.T.; Leeuwenburgh, S.C.G.; van den Beucken, J.J.J.P.; Wolke, J.G.C.; Jansen, J.A. Electrosprayed enzyme coatings as bioinspired alternatives to bioceramic coatings for orthopedic and oral implants. *Adv. Funct. Mater.* 2009, 19, 755–762.
169. Alghamdi, H.S.; van Oirschot, B.; Bosco, R.; den Beucken, J.J.J.P.; Aldosari, A.A.F.; Anil, S.; Jansen, J.A. Biological response to titanium implants coated with nanocrystals calcium phosphate or type 1 collagen in a dog model. *Clin. Oral Implant. Res.* 2012, doi:10.1111/j.1600-0501.2011.02409.x.
170. Gross, K.A.; Saber-Samandari, S. Revealing mechanical properties of a suspension plasma sprayed coating with nanoindentation. *Surf. Coatings Technol.* 2009, 203, 2995–2999.
171. Huang, Y.; Song, L.; Liu, X.; Xiao, Y.; Wu, Y.; Chen, J.; Wu, F.; Gu, Z. Hydroxyapatite coatings deposited by liquid precursor plasma spraying: Controlled dense and porous microstructures and osteoblastic cell responses. *Biofabrication* 2010, 2, 045003.
172. Sobieszczyk, S.; Zielinski A.: Coatings in arthroplasty. *Adv. Mater. Sci.* 2008, 8, 35–54.
173. Khor, K.A.; Li, H.; Cheang, P. Significance of melt-fraction in HVOF sprayed hydroxyapatite particles, splats and coatings. *Biomaterials* 2004, 25, 1177–1186.

174. Morks, M.F.; Fahim, N.F.; Kobayashi, A. Structure, mechanical performance and electrochemical characterization of plasma sprayed SiO₂/Ti-reinforced hydroxyapatite biomedical coatings. *Appl. Surf. Sci.* 2008, 255, 3426–3433.
175. Hasan, S.; Stokes, J. Design of experiment analysis of the Sulzer Metco DJ high velocity oxy-fuel coating of hydroxyapatite for orthopedic applications. *J. Therm. Spray Technol.* 2010, 20, 186–194.
176. Morks, M.F. Fabrication and characterization of plasma-sprayed HA/SiO₂ coatings for biomedical application. *J. Mech. Behav. Biomed. Mater.* 2008, 1, 105–111.
177. Morks, M.F.; Kobayashi, A.; Fahim, N.F. Abrasive wear behavior of sprayed hydroxyapatite coatings by gas tunnel type plasma spraying. *Wear* 2007, 262, 204–209.
178. Heimann, R.B. Thermal spraying of biomaterials. *Surf. Coatings Technol.* 2006, 201, 2012–2019.
179. Lima, R.S.; Dimitrievska, S.; Bureau, M.N.; Marple, B.R.; Petit, A.; Mwale, F.; Antoniou, J. HVOF-sprayed Nano TiO₂-HA coatings exhibiting enhanced biocompatibility. *J. Therm. Spray Technol.* 2010, 19, 336–343.
180. Yamashita, K.; Arashi, T.; Kitagaki, K.; Yamada, S.; Umegaki, T.; Ogawa, K. Preparation of apatite thin films through rf-sputtering from calcium phosphate glasses. *J. Am. Ceram. Soc.* 1994, 77, 2401–2407.
181. van Der Wal, E.; Oldenburg, S.J.; Heij, T.; Denier van Der Gon, A.W.; Brongersma, H.H.; Wolke, J.G.C.; Jansen, J.A.; Vredenberg, A.M. Adsorption and desorption of Ca and PO₄ species from SBFs on RF-sputtered calcium phosphate thin films. *Appl. Surf. Sci.* 2006, 252, 3843–3854.
182. Jansen, J.A.; Wolke, J.G.C.; Swann, S.; van Der Waerden, J.P.C.M.; de Groof, K. Application of magnetron sputtering for producing ceramic coatings on implant materials. *Clin. Oral Implants Res.* 1993, 4, 28–34.
183. van Dijk, K.; Schaeken, H.G.; Wolke, J.G.C.; Jansen, J.A. Influence of annealing temperature on RF magnetron sputtered calcium phosphate coatings. *Biomaterials* 1996, 17, 405–410.
184. van Dijk, K.; Schaeken, H.G.; Wolke, J.C.G.; Maree, C.H.M.; Habraken, F.H.P.M.; Verhoeven, J.; Jansen, J.A. Influence of discharge power level on the properties of hydroxyapatite films deposited on Ti6Al4V with RF magnetron sputtering. *J. Biomed. Mater. Res.* 1995, 29, 269–276.
185. Yang, J.; Cui, F.Z.; Lee, I.S.; Wang, X. Plasma surface modification of magnesium alloy for biomedical application. *Surf. Coatings Technol.* 2010, 205, S182–S187.
186. Cotell, C.M.; Chrisey, D.B.; Grabowski, K.S.; Sprague, J.A.; Gossett, C.R. Pulsed laser deposition of hydroxylapatite thin films on Ti-6Al-4V. *J. Appl. Biomater.* 1992, 3, 87–93.
187. Leon, B. *Pulsed Laser Deposition of Thin Calcium Phosphate Coatings*; Springer: New York, USA, 2009; p. 101.

188. Jedynski, M.; Hoffman, J.; Mroz, W.; Szymanski, Z. Plasma plume induced during ArF laser ablation of hydroxyapatite. *Appl. Surf. Sci.* 2008, *255*, 2230–2236.
189. Jelinek, M.; Weiserova, M.; Kocourek, T.; Zezulova, M.; Strnad, J. Biomedical properties of laser prepared silver-doped hydroxyapatite. *Laser Phys.* 2011, *21*, 1265–1269.
190. Mroz, V. Functional properties of nanostructured materials. *NATO Sci. Ser.* 2006, *223*, 183–196.
191. Johnson, S.; Haluska, M.; Narayan, R.J.; Snyder, R.L. *In situ* annealing of hydroxyapatite thin films. *Mater. Sci. Eng.* 2006, *26*, 1312–1316.
192. Junker, R.; Dimakis, A.; Thoneick, M.; Jansen, J.A. Effects of implant surface coatings and composition on bone integration: A systematic review. *Clin. Oral Implants Res.* 2009, *20*, 185–206.
193. Roy, M.; Bandyopadhyay, A.; Bose, S. Induction plasma sprayed nano hydroxyapatite coatings on titanium for orthopaedic and dental implants. *Surf. Coatings Technol.* 2011, *205*, 2785–2792.
194. Liu, X.; Chu, P.K.; Ding, C. Surface nano-functionalization of biomaterials. *Mater. Sci. Eng. Rep.* 2011, *70*, 275–302.
195. Kokubo, T.; Takadama, H. How useful is SBF in predicting *in vivo* bone bioactivity? *Biomaterials* 2006, *27*, 2907–2915.
196. Hench, L.L.; West, J.K. The sol-gel process. *Chem. Rev.* 1990, *90*, 33–72.
197. Paital, S.R.; Dahotre, N.B. Calcium phosphate coatings for bio-implant applications: Materials, performance factors, and methodologies. *Mater. Sci. Eng. Rep.* 2009, *66*, 1–70.
198. Kwok, C.T.; Wong, P.K.; Cheng, F.T.; Man, H.C. Characterization and corrosion behavior of hydroxyapatite coatings on Ti6Al4V fabricated by electrophoretic deposition. *Appl. Surf. Sci.* 2009, *255*, 6736–6744.
199. Stoch, A.; Brożek, A.; Kmita, G.; Stoch, J.; Jastrzębski, W.; Rakowska, A. Electrophoretic coating of hydroxyapatite on titanium implants. *J. Mol. Struct.* 2001, *596*, 191–200.
200. Siefert, W. Corona spray pyrolysis: A new coating technique with an extremely enhanced deposition efficiency. *Thin Solid Films* 1984, *120*, 267–274.
201. Wilhelm, O.; Mädler, L.; Pratsinis, S.E. Electrospray evaporation and deposition. *J. Aerosol. Sci.* 2003, *34*, 815–836.

Chapter III

Electrostatic Spray Deposition of Biomimetic Nanocrystalline Apatite Coating on Titanium

Ruggero Bosco*, Michele Iafisco*, Sander C. G. Leeuwenburgh, Jeroen J. J. P. van den Beucken, John A. Jansen, Maria Prat, and Norberto Roveri

Advanced Engineering Materials 14.3 (2012): B13-B20.

1. Introduction

Titanium and its alloys are widely used to manufacture orthopaedic and dental implants due to their excellent mechanical properties and corrosion resistance. However, these materials are bioinert since they do not initiate a response or an interaction with the host biological tissue. For this reason, the research has been directed his effort to the surface modification of these materials to improve bone implant contact and their biological properties [1].

Among the different materials used for this aim, the best way could be the application of a coating that replace the extracellular matrix (ECM) of bone, basically constituted of calcium phosphates, namely apatite (HA) nanocrystals [2]. The biological efficacy of calcium phosphates coating has been confirmed in numerous works, but the materials used in the last decades were ceramic calcium phosphates with several problems related to poor adhesion and limited osteoconductivity [3].

The mineral phase of bone and tooth consists of non-stoichiometric carbonated HA crystals having blade shape of approximately 100 nm width, 2-5 nm thickness and about 60 nm length [4]. Despite the large number of synthetic strategies to synthesize nanoapatites, the preparation of HA with similar physico-chemical and morphological characteristics to those of the bone mineral phase, still remains a technological challenge [5]. In fact, the biological properties of HA, such as lack of toxicity, biodegradability, biocompatibility, osteoinduction and osteointegration can be significantly increased by increase their similarity with the biogenic ones. This aim could be achieved trough the preparation of HA with nanometric dimensions, specific chemical-physical properties such as plate-shaped morphology, low crystallinity degree, non-stoichiometric composition, surface crystalline disorder and presence of carbonate ions in the crystal lattice [6]. So far, biomimetic HA coated titanium implants could be the most successful approach to overcome the problems connected to the use of ceramic based materials and improve the biological properties of the implants [7].

Among the different methods to deposit coatings, the electrostatic spray deposition (ESD) technique has received special attention since it is a simple, economical and scale-up technology and it is particularly interesting regarding deposition of coatings with controlled surface morphology and the use of low temperatures [8]. This latter is probably the main benefit of ESD, in fact it allows the preparation of coating at physiological conditions and moreover allows the simultaneous deposition of organic and inorganic compounds [9]. Briefly, the basic principle of ESD is the generation of a spray of charged, micron-sized droplets. This is accomplished by means of electrostatic atomization of precursor solutions. These spray droplets are directed towards a grounded substrate as a result of the applied potential difference. After complete solvent evaporation, a thin layer is left onto the substrate surface [8a, 10].

The aim of this work is the synthesis of biomimetic nanocrystalline HA and the evaluation of applicability of the ESD to deposit a nanostructured coating made nanocrystalline HA on titanium substrate at room temperature.

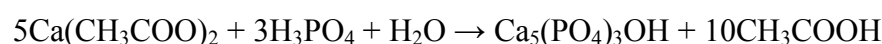
2. Experimental

2.1 Materials

Common high-purity chemical reagents were supplied from Sigma. Ultrapure water (0.22 mS, 25 °C) was used in all experiments.

2.2 Synthesis of apatite nanocrystals

Nanocrystalline apatite (HA) has been synthesised by dropping a solution of H₃PO₄ (0.21 M) into a Ca(CH₃COO)₂ suspension (0.35 M), keeping the pH at a constant value of 10 by addition of (NH₄)OH solution, to accomplish the following reaction:



The reaction mixture was kept under stirring at room temperature for 24 hours, then stirring was suspended and the mixture was left standing for 2 hours to allow deposition of the inorganic phase. This latter was repeatedly washed with water by centrifugation and freeze-dried at -60 °C under vacuum (3 mbar) overnight for the further characterizations.

2.3 Characterization of apatite nanocrystals

Specific surface area was measured with an ASAP 2010 (Micromeritics Ins. Corp., USA) by nitrogen adsorption at 77 K following the BET model (hereafter, SSA_{BET}).

The Ca/P ratio was determined by inductively coupled plasma-optical emission spectrometry (ICP-OES, Liberty 200, Varian, Clayton South, Australia). Samples were dissolved in 1% wt ultrapure nitric acid. The following analytical wavelengths were chosen: Ca 422 nm, P 213 nm.

The carbonate content was evaluated on dried samples by thermogravimetric analysis (TGA) investigations using a Thermal Analysis SDT Q 600 (TA Instruments, New Castle, DE, USA). Heating was performed in a nitrogen flow (100 ml min⁻¹) using an alumina sample

holder at a rate of 10 °C min⁻¹ up to 1200 °C. The weight of the samples was approximately 10 mg.

The infrared spectra were recorded in the wavelength range from 4000 cm⁻¹ to 400 cm⁻¹ with 2 cm⁻¹ resolution using a Thermo Nicolet 380 FT-IR spectrometer. A powdered sample (approximately 1 mg) was mixed with about 100 mg of anhydrous KBr. The mixture was pressed at 10 t pressure into 7 mm diameter discs. Pure KBr disk was used as blank. Decomposition of $\nu_3\text{CO}_3$ and $\nu_4\text{PO}_4$ was performed from FTIR spectra using GRAMS curve-fitting software.

X-ray diffraction (XRD) pattern of the powders were recorded with a Panalytical X'Pert Pro equipped with an X'Celerator detector powder diffractometer using Cu K α radiation generated at 40 kV and 40 mA. The instrument was configured with 1/2° divergence and receiving slits. A quartz sample holder was used. The 2 θ range was from 5° to 60° with a step size (°2 θ) of 0.05 and a counting time of 3 s.

The degree of HA crystallinity was calculated according to the formula (1):

$$\text{Crystallinity}[\%] = 100 \cdot \frac{C}{(A + C)} \quad (1)$$

where C was the area from the peaks in the diffraction pattern ("the crystalline area") and A was the area between the peaks and the background ("the amorphous area").

Crystal domain size along the HA axis directions were calculated applying Scherrer equation (2):

$$L_{(hkl)} = \frac{0.94\lambda}{\left[\cos \theta \left(\sqrt{\Delta r^2 - \Delta_0^2} \right) \right]} \quad (2)$$

where θ is the diffraction angle for plane (hkl), Δ_r and Δ_0 the widths in radians of reflection (hkl) at half height for the synthesized and pure inorganic hydroxyapatite (standard reference material, calcium hydroxyapatite, National Institute of Standards & Technology), respectively, and $\lambda=1.5405$ Å.

Electrophoretic determinations were performed by a Coulter DELSA apparatus. A Coulter DELSA 440 instrument measured the electrophoretic velocities of suspended particles by measuring the Doppler shift of scattered laser light simultaneously at four different scattering angles: 7.5, 15.0, 22.5 and 30.0°. The suspensions was prepared as follows: 0.05 g L⁻¹ of HA in 10⁻² M KNO₃ (constant ionic strength), at spontaneous constant pH.

High resolution transmission electron microscopy (HR-TEM) images of the materials (powder grains dispersed on lacey carbon Cu grids) were performed with a JEOL 3010-UHR with acceleration potential of 300 kV. As apatite samples might evolve under the electron beam, potentially leading to further crystallisation and/or to a loss of bulk water observations were carried out under feeble illumination conditions to avoid any modifications of the materials during the analysis.

2.4 Electrostatic spray deposition (ESD) process

Electrostatic spray deposition (ESD) was carried out using an innovative ESD device (ES-2000S, Fulence Co., Ltd., Japan). This apparatus allowed to use different set up and to have control among different parameters during deposition. A vertical ESD set-up was used in this work to deposit the inorganic coating. Machined, commercially pure (cp) Ti disks (Ø 5 mm, thickness 1.5) were used as substrates. The substrates were cleaned ultrasonically in acetone (15 minutes) and ethanol (15 minutes) prior to deposition. The distance between the nozzle (G21 (Ø 0,8 mm) stainless steel nozzle) and the substrate was varied at 20 mm and 40 mm and the temperature of samples fixed at 35 °C. A stable deposition was obtained by adjusting the potential between the nozzle and the target samples to values between 9.0 and 12.0 kV depending on the humidity selected. A laser beam was targeted to cross perpendicularly the edge of the nozzle to detect and confirm a stable cone-jet mode. The flow rate of the solution was 4 µl/min and deposition time was varied at 5, 15 and 30 minutes. Relative humidity in the

deposition chamber was varied, as well, at 20 % and 40 %. After deposition the samples were not heat-treated and air-dried.

2.5 Characterization of apatite suspension and coatings

Measurements of electrical conductivity was carried out using a portable conductivity meter (Cond 330i/SET, WTW, Germany).

Scanning Electron Microscopy (SEM) JEOL 6330 FESEM (3 kV, 12 mA) has been used to investigate the surface morphology of the coating.

X-ray diffraction (XRD) pattern of the coated samples were recorded with a Philips thin-film Panalytical X-Ray Diffractometer using Cu K α -radiation (PW3710, 40 kV, 30 mA). The coatings were analyzed by fixing the coated substrates to a position of 2.5° and scanning the detector between 20° to 50° ($^{\circ}2\theta$), with a step-size of 0.002° ($^{\circ}2\theta$), a scanning speed of 0.01 ($^{\circ}2\theta$ /s) and a sample time of 2 s/step.

The infrared spectra of the coating were recorded in the wavelength range from 4000 cm^{-1} to 400 cm^{-1} with 4 cm^{-1} resolution using a Spectrum One, Perkin-Elmer.

The amount of deposited calcium on the substrates was measured using the ortho-cresolphthalein (OCPC) method [11]. In brief, all substrates were incubated overnight in 1 ml of 0.5 N acetic acid on a shaker table. For analyses, 300 μl of work reagent was added to 10 μl aliquots of sample or standard in a 96-wells plate. The plate was incubated for 10 min at room temperature, after which the plate was read at 570 nm. Serial dilutions of CaCl_2 (0–100 $\mu\text{g ml}^{-1}$) were used for the standard curve. To evaluate the total amount of apatite deposited on samples, a standard curve have been established dissolving known amount of HA synthesized according to the method previously described.

3. Results and Discussion

3.1 Compositional and structural features of apatite nanocrystals

The code, composition, specific surface area (SSA) and ζ potential of the synthesized apatite (HA) are listed in Table 1. The bulk Ca/P ratio determined by ICP was slightly lower than the stoichiometric one (1.67), and a limited amount of carbonate groups (about 1 wt%), derived from dissolved CO₂ in the preparation media and from CO₂ adsorbed onto the materials surface during the storage, was present. The CO₂ amount was evaluated by thermogravimetric analysis (TGA), according to the weight loss occurred from 550°C to 950°C[12]. The presence of CO₂ in the structure of HA was intentionally retained, in order to better mimic the biological ones [13]. HA exhibited a high SSA in the 150-170 m² g⁻¹ range, which is in agreement with the nanometric size observed by TEM analysis.

Table 1. Code, Compositional Features (Bulk Ca/P, Carbonate Content), Specific Surface Area (SSA_{BET}), ζ Potential, Average Size of Crystal Domains (along the $[0,0,2]$ and $[3,1,0]$ Directions) and Degree of Crystallinity of the synthesised HA nanocrystals.

	Bulk Ca/P ^[a] (mol)	Carbonate species ^[b] (wt%)	SSA_{BET} (m ² g ⁻¹)	ζ Potential (mv)	D_{002} ^[c] (nm)	D_{310} ^[c] (nm)	Degree of crystallinity
HA	1.62	1.3	160 ± 16	-10.1 ± 0.8	23 ± 4	9 ± 3	61% ± 5

[a] Calculated by ICP-OES. [b] Calculated by TGA. [c] Calculated applying the Scherrer equation.

Powder X-ray diffraction pattern of HA (Figure 1) showed the characteristic diffraction maxima of hydroxyapatite single phase (JCPDS 9-432). The diffraction pattern of HA exhibited not well defined diffraction maxima indicating a relatively low degree of crystallinity and nano-dimensions. The degree of crystallinity of HA, quantified according to a previously reported method, was 61 % ± 5. The average crystal size was estimated using Scherrer's formula. The nanocrystals appeared elongated along the *c*-axis of the hexagonal structure (23 ± 4 nm average length determined from the (002) peak at $2\theta=26^\circ$). The average width thickness was 9 ± 3 nm (from the (310) peak at $2\theta = 39^\circ$ 2 θ).

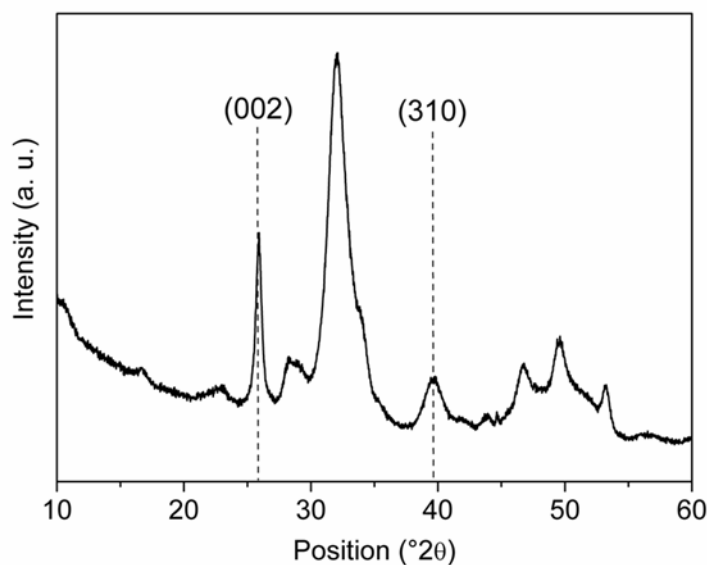


Fig. 1. X-Ray diffraction pattern of the synthesized HA nanocrystals.

The values of the crystallite domain sizes are in good agreement with the dimensions calculated by TEM image (see next). High-resolution TEM observations (Figure 2) confirmed the nanocrystalline nature of the apatite. The image reveals that they appeared as irregularly shaped platelets often agglomerated with length dimensions ranging between 25 and 35 nm.

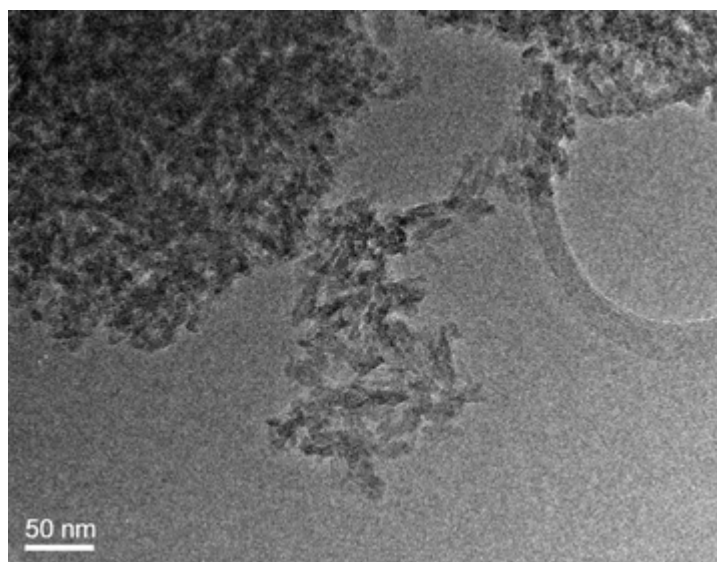


Fig. 2. High resolution transmission electron microscopy image of the synthesized HA nanocrystals.

The FT-IR spectra of HA (Figure 3A) confirmed the presence of the typical adsorption bands of apatite. The low crystalline degree of material in agreement with the diffraction data, is established by the weak resolution of all the adsorption bands. The study of the FT-IR bands characteristic of carbonate species ν_2 ($850\text{--}900\text{ cm}^{-1}$) and ν_3 ($1350\text{--}1600\text{ cm}^{-1}$) suggested type-B (carbonate substituted

for phosphate) carbonate incorporation in the apatite structure due to the presence of the bands at about 1460, 1422 and 873 cm^{-1} , with a very few carbonate ions on “non-apatitic” sites at the crystal surface. In fact, the curve fitting of the bands characteristic of carbonate species $\nu_3 \text{CO}_3$ showed the presence of the major component at 873 cm^{-1} (carbonate type B) and the band at around 864 cm^{-1} corresponds to a labile carbonate environment in both apatites (Figure 3C) [14]. The ratio “labile CO_3 /total CO_3 ” reached the value of 0.3. The FT-IR spectra also revealed the presence of phosphate and hydrogenphosphate “non-apatitic” ions. In most nanocrystalline apatite samples and especially in biological apatites additional bands are observed which do not appear in well-crystallized apatites and which have been designated as “non-apatitic environments” of the mineral ions. The curve fitting of the bands characteristic of PO_4 species indicated the presence of the apatitic PO_4^{3-} at 600, 575 and 560 cm^{-1} and of two “non apatitic” signals at 616 cm^{-1} due to PO_4^{3-} and at 533 cm^{-1} due to HPO_4^{2-} (Figure 3B). Finally, the FT-IR results pointed out the presence of a very thin hydrated layer at the surface of the apatite crystals and the presence of “non-apatitic” ions [15].

The characterization findings indicate that the synthetic apatite of this work resemble in an excellent way the chemical and morphological features of nanocrystalline apatites of biological origin.

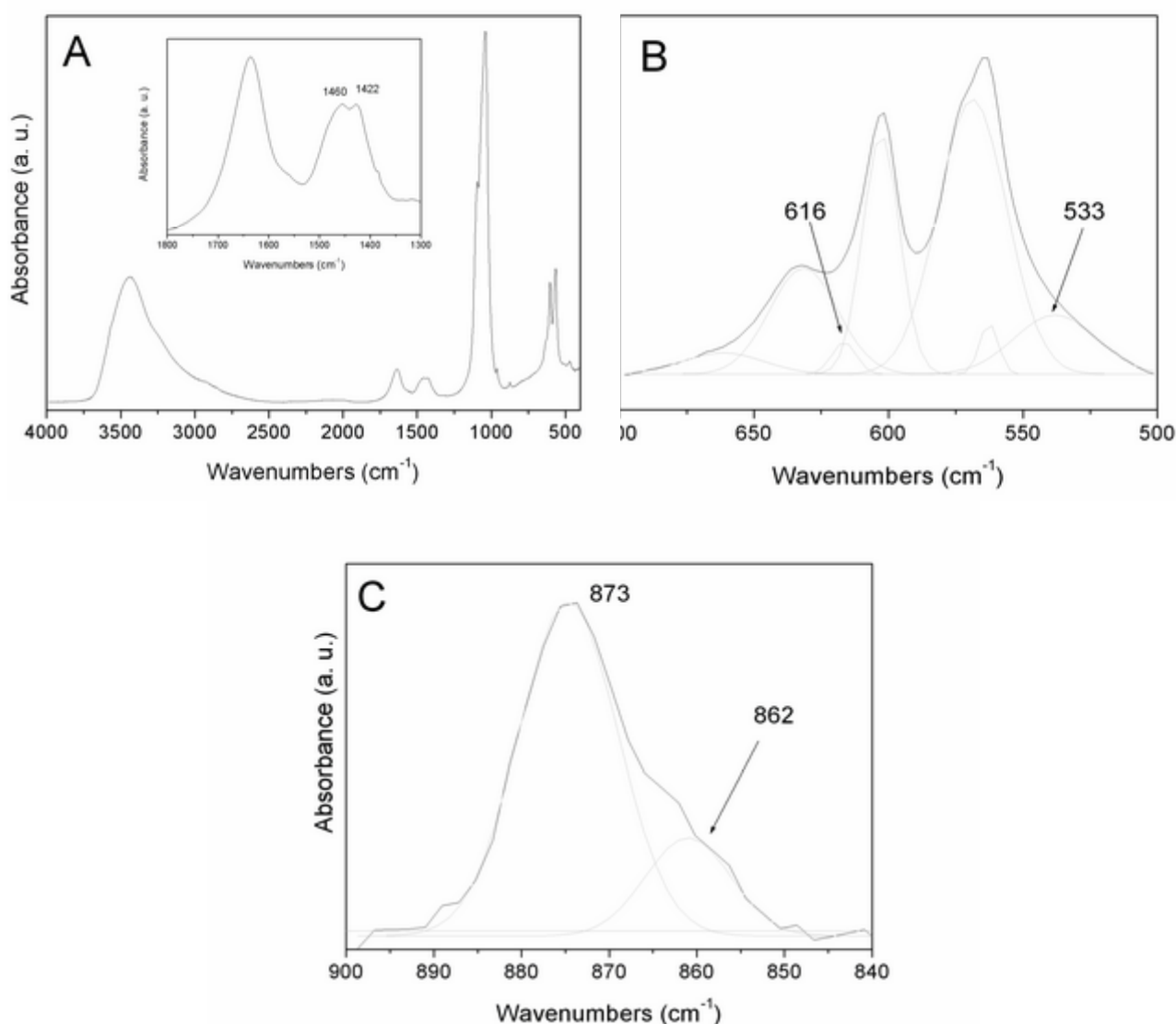


Fig. 3. FT-IR spectra of HA. The inset shows the bands of carbonate ions in the region 1800-1300 cm^{-1} (A). Curve fitting of the $\nu_4 \text{PO}_4$ bands (B) and of $\nu_3 \text{CO}_3$ (C).

3.2 Morphological and structural features of apatite coatings

In order to obtain a good HA suspension suitable for the ESD process in terms of dispersion, aggregation and stability, after 24 hours from the end of neutralization reaction the apatite nanocrystals were washed twice with ultrapure water by centrifugation and the solid residue was suspended in 100 ml of ethanol. Ethanol has been used because it is well known to give stable cone-jet mode electrohydrodynamic jetting and droplet generation [16] and its surface tension, electrical conduction and relative permittivity are key parameters in achieving this. After that, the suspension was sonicated

for 15 min, to break up the aggregate of HA nanoparticles using a probe sonicator, Ultrasonic Processor (UP50H, Hielscher, Germany), with a power and frequency of 10 W and 20 kHz, respectively, in the 0.5 cycling mode. In this way the suspension was stable without sedimentation up to 15 days. The HA nanocrystals make the ethanol more dielectric reducing the electrical conductivity from 3.4×10^{-4} to $0.7 \times 10^{-4} \text{ S m}^{-1}$. However this value is completely suitable for the ESD procedure. Finally the suspension was diluted to reach the value of 5mg/ml suspended in 50% EtOH.

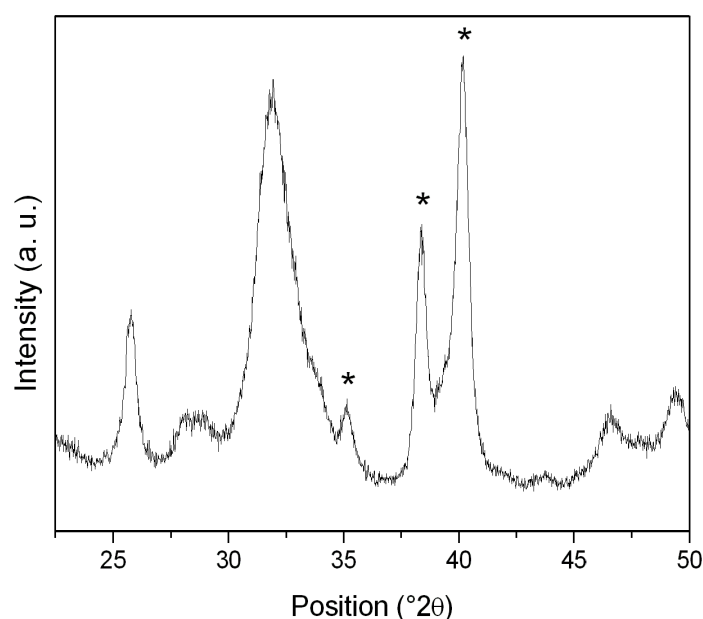


Fig. 4. X-Ray diffraction pattern of apatite ESD coating. * indicates the substrate titanium reflexes.

X-ray diffraction pattern of the apatite ESD coating (Figure 4) allowed that the titanium disk was covered by a pure apatite since only HA peaks were obtained. The presence of Ti peaks was attributed to the substrate. Moreover, the latter diffraction pattern resembled the apatite powder XRD (the (002) reflection which appears at 26° as well as the broad band at around 31° due to the deconvoluted triple peak corresponding to (211), (112) and (300) crystallographic planes) and it exhibited not well defined diffraction maxima indicating relatively low degree of crystallinity and nano-dimensions. This finding is in agreement with the fact that the solvent and the ESD did not induce any modifications in the

crystal structure of HA. In the infrared spectrum (Figure 5) only the bands characteristic of carbonate-apatite were observed, such as the broad and intense bands between $1300\text{--}1500\text{ cm}^{-1}$ and $900\text{--}1200\text{ cm}^{-1}$ correspond to ν_3 adsorptions of carbonate and phosphates, respectively. In particular, the bands at 1460 , 1422 and 873 cm^{-1} ascribed to type-B carbonate incorporation in the apatite structure, were clearly visible. This latter finding indicates that the chemical and the structural features of electrosprayed apatite on titanium are similar to the ones of apatite in the powder form.

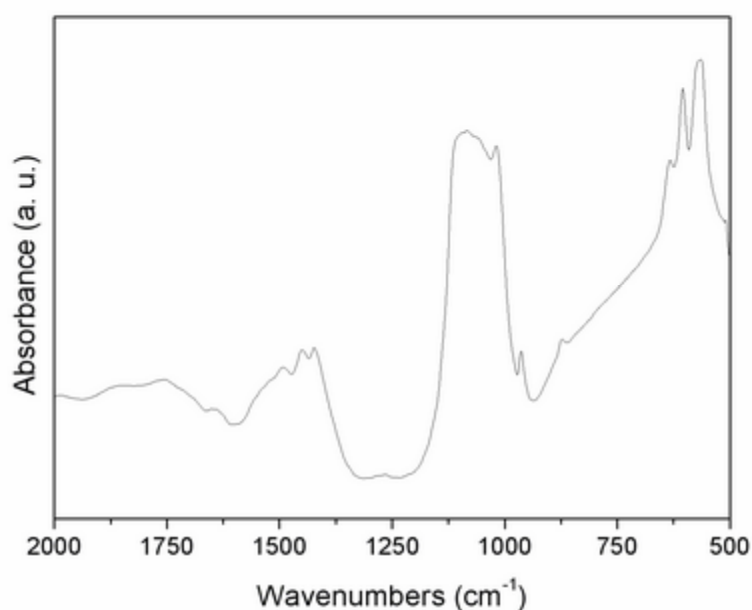


Fig. 5. *FT-IR spectra of apatite ESD coating.*

Table 2. ESD parameters for deposition of HA coatings evaluated in this work.

Nozzle to substrate distance (mm)	20	40	
Relative humidity in the deposition chamber (%)	20	40	
Deposition time (min)	5	15	30

In order to investigate the influence of processing conditions on the morphology of the coatings, several processing parameters were varied (Table 2) such as nozzle to substrate distance, relative humidity in the deposition chamber and deposition time. Figures 6 and 7 reported the SEM micrographs of the apatite coatings obtained using different conditions. It's clearly noticeable that with increasing deposition time large HA islands were formed that finally merged yielding a dense and homogeneous HA layer on the titanium substrates.

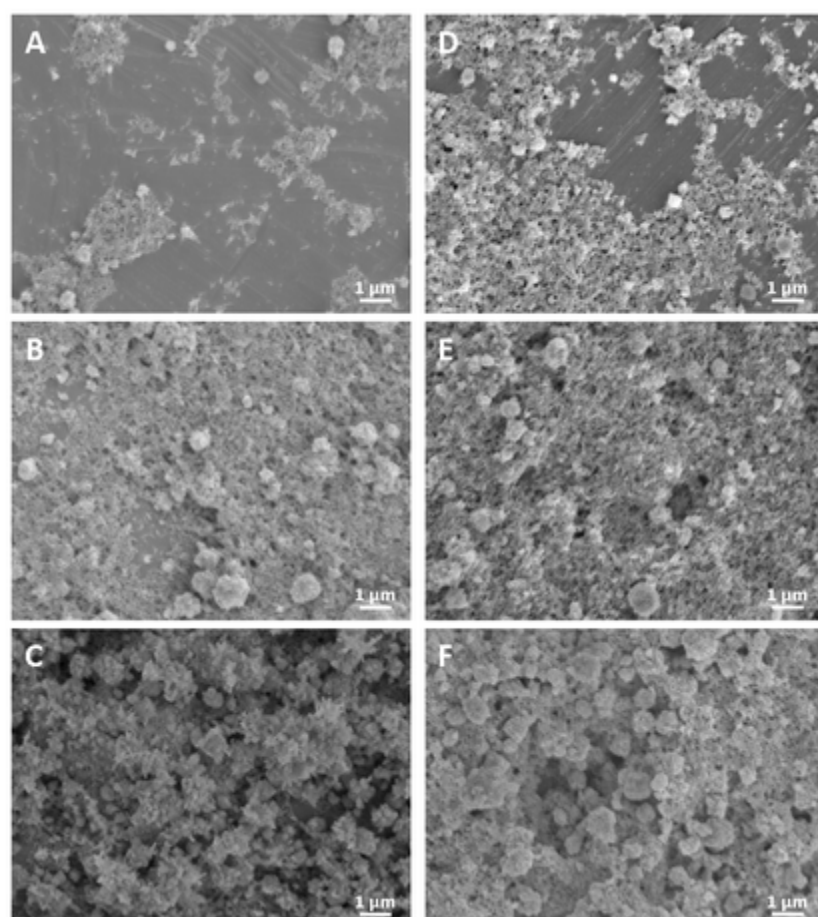


Fig. 6. SEM micrographs of apatite ESD coating morphologies. (A, B, C) Deposition parameters: nozzle to substrate distance 20 mm, relative humidity in the deposition chamber 20% and deposition time 5, 15 and 30 minutes, respectively. (D, E, F) Deposition parameters: nozzle to substrate distance 20 mm, relative humidity in the deposition chamber 40% and deposition time 5, 15 and 30 minutes, respectively.

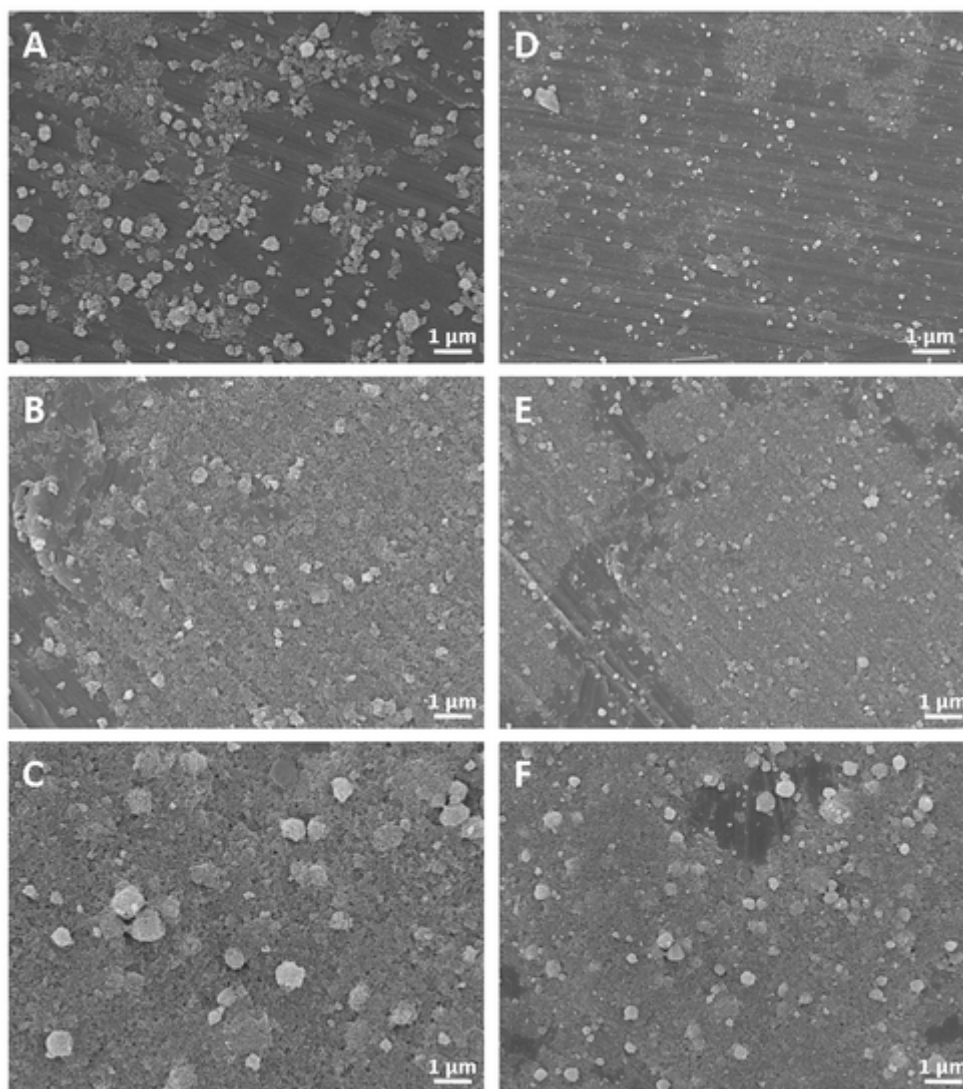


Fig. 7. SEM micrographs of apatite ESD coating morphologies. (A, B, C) Deposition parameters: nozzle to substrate distance 40 mm, relative humidity in the deposition chamber 20% and deposition time 5, 15 and 30 minutes, respectively. (D, E, F) Deposition parameters: nozzle to substrate distance 40 mm, relative humidity in the deposition chamber 40% and deposition time 5, 15 and 30 minutes, respectively.

This is confirmed by the results of the OCPC calcium assay, where a linear increase in the amount of deposited HA was measured with increasing spray times (Figure 8). Porous films made of agglomerates of plate-like apatite nanocrystals, measuring approximately 50 nm. The morphology and dimensions of these HA nanoparticles resemble that of the apatite powder and thus that of the natural bone apatite mineral.

SEM results showed that the coating morphology was different for short deposition time using different nozzle-to-substrate distances. A longer distance induced a longer flight time of the droplets that reached the surface in a dry condition. This leads to the formation of highly porous, fractal-like

coating morphologies. This phenomenon explained the increased homogeneity in 5 minutes deposition at 20 mm of distance compared to 40 mm where it was possible to notice formation of crystals agglomeration. Evaporation of the solvent used to deliver nanoparticles on the surface can be retarded or promoted in this way to detect the ideal level to obtain an increased homogeneity of the coating. Prolonged time reduced this difference in coating quality as it was showed after 15 minutes of deposition. However formation of a dielectric ceramic layer during deposition has also an effect on the morphology of the coating. During long time deposition change of local conductivity and wettability, due to the presence of coating, reduce the role of solvent evaporation to achieve homogeneity. Relative humidity was set during deposition at 20% and 40% without showed a significative effect on morphology.

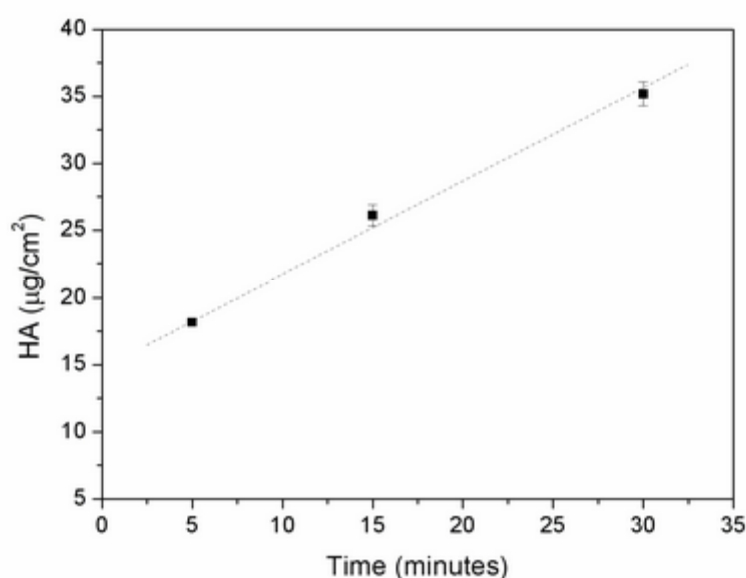


Fig. 8. Amount of deposited HA as a function of ESD time. (Linear fitting, dotted line)

4. Conclusions

The aim of this study was to investigate the applicability of the electrostatic spray deposition (ESD) technique for the deposition of nanostructured uniform apatite coating onto commercially pure cp-Ti substrates at room temperature. Therefore poorly crystalline bone-like carbonate-apatite nanocrystals were synthesised and well characterized. The apatite suspension suitable for the ESD process in terms of dispersion, aggregation and stability has been set up and some processing parameters such as nozzle to substrate distance, relative humidity in the deposition chamber and deposition time were varied in order to assess the morphological possible modifications.

Spectroscopic and diffractometric characterizations confirmed that the chemical and the structural features of electrosprayed apatite on titanium are similar to the ones of apatite in the powder form. Porous films made of agglomerates of plate-like apatite nanocrystals, measuring approximately 50 nm with morphology and dimensions resembling that of the natural bone apatite mineral have been formed. With increasing deposition time large apatite islands were formed that finally merged yielding a dense and homogeneous layer. The amount of deposited HA measured in function of the increasing spray times, confirmed a linear trend. Relative humidity did not show a significative effect on the morphology of coating, whereas the nozzle-to-substrate distances influenced the quality of the deposited layer in terms of crystals agglomerations. Shorter distance induced a shorter flight time of the droplets that reached the surface in a wet condition increasing the coating homogeneity and avoiding agglomerations.

The current study shows the feasibility of the ESD technique for the production of thin apatite coatings with a nanosized surface morphology onto commercially titanium substrates. The ability of these nanocrystals to bind a wide variety of molecules and most therapeutic agents for bone diseases [6] due to their very high specific surface area and the well known capability of ESD to produce coating at physiological conditions allowing the simultaneous deposition of organic and inorganic compounds, makes this work a first step for the set up of coating for bone implants based of surface activated apatite with improved functionality. The biologic efficacy of the ESD coatings made of pure apatite and functionalized apatite has to be proven in future *in vitro* and *in vivo* studies.

References

- [1] Y. Ramaswamy, C. Wu, H. Zreiqat, *Expert Review of Medical Devices* **2009**, 6, 423.
- [2] a) G. M. Luz, J. F. Mano, *Composites Science and Technology* **2010**, 70, 1777; b) B. Palazzo, D. Walsh, M. Iafisco, E. Foresti, L. Bertinetti, G. Martra, C. L. Bianchi, G. Cappelletti, N. Roveri, *Acta Biomater* **2009**, 5, 1241.
- [3] E. M. Christenson, K. S. Anseth, J. J. J. P. van den Beucken, C. K. Chan, B. Ercan, J. A. Jansen, C. T. Laurencin, W.-J. Li, R. Murugan, L. S. Nair, S. Ramakrishna, R. S. Tuan, T. J. Webster, A. G. Mikos, *Journal of Orthopaedic Research* **2007**, 25, 11.
- [4] N. Roveri, B. Palazzo, M. Iafisco, *Expert Opin Drug Deliv* **2008**, 5, 861.
- [5] Y. Sakhno, L. Bertinetti, M. Iafisco, A. Tampieri, N. Roveri, G. Martra, *The Journal of Physical Chemistry C* **2010**, 114, 16640.
- [6] a) M. Iafisco, B. Palazzo, G. Falini, M. D. Foggia, S. Bonora, S. Nicolis, L. Casella, N. Roveri, *Langmuir* **2008**, 24, 4924; b) B. Palazzo, M. Iafisco, M. Laforgia, N. Margiotta, G. Natile, C. L. Bianchi, D. Walsh, S. Mann, N. Roveri, *Advanced Functional Materials* **2007**, 17, 2180; c) M. Iafisco, J. G. Morales, M. A. Hernandez-Hernandez, J. M. Garcia-Ruiz, N. Roveri, *Advanced Engineering Materials* **2010**, 12, B218.
- [7] E. S. Thian, X. Li, J. Huang, M. J. Edirisinghe, W. Bonfield, S. M. Best, *Thin Solid Films* **2011**, 519, 2328.
- [8] a) S. C. G. Leeuwenburgh, M. C. Heine, J. G. C. Wolke, S. E. Pratsinis, J. Schoonman, J. A. Jansen, *Thin Solid Films* **2006**, 503, 69; b) S. C. G. Leeuwenburgh, J. G. C. Wolke, M. C. Siebers, J. Schoonman, J. A. Jansen, in *Thin Calcium Phosphate Coatings for Medical Implants* (Eds.: B. León, J. Jansen), Springer New York, **2009**, pp. 1.
- [9] a) L. T. de Jonge, S. C. Leeuwenburgh, J. J. van den Beucken, J. te Riet, W. F. Daamen, J. G. Wolke, D. Scharnweber, J. A. Jansen, *Biomaterials* **2010**, 31, 2461; b) L. T. De Jonge, S. C. G. Leeuwenburgh, J. J. J. P. Van De Beucken, J. G. C. Wolke, J. A. Jansen, *Adv. Funct. Mater.* **2008**; c) L. T. de Jonge, S. C. Leeuwenburgh, J. G. Wolke, J. A. Jansen, *Pharm Res* **2008**, 25, 2357.

-
- [10] a) S. Leeuwenburgh, J. Wolke, J. Schoonman, J. Jansen, *Journal of Biomedical Materials Research - Part A* **2003**, 66, 330; b) S. Leeuwenburgh, J. Wolke, J. Schoonman, J. A. Jansen, *Journal of Biomedical Materials Research - Part A* **2005**, 74, 275; c) S. C. Leeuwenburgh, J. G. Wolke, M. C. Siebers, J. Schoonman, J. A. Jansen, *Biomaterials* **2006**, 27, 3368; d) S. C. G. Leeuwenburgh, J. G. C. Wolke, M. C. Siebers, J. Schoonman, J. A. Jansen, *Biomaterials* **2006**, 27, 3368.
- [11] J. van den Dolder, G. N. Bancroft, V. I. Sikavitsas, P. H. M. Spauwen, J. A. Jansen, A. G. Mikos, *Journal of Biomedical Materials Research Part A* **2003**, 64A, 235.
- [12] M. Iafisco, E. Varoni, E. Battistella, S. Pietronave, M. Prat, N. Roveri, L. Rimondini, *Int J Artif Organs* **2010**, 33, 765.
- [13] N. Roveri, M. Iafisco, in *Advances in Biomimetics* (Ed.: A. George), InTech, **2011**, pp. 75.
- [14] C. Rey, B. Collins, T. Goehl, I. R. Dickson, M. J. Glimcher, *Calcified Tissue International* **1989**, 45, 157.
- [15] C. Rey, C. Combes, C. Drouet, H. Sfihi, A. Barroug, *Materials Science & Engineering C-Biomimetic and Supramolecular Systems* **2007**, 27, 198.
- [16] J. M. Grace, J. C. M. Marijnissen, *Journal of Aerosol Science* **1994**, 25, 1005.

Chapter IV

Configurational effects of collagen/ALP coatings on enzyme immobilization and surface mineralization

R Bosco, SCG Leeuwenburgh, JA Jansen, JJJP van den Beucken*

Applied Surface Science, Volume 311, 30 August 2014, Pages 292 -299.

1 Introduction

The primary scope of surface modifications for bone implants is to enhance bone integration to obtain early and strong fixation for functional application of the implant even under load bearing conditions. Bone is a connective tissue characterized by a multi-phase structure of collagen (organic) and hydroxyapatite crystals (inorganic). The inorganic phase is responsible for mechanical properties, such as hardness and compression resistance and the organic phase confers flexibility, resilience and fatigue resistance to the tissue[1, 2]. For decades, titanium has proved to be the most successful material for bone implants due to its suitable mechanical properties and biocompatibility. However, although the bulk properties of titanium are optimal for load bearing applications, the relative passive surface properties are a limitation for rapid integration into bone tissue[3].

Especially at the interface between implants and bone, a rapid and strong bonding that allows load and stress transfer to stimulate bone formation defined by the so called Wolff's law is required[4]. In view of the fundamental role of the interface in integration, the deposition of a thin layer of calcium phosphate onto titanium implant surfaces has been used frequently in the last decades to improve biological responses[5]. Additionally, several bioinspired strategies and compounds have been tested to obtain implant surfaces with a chemical composition similar to the inorganic phase of bone tissue. Hydroxyapatite (HA) has been most intensively investigated for bone applications. In vitro experiments demonstrated that HA can increase mesenchymal stem cell[6] and primary human osteoblast cell[7] proliferation and differentiation. Surface modifications based on HA-coatings have proven effects on the in vitro and in vivo performance compared to non-coated titanium controls[8]. A wide range of in vivo and clinical investigations have indicated an improved fixation of HA-coated implants compared to non-coated controls[9-15].

A relatively unexplored area for bioinspired surface engineering is the use of organic moieties. As the organic phase plays an important role during the biological mineralization

process[16], particularly collagen fibers and alkaline phosphatase (ALP) are appealing proteins for surface engineering approaches. In fact, the mineralization of bone tissue is a biphasic process in which the first phase is characterized by enzymatic interactions that increase Ca^{2+} and PO_4^{3-} ions within so-called matrix vesicles toward the formation of calcium phosphate (CaP) crystals, and the second phase comprises the exposure of formed CaP crystals into the extracellular matrix (ECM) to trigger nucleation[16]. During the first phase, ALP catalyzes the hydrolysis of organic phosphate monoesters, such as β -glycerophosphate, increasing the local concentration of inorganic phosphate required for bone physiological mineralization. The second phase, described as mineral propagation, is based on the transition of the accumulated CaP crystals on collagen fibers that would begin to play a major role in nucleating and orienting the newly formed crystals[17].

In previous work by De Jonge et al.[18], ALP was used as a single component in a coating procedure to induce surface mineralization via local increase of phosphate anions by hydrolysis of organic phosphate-monoesters. With these ALP-based coatings, Schouten et al. showed their capacity to enhance osteogenic responses in a rat model[19]. Despite low ALP retention on their surface, the engineered surfaces in these studies showed intriguing results that led to the hypothesis that the performance of ALP-based coatings may be substantially improved if the ALP immobilization can be optimized. In order to augment ALP retention, collagen represents a bioinspired option that can be easily introduced into the coating procedure and could potentially perform a dual role: (i) improve the retention of ALP by protein-protein interactions, and (ii) improve surface mineralization by CaP-collagen interactions.

The aim of this study was to generate collagen-ALP coatings onto titanium disks, and to evaluate whether configurationally different compositions of collagen-ALP coating affect enzyme retention and in vitro biomineralization. For coating deposition, electrospray deposition (ESD) was used due to the possibility to deposit materials from aqueous solutions and

its advantages regarding low temperature conditions[20-22]. Collagen and ALP coatings were deposited onto Ti disks as subsequent layers or in a mixed configuration; single compound coatings of collagen or ALP served as controls. These coatings were analysed via ALP-activity assays to determine ALP retention and in vitro mineralization assays to evaluate their surface mineralization capacity.

2 Materials and Methods

2.1 Materials

Commercially pure Ti disks (\varnothing 5 mm, thickness 1.5 mm) were used as substrates for coating deposition. Prior to coating deposition, disks were cleaned ultrasonically in acetone and ethanol (15 minutes each). ALP (P7640, 28 U/COL-ALP-M, Sigma Aldrich Ltd, Munich, Germany) was dissolved in an aqueous solution (1 mg/ml in 10:90 ethanol: mQ) and collagen (type I, rat tail; BD354236, Becton Dickinson Bioscience (BD) Breda, The Netherlands) was used to prepare a solution using 100% ethanol and 0.01 M acetic acid (in a ratio of 1:1) to a final collagen concentration of 0.5 mg/ml.

2.2 Coating deposition

All coatings were deposited using a commercially available vertical ESD device (ES 2000s, Fulence Ltd., Tokyo, Japan). Electrospraying was performed under controlled atmosphere conditions (relative humidity <15% and temperature 25°C) to prevent protein denaturation. Depositions were performed at a fixed nozzle-substrate distance of 40 mm, a flow rate of 4 μ l/min and an applied voltage of 10-12 kV. Different experimental groups were designed to determine the role and effect of collagen combined with ALP:

1. Collagen mono layer (COL)
2. ALP mono layer (ALP)
3. Collagen-ALP layered configuration (COL-ALP-L)

4. Collagen-ALP mixed configuration (COL-ALP-M)

COL was obtained using 0.5 mg/ml of collagen dissolved in 0.01 M acetic acid and 100% ethanol (ratio 1:1) sprayed for 30 minutes. ALP was made with deposition of 1 mg/ml of ALP dissolved in 10% ethanol for 30 minutes. COL-ALP-L was obtained with a dual step procedure as COL (1st step) and ALP (2nd step) as sequential depositions. COL-ALP-M was made of 0.5 mg/ml collagen + 1 mg/ml ALP dissolved in 0,01 M acetic acid and 100% ethanol (ratio 1:1) sprayed for 30 minutes. A schematic representation of coating groups is given in Figure 1A. All coated disks were lyophilized overnight and stored at -20 °C until further use.

2.3 Coating Characterization

2.3.1 Alkaline phosphatase activity

Alkaline phosphatase (ALP) activity was measured as described previously[23]. In brief, a volume of 200 µl mQ, 50 µl of buffer solution (5 mM MgCl₂, 0.5M 2-amino-2-methyl-1-propanol) and 250 µl of substrate solution (5 mM para-nitro-phenyl-phosphate) was added to coated titanium disks in a 24-well plate and incubated for 1 hour at 37°C. Subsequently, the reaction was stopped by adding 100 µl stop solution (0,3N NaOH), after which 100 µl solution was transferred to a 96-wells plate and read in an ELISA reader at 405 nm. Results were calibrated using a standard curve made by serial dilutions of freshly dissolved ALP (0 – 250 ng/ml).

2.3.2 Enzyme retention test

In order to evaluate the role of collagen in ALP retention, the enzymatic activity of all coated samples was analyzed before and after immersion in mQ. To perform this retention test, coated disks (n=3) of all groups were immersed in mQ (37°C) for 1 hour in static conditions. After this period, ALP activity of coated disks was evaluated using the aforementioned ALP

activity test and results obtained were compared with the enzymatic activity of coated disks before the soaking test and expressed as relative activity (%).

2.4 *In vitro* biomineralization test

Surface mineralization capacity of coated disks was evaluated *in vitro* by immersion of disks in cell culture medium (CCM) in accordance to the method described by de Jonge et al.[24]. Briefly, CCM consisted of alpha minimal essential medium (α -MEM, Gibco, Invitrogen, life technology corporation, Carlsbad, US) with addition of 10% v/v fetal calf serum, 50 μ g/ml ascorbic acid, 10^{-8} dexamethason, 50 μ g/ml gentamicin and 10 mM sodium β -glycerophosphate (Sigma). Coated disks were immersed in 1 ml of CCM in a 24 wells plate in static condition for 1, 2, 4, 10 and 14 days (n=3) at 37°C and medium was refreshed every 2 days. After each time point, disks were washed thoroughly with mQ water and kept at -20°C. Quantification of deposited calcium on titanium disks was performed with the *o-cresol*-phthalein complexone (OCPC) method (Sigma Aldrich co. Ltd.,Munich, Germany) [25], for which samples were immersed overnight in 0.5 N acetic acid on a shaker table. For analyses, 300 μ L of work reagent was added to 10 μ L aliquots of sample or standard in a 96-wells plate. The plate was incubated for 10 min at room temperature and then read at 570 nm. Serial dilutions of CaCl_2 (0–100 μ g / ml) were used for the standard curve.

2.5 *Coating and biomineralization morphology*

Field Emission Scanning Microscopy (JEOL FESEM 6330, Tokyo, Japan) was used to evaluate surface homogeneity of all experimental samples after coating deposition. SEM was also used to detect and characterize the biomineralization on the surface after soaking in CCM for different time points (1, 2, 4, 10 and 14 days). To evaluate surface composition after biomineralization experiments, Fourier transform infrared analysis (FTIR, Perkin-Elmer,

Spectrum One, Groningen, The Netherlands) was performed on samples at day 4 and 10 of the in vitro biomineralization test[26].

2.6 *Statistical analysis*

Statistical analyses on the data of the in vitro biomineralization experiments were performed with GraphPad InStat software (GraphPad software Inc., La Jolla, USA) using a one-way ANOVA combined with post-hoc Tukey–Kramer Multiple Comparisons test. The significance level was set at $p < 0.05$.

3 Results

3.1 Coating morphology

All experimental samples were analyzed for surface morphology with scanning electron microscopy after deposition. For all groups, an apparent homogenous and complete surface coverage was observed using a 30 minute deposition time. Figure 1 shows a schematic representation (A) of the experimental groups and the corresponding scanning electron microscopy images (B) of the coating surface morphology. A scratch was made on COL to detect the thin collagen layer as shown in Figure 1B.

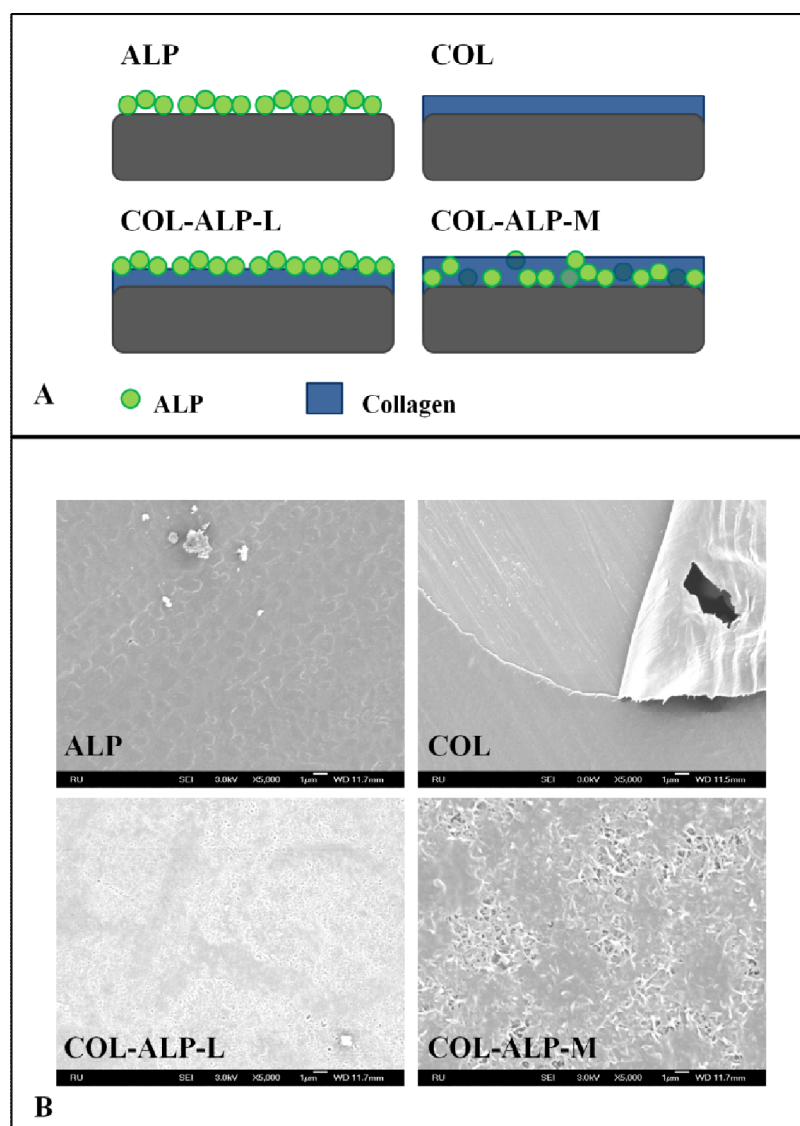


Figure 1 Groups overview: (A) Schematic representation of coating composition and conformation. (B) SEM images of titanium disks surfaces after ESD coating

3.2 Enzyme retention

For all ALP-containing experimental samples, the retention of the enzyme ALP within the coating decreased significantly after overnight immersion in mQ compared to virgin samples (Figure 2). For ALP, COL-ALP-L, and COL-ALP-M, the relative retention of the enzymatic ALP-activity within the coating was 5%, 20%, and 50% of their virgin equivalents, respectively. Among the experimental groups, the relative retention of the enzymatic ALP-activity within the coating of COL-ALP-L was significantly higher ($p < 0.01$) compared to ALP, and that of COL-ALP-M was significantly higher ($p < 0.001$) compared to both COL-ALP-L and ALP. No enzymatic ALP-activity was observed for COL coatings, neither before nor after overnight immersion in mQ.

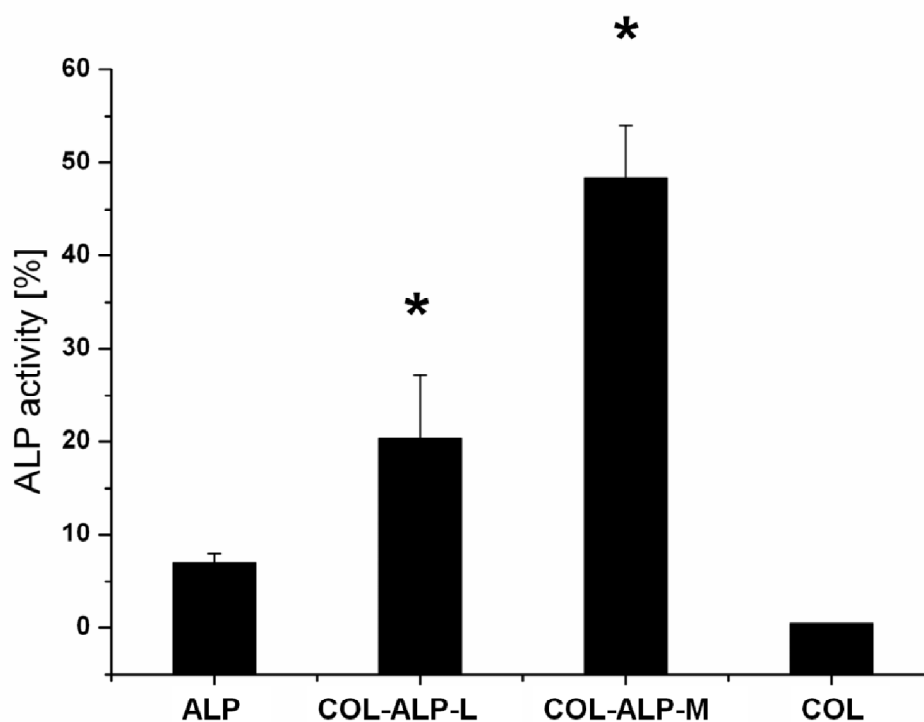


Figure 2 ALP activity retained after soaking test. Values are normalized to the ALP activity of each coating group before soaking. The * indicates a significant difference compared to ALP. The # indicates a significant difference compared to COL-ALP-L (*, # $p < 0,05$).

3.3 *In vitro* biomineralization test

Mineralization was evaluated through quantification of calcium deposition upon immersion of the experimental samples in CCM. For all groups except COL, calcium deposition was observed from day 1 of immersion onward. COL-ALP-L showed the fastest mineralization with the highest calcium content at day 1 reaching $40 \mu\text{g}/\text{cm}^2$, while ALP and COL-ALP-M reached similar calcium contents of $18 \mu\text{g}/\text{cm}^2$ and $12 \mu\text{g}/\text{cm}^2$, respectively. At day 2 COL-ALP-M reported the highest value of calcium content ($77 \mu\text{g}/\text{cm}^2$) higher than ALP and COL-ALP-L (with value of 30 and $61 \mu\text{g}/\text{cm}^2$, respectively). Day 4 represents a particular time point in which all the ALP containing group reach a similar value of calcium content (ALP $62 \mu\text{g}/\text{cm}^2$, COL-ALP-L $66 \mu\text{g}/\text{cm}^2$ and COL-ALP-M $76 \mu\text{g}/\text{cm}^2$). All the group increase their calcium content at day 10, COL-ALP-M reached a higher mineralization value compared to COL-ALP-L (COL-ALP-M $106 \mu\text{g}/\text{cm}^2$ and COL-ALP-L $76 \mu\text{g}/\text{cm}^2$) and ALP increased the calcium content up to a value comparable to COL-ALP-M ($95 \mu\text{g}/\text{cm}^2$). At the end of the biomineralization test, at day 14, the calcium content in ALP and COL-ALP-L was increased but comparable to their value at day 10 (respectively 106 and $93 \mu\text{g}/\text{cm}^2$). In contrast, COL-ALP-M at day 14 markedly increased the calcium content with values (over $150 \mu\text{g}/\text{cm}^2$) significantly higher than the corresponding value of the other ALP containing coating at the last time point ($p < 0.05$). Results of the quantified mineralization at all the time points are displayed in Figure 3.

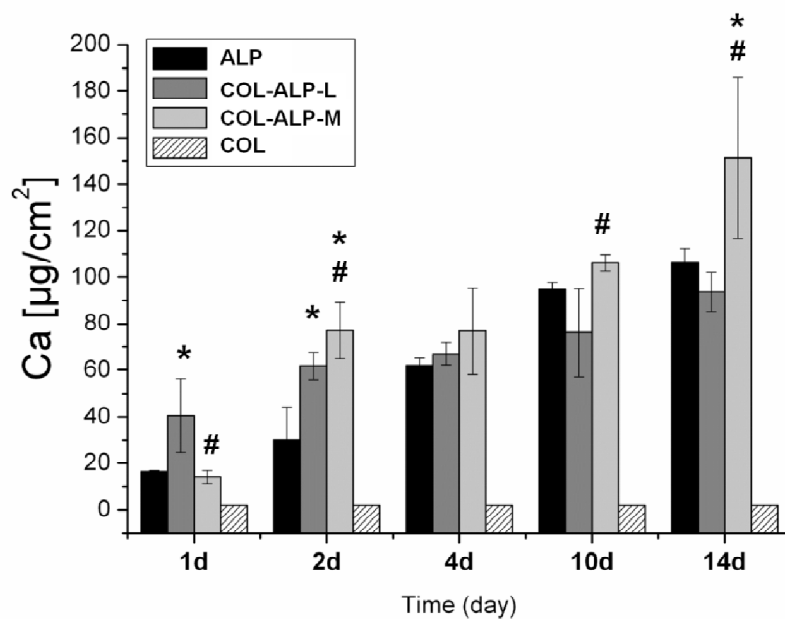


Figure 3 Quantification of deposited Ca (OCPC) after different days of immersion in CCM. The * indicates a significant difference compared to ALP. The # indicates a significant difference compared to COL-ALP-L (*, # $p < 0,05$).

FTIR at day 4 and 10 indicated the presence of calcium phosphate on the surface (Figure 4). For ALP, COL-ALP-L and COL-ALP-M, characteristic phosphate bands were detected at 550–600 (ν_4 PO_4 stretching), 960 (ν_1 PO_4 stretching), 1020 (ν_3 PO_4 stretching) cm^{-1} , COL group, instead, showed none of this fingerprint bands as presented in Figure 4.

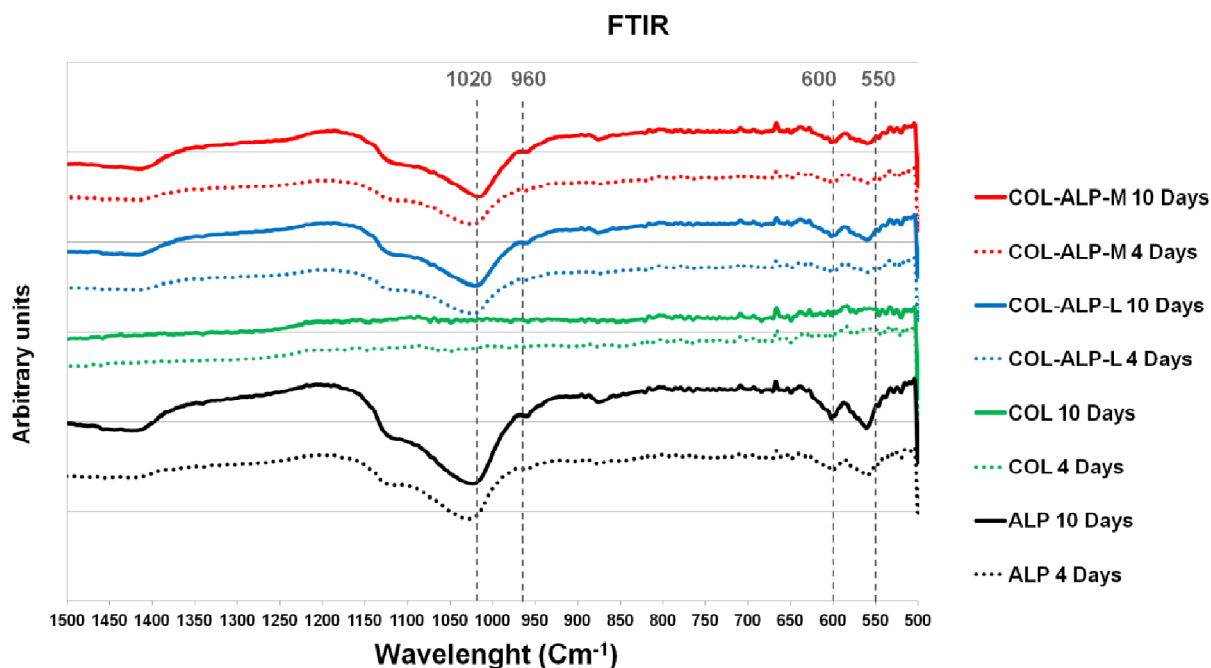


Figure 4 Infrared analysis (FTIR) performed on coated disks surfaces after biomineralization test at day 4 (dotted line) and 10 (continued line). The Y axis reports arbitrary units and the curves disposition is not quantitative.

3.4 Surface morphology after biomineralization

Scanning electron microscopy was used to observe the morphology of biomineralized surfaces (Figure 5) on all experimental samples after different immersion periods in CCM. An overview, per experimental sample, of the surface before mineralization (day 0) and after 14 days is presented in Figure 5. After 14 days, all experimental groups containing the enzyme ALP within the coating showed mineralization on the surface. In contrast, COL showed no mineral phase on their surface. ALP and COL-ALP-L demonstrated a similar mineralization process and the structure of the mineralized layer was homogeneous and uniform. On the contrary, COL-ALP-M induced the formation of spherical, agglomerated crystals with a size of 1-2 μm . These micro-scale agglomerations were interconnected with a matrix of nanoscale fibers.

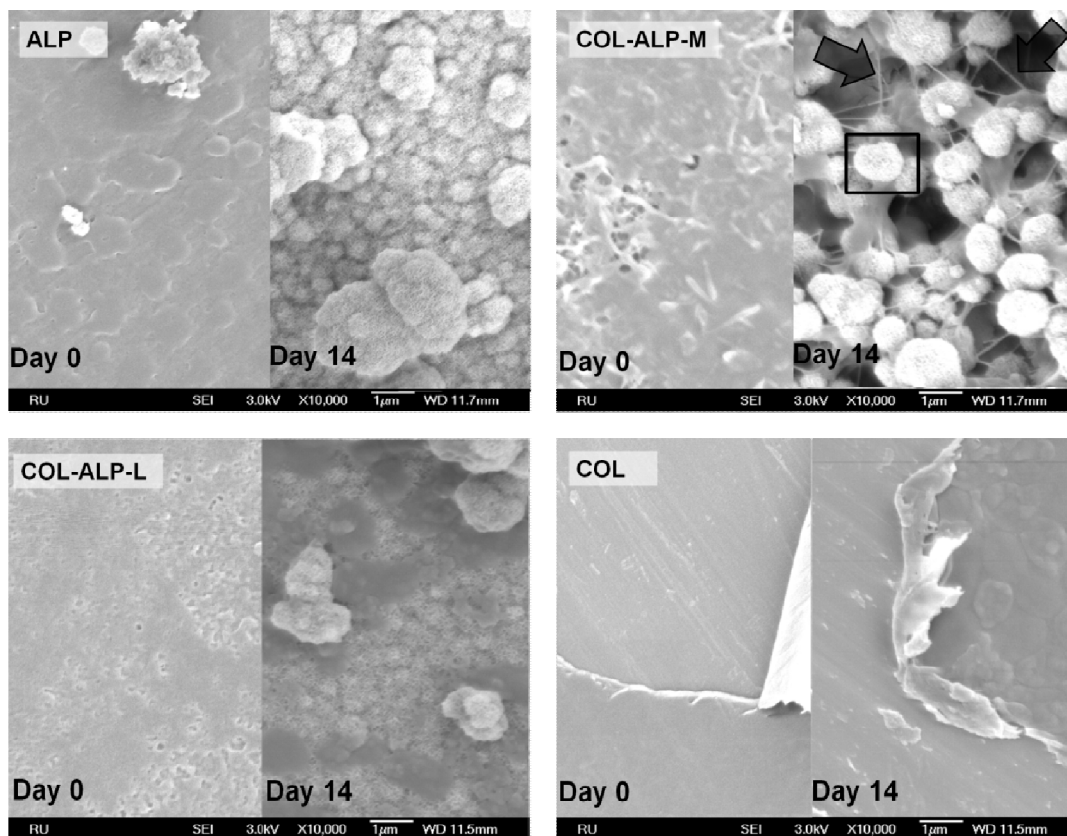


Figure 5 SEM images to obtain surface evaluation at day 0 and day 14 of biomineralization test. On COL-ALP-M surface micro-scale crystal agglomeration is indicated by a square and nano fibers are indicated by an arrow.

Figure 6 presents the evolution of the complex crystals agglomeration and interconnecting nano fiber formation during the 14 days of biomineralization. The SEM images revealed initial formation of interconnected fibers at day 1 when the first agglomerations started to form on top of a mineralized layer. The mineralized networks increased during immersion and at day 14 the presence of micro-scale crystal agglomerations interconnected by collagen fibers network was observed for the entire surface(Figure 7).

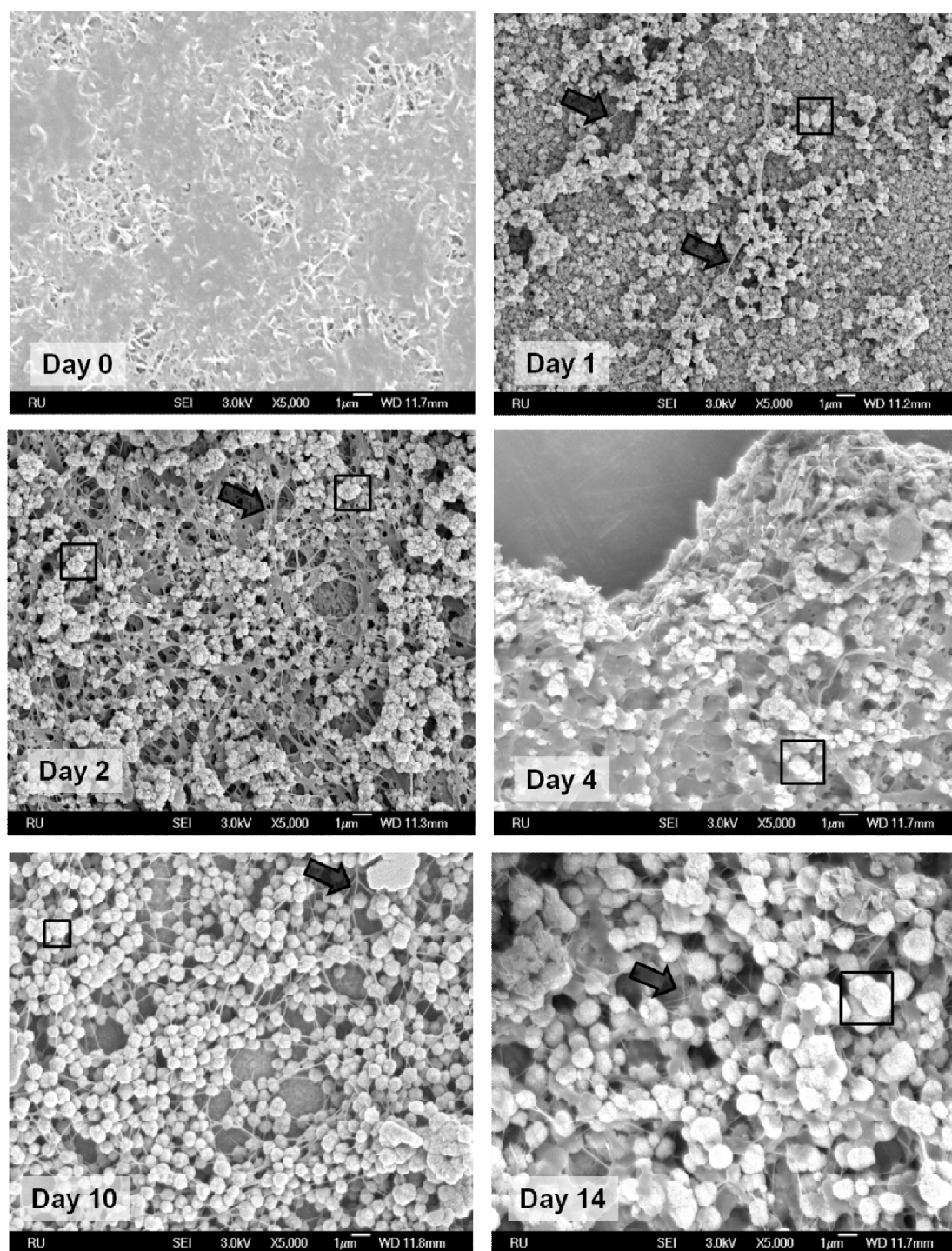


Figure 6 SEM images of mineralized surface on COL-ALP-M. The biomineralization process is documented among all the time points (1, 2, 4, 10, 14 days) to offer an overview of the phenomenon. Surface micro-scale crystal agglomeration is indicated by a square and nano fibers are indicated by an arrow.



Figure 7 SEM evaluation after scratch of a COL-ALP-M coated disk at day 14. This image offer a particular point of view of the biomineralization phenomenon offering the view of how both the side of the coating layer (the one facing the titanium and the external one) are characterized by crystals agglomerations and interconnecting fibers.

4 Discussion

The aim of this study was to generate collagen-ALP coatings onto titanium disks, and to evaluate whether configurationally different compositions of collagen-ALP coatings would affect enzyme retention and *in vitro* biomineralization. ALP and collagen coatings, deposited with ESD, were obtained in a layered and mixed configuration and compared with mono compound coating as controls. All the coatings were tested via a soaking test and an *in vitro* biomineralization test to evaluate the effect of collagen on ALP coatings. The hypotheses were that collagen might act as a “glue” to increase the retention of ALP, therefore augmenting the enzymatic efficiency, and that collagen might synergistically increase the biomineralization process by entrapping calcium phosphate crystals. Data presented in this study indicate that addition of collagen affected mineralization performances of ALP based coatings. More interestingly collagen and ALP coating configuration played a role in formation of mineralized layer onto coated samples.

Surface modifications based on addition of biomolecules on the surface are usually focused on the biological and cellular effect of such biomaterials [3, 27]. The approach used in this study is different and focus on obtaining a mineralization phenomenon without cells on titanium surface. The conducted investigation was aiming to obtain biomineralization, through the use of ALP and collagen, inspired by the natural mechanism as described by Anderson et al.[16, 17]. An approach to obtain mineralization from ECM molecules, in combination with collagen, was performed by Zurick et al.[28] using osteopontin, bone sialoprotein and dentin phosphoprotein. In Zurick's study the mineralization attempt is limited to few hours and not on titanium surface. An intriguing method to obtain mineralization on surface is offered by Nijhuis et al.[29] using the enzymatic properties of urease to control pH and obtain mineral deposition on titanium and polystyrene from SBF. In previous studies de Jonge[24] and Schouten[30] used ALP coated titanium to obtain mineralization on the surface using a cheaper and stable ECM molecule.ESD have demonstrated its applicability for thin coating made of organic materials and tailorable substrate composition [24, 31, 32]. Previous research showed the capability of ALP as organic and bioinspired material for orthopaedic applications, in particular to obtain mineralization and increased bone to implant contact [24, 30, 31]. In this work ESD was successfully used to deposit COL, ALP, COL-ALP-M and COL-ALP-L onto titanium controlling the coatings configurations.

In this study, ALP was exploited as an active enzymatic compound for surface immobilization to induce biomineralization. More specifically, its role was to increase the local concentration of phosphate groups and hence to mimic the natural biomineralization process. In fact, in the mineralization process proposed in this study, the main source for phosphate groups was the addition of β -glycerophosphate (10 mM) and the only available source for calcium was calcium chloride (CaCl_2 200mg/L). ALP was responsible to create free PO_4^{3-} ions from β -glycerophosphate that interact with Ca^{2+} to form CaP crystals. This phenomenon was already described by de Jonge[18] and it represented the starting point for this study.

The first hypothesis in this study was concerning the role of collagen in ALP retention. In the work of de Jonge[18] was suggested that ALP could act as a surface-active enzyme and therefore its activity could be limited to the coated surface area. For this reason ALP (mono compound) was used as reference and comparison to evaluate the effect of collagen in increasing ALP retained activity. ALP activity after deposition and soaking test showed different efficiency of coatings among all the different groups. Addition of collagen increased surface immobilization of the enzyme ALP as indicated by a significantly increased enzymatic ALP-activity, for groups with dual compounds, of 3 and 7 times higher for COL-ALP-L and COL-ALP-M, respectively. ALP activity tested on COL was equal to zero, so it is possible to exclude any effect on the ALP assay induced by the presence of collagen. The increased retained activity of COL-ALP-L and COL-ALP-M could be related to a more favourable adhesion of ALP to collagen compared to ALP to titanium. The conformation with ALP “entrapped” in a collagen mix appears able to preserve a higher ALP activity compared to all the other conformation. In an ALP retention study performed by Douglas et al[33] using different hydrogels is offered a description of non crosslinked collagen in ALP retention. Douglas showed that collagen based hydrogel were able to entrap ALP, even if the test was performed only for few hours. Vittur et al.[34] offered an explanation of ALP and collagen binding. Vittur, in fact, showed that ALP is bound to collagen through ionic forces as demonstrated by ALP release was conditioned by addition of NaCl. Vittur’s theory is therefore confirmed in the results of this paper; in fact COL-ALP-M showed the highest retention level because ALP was embedded in the collagen structure. ALP requires free collagen binding sites to attach and the mixed configuration is obviously offering more binding sites than the layered configuration where only the binding sites at the surface were available.

Further, the role of collagen in the biomineralization process was studied after it was demonstrated its effect in improving ALP retention. According to Dey et al. [35], collagen

plays a fundamental role in mineralization sub sequentially to the formation of “prenucleation clusters”. As was also reported by Nudelman et al. [36], collagen is essential to guide the mineral phase in bone mineralization in presence of CaP. In their study, in fact, the crystal phase was obtained on collagen using CaCl_2 and K_2HPO_4 (a highly soluble potassium salt) to obtain the ions and cations required to form CaP instead of the use of non collagenous proteins responsible of mineral formation (such as ALP). In the study here presented, the active role of ALP in recruiting PO_4^{3-} was maintained and improved by the presence of collagen and it was the principal element of investigation.

The effect of collagen in a biomineralization process, activated by ALP, was evaluated by the quantification and the morphology of the mineralization during time. Presence of collagen also increased the amount of mineral phase that was formed onto the disk proving that a synergistic effect with ALP was obtained. ALP is an enzyme and its ability to produce free phosphate ions is related to its availability and not to its quantity. As demonstrated in this study collagen is capable to increase ALP retention on the surface of the coated samples and therefore the presence of ALP should be able to increase the mineral formation. Biomineralization data indicated a substantial increase in mineral content (at day 14) if compared with the results obtained by de Jonge[18] (110 vs 20 $\mu\text{g}/\text{cm}^2$ respectively). It has to be remarked that despite the similarity of the approach in this study and the one conducted by de Jonge, a fundamental difference can be found in the biomineralization test; in the study here presented medium was refreshed every 2 days offering a constant source of unprocessed β -glycerophosphate, on the contrary in de Jonge’s experiment there is no reference to medium refreshment.

Despite the increased amount of retained ALP the mineralization process is not proportionally augmented. COL-ALP-M showed a retained enzymatic activity 7 folds higher than ALP but on day 14 COL-ALP-M compared to ALP has only 1,6 folds increased mineral content. Retention test was performed in 1 hour and in mQ and therefore it can be related only to an

initial retention of ALP that cannot be compared with 14 days of mineralization test in CCM. Nevertheless biomineralization trend was monotonic and time dependent for ALP, COL-ALP-L and COL-ALP-M coatings. COL showed no mineralization during the experiment clarifying any chance that the collagen itself could have induced some mineralization. The increase of mineral content is related to the amount of crystals that are present on the surface of coated samples. It was previously reported by Beertsen et al.[37] that collagen enriched with ALP mineralize more, even in vivo, due to the local effect of ALP that induce crystal formation in proximity of collagen and so with more chance to be entrapped by collagen. In the study here presented a similar effect can be deduced, in fact retained ALP could induce mineral formation onto titanium disk and not in the medium continuously refreshed. The structure of collagen and embedded ALP in COL-ALP-M is responsible of this improvement. Collagen is capable of attracting CaP crystals in its negative sites and the presence of ALP inside a collagenous structure is improving this effect. In fact embedded ALP is responsible of a crystals nucleation phenomenon that starts not only merely at surface but also inside the collagen matrix as suggested in other mineralization models[36].

Collagen and ALP coatings configuration can also affect the morphology of mineralization. As reported by Nudelman[36] and previously by Mann[38] biomineralization required strategies such as a) chemical control, b) spatial control and c) structural control. Nudelman remarked the role of a 3D structural composition of collagen and crystals-nucleating biomolecules (such as ALP) is essential to modulate the mineralization process. Collagen can play a role as a template or scaffold where the mineralization process can be initiated and maintained thanks to collagen binding sites. An example, in the study here presented, is given by COL-ALP-M samples that showed an altered and unique biomineralization pattern. COL-ALP-M created a nano fibrous matrix, which closely resembles ECM, with agglomeration of nano sized crystals interconnected with collagen filaments. Analysis of COL-ALP-M biomineralization process during the time point, using SEM images, show that micro-sized

agglomeration of crystals are formed since the early phase (day 4) and retained by the nano fibrils among all the mineralization process resulting in an increased amount of calcium phosphate onto the disk compared with the other groups.

A detail of the biomineralized layer obtained with COL-ALP-M after 14 days revealed that the crystals agglomeration and matrix structure is present in both the side of the coating. The COL-ALP-M mineralized coating was strongly cohesive as indicated by peeling of the coating after a scratch for SEM evaluation; the crystals agglomerations and the matrix structure resist to the scratch maintaining their formation. The structure of this unique biomineralization pattern is able to explain the increased quantitative results obtained for calcium assay and ALP activity on COL-ALP-M. The collagen network entrapped the ALP and increased its total retention, the presence of more ALP induced an augmented mineralization process that was kept by the cohesive strength of collagen that preserved crystal agglomerations to be released from the titanium surface.

Collagen, undeniably, played a dual role improving the ALP based coatings in terms of enzymatic retained ability and mineralization capacity. COL-ALP-M was characterized by the highest retained ALP activity and the maximum mineral content and therefore COL-ALP-M is an improvement to the previous ALP coatings. ALP was already an intriguing coating material that obtained successful results *in vitro* [18] and *in vivo* [19]; the improvement added by the presence of collagen is certainly a promising innovation for organic coatings. COL-ALP-M was also unique in the ECM-like biomineralized structure that was formed during the mineralization test. Such ECM-like structure can be a positive environment for osteoblast biological response, due to the similarity to the natural bone-like ambient. COL-ALP-M could therefore be used as a successful coating solution to mimic the biomineralization mechanism of bone tissue and could result in a bioactive surface modification able to trigger cellular response (*in vitro*) or a positive bone reaction (*in vivo*).

5 Conclusions

This study showed a marked role of collagen to increase retention of the ALP coating onto titanium disks as proved by residual enzymatic activity after rinses in mQ water. ESD resulted to be an optimal coating method that preserved functionality of bio molecules. ALP was also able to dissociate phosphate groups that attract Ca (dissolved in CCM) and let them react to obtain calcium phosphate crystals mimicking the process of crystals deposition in bone tissue (biomineralization). In every test performed the mixed conformation (COL-ALP-M) manifested superior results compared with the other samples in terms of ALP remaining activity after soaking (retention) and formation of mineral layer (activity). Also the unique pattern that mineralization assumed during time, with the formation of collagen nano fibers, is a result that induce us to plans further investigation.

REFERENCES

1. Ramakrishna, S., et al., *Biomedical applications of polymer-composite materials: a review*. Composites Science and Technology, 2001. **61**(9): p. 1189-1224.
2. Flanagan, D., et al., *Measurement of the Fatigue Life of Mini Dental Implants: A Pilot Study*. Journal of Oral Implantology, 2008. **34**(1): p. 7-11.
3. Bosco, R., et al., *Instructive coatings for biological guidance of bone implants*. Surface and Coatings Technology, (0).
4. Ahn, A.C. and A.J. Grodzinsky, *Relevance of collagen piezoelectricity to "Wolff's Law": A critical review*. Medical Engineering and Physics, 2009. **31**(7): p. 733-741.
5. Dorozhkin, S.V., *Calcium orthophosphate coatings, films and layers*. Progress in Biomaterials, 2012. **1**(1): p. 1-40.
6. Guo, H., et al., *Biocompatibility and osteogenicity of degradable Ca-deficient hydroxyapatite scaffolds from calcium phosphate cement for bone tissue engineering*. Acta Biomaterialia, 2009. **5**(1): p. 268-278.
7. Douglas, T., et al., *Porous polymer/hydroxyapatite scaffolds: characterization and biocompatibility investigations*. Journal of Materials Science: Materials in Medicine, 2009. **20**(9): p. 1909-1915.
8. Shadanbaz, S. and G.J. Dias, *Calcium phosphate coatings on magnesium alloys for biomedical applications: A review*. Acta Biomaterialia, 2012. **8**(1): p. 20-30.
9. Dinda, G.P., J. Shin, and J. Mazumder, *Pulsed laser deposition of hydroxyapatite thin films on Ti-6Al-4V: Effect of heat treatment on structure and properties*. Acta Biomaterialia, 2009. **5**(5): p. 1821-1830.
10. Suchanek, W. and M. Yoshimura, *Processing and properties of hydroxyapatite-based biomaterials for use as hard tissue replacement implants*. Journal of Materials Research, 1998. **13**(1): p. 94-117.
11. Paital, S.R. and N.B. Dahotre, *Calcium phosphate coatings for bio-implant applications: Materials, performance factors, and methodologies*. Materials Science and Engineering: R: Reports, 2009. **66**(1&2): p. 1-70.
12. Sima, L.E., et al., *Differentiation of mesenchymal stem cells onto highly adherent radio frequency-sputtered carbonated hydroxylapatite thin films*. Journal of Biomedical Materials Research - Part A. **95**(4): p. 1203-1214.
13. Saithna, A., *The influence of hydroxyapatite coating of external fixator pins on pin loosening and pin track infection: A systematic review*. Injury. **41**(2): p. 128-132.
14. Barrere, F., et al., *Osteointegration of biomimetic apatite coating applied onto dense and porous metal implants in femurs of goats*. J Biomed Mater Res B Appl Biomater, 2003. **67**(1): p. 655-65.
15. Morris, H.F., et al., *Periodontal-type measurements associated with hydroxyapatite-coated and non-HA-coated implants: uncovering to 36 months*. Ann Periodontol, 2000. **5**(1): p. 56-67.
16. Anderson, H.C., *Molecular biology of matrix vesicles*, 1995. p. 266.
17. Anderson, H.C., R. Garimella, and S.E. Tague, *The role of matrix vesicles in growth plate development and biomineralization*. Front Biosci, 2005. **10**(882-837).
18. de Jonge, L.T., et al., *Electrosprayed Enzyme Coatings as Bioinspired Alternatives to Bioceramic Coatings for Orthopedic and Oral Implants*. Advanced Functional Materials, 2009. **19**(5): p. 755-762.
19. Schouten, C., et al., *The effect of alkaline phosphatase coated onto titanium alloys on bone responses in rats*. Biomaterials, 2009. **30**(32): p. 6407-6417.

20. Nijhuis, A.W., S.C. Leeuwenburgh, and J.A. Jansen, *Wet-chemical deposition of functional coatings for bone implantology*. Macromol Biosci. **10**(11): p. 1316-29.
21. Morozov, V.N. and T.Y. Morozova, *Electrospray Deposition as a Method To Fabricate Functionally Active Protein Films*. Analytical Chemistry, 1999. **71**(7): p. 1415-1420.
22. Iafisco, M., et al., *Electrostatic spray deposition of biomimetic nanocrystalline apatite coatings onto titanium*. Advanced Engineering Materials, 2012.
23. De Ruijter, J., et al., *Analysis of integrin expression in U2OS cells cultured on various calcium phosphate ceramic substrates*. Tissue Engineering, 2001. **7**(3): p. 279-289.
24. de Jonge, L.T., et al., *In vitro responses to electrosprayed alkaline phosphatase/calcium phosphate composite coatings*. Acta Biomaterialia, 2009. **5**(7): p. 2773-2782.
25. van den Dolder, J., et al., *Flow perfusion culture of marrow stromal osteoblasts in titanium fiber mesh*. Journal of Biomedical Materials Research Part A, 2003. **64A**(2): p. 235-241.
26. Raynaud, S., et al., *Calcium phosphate apatites with variable Ca/P atomic ratio I. Synthesis, characterisation and thermal stability of powders*. Biomaterials, 2002. **23**(4): p. 1065-1072.
27. Nijhuis, A.W., S.C. Leeuwenburgh, and J.A. Jansen, *Wet-Chemical Deposition of Functional Coatings for Bone Implantology*. Macromolecular bioscience, 2010. **10**(11): p. 1316-1329.
28. Zurick, K.M., C. Qin, and M.T. Bernards, *Mineralization induction effects of osteopontin, bone sialoprotein, and dentin phosphoprotein on a biomimetic collagen substrate*. Journal of Biomedical Materials Research Part A, 2013. **101A**(6): p. 1571-1581.
29. Nijhuis, A.W.G., et al., *Enzymatic pH control for biomimetic deposition of calcium phosphate coatings*. Acta Biomaterialia, (0).
30. Schouten, C., et al., *The effect of alkaline phosphatase coated onto titanium alloys on bone responses in rats*. Biomaterials, 2009. **30**(32): p. 6407-6417.
31. de Jonge, L.T., et al., *In vitro responses to electrosprayed alkaline phosphatase/calcium phosphate composite coatings*. Acta Biomaterialia, 2009. **5**(7): p. 2773-2782.
32. de Jonge, L.T., et al., *The osteogenic effect of electrosprayed nanoscale collagen/calcium phosphate coatings on titanium*. Biomaterials. **31**(9): p. 2461-2469.
33. Douglas, T.E., et al., *Enzymatic Mineralization of Hydrogels for Bone Tissue Engineering by Incorporation of Alkaline Phosphatase*. Macromolecular bioscience, 2012. **12**(8): p. 1077-1089.
34. Vittur, F., et al., *Alkaline phosphatase binds to collagen; a hypothesis on the mechanism of extravesicular mineralization in epiphyseal cartilage*. Experientia, 1984. **40**(8): p. 836-837.
35. Dey, A., et al., *The role of prenucleation clusters in surface-induced calcium phosphate crystallization*. Nature materials, 2010. **9**(12): p. 1010-1014.
36. Nudelman, F., et al., *The role of collagen in bone apatite formation in the presence of hydroxyapatite nucleation inhibitors*. Nature materials, 2010. **9**(12): p. 1004-1009.
37. Beertsen, W. and T. Van den Bos, *Alkaline phosphatase induces the mineralization of sheets of collagen implanted subcutaneously in the rat*. Journal of Clinical Investigation, 1992. **89**(6): p. 1974.
38. Mann, S., *Biomineralization: the form (id) able part of bioinorganic chemistry!**. Journal of the Chemical Society, Dalton Transactions, 1997(21): p. 3953-3962.

Chapter V

**Nano-sized hydroxyapatite crystals functionalized with
alendronate as bioactive components for bone implant coatings to
decrease osteoclastic activity.**

Ruggero Bosco, Michele Iafisco, Anna Tampieri, John A Jansen, Sander CG Leeuwenburgh,

Jeroen JJP van den Beucken

1. Introduction

The success of bone implants for load-bearing applications is related to the quality of bone at the interface[1]. Titanium implants have strong mechanical characteristics but lack active properties fundamental to trigger biological responses. Coatings are deposited on titanium to improve the biological properties at the interface with bone tissue. Since the inorganic phase of bone tissue is composed of nano-sized platelet-shaped hydroxyapatite (HA) crystals, various surface modification strategies have been explored to deposit HA onto titanium implants [2]. HA coatings are widely used to improve the biological performance of bone implants in terms of bone contact and new bone formation[3].However, in view of an increased life-expectancy and hence increasing number of medically compromised patients (e.g. wound healing disorders and osteoporosis), the application of bone implants for such patients is a growing challenge for orthopaedic and dental surgeons [4].Consequently, surface modification approaches for bone implants are evolving from passive materials, that merely aim to mimic the composition of bone, to active compounds which trigger desired biological responsesand improve rapid and permanent implant fixation within native bone tissue [5].

Osteoporosis is a bone metabolic disease that causes an imbalance in the bone turnover in favor of bone resorption, leading to a decreasein bone mechanical strength [6]. Alterations of bone turnover correspond to a change in the balance between osteoblast and osteoclast activity [7]. Such an imbalance between formation and resorption has an immediate effect on bone quality with a consequential reduced performance of bone implants in terms of osteointegration, bone to implant contact and in general mechanical fixation [8-10].

Generally, patients diagnosed with osteoporosis are treated systemically via oral administration of bisphosphonates to reduce osteoclast number or activity and hence decrease bone resorption[11].Bisphosphonates are based on a common backbone of P-C-P (where C is a carbon and P a phosphonate moiety) and are widely used for medical treatment since 40 years in view of their high affinity for bone apatite [12, 13]. Conventional, systemic delivery

of bisphosphonates is often associated with serious side-effects, which have raised a negative attitude by patients and the medical community toward their use. Particularly, controversies arise concerning oral administration that is often associated to osteonecrosis of the jaw (ONJ)[14] and gastric-digestive associated pathologies[15]. To circumvent these disadvantages of conventional bisphosphonate-based treatment, a therapy based on local (rather than systemic) effects of bisphosphonates is particularly appealing. Additionally, local treatment is capable of reducing the amount of drug used, which has been demonstrated for bisphosphonates by showing reduced osteoclastic activity even at low doses upon local delivery [16-18].

Boanini et al. demonstrated that nano-sized HA crystals synthesized in presence of bisphosphonates (alendronate or zoledronate) reduce osteoclast proliferation and induce osteoclast apoptosis [19]. Poorly crystalline nano-sized HA crystals (nHA) are particularly useful material in view of their specific physicochemical properties (e.g. increased specific surface area, SSA) and improved biological affinity in terms of favorable cell proliferation due to their similarity with biological ones[20]. As a strong correlation exists between nano-scale dimension (< 100 nm) and cell responses[21], the concept of using nHA for biomedical applications to control cell fate in terms of proliferation and apoptosis control is straightforward [22]. Particularly, the functionalization of nHA with bisphosphonate and subsequent deposition of this material as a coating onto bone implants represents an approach with high potential for improving bone implant fixation and survival in patients suffering from osteoporosis.

The aim of this study was to (i) quantitatively evaluate the effect of bisphosphonate-functionalized nHA (nHA_{ALE}) on osteoclast behavior, and (ii) determine the feasibility to use nHA_{ALE} to obtain a coating for bone implants. nHA was synthesized according to a previously established method[23], hereafter the amino-bisphosphonate alendronate was attached to nHA particles to obtain nHA_{ALE}. This nHA_{ALE} was characterized and its effect on osteoclast

behavior was evaluated in vitro. Further, nHA_{ALE} was deposited as a thin nanoscale coating on titanium using electrospray deposition (ESD), a coating method that offers control over the coating process and preserves the biological activity of biomolecules [24]

2. Material and methods

2.1 Synthesis and characterization of nHA

Nanosized hydroxyapatite (nHA) was synthesized and characterized according to a previously established method[23]. Briefly, nanocrystals were precipitated from a suspension of Ca(CH₃COO)₂ (0.35 M) by slow addition (1 drop s⁻¹) of an aqueous solution of H₃PO₄ (0.21 M), keeping the pH at a constant value of 10 by the addition of (NH₄)OH solution. At 24 h after the end of this precipitation reaction, the solid residue was collected by centrifugation, washed four times with ultrapure water, and suspended in 100 ml of ethanol (EtOH). Inductively coupled plasma-optical emission spectrometry (ICP-OES, Liberty 200, Varian, Clayton South, Australia) was used to determine the Ca/P ratio of nHA. For ICP-OES, nHA samples were dissolved in 1 wt% ultrapure nitric acid and the analytical wavelengths were chosen accordingly: Ca 422 nm, P 213 nm. Further, nHA was analyzed using i) transmission electron microscopy (TEM; Philips CM 100 instrument (80 kV). The powdered samples were dispersed in milliQ water and a few droplets of the slurry deposited on holey-carbon foils supported on conventional copper microgrids) to determine the dimensions, ii) x-ray diffraction (XRD; PANalytical X'Pert Pro powder diffractometer using Cu K α radiation generated at 40 kV and 40 mA, the instrument was configured with 1/2° divergence and receiving slits. The 2 θ range was from 5° to 60° with a step size (2 θ) of 0.05° and a counting time of 3 s to determine crystallinity and crystallite size, and iii) quantification of nitrogen adsorption, at 77 K following the BET model, to determine the specific surface area (SSA). The carbonate content was evaluated on dried samples by thermogravimetric analysis (TGA; Thermal Analysis SDT Q 600, TA Instruments, New Castle, DE, USA), for which the heating procedure was performed in a nitrogen flow (100 mLmin⁻¹) using an alumina sample

holder at a rate of $10\text{ }^{\circ}\text{C} \cdot \text{min}^{-1}$ up to $1200\text{ }^{\circ}\text{C}$. The degree of nHA crystallinity was calculated according to the formula (1):

$$\text{Crystallinity}[\%] = 100 \times \frac{C}{(C+A)} \quad (1)$$

where C is the area from the peaks in the XRD pattern (“the crystalline area”) and A is the area between the peaks and the background (“the amorphous area”).

2.2 Alendronate adsorption to nHA

Different amounts of alendronate sodium (A4978, Sigma Aldrich co. Ltd.) were dissolved in $500\text{ }\mu\text{l}$ of milliQ water ($0.5\text{--}2\text{ mgml}^{-1}$) and mixed with $500\text{ }\mu\text{l}$ of a suspension of nHA in EtOH for 24 h at 37°C to obtain complete adsorption of alendronate onto the nano crystals (nHA_{ALE}). Alendronate adsorption was evaluated by measuring the alendronate concentration in the supernatant solution using UV-Vis spectroscopy based on the reaction of the primary amino group with ninhydrin in a methanol medium containing 0.05 M sodium bicarbonate. The colored reaction product was measured at 568 nm $\varepsilon = 29\text{ M}^{-1}\text{cm}^{-1}$ [25]. Additionally, the amount of adsorbed alendronate was compared to the adsorption model described by a Langmuir type isotherm, in agreement with the data reported in previous studies[25], using the following equation:

$$Q_e = Q_m (K_L C_e) / (1 + (K_L C_e)) \quad (2)$$

where C_e and Q_e are the drug concentration in solution and the amount of drug adsorbed to hydroxyapatite, respectively, Q_m is the maximum saturation load, K_L is the Langmuir affinity constant of the drug to the nanocrystal surface. Thermogravimetric analyses (TGA) were carried out on the nHA_{ALE} after extensive washings and freeze-drying to discriminate between physically adsorbed (physisorbed) and strongly linked alendronate. The relative amount of linked alendronate was calculated using the following equation:

$$\text{Alendronate (wt \%)} = 100 - (\Delta w\%_{\text{Alendronate}} - \Delta w\%_{\text{nHA}_{\text{ALE}}}) \times 100 / (\Delta w\%_{\text{Alendronate}} - \Delta w\%_{\text{nHA}}) \quad (3)$$

where $\Delta w\%_{\text{Alendronate}}$, $\Delta w\%_{\text{HAA}}$ and $\Delta w\%_{\text{nHAA}_{\text{ALE}}}$ are the relative weight loss in the range 120-1200 °C of pure alendronate, nHA and nHA_{ALE}, respectively.

2.3 *Invitro osteoclast apoptosis model*

RAW 264.7 cells (ATCC, LGC Standards GmbH, Wesel, Germany) were cultured in proliferation medium consisting of α MEM (22571, Gibco, Invitrogen, life technology corporation, Carlsbad, US), 10% fetal bovine serum (FBS, Gibco), 1% gentamicin (15750, Gibco).

In order to evaluate osteoclast apoptosis, RAW 264.7 cells were seeded at 2000 cells/cm² in 8-well glass chamber slides (Thermo Scientific, 177402, Rochester, NY, USA) using proliferation medium enriched with 50 ng/ml RANKL (sRANKL, Peprotech, Rocky Hill, US) to induce osteoclastogenesis (osteoclastogenesis medium). Medium was refreshed every 2 days after the first day of seeding.

TRAP-staining (386A, Sigma Aldrich co. Ltd.) and DAPI staining (10236276, Roche, Woerden, The Netherlands) were used to visualise osteoclastic differentiation after 4 days of culture. A single osteoclast-like cell was defined as a TRAP positive cell with at least 3 nuclei, corresponding to earlier work [26]. After 4 days of culture in osteoclastogenic medium, 4 experimental groups were added (Table 2) thereafter the cell culture was extended for another 4 days:

- | | |
|-----------------------|--------------------------------------|
| • Control | no added components |
| • nHA | 32 μ g/ml (final concentration) |
| • nHA _{ALE} | 32 μ g/ml (final concentration) |
| • Alendronate control | 3.2 μ g/ml (final concentration) |

The ratio between attached alendronate and hydroxyapatite was fixed to 1:10 (wt:wt) for the in vitro experiment. This ratio was set to assure that 100% of dissolved alendronate would be adsorbed on the suspended nHA in 24 hrs according to previous test performed (data not

shown). Quantification of osteoclast-like cells was performed by counting the number of osteoclast-like cells per field of view using a light microscope equipped with a digital camera (Axio Imager Microscope Z1, Carl Zeiss Micro imaging GmbH, Göttingen, Germany).

2.4 Coating deposition

Titanium substrates (commercially pure, 5 mm Ø, 2 mm thickness) and silicon wafer (Wafernet, Siltronic, Portland, USA) were coated using electrospray deposition (ESD) with commercially available vertical ESD equipment (ES-2000s, Fience Ltd., Japan). Suspensions of nHA and nHA_{ALE} were prepared at a final concentration of 3 mg/ml in EtOH/H₂O (50/50 vol%). During deposition, the following settings were applied: flow rate 4 µl/min, nozzle to substrate distance 40 mm, humidity 40%, voltage 10-12 kV[27, 28]. The deposition time was 5, 15 or 30 minutes for titanium disks and 30 minutes for silicon wafers used to determine coating thickness.

2.5 Coating characterisation

The calcium amount within the deposited coatings was determined using the ortho-cresolphthalein (OCPC) method (Sigma Aldrich co. Ltd.)[29] after immersing coated titanium substrates overnight in 0.5 N acetic acid on a shaker table. For analyses, 300 µL of work reagent was added to 10 µL aliquots of sample or standard in a 96-wells plate. The plate was incubated for 10 min at room temperature, and then the plate was read at 570 nm. Serial dilutions of CaCl₂ (0–100 µg · mL⁻¹) were used for the standard curve. To evaluate the total amount of hydroxyapatite deposited on samples, a standard curve was made by dissolving known amounts of nHA synthesized according to the method described above.

Morphological analysis of the coating after deposition was performed using scanning electron microscopy (SEM; FESEM, JEOL 6330, Tokyo Japan). Atomic force microscopy (AFM) was carried out directly on the titanium disks and on silicon wafers. AFM imaging was performed

using a Digital Instruments Nanoscope IIIa Multimode SPM (Digital Instruments, Santa Barbara, CA, USA). The samples were analysed in contact mode using a J scanner and silicon nitride tips (200 μm long with nominal spring constant of 0.06 N/m). Coating thickness and roughness (R_a) were determined using atomic force microscopy (AFM) on coated silicon wafers.

Chemical analysis of the coating was investigated using x-ray photoemission spectroscopy (XPS). Analyses were performed in an S-Probe (Surface Science Instruments, Mountain View, CA, USA) instrument equipped with a monochromatic Al K α source (1486.6 eV) at a spot size of 200 \times 750 μm and a pass energy of 25 eV, providing a resolution of 0.74 eV.

2.6 Statistical analysis

Analysis of quantitative data was performed using a one-way ANOVA combined with a post-hoc Tukey-Kramer multiple comparison test to detect significant differences at a significance (p-value) level of $p < 0.05$. Comparison between average of pair sets of data was performed using Student's t-test. Results are reported as mean \pm standard deviations.

3. Results

3.1 Synthesis and characterization of nHA

nHA was obtained via precipitation from calcium acetate and phosphoric acid. TEM showed that nHA had plate-like shape and nanometric dimensions (<50 nm, data not shown). ICP indicated a bulk Ca/P ratio of 1.62 and TGA revealed the presence of carbonate species at 1.3 wt%. The specific surface area (SSA) was determined at $160 \pm 16 \text{ m}^2\text{g}^{-1}$ and XRD analysis (data not shown) revealed a semi-crystalline (61% crystallinity) structure and crystallite size of 23 and 9 nm (determined along the (002) and (310) directions, respectively) [23]. An overview of the composition, SSA, crystallite size and crystallinity is presented in Table 1.

Table 1 Compositional features (bulk Ca/P, carbonate content), specific surface area (SSA), average size of crystal domains (along the $[0, 0, 2]$ and $[3, 1, 0]$ directions), and degree of crystallinity of the synthesized HA nanocrystals.

	Bulk Ca/P [mol]	Carbonate species [wt%]	SSA [m^2g^{-1}]	D_{002} [nm]	D_{310} [nm]	Degree of Crystallinity
nHA	1.62 ± 0.02	1.3 ± 0.1	160 ± 16	23 ± 4	9 ± 3	$61\% \pm 5$

3.2 nHA functionalized with alendronate

Quantification of the total adsorbed alendronate onto nHA (physisorbed and strongly attached) is presented as an isotherm in Figure 1A, where the alendronate amount (mg of alendronate on mg of nHA) is plotted as a function of the drug concentration remaining in solution after adsorption. The amount adsorbed (Q_m) was 0.43 mg/mg and the affinity constant for alendronate (K_L) was 10.9 ml/mg were calculated according to the Langmuir adsorption model. The obtained value of K_L is similar to those already reported for alendronate adsorption[30]. The presence of the adsorption plateau at low equilibrium concentration is an indicator of high affinity of alendronate for the surface of nHA. The increase of alendronate concentration in contact with the nanocrystals increased the surface coverage, reaching a maximum amount of drug surface immobilization of 0.39 mg/mg (calculated as plateau value of the isotherm curve).

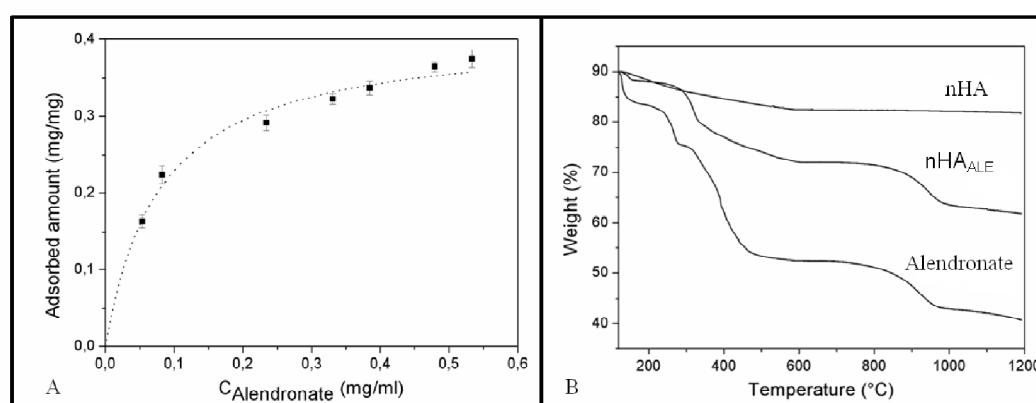


Figure 4. (A) Adsorption isotherm of alendronate on nHA. Separate points are experimental data, dotted line is the curve fitting according to the Langmuir model. The adsorbed amount is determined as difference between the known quantity of added alendronate and the amount detected in the supernatant. $C_{\text{Alendronate}}$ represents the remaining concentration of alendronate in the solution after the adsorption. (B) Thermogravimetric analyses (TGA) curves of nHA, nHA_{ALE} and alendronate.

The TGA curves of nHA, alendronate and nHA_{ALE} (loaded with a maximum amount of drug) are presented in Figure 1B. The amount of alendronate attached to nHA calculated by TGA was 29.5 wt%, which corresponds to a maximum drug surface immobilization on nHA of about 0.42 mg/mg. This value is very close to the one calculated by isotherm indicating that

all the alendronate used for the functionalization is strongly attached to nHA and that the maximum drug surface immobilization on nHA was about 0.41 mg/mg.

The bound of alendronate to nHA was verified by FTIR analysis (Figure 2). The FTIR spectra of the nHA_{ALE} showed the typical molecular fingerprints of apatite (1045, 609 and 580 cm⁻¹) [31] and alendronate (1545, 1137, 1073 cm⁻¹) [32]. The wavelengths of the bands recorded for the free alendronate attributed to the phosphonates groups (900-1200 cm⁻¹) were slightly shifted in the spectra of nHA_{ALE} confirming the formation of a chemical link on with the nHA surface.

For the in vitro tests as well as for the ESD deposition, nHA_{ALE} was designed with 10 wt% of alendronate to reduce the amount of drug dissolved in solution.

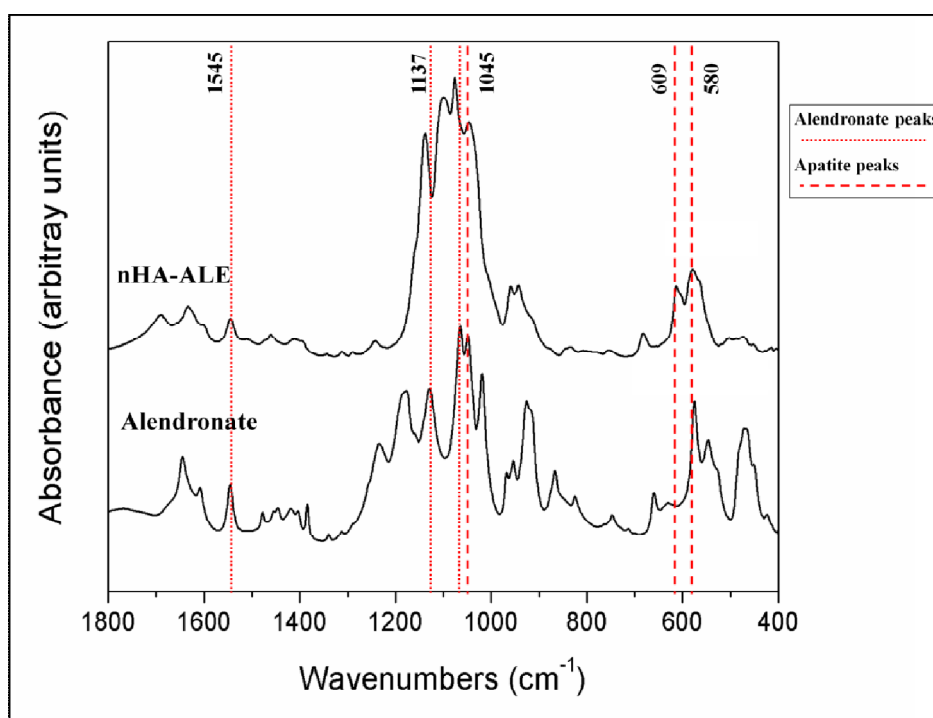


Figure 2. FTIR spectra of alendronate and nHA_{ALE}. Representative peaks of the hydroxyapatite and of alendronate are also reported

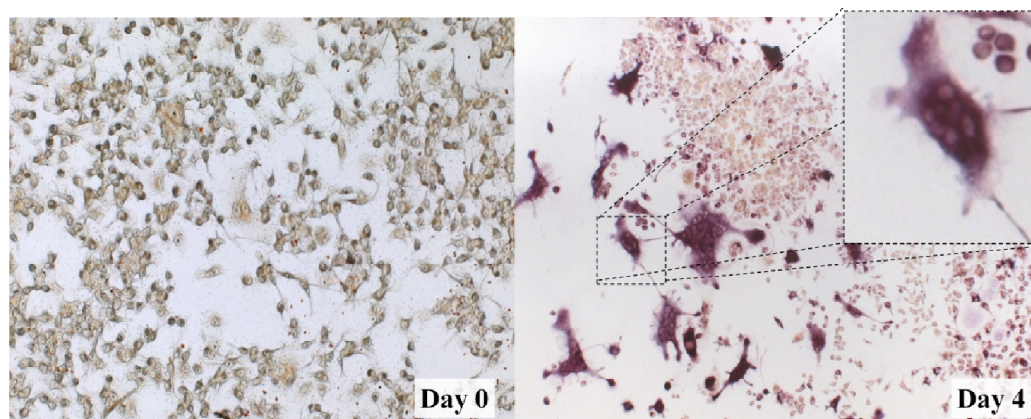


Figure 3 Osteoclastogenesis. Effect on RAW 264.7 cells after 4 days of culture in medium enriched with RANKL [50ng/ml]. TRAP staining and presence of 3 or more nuclei were used as parameters to detect formation of osteoclast-like cells.

3.3 In-vitro osteoclast apoptosis model

Therefore nHA_{ALE} was designed with 10 wt% of adsorbed alendronate to obtain the total chemical adsorption onto nHA, reducing the amount of alendronate dissolved in solution. Osteoclastogenesis was confirmed by TRAP and DAPI stains performed at day 4 on RAW 264.7 cells cultured with RANKL-enriched medium. The changes in cell morphology and appearance are indicators of the formation of osteoclast-like cells (TRAP positive membrane, 3 or more nuclei) as shown in Figure 3.

Figure 4A presents representative microscopic images for each experimental group at the end of the culture, showing the effect of the different compounds added to osteoclastogenesis medium on the cells. The number of osteoclast-like cells was reduced for ALE and nHA_{ALE} compared to the control and nHA. Further, all experimental groups show multiple viable undifferentiated cells.

Quantitative analysis of the number of osteoclast-like cells per field of view is presented in Figure 4B. The average number of osteoclast-like cells that were alive at day 8 was calculated and compared to the control group. The presence of nHA_{ALE} (4 ± 2 cells/field of view) and ALE (1 ± 1 cells/field of view) significantly ($p < 0.01$) reduced the number of osteoclast-like

cells compared to the control (20 ± 2 cells/field of view). The addition of nHA has no effect in the osteoclast-like cells number (16 ± 3 cells/field of view).

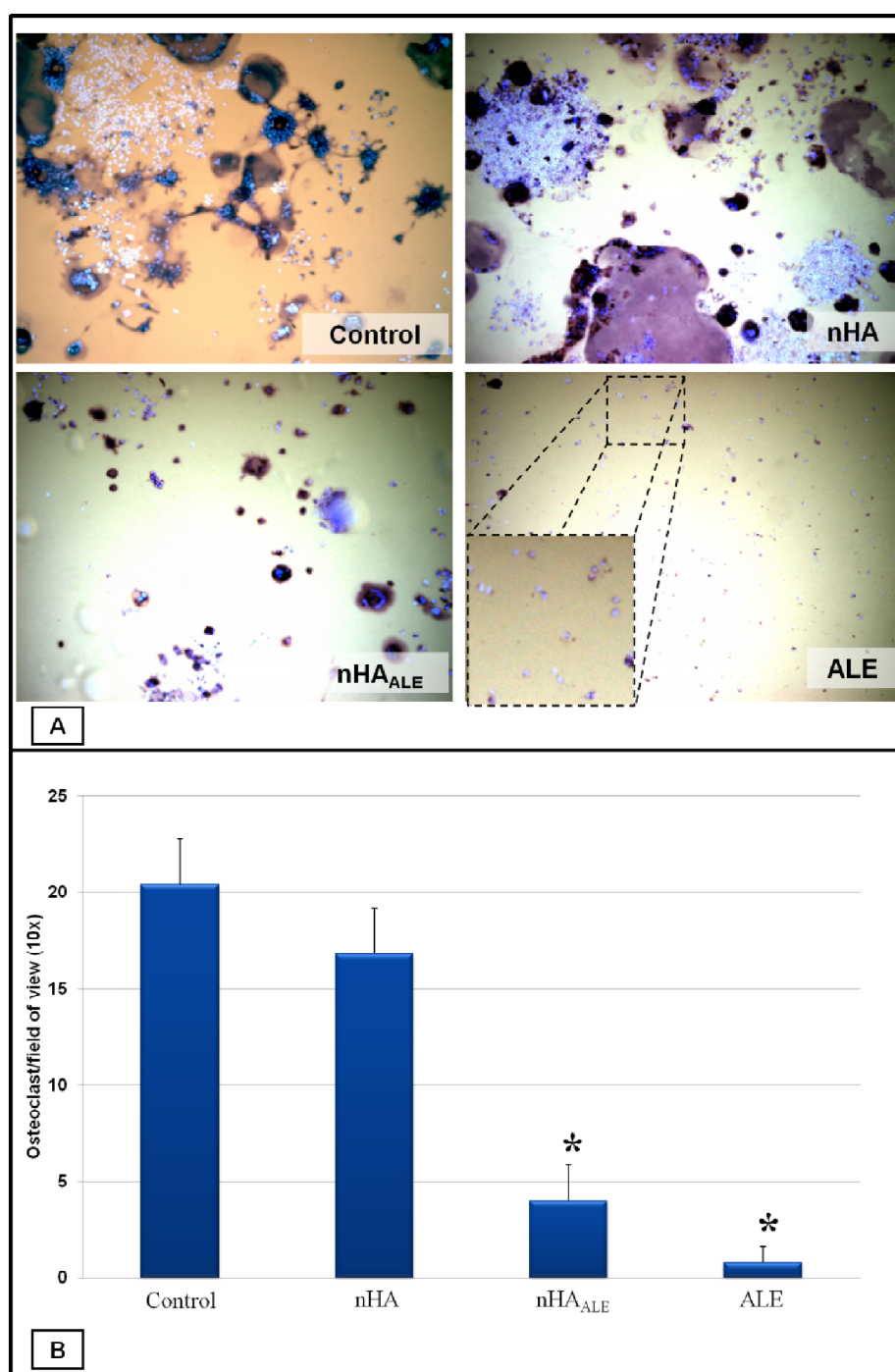


Figure 4 Effect of alendronate-hydroxyapatite on osteoclasts. (A) Visualization at day 8 of apoptosis in control group, nHA, nHA_{ALE} and alendronate. TRAP and DAPI staining, 10x magnification, day 4, 2000 cells/cm². (B) Quantification of osteoclasts per field of view. Osteoclasts have been counted only in presence of 3 or more nuclei and TRAP positive membrane. Variance analysis has been performed (ANOVA); * indicate a significant difference ($p < 0,01$) compared to control group.

3.4 Deposition and coating characterization

The coatings prepared using nHA and nHA_{ALE} showed a complete coverage at 30 minutes (Figure 5 A, B) based on SEM images and AFM analysis. Titanium disks coated with nHA_{ALE} revealed a tendency of the nanocrystals to agglomerate into microstructures (0.5-1 μm) compared to nHA. AFM performed on silicon wafers revealed a thickness of 570 nm for nHA and 771 nm for nHA_{ALE}. R_a calculation showed a significantly ($p = 0.034$, $n=5$) increased roughness on nHA_{ALE} (290 nm) compared to nHA (235 nm) coated wafers as reported in Figure 5B.

The amount of nHA and nHA_{ALE} coated onto titanium disks showed a linear increase in coating thickness as a function of deposition time (Figure 5C). Titanium disks coated with nHA_{ALE} showed a higher amount of deposited material at all time points. After 30 minutes of deposition, the analyzed samples were coated with up to 9 $\mu\text{g}/\text{cm}^2$ of nHA_{ALE} and 3 $\mu\text{g}/\text{cm}^2$ of nHA despite the identical starting concentration.

XPS spectroscopy of coated disks confirmed the presence of alendronate after deposition (Table 3), as shown by a nitrogen (N) signal and the increased relative amount of P with the resulting decrease of Ca/P ratio. The titanium (Ti) signal appeared only in the coating made of sprayed alendronate, indicating good coverage and homogeneity obtained for coatings consisting of nHA as well as nHA_{ALE}.

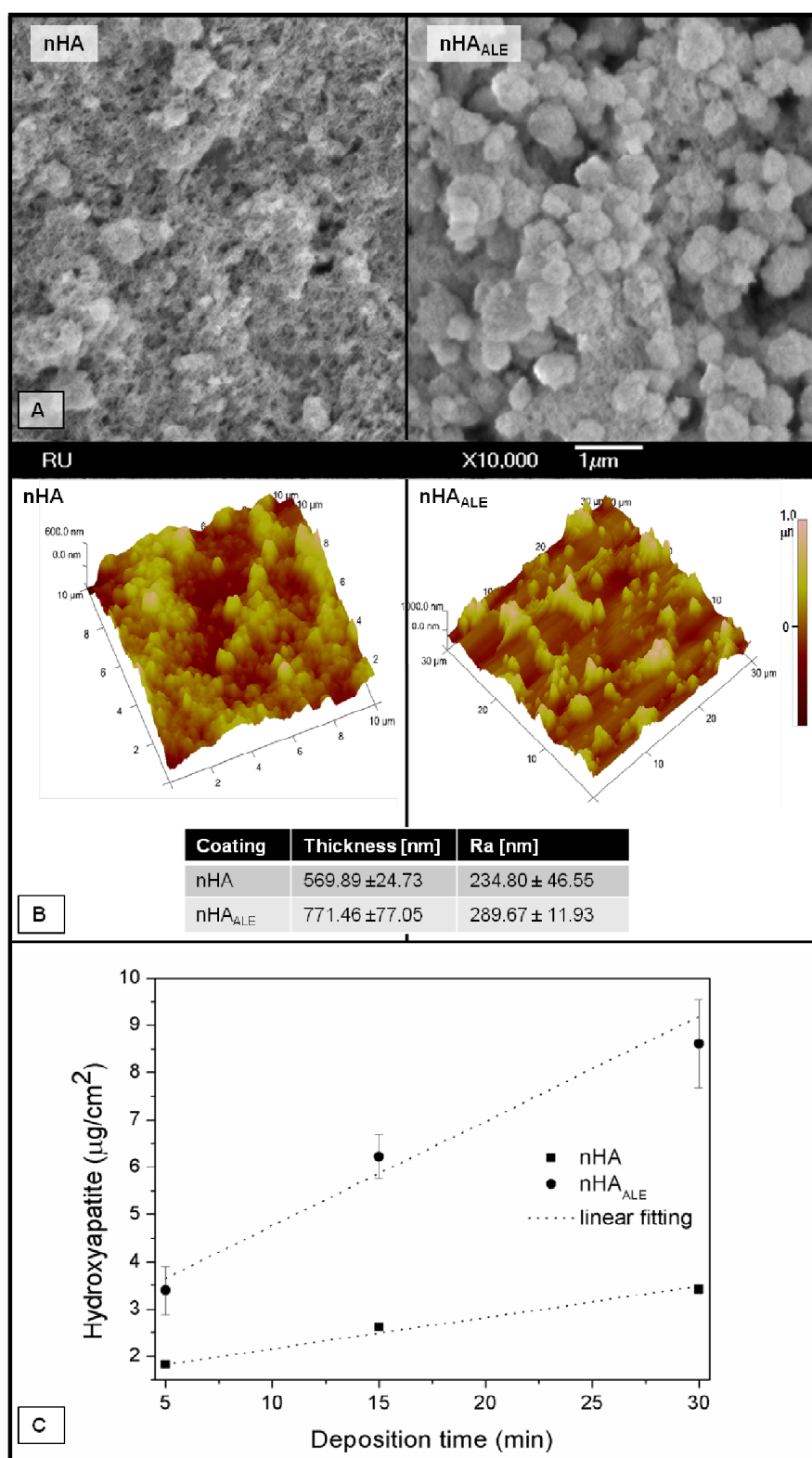


Figure 5 (A) FESEM surface morphology evaluation of nHA and nHA_{ALE} coated Ti after ESD deposition. (B) AFM analysis: images of coated titanium and thickness characterization performed on silicon wafers. (C) Quantification of deposited hydroxyapatite performed with modified OCPC. Disks were freeze dried before analysis

4. Discussion

The aims of this study were to evaluate i) the efficacy of functionalized alendronate-hydroxyapatite nanocrystals (nHA_{ALE}) to reduce osteoclast number, and ii) the feasibility to use this material for the preparation of bone implant coatings with a specific therapeutic effect. For this purpose, nHA was synthesized to obtain crystals within the nanoscale range (<100 nm) and with a highSSA (160 m²/g). Alendronate, a well-established anti-osteoporotic drug, was adsorbed to nHA to obtain nHA_{ALE}. The hypotheses were that a potent osteoclast inhibitor drug could be adsorbed to nanocrystals and preserve its ability to induce osteoclast apoptosis. The therapeutic capacity of nHA_{ALE} was tested as well as the feasibility of generating bone implant coatings with nHA_{ALE}. Using an in vitro osteoclast apoptosis model, it was shown that nHA_{ALE} significantly reduced the number of osteoclast-like cells. Further, the preparation of nHA_{ALE} coatings using ESD was shown to be feasible resulting in homogeneous, alendronate-containing nanoscale coatings with a slightly increased roughness compared to alendronate-free nHA coatings.

The method to synthesize nHA was selected to obtain nanocrystals with a high SSA able to bind a high percentage (in weight) of bisphosphonate (BP) that has been estimated to reach up to 30 wt%. The presence of alendronate on the crystals after interaction was proven by FTIR and TGA analysis. The adsorption isotherm fitted well with a Langmuir type isotherm in agreement with the data reported in previous studies[30], suggesting that BPs are strongly attached to nHA by interactions at the calcium site where the bidentate and tridentate coordination of the P-C-P and -OH domains of the BPs are known to act. The obtained values are in good agreement with the maximum alendronate uptake calculated by UV-Vis (0.39 mg/mg), by TGA (0.42 mg/mg) and with the theoretical maximum amount calculated according to the Langmuir model (0.43 mg/mg), indicating that all alendronate adsorbed on nHA was chemically linked and that the amounts of physisorbed drug were negligible. These findings confirm the strong interaction of alendronate to the nHA, most likely by the chemical

link of phosphonate groups of alendronate with the calcium ions of nHA and through the formation of hydrogen bonds of the alendronate amino group with the nHA surface[33]. Moreover, the presence of amine moieties in alendronate allows additional interactions due to the formation of N-H-O hydrogen bonds on the nHA surface[33].

A modified in vitro test[34] was designed to evaluate the biological activity of nHA_{ALE}. RAW 264.7 cells were selected to obtain osteoclast-like cells via an osteoclastogenesis procedure. The in vitro set-up was designed with dispersed ceramic nanoparticles (i.e. nHA or nHA_{ALE}) or dissolved alendronate in the medium to test the biological efficacy of nHA_{ALE} without any potential effects of coating topography. Osteoclast-like cells cultured for 4 days in medium containing alendronate or nHA_{ALE} showed a tendency of precocious apoptosis when compared to the control group or nHA-enriched medium. These results indicated an active role for nHA_{ALE} in decreasing the number of viable osteoclasts. Potential cytotoxic effects of the nanocrystal materials can be excluded, as the presence of several viable undifferentiated RAW 264.7 cells were observed in all culture wells, even after treatment with alendronate or nHA_{ALE}. The effect of nHA_{ALE} was comparable to the effect of the same amount of pure alendronate; osteoclast-like cells number was reduced about five folds compared to the control group.

Bioinorganic coatings with anti-osteoporotic properties could be a promising solution for numerous compromised implant applications since the presence of a drug regulating bone turnover such as alendronate, released only in situ and in close presence of osteoclasts, is interesting to obtain biomaterials which are able to locally improve the bone/implants interaction in osteoporotic conditions. Electrospray deposition (ESD) has been used to achieve deposition without compromising the biological activity of adsorbed alendronate. Deposition was performed at room temperature and with aqueous solutions to preserve the chemical structure of the bisphosphonate; nHA_{ALE} was deposited with a thickness of 700 nm and a roughness (Ra) of 290 nm. Elemental analysis (performed using XPS) confirmed the presence

of nitrogen and an increased amount of phosphorous on the surface of nHA_{ALE} coated disks. These traces were considered proof for the nHA-mediated immobilization of amino-bisphosphonate alendronate onto coated disks. The comparison of nHA and nHA_{ALE} coatings showed a threefold difference in the quantity of deposited material in favor of nHA_{ALE}. Analyses performed with SEM induced to consider the increased roughness and the presence of micro a reason for this discrepancy.

Despite other methods to incorporate alendronate or other bisphosphonates onto bone implants, in this study alendronate was directly linked to nHA. Previous approaches used dual step procedures where implants pre-coated with calcium phosphate were immersed in a medium containing dissolved bisphosphonate. Such procedures lack control over drug quantity and the amounts of loaded bisphosphonate (via adsorption to the outer layer of the coating) are limited [18]. The advantage that was obtained with nHA_{ALE} in combination with ESD is the strong control over the quantity of bisphosphonate loading. The strong linearity between time and amount of deposited material allows regulating and controlling the final amount of deposited drug. Other methods to incorporate bisphosphonate as a co-precipitation compound during the synthesis of calcium phosphate crystals could reduce the therapeutic effect of the bisphosphonate loaded onto bigger hydroxyapatite crystals obtained due to high temperature of synthesis (90 ° C). Co-precipitation can also suffer from a lack of efficiency requiring to dissolve more bisphosphonate to obtain loaded value comparable to the one that was described in this study [19, 35].

5. Conclusions

Since the unbalance between osteoclasts and osteoblasts in patients with bone metabolic disease can be an obstacle to bone implant success, coatings that actively aim at correcting this unbalance are required to recover bone turnover and improve osteointegration of bone implants. In the presented study, it was described a method to adsorb anti-osteoporotic drug onto nano-sized hydroxyapatite crystals and a solution to deposit such materials onto titanium implants. Nano hydroxyapatite crystals mimicking natural bone size and shape, but enriched with bisphosphonate, could represent a potent material able to target specifically osteoclast cells and capable of reducing the amount of administered drug. Osteoporotic patients can benefit from such coated implants to regain load-bearing functions (i.e. mastication or gait cycle) owing to a locally improved bone quality.

References

- [1] Albrektsson, T., et al., *The interface zone of inorganic implantsIn vivo: Titanium implants in bone*. Annals of biomedical engineering, 1983. **11**(1): p. 1-27.
- [2] Furlong, R. and J. Osborn, *Fixation of hip prostheses by hydroxyapatite ceramic coatings*. Journal of Bone & Joint Surgery, British Volume, 1991. **73**(5): p. 741-745.
- [3] Alghamdi, H.S., et al., *Biological response to titanium implants coated with nanocrystals calcium phosphate or type I collagen in a dog model*. Clinical oral implants research, 2012. **24**(5), p. 475-483
- [4] Bosco, R., et al., *Surface Engineering for Bone Implants: A Trend from Passive to Active Surfaces*. Coatings, 2012. **2**(3): p. 95-119.
- [5] Bosco, R., et al., *Instructive coatings for biological guidance of bone implants*. Surface and Coatings Technology, 2013. **233**, p. 91-98.
- [6] Risk, W.S.G.o.A.o.F. and i.A.t.S.f.P. *Osteoporosis, Assessment of fracture risk and its application to screening for postmenopausal osteoporosis*. 1994: World Health Organization.
- [7] Manolagas, S.C. and R.L. Jilka, *Bone marrow, cytokines, and bone remodeling. Emerging insights into the pathophysiology of osteoporosis*. The New England journal of medicine, 1995. **332**(5): p. 305.
- [8] Wronski, T., C. Walsh, and L. Ignaszewski, *Histologic evidence for osteopenia and increased bone turnover in ovariectomized rats*. Bone, 1986. **7**(2): p. 119-123.
- [9] Keller, J.C., et al., *Osteoporosis-like bone conditions affect osseointegration of implants*. The International journal of oral & maxillofacial implants, 2004. **19**(5): p. 687.
- [10] Fini, M., et al., *Osteoporosis and biomaterial osteointegration*. Biomedicine & Pharmacotherapy, 2004. **58**(9): p. 487-493.
- [11] Russell, R.G.G. and M.J. Rogers, *Bisphosphonates: from the laboratory to the clinic and back again*. Bone, 1999. **25**(1): p. 97-106.
- [12] Russell, R.G.G., et al., *Mechanisms of action of bisphosphonates: similarities and differences and their potential influence on clinical efficacy*. Osteoporosis International, 2008. **19**(6): p. 733-759.
- [13] Abtahi, J., P. Tengvall, and P. Aspenberg, *Bisphosphonate coating might improve fixation of dental implants in the maxilla: A pilot study*. International journal of oral and maxillofacial surgery, 2010. **39**(7): p. 673-677.
- [14] Ruggiero, S.L., et al., *Osteonecrosis of the jaws associated with the use of bisphosphonates: a review of 63 cases*. Journal of oral and maxillofacial surgery, 2004. **62**(5): p. 527-534.
- [15] Cryer, B. and D.C. Bauer, *Oral Bisphosphonates and Upper Gastrointestinal Tract Problems: What Is the Evidence?* Mayo Clinic Proceedings, 2002. **77**(10): p. 1031-1043.
- [16] Sato, M., et al., *Bisphosphonate action. Alendronate localization in rat bone and effects on osteoclast ultrastructure*. Journal of Clinical Investigation, 1991. **88**(6): p. 2095.
- [17] Marx, R.E., et al., *Bisphosphonate-induced exposed bone (osteonecrosis/osteopetrosis) of the jaws: risk factors, recognition, prevention, and treatment*. Journal of oral and maxillofacial surgery, 2005. **63**(11): p. 1567-1575.
- [18] Cattalini, J.P., et al., *Bisphosphonate-based strategies for bone tissue engineering and orthopedic implants*. Tissue Engineering Part B: Reviews, 2012. **18**(5): p. 323-340.
- [19] Boanini, E., et al., *Alendronate-hydroxyapatite nanocomposites and their interaction with osteoclasts and osteoblast-like cells*. Biomaterials, 2008. **29**(7): p. 790-796.
- [20] Zhou, H. and J. Lee, *Nanoscale hydroxyapatite particles for bone tissue engineering*. Acta Biomaterialia, 2011. **7**(7): p. 2769-2781.
- [21] Shi, Z., et al., *Size effect of hydroxyapatite nanoparticles on proliferation and apoptosis of osteoblast-like cells*. Acta Biomaterialia, 2009. **5**(1): p. 338-345.
- [22] Zhou, G.S., et al., *Different effects of nanophase and conventional hydroxyapatite thin films on attachment, proliferation and osteogenic differentiation of bone marrow derived mesenchymal stem cells*. Bio-medical materials and engineering, 2007. **17**(6): p. 387-395.
- [23] Iafisco, M., et al., *Electrostatic Spray Deposition of Biomimetic Nanocrystalline Apatite Coatings onto Titanium*. Advanced Engineering Materials. **14**(3): p. B13-B20.
- [24] de Jonge, L.T., et al., *Organic-inorganic surface modifications for titanium implant surfaces*. Pharmaceutical research, 2008. **25**(10): p. 2357-2369.

-
- [25] Iafisco, M., et al., *Adsorption and conformational change of myoglobin on biomimetic hydroxyapatite nanocrystals functionalized with alendronate*. Langmuir, 2008. **24**(9): p. 4924-30.
- [26] TAKAHASHI, N., et al., *Osteoclast-like cell formation and its regulation by osteotropic hormones in mouse bone marrow cultures*. Endocrinology, 1988. **122**(4): p. 1373-1382.
- [27] de Jonge, L.T., et al., *In vitro responses to electrosprayed alkaline phosphatase/calcium phosphate composite coatings*. Acta Biomaterialia, 2009. **5**(7): p. 2773-2782.
- [28] Leeuwenburgh, S.C.G., et al., *Influence of precursor solution parameters on chemical properties of calcium phosphate coatings prepared using Electrostatic Spray Deposition (ESD)*. Biomaterials, 2004. **25**(4): p. 641-649.
- [29] van den Dolder, J., et al., *Flow perfusion culture of marrow stromal osteoblasts in titanium fiber mesh*. Journal of Biomedical Materials Research Part A, 2003. **64A**(2): p. 235-241.
- [30] Pascaud, P., et al., *Interaction between a Bisphosphonate, Tiludronate, and Biomimetic Nanocrystalline Apatites*. Langmuir, 2013. **29**(7): p. 2224-2232.
- [31] Rehman, I. and W. Bonfield, *Characterization of hydroxyapatite and carbonated apatite by photo acoustic FTIR spectroscopy*. Journal of Materials Science: Materials in Medicine, 1997. **8**(1): p. 1-4.
- [32] Ananchenko, G., J. Novakovic, and A. Tikhomirova, *Alendronate sodium*. Profiles of drug substances, excipients, and related methodology, 2012. **38**: p. 1-33.
- [33] Russell, R.G., et al., *Mechanisms of action of bisphosphonates: similarities and differences and their potential influence on clinical efficacy*. Osteoporos Int, 2008. **19**(6): p. 733-59.
- [34] Félix Lanao, R.P., et al., *RANKL delivery from calcium phosphate containing PLGA microspheres*. Journal of Biomedical Materials Research Part A, 2013. **101**(11), p.3123-3130.
- [35] Bigi, A., et al., *Biofunctional alendronate-hydroxyapatite thin films deposited by matrix assisted pulsed laser evaporation*. Biomaterials, 2009. **30**(31): p. 6168-6177.

Chapter VI

Synergistic effects of bisphosphonate and calcium phosphate nanoparticles on peri-implant bone response in osteoporotic rats

Hamdan S. Alghamdi[†], Ruggero Bosco[†], Sanne K. Both, Michele Iafisco, Sander C.G. Leeuwenburgh, John A. Jansen, Jeroen J.J.P. van den Beucken

Biomaterials, 2013, 34.15: 3747-3757.

1. Introduction

The use of bone implants in dental or orthopedic rehabilitation is generally successful as reflected by 10-year survival rates of 95% in healthy patients.^[1] In the clinic, however, the aging patient population challenges the use of implants due to general as well as oral health issues in modern societies. For instance, osteoporosis, a common systemic bone disease, develops with age and is more prevalent in women and men aged above 50 years.^[2] The prevalence of osteoporosis has been reported to increase up to 70% in patients at 80 years old. Worldwide, osteoporosis affects approximately 200 million people and the national osteoporosis foundation (NOF) estimates that over 40 million people in the USA already have osteoporosis or are at high risk in 2020.^[3,4] Osteoporosis is characterized by a severe decrease in bone mass and alteration of trabecular bone microstructure due to an imbalance between bone resorption (by osteoclasts) and bone formation (by osteoblasts).^[5] Further, it has been shown that bone healing in osteoporosis is impaired and the biological activity of bone cells is negatively influenced.^[6] For bone implant treatment in osteoporotic patients, the osteoporotic condition impedes primary stability, biological fixation and final osseointegration.^[7] As such, the application of bone implants in osteoporotic patients remains a clinical challenge in dental and orthopedic surgery.

For successful implant osseointegration, the bone-implant interface has to interact optimally with the bone tissue in the implant vicinity. For medically healthy patients, new bone (i.e. woven bone) is formed directly in contact with the implant surface by osteoblastic cells, where after it transforms into mature bone.^[8] This interaction can be improved by implant-related factors, such as implant design, surgical technique, and osteophilicity of the implant surface.^[9] Because the implant surface directly interacts with bone tissue, a variety of surface modifications have been explored.^[10] The currently available surface modifications aim to combine advantages of physical properties (e.g. roughness) with bioactive cues (i.e. bone-bonding) to improve implant integration.^[11] Over the past two decades, calcium phosphate

(CaP) coatings have demonstrated to favor the healing response to the implant surface and hence to enhance peri-implant bone formation.^[12,13] The presence of a CaP coating at the implant surface is anticipated to facilitate colonization by mesenchymal precursor cells and upregulate specific gene expression in the vicinity of the implant.^[14] Recently, it was shown that electrostatic spray deposition (ESD) enables the functionalization of implant surfaces with CaP nanoparticles (nCaP) that mimic the mineral component of natural bone.^[15] An additional advantage of ESD is that it enables the deposition of nCaP in combination with organic biomolecules such as collagen proteins, growth factors, peptides, or other therapeutic agents.^[16] As a consequence, a novel generation of therapeutic implant coatings can be synthesized that instruct bone cells by releasing drug molecules locally around the implant surface, especially for compromised conditions such as osteoporosis.^[17,18] In clinical practice, the deposition of nCaP in combination with therapeutic implant coatings might have a dual effect during bone-implant integration, and their concomitant use may offer a simultaneous targeting of peri-implant bone anabolic/catabolic processes. Particularly bisphosphonates (BPs) are appealing for such purpose, as their therapeutic function to inhibit osteoclast proliferation and activity can be exploited for local effects in the vicinity of an implant surface toward improved implant fixation^[19]. In view of this, the idea for therapeutic nCaP/BP coatings for bone implants represents an appealing approach to improve bone responses and implant integration in osteoporotic conditions.

The present study aimed to evaluate the efficacy of an ESD-derived nCaP/BP coating on peri-implant bone response in osteoporotic as well as healthy conditions using an established rat femoral condyle implantation model.^[20] At 4 weeks post-implantation, histological, histomorphometrical, and microcomputed tomography (μ CT) were performed. In addition to conventional histological analysis, we also performed real-time polymerase chain reaction (RT-PCR) after 4 weeks of healing to evaluate osteogenic gene expression in the peri-implant bone in osteoporotic and healthy conditions.

2. Results

2.1. Rat osteoporotic model

To establish an osteoporotic condition, 60 skeletally-mature male Wistar rats were subjected to gonadal tissue removal and sham operations.^[20,21] *In vivo*, 6-weeks monitoring of trabecular bone in femoral condyles (i.e. implantation site) via small-animal micro-computed tomography (*in-vivo* μ CT) imaging showed rapid bone morphological changes for hypo-gonadism rats. The measurements revealed significantly lower trabecular bone volume (%BV), trabecular thickness (Tb.Th mm), trabecular number (Tb.N mm⁻¹), and significantly higher trabecular spacing (Tb.Sp mm) for hypo-gonadism compared to healthy rats (Table 1). After confirmation of the osteoporotic condition in hypo-gonadism rats, implants coated with nCaP, bisphosphonate, or bisphosphonate-loaded nCaP were installed bilaterally in the femoral condyles of hypo-gonadism (osteoporotic) and sham-operated (healthy) rats. Non-coated implants served as control. Post-operatively, rats were allowed to move freely without any restrictions. The animals returned to normal activity within 12 hours following implantations. Daily monitoring did not show significant changes in animal activity and feeding behavior. No wound complications or implant failures were observed within the 4-week implantation period.

Table 1: Quantifying trabecular bone morphology post-hypogonadism using *in-vivo* μ CT. The measurements (mean \pm SD) represent trabecular bone volume (%BV), thickness (Tb.Th mm), number (Tb.N mm⁻¹), and spacing (Tb.Sp mm).

	%BV	Tb.Th mm	Tb.N mm ⁻¹	Tb.Sp mm
Osteoporotic condition	14.69 \pm 2.90	0.06 \pm 0.01	2.64 \pm 0.23	0.33 \pm 0.04
Healthy condition	33.05 \pm 4.81*	0.07 \pm 0.01*	4.58 \pm 0.18*	0.15 \pm 0.02*

* indicates significant difference between rows (P<0.05)

2.2. Bone-implant interfacial histology after 4 weeks

The morphology of the bone tissue in the peri-implant area was investigated histologically (methylene blue and basic fuchsin stain). Figure 1.a,b shows overview images of the peri-implant area for all experimental implants and magnifications of the implant-bone interface. High amounts of remote bone tissue were observed around nCaP/BP- and BP-coated implants for both osteoporotic and healthy conditions. Lower amounts of bone, occasionally with layers of fibrous tissue at the bone-implant interface, were observed for non-coated and BP-coated implants. Trabecular bone was observed in direct contact with the surfaces of nCaP- and nCaP/BP-coated implants for both osteoporotic and healthy conditions. Further, newly formed bone could be clearly discriminated from old bone in the bone/implant interfacial area of nCaP/BP-coated implants (Figure 1.c).

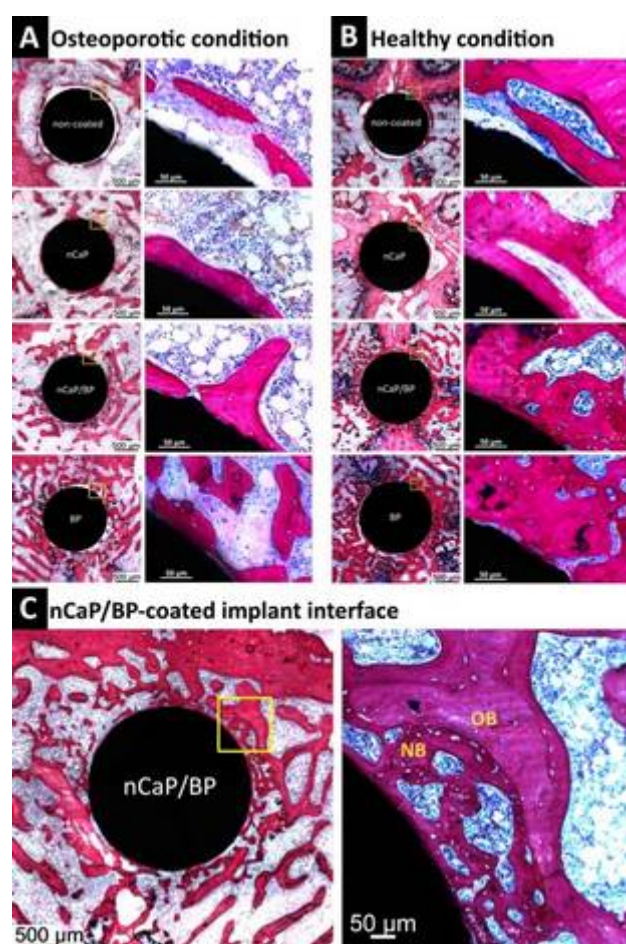


Figure 1. Histology sections of implants with various coating demonstrating the morphology of the bone tissue in the peri-implant interfaces at 4-weeks. (A and B) Images for all experimental implants and magnifications (x400) of yellow boxes show high amount of bone tissue around the nCaP/BP- and BP-coated implants in osteoporotic and healthy conditions compared to non-coated implants. Trabecular bone shows in direct contact with the surfaces of nCaP- and nCaP/BP-coated implants in both osteoporotic and healthy conditions. (C) Newly formed bone (NB) could be clearly discriminated from old bone (OB) in the bone/implant interfacial area of nCaP/BP-coated implants.

Table 2. Quantifying peri-implant bone formation and integration by ex-vivo μ CT and histomorphometrical analyses after 4-weeks. Data represents mean \pm SD for experimental groups in osteoporotic and healthy conditions.

		Ex-vivo μ CT examination		Histomorphometrical analysis		
		n	Bone volume [%BV]	n	Bone area [%BA]	Bone-implant contact [%BIC]
Osteoporotic condition	<i>non-coated</i>	4	25.62 \pm 8.97	7	33.02 \pm 10.02	9.5 \pm 10.53
	<i>nCaP</i>	4	31.52 \pm 5.66	7	29.28 \pm 11.30	49.13 \pm 32.02 ^a
	<i>nCaP/BP</i>	4	47.04 \pm 11.64 ^a	7	39.66 \pm 11.57	50.50 \pm 42.94 ^a
	<i>BP</i>	4	44.69 \pm 1.94 ^a	7	49.47 \pm 7.39 ^a	9.51 \pm 8.66
Healthy condition	<i>non-coated</i>	4	32.96 \pm 11.45	6*	35.69 \pm 10.50	19.16 \pm 8.23
	<i>nCaP</i>	4	34.77 \pm 9.09	7	36.84 \pm 15.37	64.06 \pm 30.40 ^b
	<i>nCaP/BP</i>	4	36.64 \pm 20.46	7	58.79 \pm 10.73 ^b	70.02 \pm 31.84 ^b
	<i>BP</i>	4	61.85 \pm 6.17 ^b	6*	50.61 \pm 19.57	24.73 \pm 16.60

*One sham-operated rat died.

^a indicates significant difference compared to non-coated implants in osteoporotic conditions ($P < 0.05$).^b indicates significant difference compared to non-coated implants in healthy conditions ($P < 0.05$).

2.3. Quantifying peri-implant bone formation at 4 weeks

Micro-computed tomography was performed to quantify the peri-implant bone volume (BV) fraction. In corresponding two-dimensional (2D) μ CT slices (Figure 2.a,b), we observed more bone formation toward nCaP/BP- and BP-coated implants in both osteoporotic and healthy conditions. The peri-implant trabecular bone volume (%BV) after 4 weeks of implantation was calculated in a standard volume-of-interest (VOI) 500 μ m surrounding implants (Figure 2.c, Table 2). In osteoporotic conditions, nCaP/BP- and BP-coated implants significantly increased %BV (i.e. 1.8-fold and 1.7-fold, respectively) compared to non-coated implants ($P < 0.05$). In healthy conditions, %BV increased considerably (i.e. 1.9-fold) around BP-coated implants compared to non-coated implants ($P < 0.05$). The nCaP- and nCaP/BP-coated implants showed a similar %BV in osteoporotic bone compared to healthy conditions ($P > 0.05$).

Histomorphometrical analysis was performed to quantify and compare peri-implant bone formation (bone area; %BA) in a standard region-of-interest (ROI) of 500 μm surrounding implants (Figure 2.d and Table 2). In osteoporotic conditions, BP-coated implants showed significantly ($P<0.05$) increased %BA compared to non-coated implants (i.e. 1.5-fold), whereas nCaP and nCaP/BP-coated implants showed comparable %BA to controls ($P>0.05$). In healthy conditions, the %BA values were significantly increased around nCaP/BP implants (i.e. 1.6-fold) compared to non-coated implants ($P<0.05$), whereas nCaP- and BP-coated implants showed a comparable %BA to non-coated implants ($P>0.05$).

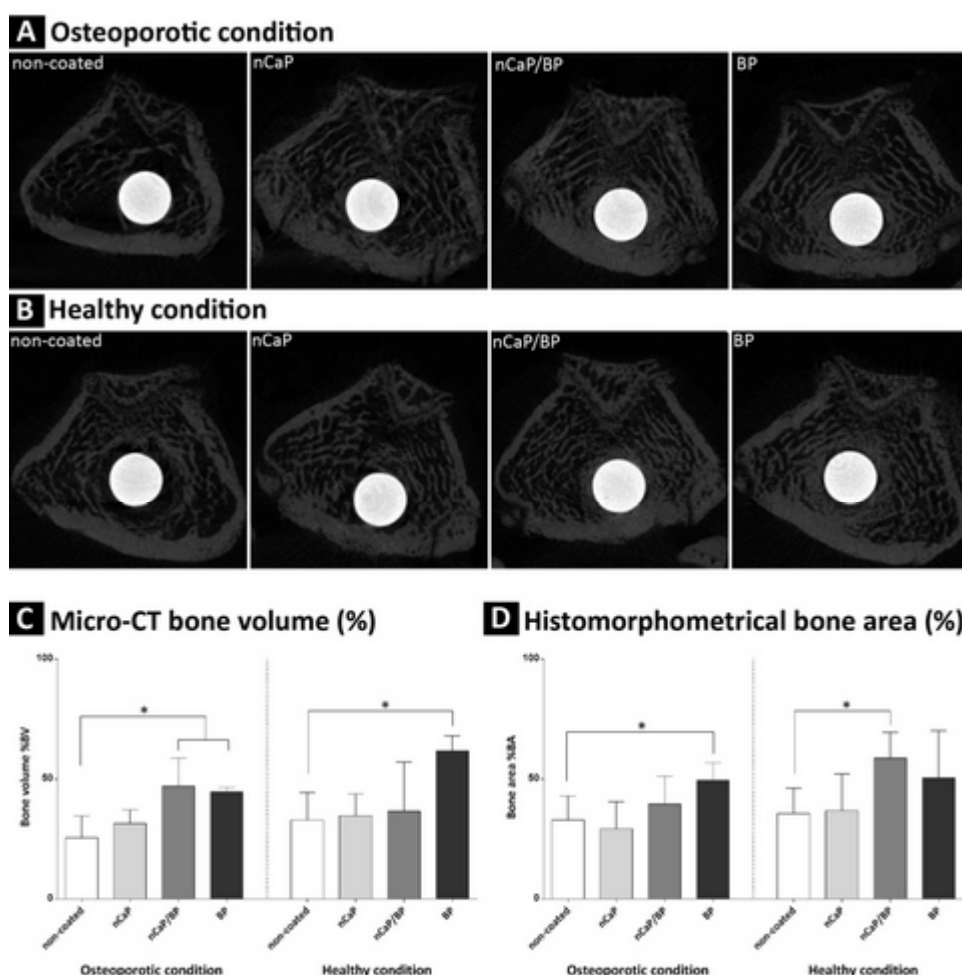


Figure 2. Visualizing and quantifying peri-implant bone formation after 4-weeks. (A and B) Representative ex-vivo μCT 2-dimentional imaging of non-coated and coated implants in osteoporotic and healthy conditions. (C) %BVs were calculated by μCT ($n = 4$). (D) Histomorphometrical %BAs were also measured for all experimental implant groups ($n = 6$ to 7). * $P<0.05$, one-way ANOVA with Dunnett's post-hoc test.

2.4. Histomorphometrical analysis of the bone-implant interface after 4 weeks

nCaP/BP-coated implants were anticipated to lead to an osseointegrative tissue response, in which bone would grow intimately along the implant surface and form a mechanically strong bone-implant interface.^[8,22] As an advantage of retaining the implant for histological sectioning, we were able to quantify the direct bone-to-implant contact at high magnification. Figure 3 and Table 2 show the quantitative results of bone-to-implant contact (%BIC). At 4 weeks, implants with nCaP and nCaP/BP coatings demonstrated significantly higher %BIC compared to non-coated implants for both osteoporotic and healthy conditions ($P < 0.05$). Quantitative measurements for BP-coated implants showed a comparable %BIC to non-coated implants for both osteoporotic and healthy conditions ($P > 0.05$).

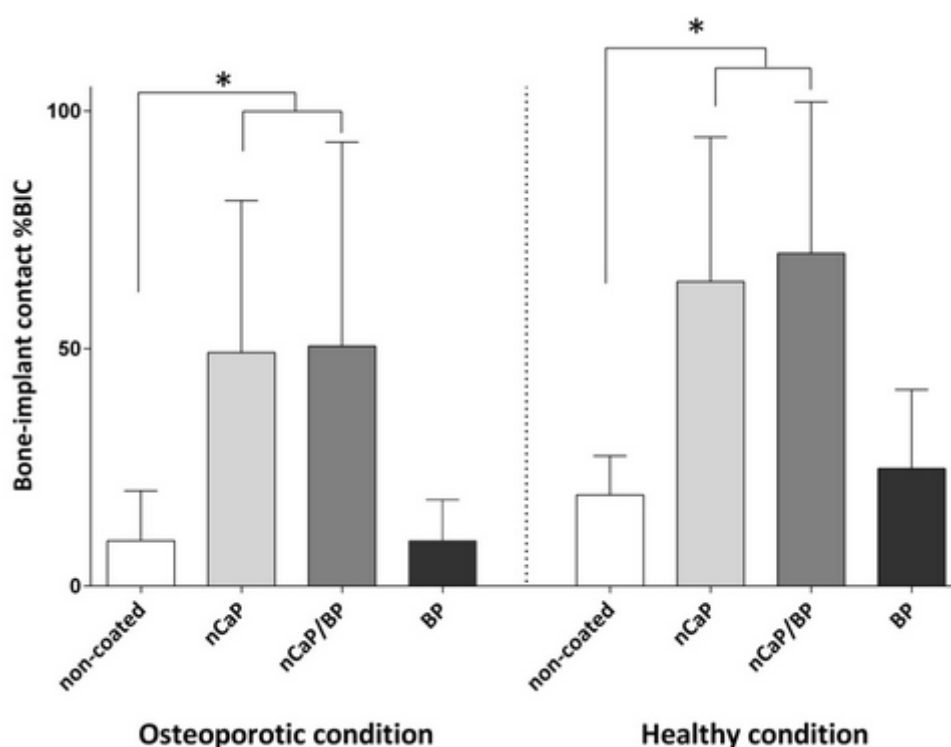


Figure 3. Representative histomorphometrical analysis showing bone-to-implant contact (%BIC). The statistical results depict implants with nCaP and nCaP/BP coatings had higher mean %BIC compared to control implants in both osteoporotic and healthy conditions. * $P < 0.05$, one-way ANOVA with Dunnett's post-hoc test.

2.5. Relative gene expression in peri-implant tissue after 4 weeks

Identification of osteogenic genes that are upregulated during implant-bone interfaces for osteoporotic and healthy conditions is pertinent to successfully address clinical needs. In the

present study, peri-implant tissues were carefully retrieved at 4-weeks post-implantation and analyzed via real-time PCR using the relative comparative (Ct) method ^[23] while non-coated implants in healthy conditions served as a reference. The results of real-time PCR are shown in Figure 4.a-g. The relative gene expression (fold changes) showed similar osteogenic gene expression for all experimental groups.

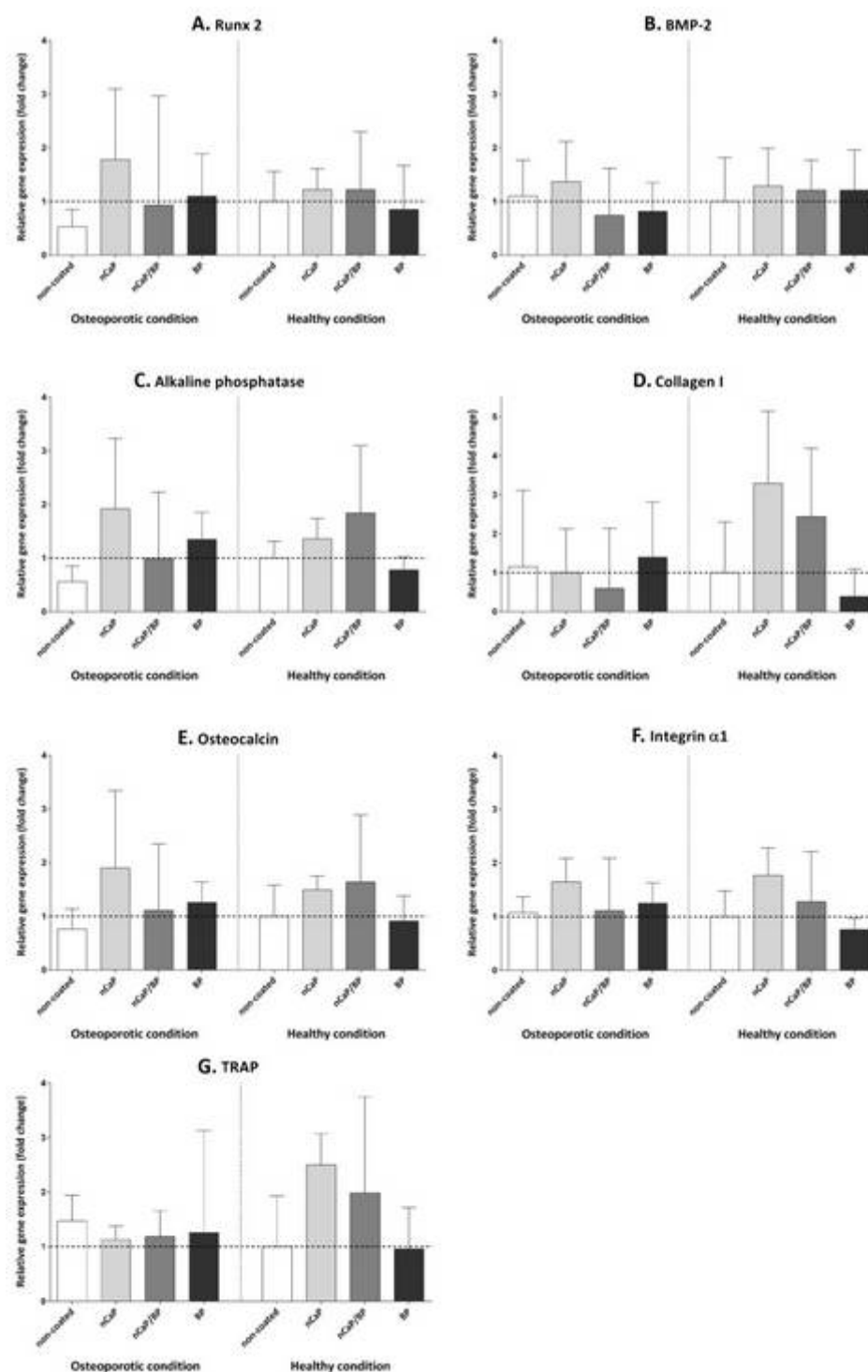


Figure 4. Results of the relative quantification of gene expression (fold changes) at 4-weeks. (A to F) Data (mean±SD) present peri-implant osteoblastic-specific genes for all experimental groups. (G) The osteoclastic TRAP markers also compared between coated and control implants in both osteoporotic and healthy conditions. * $P < 0.05$, one-way ANOVA with Dunnett's post-hoc test.

3. Discussion

Osteoporosis is expected to affect a large proportion of the aged population in the near future. In the clinic, however, an osteoporotic condition challenges the use of bone implant-based rehabilitation due to the impaired osseointegration and high risk of implant loosening.^[1, 2] In the present study, we used a combination of calcium phosphate nanoparticles (nCaP) and bisphosphonate (alendronate) to generate coatings onto titanium implants in an approach to enhance bone-implant integration for osteoporotic and healthy patients. Interestingly, by detailed histomorphometrical analysis, we observed a significant increase in bone-to-implant contact (%BIC) associated with the deposition of nCaP and nCaP/bisphosphonate onto implant surfaces at 4-weeks post-implantation compared to non-coated implants in both osteoporotic and healthy conditions. Clinically, bone implant osseointegration is achieved by direct bone formation and bonding at the implant surface, which is clinically relevant for high success rates of bone implants.^[8] This preferred biological response requires early recruitment, attachment, and proliferation of bone cells to the implant surface, which can be improved by surface modifications, most often by depositing synthetic CaPs that resemble the mineral component of bone.^[24] The beneficial effect of the ESD nCaP-coating has already been explored *in vitro*,^[25] showing an increased adhesion of osteoblast-like cells to nCaP-coated substrates. This is also in accordance with the observations in a recent rat study using ESD nCaP-coated implants.^[26]

Evidently, we noticed that the presence of a nCaP-coating generates a beneficial effect at the osteoporotic bone-implant interface, but not on the bone tissue at more remote distances away from the implant surface. Consequently, new surface coating strategies with therapeutic capacity including bisphosphonates are currently introduced to target osteoporotic bone also at more remote distances from the implant surface.^[27,28] In this study, we proved that the synergistic action of bisphosphonates and nCaP on successfully increased the quantity of bone formation at the implant interface and within a peri-implant area of 500 μm compared to non-

coated implants for both osteoporotic and healthy conditions. In contrast, the single deposition of bisphosphonate only onto the implant surface effectively increased peri-implant bone volume/area in osteoporotic conditions, but not the bone-to-implant contact, which corroborates with the study of Wermelin et al.^[29]. These findings also endorse previous in vivo observations that the combination of bisphosphonate and CaP coating significantly improves both bone-implant contact and the amount of bone surrounding implants.^[19,30,31,32] The implications of these observations are still unknown, but we assume that bisphosphonates are less firmly bound to the titanium surface compared to nCaP in view of the high calcium-binding affinity of BPs. As a consequence, release of bisphosphonates from CaP-free bisphosphonate coatings will affect bone formation at distance larger than 500 μm from implant surface, whereas the more localized site of action of nCaP-bound bisphosphonates is the direct implant/tissue interface. Our data further confirmed that deposited nCaP coatings can also serve as a local drug-delivery vehicle to favor the bone healing process at the implant interface in a dual manner.^[29,30,33]

The effect of nCaP on the bone-implant interface can be due to different mechanisms of action. For instance, the dissolution of Ca^{2+} and PO_4^{3-} ions from a CaP-coating has been suggested to stimulate cellular and intracellular signaling and to favor osteoblastic cell activity in the process of bone formation.^[24,34] Further, Ca^{2+} ions might increase osteogenic cell chemotaxis and migration toward the coated surface via the activation of calcium signaling.^[35] Ca^{2+} and PO_4^{3-} ions also play an essential role in bone mineralization, and can facilitate the precipitation of bone-like apatite on the implant surface.^[36] On the other hand, bisphosphonates have been demonstrated to inhibit osteoclast-mediated resorption of newly formed bone, leading to an increased peri-implant bone amount.^[17] Pharmaceutically, the potency of bisphosphonates is determined by the presence of specific lateral chains (R1 and R2 groups), which bind to bone (CaP) minerals and then target different cellular and molecular processes in osteoclasts.^[33] Bisphosphonates, specifically alendronate, possess the

ability to inhibit the enzyme farnesyl pyrophosphate (FPP) synthase, thereby disrupting the mevalonate pathway, which reduces osteoclastic function and activity.^[33, 37] Beside effects on osteoclastic activity, an in vitro study showed that bisphosphonates increase osteoblast anabolic activity via binding and opening of cell-membrane hemichannels, which ultimately activate osteoblastic-cell surviving processes.^[38]

Apart from the molecular mechanisms involved in the effect of nCaP and bisphosphonate coatings on peri-implant bone healing, real-time PCR analysis at 4-weeks revealed similar effects of the experimental coatings on gene expression levels involved in peri-implant osteogenesis. This corroborates earlier findings,^[39] which also showed similar levels of bone-specific gene expression at the interface of nCaP-incorporated implants compared to non-coated implants after 4-weeks of healing. Despite these similar gene expression levels after 4 weeks of bone healing, the amounts of new bone formation and remodeling around the coated implants were increased after 4 weeks,^[40] suggesting that the influence of implant surface coatings on the process of osteoconduction might be more effective during the early stages of osseointegration. Further, the histologically observed peri-implant bone healing differences at 4-weeks post-implantation are likely to be preceded by distinct gene expression in the peri-implant region of the different experimental groups, for which gene expression confirmation of histological observations are difficult to obtain via an experimental set-up with one single time point for sampling. We also expected to observe a significantly decreased osteoclastic cell activity (i.e. levels of TRAP gene expression) in the presence of bisphosphonate-containing coatings compared to non-coated implants, especially in osteoporotic conditions. The absence of this observation might suggest that in osteoporotic conditions, bisphosphonate at the amount electrosprayed onto titanium implants in the present study does not effectively inhibit osteoclastic cell activity. As such, this warrants further investigation of the pharmaceutical dose-efficacy of drug-loaded implants before translating towards clinical translation.

Because of the limited opportunity to undertake human studies, we have used animal models to investigate a drug-loaded method to improve peri-implant interface processes in osteoporotic conditions. Although the rat is one of the most commonly used species in medical research, further investigations in large animals are needed for simulating implant integration under a complex clinical condition (i.e. loading).

4. Conclusion

The results of this study demonstrate that the combined use of nCaP and bisphosphonate increases bone formation at the implant interface compared to non-coated implants. It is suggested that simultaneous targeting of bone formation (by nCaP) and bone resorption (by BP) using nCaP/BP surface coatings represents an effective strategy for improving bone-implant integration, especially in osteoporotic conditions. On the molecular level, real-time PCR analysis at 4-weeks revealed similar effects of the experimental coatings on gene expression levels involved in peri-implant osteogenesis.

5. Experimental Section

Preparation of implants: Pin-shaped implants (Figure S1) were made of commercially-pure titanium with main diameter of 3.1 mm and length of 7.0 mm. The implant model was featured by a pin part (diameter: 1.5 mm and length: 4 mm) to facilitate a standard method of harvesting bone-implant tissues for histological and genetic analyses. All implants were grit-blasted (roughness, $Ra = 0.5 \mu\text{m}$) and cleaned ultrasonically in nitric acid 10% (15 min), acetone (15 min), and ethanol (15 min) and thereafter air-dried.

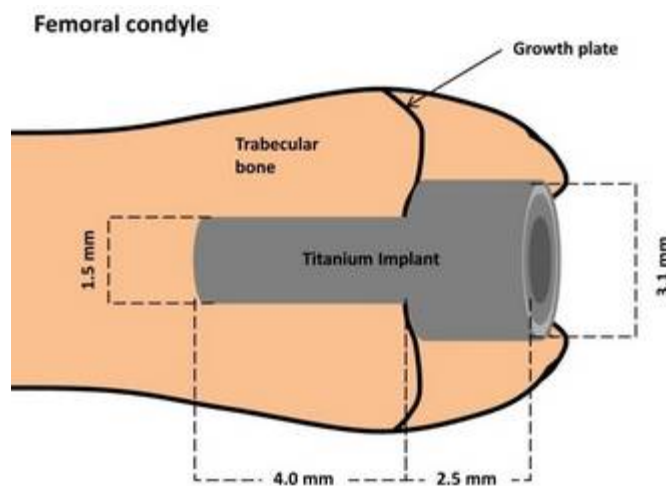


Figure S1. Schematic illustration of pin-shaped implants used in the present study. Implant was designed with a pin part to facilitate a standard method of harvesting bone-implant tissues.

Electrostatic spray deposition (ESD) of coatings: ESD coatings were deposited as previously described^[26] using a commercially available electrostatic spray deposition (ESD) device (ES-2000S, Fulence Co., Ltd., Japan). The following standardized conditions were applied: 20% relative humidity; 30°C substrate holder temperature; 40 mm nozzle-to-substrate distance; 4 $\mu\text{l}/\text{min}$ liquid flow rate; and 10-12 kV applied voltage. For deposition of nCaP coatings, nano-sized apatite crystals were synthesized according to a previously described method.^[41] Briefly, nCaP crystals were obtained from a suspension of $\text{Ca}(\text{CH}_3\text{COO})_2$ (0.35 M) by the slow addition (1 drop/second) of an aqueous solution of H_3PO_4 (0.21 M). The pH was kept constant (pH= 10) by the addition of a $(\text{NH}_4)\text{OH}$ solution. After 24 h, the solid residue was collected

by centrifugation, washed four times with ultrapure water and then suspended in 100 ml of ethanol. For nCaP/BP coatings, alendronate sodium trihydrate $\geq 97\%$ powder (A4978; Sigma-Aldrich, Munich, Germany) was added to a suspension containing nCaP crystals at a concentration of 3 mg/ml and weight ratio of 1:10 for 24 h. The attached percentage of alendronate onto nCaP crystals was determined by measuring the drug concentration in the supernatant solution using ultraviolet-visible spectroscopy based on the detection of the primary amino group with ninhydrin as previously described.^[41,42] For BP coatings, a solution of alendronate sodium powder was dissolved in milli-Q and adjusted with ethanol to a final concentration of 0.3 mg/ml. The medium used for deposition of all the coating groups consisted in a solution of 50% ethanol. Thereafter, ESD coating was performed in three separate runs (with in between implant turning of 120°) of 30 min each to obtain complete coating coverage. The amount of nCaP coating was measured using the ortho-cresolphthalein (OCPC) method (Sigma-Aldrich, Munich, Germany) as previously described.^[41,43] In brief, 300 μL of work reagent was added to 10 μL aliquots of sample or standard in a 96-wells plate. The plate was incubated for 10 min at room temperature, and then the plate was read at 570 nm. Serial dilutions of CaCl_2 ($0\text{--}100\text{ }\mu\text{g} \cdot \text{mL}^{-1}$) were used for the standard curve. To evaluate the total amount of nCaP/BP coating, a standard curve was made by dissolving known amounts of nCaP/BP synthesized according to the method described above. Based on OCPC method, the amount of nCaP/BP coating was measured $8 \pm 0.9\text{ }\mu\text{g}/\text{cm}^2$ and weight ratio of 1:10. For BP coating, the quantity of the drug was estimated $0.8\text{ }\mu\text{g}/\text{cm}^2$. Finally, implants were provided with 3 types of coating or left non-coated:

A: non-coated implants

B: nCaP

C: nCaP/BP

D: BP

Implants were sterilized using ethylene oxide (EO; Synergy Health plc, Venlo, The Netherlands).

Animal model and surgical procedures: The study was approved by the Animal Ethical Committee of the Radboud University Nijmegen Medical Centre (DEC-2011-258). All *in vivo* experiments obeyed the guidelines (national and international) for animal care and the Dutch law concerning animal welfare and conformed to the ARRIVE guidelines. For animal experiments, male Wistar rats (12-weeks old, weight ~350 g) underwent orchidectomy (ORX) surgery to induce osteoporosis through a loss of gonadal function (hypo-gonadism). Osteoporotic conditions were allowed to establish for 6 weeks before implants were installed bilaterally in the femoral condyles. At the intercondylar notch, a cylindrical hole (diameter: 1.5 mm and depth: 7 mm) was initially prepared parallel to the long axis of the femur. Then, implants were placed (press-fit) into the predrilled pin-shaped hole. Details are in the Supporting Information.

A power-analysis was performed to calculate the study sample number using the following formula: $n = 1 + 2C(s/d)^2$. We assumed a standard deviation (s) of 12.5 and an effect size (d) of 15. C-value was fixed at 7.85 (resulting from $1 - \beta = 0.8$ and $\alpha = 0.05$). There were a total of four experimental (coated and non-coated implants) groups with at least 30 test animals per condition (osteoporotic and healthy). Each animal has one implant in each leg (considered independent). A 4-weeks endpoint was predetermined to evaluate the temporal effect of coatings of peri-implant bone formation and implant-bone integration in osteoporotic and healthy conditions. Within each experimental group, (i) specimens ($n = 6$ to 7 per implant group) were subjected to histomorphometrical evaluations after (undecalcified) embedding in poly(methylmethacrylate) (pMMA), (ii) specimens ($n = 4$ per implant group) were selected

for *ex-vivo* micro-CT examination, and (iii) specimens ($n = 4$ per implant group) were used for molecular (real-time PCR) analysis. All experiments were randomized and blinded.

Ex-vivo μ CT examination: At 4-weeks of implantation, rats were euthanized by CO₂-suffocation. Femoral condyles were dissected from adhering tissues. After fixation in 10% formalin solution, specimens were scanned with a desktop X-ray micro-tomography system scanner (Skyscan[®] 1072, Kontich, Belgium). Before scanning, each specimen was wrapped in Parafilm[®] (SERVA Electrophoresis GmbH, Heidelberg, Germany) to prevent drying during scanning, and placed vertically onto the sample holder. Subsequently, a scan resolution of 11 μ m was set for all the samples. Scans were recorded at 100 kV and 98 μ A, with the use of a 1 mm thick aluminum filter to optimize the contrast, a 180° rotation, 5-frames averaging, a rotation step of 0.90° (206 images per scan), and exposure time of 3.8 sec. After 3D reconstruction using NRecon v.1.4.4 (Skyscan[®], Kontich, Belgium), a constant volume of interest (VOI) was chosen to include bone tissue surrounding the implant bed by using CT analyzer software (CTAn v.1.8, Skyscan[®], Kontich, Belgium). Thereafter, per sample, a fixed threshold was manually selected to segment peri-implant bone tissue and preserves its morphology. Finally, trabecular bone volume fraction was visualized and measured in a defined ROI using a ring with a radius of 500 μ m from the implant surface.

Histological evaluation of bone-implant interface: After euthanasia and fixation in 10% formalin solution, specimens with implant in situ were dehydrated in ascending grades of alcohol from 70 to 100% and subsequently embedded into pMMAresin. After polymerization, serial cross-sections (perpendicular to the long axis of the implant) were cut at a thickness of ~10 μ m, using a modified sawing microtome technique, and were stained with methylene blue and basic fuchsin. Blinded histological and histomorphometrical evaluations were carried out using a light microscope (Axio Imager Microscope Z1, Carl Zeiss Micro imaging GmbH,

Göttingen, Germany). Histomorphometrical bone area (%BA) was calculated in a circular peri-implant ROI, i.e. 0-500 μm from the implant surface. Additionally, bone-to-implant contact (%BIC) was measured.

RNA isolation, complementary DNA (cDNA) synthesis, and quantitative real-time PCR: After euthanasia, an aseptic procedure was employed to harvest implants for the molecular (genetic) analysis. In brief, the skin above the implant was shaved, disinfected with 10% povidone iodine, and then incised to expose completely the top part of implant. A trephine guide (3.1 x 3.0 mm) was connected to the implant. Then, the implant was trephined using ACE easyretrieve trephine system (ACE Surgical Supply Company, Inc., Brockton, MA, USA) with inner diameter of 3.2 mm (Figure S2). The retrieved implant along with the surrounding bone *en bloc* was placed in a Cryo.sTM 2 ml sterilized tube (Greiner Bio-One GmbH, Frickenhausen, Germany) and frozen at -80°C until analysis.

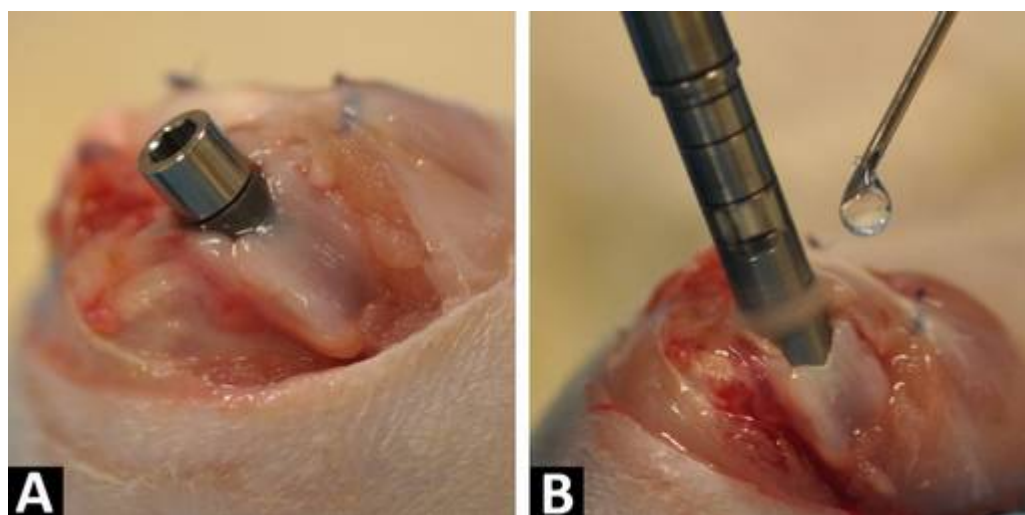


Figure S2. Method of harvesting implants for the molecular (real-time PCR) analysis. First, a trephine guide (A) was connected to the implant. Then, (B) ACE easyretrieve trephine system was used to trephine the implant.

For molecular analysis, bone tissue attached to the implant was pulverized to a fine powder using the Mikro-Dismembrator (B. Braun Biotech International GmbH, Melsungen, Germany). Then, total cellular RNA was isolated using Trizol[®] reagent (Invitrogen Life Technologies, Carlsbad, CA, USA). Total RNA concentration was quantified using a NanoDrop[™] 2000 spectrophotometer (NanoDrop products, Wilmington, DE, USA). The extracted RNA was reverse transcribed following a conventional protocol to synthesize complementary DNA (cDNA). cDNA synthesis was performed using 1 µg RNA dissolved in 10 µl nuclease-free water containing 2 µl 5x iScript reaction mix and 0.5 µl iScript reverse transcriptase (iScript[™] cDNA synthesis kit, Bio-Rad Laboratories B.V., Veenendaal, The Netherlands) according to the manufacturer's protocol. The cDNA was used as a template in real-time PCR. Quantitative real-time PCR was performed in a total volume of 23 µl buffer solution containing 1 µl of template cDNA, 12.5 µl SYBR Green MasterMix (Eurogentec S.A., Seraing, Belgium), 8.5 µl nuclease-free water, and 1 µl of each primer. PCR reactions were performed using rat-specific primers designed by Primerdesign[®] (PrimerDesign Ltd, Southampton, UK) according to manufacturer's instructions (Table S1). Osteoblastic cell differentiation was monitored by the expression of runt-related transcription factor-2 (Runx-2), bone morphogenetic protein-2 (BMP-2), collagen type I (Col I), integrin α 1, alkaline phosphatase (ALP), and osteocalcin (OC). The expression of the osteoclast-specific gene tartrate-acid resistant phosphatase (TRAP) was also monitored. Glyceraldehyde-3-phosphate dehydrogenase (GAPDH) was used as house-keeping gene control. Real-time PCR was performed using the SYBR Green PCR kit (Eurogentec, Liege, Belgium) and controlled in C1000[™] Thermal Cycler PCR system (Bio-Rad, Veenendaal, The Netherlands). The quantification of a target gene expression in comparison to a reference gene (GAPDH) was mathematically determined. After the real-time PCR run, the cycle threshold (Ct) value of target gene was calculated relative to GAPDH as an internal control ($\Delta Ct = Ct_{\text{target}} - Ct_{\text{GAPDH}}$). Then, fold-differences in gene expression were calculated by the comparative ($\Delta\Delta Ct =$

$\Delta\text{Ct}_{\text{target}} - \Delta\text{Ct}_{\text{control}}$) and $2^{-\Delta\Delta\text{Ct}}$ value method as previously described.^[23] Non-coated implants in healthy conditions were set as control; 1.0-fold expression level.

Table S1: Bone-specific rat primers for real-time PCR designed by Primerdesign® (PrimerDesign Ltd, Southampton, UK).

Gene	Supplier Accession No.	Amplicon length (bp)
Runx-2	XM_346016	120
PMB-2	NM_017178	139
Collagen I	XM_213440	100
Osteocalcin	NM_013414	103
ALP	NM_013059	105
Integrin α1	NM_030994	125
TRAP	NM_019144	92

Statistics: Data were analyzed by SPSS version 16.0 (SPSS Inc., Chicago, IL, USA) and are presented as mean \pm SD. Independent *t*-tests were used for two group comparisons to confirm changes in bone morphological parameters in osteoporotic conditions compared to healthy conditions. For histomorphometrical data, BIC values were assumed to display unequal variances ($P < 0.05$). Consequently, parameters of BIC were categorized (dichotomized) into two groups according to bone-implant contact level, either equal or above the zero value, using crosstab and chi-square calculations method. Then, the association between BIC values (above the zero) and types of surface coatings were assessed. One-way ANOVA with Dunnett's *post-hoc* test was performed to compare variables of coated implants to non-coated implants in osteoporotic and healthy conditions, separately. The level of significance was set at $P < 0.05$.

Supporting Information

Supporting Information is available online from the Wiley Online Library or from the author.

References

- [1] I. D. Learmonth, C. Young, C. Rorabeck, *Lancet***2007**, 370,1508.
- [2] A. Klibanski, L. Adams-Campbell, T. Bassford, S. Blair, S. Boden, K. Dickersin, D. Gifford, L. Glasse, S. Goldring, K. Hruska, *JAMA***2001**, 285, 785.
- [3] B. M. Kuehn, *JAMA* **2005**, 293,2453.
- [4] C. H. Chesnut III, *JAMA* **2001**, 286,2865.
- [5] H. G. Bone, D. Hosking, J.-P. Devogelaer, J. R. Tucci, R. D. Emkey, R. P. Tonino, J. A. Rodriguez-Portales, R. W. Downs, J. Gupta, A. C. Santora, *N. Engl. J. Med.* 2004, 350, 1189.
- [6] P. A. Downey, M. I. Siegel, *Phys. Ther.***2006**, 86, 77.
- [7] F. Marco, F. Milena, G. Gianluca, O. Vittoria, *Micron***2005**, 36, 630.
- [8] D. Puleo, A. Nanci, *Biomaterials***1999**, 20, 2311.
- [9] K. Kieswetter, Z. Schwartz, D. D. Dean, B. D. Boyan, *Crit. Rev. Oral Biol. Med.***1996**, 7, 329.
- [10] M. Browne, P. Gregson, *Biomaterials***1994**, 15, 894.
- [11] G. Mendonça, D. Mendonça, F. J. Aragao, L. F. Cooper, *Biomaterials***2008**, 29, 3822.
- [12] R. Junker, A. Dimakis, M. Thoneick, J. A. Jansen, *Clin. Oral Implants Res.***2009**, 20 Suppl 4, 185.
- [13] R. Bosco, E. R. U. Edreira, J. G. Wolke, S. C. Leeuwenburgh, J. J. van den Beucken, J. A. Jansen, *Surf. Coat. Technol.***2013**. <http://dx.doi.org/10.1016/j.surfcoat.2013.02.039>.
- [14] K. Anselme, *Biomaterials***2000**, 21, 667.
- [15] S. C. Leeuwenburgh, J. G. Wolke, M. C. Siebers, J. Schoonman, J. A. Jansen, *Biomaterials***2006**, 27, 3368.
- [16] L. T. de Jonge, S. C. G. Leeuwenburgh, J. G. C. Wolke, J. A. Jansen, *Pharm. Res.***2008**, 25, 2357.

- [17] J. P. Cattalini, A. R. Boccaccini, S. Lucangioli, V. Mourino, *Tissue Eng. Part B Rev.***2012**, 18, 323.
- [18] M. Ginebra, T. Traykova, J. Planell, *J. Control. Release***2006**, 113, 102.
- [19] B. Peter, O. Gauthier, S. Laib, B. Bujoli, J. Guicheux, P. Janvier, G. H. van Lenthe, R. Muller, P. Y. Zambelli, J. M. Bouler, D. P. Pioletti, *J. Biomed. Mater. Res A***2006**, 76, 133.
- [20] H. S. Alghamdi, J. J. van den Beucken, J. A. Jansen, *Tissue Eng. Part C Methods***2013**. doi:10.1089/ten.TEC.2013.0327
- [21] H. S. Alghamdi, R. Bosco, J. J. van den Beucken, X. F. Walboomers, J. A. Jansen, *Biomaterials***2013**, 34, 3747.
- [22] L. L. Hench, J. M. Polak, *Science***2002**, 295, 1014.
- [23] T. D. Schmittgen, K. J. Livak, *Nat. protoc.***2008**, 3, 1101.
- [24] Y. C. Chai, A. Carlier, J. Bolander, S. J. Roberts, L. Geris, J. Schrooten, H. V. Oosterwyck, F. P. Luyten, *Acta Biomater.* **2012**, 8, 3876.
- [25] L. T. de Jonge, J. J. van den Beucken, S. C. Leeuwenburgh, A. A. Hamers, J. G. Wolke, J. A. Jansen, *Acta Biomater.***2009**, 5, 2773.
- [26] L. T. de Jonge, S. C. Leeuwenburgh, J. J. van den Beucken, J. te Riet, W. F. Daamen, J. G. Wolke, D. Scharnweber, J. A. Jansen, *Biomaterials***2010**, 31, 2461.
- [27] M. Yoshinari, Y. Oda, T. Inoue, K. Matsuzaka, M. Shimono, *Biomaterials***2002**, 23, 2879.
- [28] M. Yoshinari, Y. Oda, H. Ueki, S. Yokose, *Biomaterials***2001**, 22, 709.
- [29] K. Wermelin, F. Suska, P. Tengvall, P. Thomsen, P. Aspenberg, *Bone***2008**, 42, 365.
- [30] B. Peter, D. P. Pioletti, S. Laib, B. Bujoli, P. Pilet, P. Janvier, J. Guicheux, P. Y. Zambelli, J. M. Bouler, O. Gauthier, *Bone***2005**, 36, 52.
- [31] J. D. Bobyn, K. McKenzie, D. Karabasz, J. J. Krygier, M. Tanzer, *J. Bone Joint Surg. Am.***2009**, 91 Suppl 6, 23.

-
- [32] Y. Nakamura, K. Hayashi, S. Abu-Ali, M. Naito, A. Fotovati, *J. Bone Joint Surg. Am.***2008**, 90, 824.
- [33] G. A. Rodan, *Annu. Rev. Pharmacol. Toxicol.***1998**, 38, 375.
- [34] A. Barradas, H. A. M. Fernandes, N. Groen, Y. C. Chai, J. Schrooten, J. van de Peppel, J. P. T. M. van Leeuwen, C. A. van Blitterswijk, J. de Boer, *Biomaterials***2012**, 33, 3205.
- [35] D. E. Clapham, *Cell***2007**, 131, 1047.
- [36] T. Kokubo, H. Takadama, *Biomaterials***2006**, 27, 2907.
- [37] M. J. Rogers, J. C. Crockett, F. P. Coxon, J. Monkkonen, *Bone***2011**, 49, 34.
- [38] L. I. Plotkin, R. S. Weinstein, A. M. Parfitt, P. K. Roberson, S. C. Manolagas, T. Bellido, *J. Clin. Invest.***1999**, 104, 1363.
- [39] R. Jimbo, Y. Xue, M. Hayashi, H. O. Schwartz-Filho, M. Andersson, K. Mustafa, A. Wennerberg, *J. Dent. Res.***2011**, 90, 1422.
- [40] G. Mendonça, D. Mendonça, L. G. Simões, A. L. Araújo, E. R. Leite, W. R. Duarte, F. J. Aragão, L. F. Cooper, *Biomaterials***2009**, 30, 4053.
- [41] M. Iafisco, R. Bosco, S. C. G. Leeuwenburgh, J. J. J. P. van den Beucken, J. A. Jansen, M. Prat, N. Roveri, *Adv. Eng. Mater.***2012**, 14, 13.
- [42] M. Iafisco, B. Palazzo, G. Falini, M. D. Foggia, S. Bonora, S. Nicolis, L. Casella, N. Roveri, *Langmuir***2008**, 24, 4924.
- [43] J. van den Dolder, G. N. Bancroft, V. I. Sikavitsas, P. H. Spauwen, J. A. Jansen, A. G. Mikos, *J Biomed Mater Res A***2003**, 64, 235.

Supporting Information

Experimental details

Surgical procedure for orchidectomy (hypo-gonadism): To establish an osteoporotic condition, skeletally-mature male Wistar rats (Charles River Laboratories International, MA, USA) were subjected to gonadal tissue removal and sham operations. Prior to surgery, pain control medication, Carprofen (Rimadyl[®], 5.0 mg/kg) and Buprenorphine (Temgesic[®], 0.02 mg/kg), were injected subcutaneously 15 min pre-operation and every 8h for 2 days after the surgery. After inhalational anesthesia was induced and maintained by 2% Isoflurane[®] by volume (Rhodia Organique Fine Ltd, Avonmouth, Bristol, UK), the abdominal region was completely shaved and cleaned with 10% povidone iodine. Animal was placed in supine position on an electric heating blanket. A 1 cm midline skin incision was made in order to enter the abdominopelvic cavity. Then, the gonadal tissues were gently pulled through and a single ligature (Vicryl[®] 3.0, Ethicon Products, Amersfoort, The Netherlands) was placed around the blood vessels, after which both testes were removed. After confirming that no massive bleeding was occurring, the abdominal muscle layers were closed with absorbable sutures (Vicryl[®] 3.0) and the skin was stapled by metal wound clips (Agraven[®], InstruVet Bv, Cuijk, The Netherlands). The sham operations were also performed following the same surgical procedure except for the removal of testes. The animals were monitored for signs of pain, infection and proper activity. After ORX intervention, rats had free access to water and a low-calcium pellet (0.01% Ca and 0.77% P) and followed an osteoporotic diet (ssniff Spezialdiäten GmbH, Soest, Germany). The sham-operated rats had unrestricted access to the normal pellet food containing 1.17% calcium (Ca) and 0.91% phosphorus (P).

Assessment of osteoporosis condition: After 6 weeks, ORX rats as well as the sham-operated rats ($n = 3$ of each animals group) were scanned by small-animal *in-vivo* μ CT imaging system

(Inveon; Siemens Medical Solutions, Knoxville, TN). Before scanning, small animal anesthetic machine (Rhodia Organique Fine Ltd, Avonmouth, Bristol, UK) was added to the scanner cabinet. Then, animal was placed supine on the scan stage and was sedated under inhalational anesthesia (2% Isoflurane[®] by volume) using a mask held over the rat's snout and then secured with a strap. The two hind-limbs were bended and held in place with a strap. The distal femoral regions were manually located via the scout viewer (Inveon Acquisition Workplace software, Siemens Medical Solutions, Knoxville, TN) as the region of interest for optimal focused scanning resolution. Then, CT images were acquired with the manufacturer recommended parameters: voltage 80 kVp, anode current 500 μ A, angular sampling 1° per projection for a full 360° scan, effective pixel size 30 μ m, and exposure time of 1 sec. The X-ray source-to-detector distance was 357.8 mm and source-to-object distance was 160.7 mm. Total acquisition time was 30 min. Thereafter, all projection data were reconstructed using cone beam algorithm according to the manufacturer's default values. The scanned micro-CT data for right and left femoral condyles were imported into Inveon Research Workplace 3.0 program (Siemens Medical Solutions USA Inc, Knoxville, USA). Trabecular bone was selected by drawing volume of interest (VOI) in metaphyseal region. To generate a standard VOI selection, a region-of-interest with a length of 2.1 mm (= 70 slices) was chosen manually (excluding the cortical bone) and distanced from the growth plate area. Thereafter, the gray-value images were adjusted to remove noise and a fixed threshold was manually determined to extract trabecular bone phase and bone marrow phase separately. Using the Inveon Research Workplace 3.0 software, the following trabecular bone morphological parameters were automatically computed: (1) bone volume fraction (%BV), (2) trabecular thickness (Tb.Th mm), (3) trabecular number (Tb.N mm⁻¹), and (4) trabecular separation (Tb.Sp mm).

Surgical procedure for installation of implants: After confirmation of the osteoporotic conditions, the pin-shaped implants were installed in the femoral condyles under inhalation

anesthesia (2% Isoflurane[®] by volume). The rat was immobilized supine with the knee joint in a maximally flexed position and the hind limbs were shaved, washed and disinfected with 10% povidone iodine. The knee joint capsule was incised longitudinally, and by lifting the patellar ligament gently and moving it laterally, the knee joint became fully exposed. This maneuver was facilitated by a slight extension of the knee. At the intercondylar notch, a cylindrical hole (diameter: 1.5 mm and depth: 7 mm) was initially prepared parallel to the long axis of the femur, using dental burs and surgical motor (Elcomed 100, W&H Dentalwerk Burmoos, Austria) with low rotational drill speed (800 rpm) and continuous external cooling with saline. Then, only the top part of the prepared hole (3 mm in depth) was increased in diameter to 3.2 mm. thereafter, implants were placed (press-fit) bilaterally into the predrilled holes, resulting in two implants per rat randomly. After insertion of the implants, the soft tissue layers and skin were closed with resorbable sutures (Vicryl[®] 4.0, Ethicon Products, Amersfoort, The Netherlands). To reduce post-operative pain, Rimadyl[®] (5.0 mg/kg) and Temgesic[®] (0.02 mg/kg) were used three times a day for 2 days. Animals were monitored on a daily basis. After implantation procedures, all rats had free access to normal pellet food (1.17% Ca and 0.91% P) and water.

Chapter VII

Electrospray deposition of strontium-substituted nano-hydroxyapatite to stimulate the response of osteoblastic cells to titanium implants.

R Bosco, M Bianchi, M Iafisco, SCG Leeuwenburgh, JA Jansen, JJJP van den Beucken

1 Introduction

The preservation of biomechanical functions of bone tissue is fundamental to maintain a sufficient healthy quality of life. Movement, support, posture and mastication are achieved thanks to the mechanical properties of bone tissue. When joints are damaged or bone-anchored elements are lost, metallic implants are commonly used in orthopedics and dentistry to replace load-bearing and structural function[1]. Aside from their excellent mechanical properties and biocompatibility, metallic implants are inert materials that are limited in their capacity to form mechanically stable bonds with bone tissue.

To overcome interface limitations for implants while maintaining bulk material properties, research efforts have focused on the deposition of coatings made of different constituents. Hydroxyapatite ($\text{Ca}_{10}(\text{PO}_4)_6(\text{OH})_2$; HA) has long been investigated as an implant coating material, due to the similarity with bone mineral and anticipated improvement of osteoconductivity and fixation within the native bone[2]. HA has been successfully applied as a coating using several different methods, including plasma-spraying, magnetron sputtering, ion-beam coating, electrophoretic deposition, anode oxidation, anodic spark deposition, pulsed-laser deposition, electrospray deposition and biomimetic deposition from supersaturated solutions[3-6].

Recently, research interests for modified hydroxyapatite-like crystal structures have increased, since HA can be doped with ions such as K^+ , Mg^{2+} , Na^+ , CO_3^{2-} , F^- and Sr^{2+} that substitute for Ca^{2+} cations in the crystal lattice. From a bio-inorganic[7] point of view, these ions can play relevant roles in the overall solubility and bioactivity of the mineral phase[8]. In particular, strontium (Sr^{2+}) is chemically and physically similar to calcium and present in bone tissue, especially at regions of high metabolic turnover[9]. Further, in vitro and in vivo studies have shown that Sr^{2+} stimulates bone formation by increasing osteoblast activity and reducing bone resorption by decreasing osteoclast activity[10, 11].

Interestingly, Sr^{2+} can be added to calcium phosphate crystals during their formation as a substituting cation for calcium in the crystal lattice for the whole range of CaP compositions, due to the chemical similarity between the two ions[12]. Sr^{2+} -substituted-HA (SrHA) coatings can be obtained either by adding strontium ions during the HA synthesis reaction and using this material for deposition techniques (e.g. plasma spraying, magnetron sputtering or pulsed laser deposition)[13, 14] or by wet apatite nucleation from simulated body fluid (SBF) enriched with strontium ions[15].

Among the currently available coating deposition techniques for CaP deposition, benefits and limitations apply for each of these, e.g. physical deposition methods provide controlled coatings at higher deposition rates, but require high temperatures that can compromise or modify coating properties[16]. In contrast, wet chemical deposition techniques can generate coatings more similar to the bone mineral phase, but long deposition times are required and the adhesive properties are poor[17]. Electrospray deposition (ESD) is a wet-chemical deposition technique that can fabricate coatings on top of implant materials even at low temperatures (25 °C)[18]. Briefly, the basic principle of ESD is the generation of a spray of charged, micron-sized droplets. This is accomplished by means of electrostatic atomization of precursor solutions. These spray droplets are directed toward a grounded substrate using a potential difference[19]. After complete solvent evaporation, a coating layer is left on the substrate surface. ESD has been successfully applied for experimental bone implant applications, preparing thin coatings based on ceramics (e.g. CaP and nano-HA)[20, 21], proteins (e.g. alkaline phosphatase and collagen)[22, 23], and combinations[24, 25].

The aim of this study was to deposit nano-sized SrHA, with different levels of substitution, on titanium by ESD and to evaluate the effect of different amounts of Sr^{2+} -substitution in the coatings on the proliferation and differentiation of osteoblastic cells. We hypothesized that (i)

ESD is a feasible method to deposit SrHA on titanium, and that (ii) the level of Sr^{2+} -substitution can modulate osteoblastic cell response in a level-dependent manner.

2 Materials and methods

2.1 Synthesis of HA nanocrystals

Nanosized hydroxyapatite (HA) was synthesized and characterized according to a previously established method[21]. Briefly, nanocrystals were precipitated from a basic suspension of $\text{Ca}(\text{CH}_3\text{COO})_2$ (0.035 M) by slow addition (1 drop s^{-1}) of an acid solution of H_3PO_4 (0.021 M), keeping the pH constant ($\text{pH}=10$) by the addition of $(\text{NH}_4)\text{OH}$ solution. Sr^{2+} -doped HA was obtained by adding $\text{Sr}(\text{NO}_3)_2$ in the basic suspension at 1 and 10% Ca moles. In more detail, 1% Sr-doped hydroxyapatite (SrHA1) was obtained from a basic solution made of $\text{Ca}(\text{CH}_3\text{COO})_2$ (0.03465 M) and $\text{Sr}(\text{NO}_3)_2$ (0.00035 M); 10% Sr-doped hydroxyapatite (SrHA10) basic solution was made of $\text{Ca}(\text{CH}_3\text{COO})_2$ (0.0315 M) and $\text{Sr}(\text{NO}_3)_2$ (0.0035 M). Quantities and formulas are reported in Table 1. At 24 h after the end of this precipitation reaction, the solid residue was collected by centrifugation, washed four times with ultrapure water, and suspended in 100 ml of ethanol (EtOH). Inductively coupled plasma-optical emission spectrometry (ICP-OES, Liberty 200, Varian, Clayton South, Australia) was used to determine the Ca/P ratio of HA. For ICP-OES, HA samples were dissolved in 1 wt% ultrapure nitric acid and the analytical wavelengths were chosen accordingly: Ca 422 nm, P 213 nm.

Table 1. Precursors material and composition used for crystals precipitation. The acid solution is constant for all the precipitations. Basic suspension was adapted to incorporate Sr as Ca substitute.

Precipitated powder	Basic suspension	Acid Solution
Nano hydroxyapatite (HA)	$\text{Ca}(\text{CH}_3\text{COO})_2$ (0.035 M)	H_3PO_4 (0.1 M)
1% Sr-doped hydroxyapatite (SrHA1)	$\text{Ca}(\text{CH}_3\text{COO})_2$ (0.0346 M) + $\text{Sr}(\text{NO}_3)_2$ (0.00035 M)	
10% Sr-doped hydroxyapatite (SrHA10)	$\text{Ca}(\text{CH}_3\text{COO})_2$ (0.0315 M) + $\text{Sr}(\text{NO}_3)_2$ (0.0035 M)	

2.2 Coating deposition

All coatings were deposited using a commercially available vertical ESD device (ES 2000s, Fuence Ltd., Tokyo, Japan). Titanium disks were used as a target for deposition (machined surface, 5 mm Ø, and 2 mm thickness). Electrospraying was performed under controlled atmosphere conditions (relative humidity <20% and temperature 25°C). Depositions were performed at a fixed nozzle-substrate distance of 40 mm, a flow rate of 4 µl/min and an applied voltage of 10-14 kV. Four different experimental groups were designed to determine the effect of HA and SrHA on coating properties:

1. Uncoated (Ti)
2. HA coated (HA)
3. 1% Sr-substituted HA (SrHA1)
4. 10% Sr-substituted HA (SrHA10)

HA, SrHA1, and SrHA10 were obtained from a 0.3 mg/ml suspension of crystals in 50% ethanol and sprayed for 30 minutes. Sterilization of all the coated samples was obtained through UV irradiation (254 nm) for 1 hour. All coated disks were lyophilized overnight and stored at -20 °C until further use.

HA, SrHA1 and SrHA10 were analyzed using x-ray diffraction (XRD; PANalytical X'Pert Pro powder diffractometer, Almelo, The Netherlands) using Cu K α radiation generated at 40 kV and 30 mA. The instrument was configured with ½° divergence and receiving slits. The 2 θ range was from 5° to 60° with a step size (2 θ) of 0.05° and a counting time of 3 s to determine crystallite size, based on the 002 reflection, according to Formula 1:

$$C = \frac{CC}{CCCCC} \quad (1)$$

where D is the mean size of the ordered (crystalline) domains, which may be smaller or equal to the grain size; K is a dimensionless shape factor, with a value close to unity that was set at 0.9, λ is the X-ray wavelength, β is the line broadening at half the maximum intensity and θ is the Bragg angle.

The infrared spectra (FTIR) of the coatings were recorded in the wavelength range from 4000 to 400 cm^{-1} with 4 cm^{-1} resolution using a Spectrum One (Perkin-Elmer, Waltham, MA, USA).

2.3 In vitro experiment

Preosteoblastic, mouse-derived cells (MC3T3-E1, ATCC-CRL-2593; ATCC, Wesel, Germany) were pre-cultured and expanded in proliferation medium consisting of α MEM (10490, Gibco, Invitrogen, life technology corporation, Carlsbad, US), 10% fetal bovine serum (FBS, Gibco), 10^{-8} M dexamethasone (Sigma-Aldrich, St. Louis, USA), 10mM β -glycerophosphate (Sigma-Aldrich) and 1% gentamicin (15750, Gibco). In order to obtain osteoblast-like cells, ascorbic acid (50mg/L) was added in the proliferation medium to form osteogenic medium. Osteoblast-like cells were seeded in 48-wells plates onto coated disks at 2×10^4 cells/ cm^2 and on tissue culture plastic (TCP) for up to 4 weeks in osteogenic medium with medium refreshments two times per week. After 1 day of culture, disks were transferred to fresh wells to exclude the effect of cells not seeded on the disks but on the tissue culture plastic.

DNA content and alkaline phosphatase (ALP) activity was evaluated at day 7, 21 and 28 to determine cell proliferation and differentiation. All the samples were washed in PBS for 30 minutes at 37 °C and then frozen in mQ at -20 °C. At the time of analyses, all the samples were subjected to three freeze-thaw cycle at -80 °C. A total of $n = 4$ replicates per time point for each experimental condition were used. Proliferation was determined with the fluorometric QuantiFluor dsDNA System (Promega, Leiden, The Netherlands) following the protocol of

the manufacturer and the fluorescence measurement at 530 nm was performed using a FLx800 fluorescence microplate reader (Bio-Tek Instruments, Winooski, VT, USA). Differentiation was deduced from ALP activity and it was measured using a diagnostic kit (Sigma). Briefly, the absorbance of each well was read at 405 nm using a PowerWave X340 microplate spectrophotometer (Bio-Tek Instruments, Winooski, VT, USA). Absorbance values of the samples were normalized to the amount of DNA.

At days 7 and 28, to assess cellular morphology samples were washed with 1x PBS, fixed for 5 minutes in 2% glutaraldehyde, rinsed for 5 minutes with 0.1M sodium-cacodylate buffer (pH7.4; Acros Organics, Geel, Belgium), dehydrated in a graded series of ethanol and air dried in tetramethylsilane (Acros Organics).

2.4 Statistical analyses

Statistical analyses on the data of the in vitro experiments were performed with GraphPad InStat software (GraphPad software Inc., La Jolla, USA) using a one-way ANOVA combined with post-hoc Tukey–Kramer Multiple Comparisons test. The significance level was set at $p < 0.05$.

3 Results

3.1 Synthesis of HA nanocrystals

Synthesized powders were analyzed with ICP to detect the percentage of effective cationic substitution (Table 2). The results indicated that Sr^{2+} incorporation increases with increasing the Sr^{2+} ion concentration in the basic suspension used for the precipitation reaction. Data showed that the Sr/Ca ratio was 0.61 and 7.49 respectively for SrHA1 and SrHA10. The total Sr wt% incorporated in HA was proportional to the Sr wt% used during precipitation; SrHA10 contained 10-fold more Sr than SrHA1 (4.98 and 0.47 wt%, respectively). Stoichiometrically, the obtained ceramic powders showed large similarity between SrHA1 and HA (Ca/P ratio 1.71 and 1.73, respectively; (Sr+Ca)/P ratio 1.72 and 1.73, respectively) while SrHA10 showed a substantially changed molar composition (Ca/P ratio 1.46; (Sr+Ca)/P ratio 1.57).

Table 2 ICP analysis of synthesized powder. The amount of Ca, P and Sr is expressed as wt%. Stoichiometric values of Ca/P and (Sr+Ca)/P (Molar). Ratio between Sr/Ca and Sr/(Ca+Sr) in moles %

		HA	SrHA1	SrHA10
Ca	wt. %	35.97	35.23	30.43
P	wt. %	16.09	15.94	16.11
Sr	wt. %	0.00	0.47	4.98
Ca/P	Molar	1.73	1.71	1.46
(Sr+Ca)/P	Molar	1.73	1.72	1.57
Sr/Ca	moles %	0.00	0.61	7.49
Sr/(Ca+Sr)	moles %	0.00	0.01	0.07

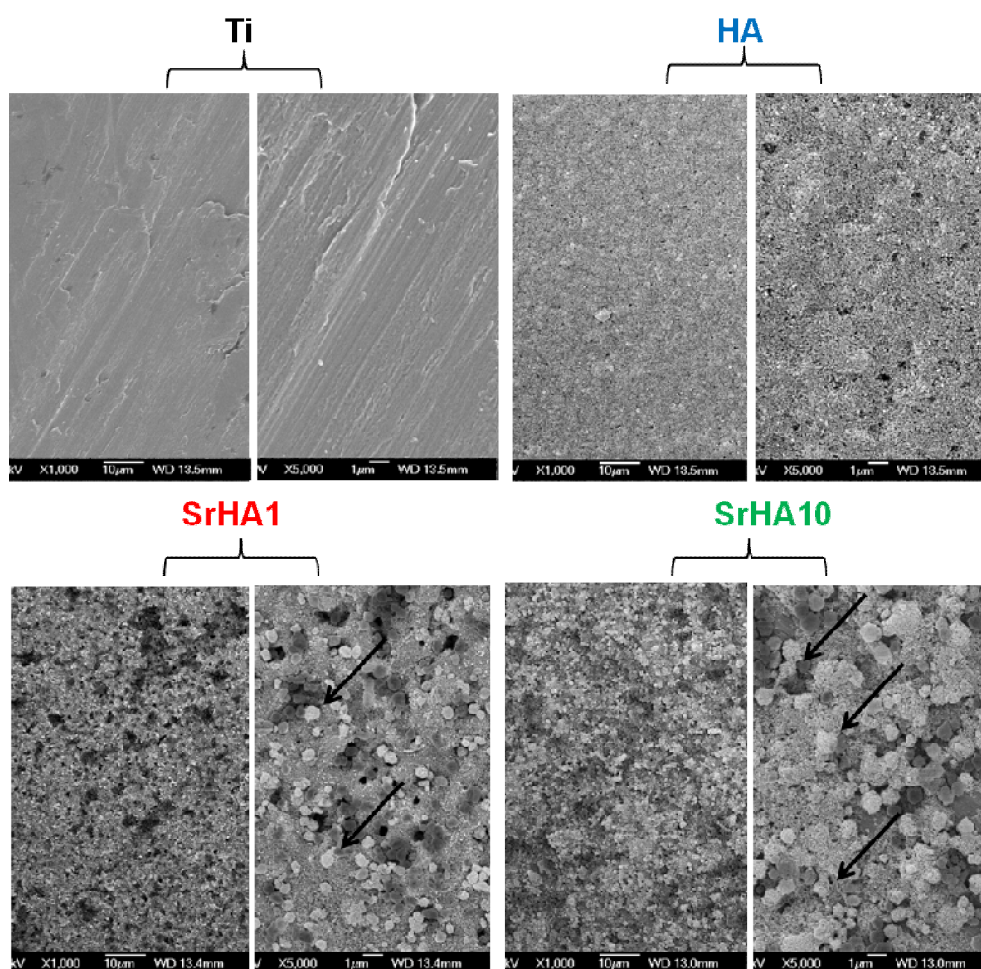


Figure 1 SEM pictures of Ti, HA, SrHA1 and SrHA10 at 1000 and 5000 magnification after deposition and lyophilization. Examples of crystal agglomerations on SrHA1 and SrHA10 are indicated by black arrows.

3.2 Coating characterization

ESD allowed deposition of all synthesized nano-sized CaP powders and SEM evaluation showed the presence of coating on the titanium substrates as indicated in Figure 1. All the analyzed disks revealed a homogeneous coating layer. The surface of coated disks showed the presence of a coating made of single nano-sized crystals covering the entire surface. Both types of Sr^{2+} -doped coatings showed the presence of agglomerations on the coated surface, which increased in number density with increasing Sr % substitution.

Figure 2 shows the crystalline structure of the deposited coatings (HA, SrHA1 and SrHA10) as analyzed with XRD. The characteristic apatitic peaks (associated to 002 and 211,112 crystal reflections, respectively) were observed for all three experimental coatings. XRD illustrated the shift at both peaks and related to the percentage of Sr substitution. The full width at half maximum (FWHM), measured for the (002) crystal reflection, was increased for Sr-doped HA accordingly to the increased ionic substitution. Data, reported in Table 3, indicated a progressive increase from 0.40° to 0.47° and to 0.50° for HA, SrHA1 and SrHA10, respectively. Therefore the mean crystallite size decreased progressively with addition of Sr^{2+} in the lattice from 27.2 nm (HA) to 21.4 (SrHA1) nm and 20.4 nm (SrHA10). FTIR analysis performed on surfaces coated with HA, SrHA1 and SrHA10 showed similar spectra as reported in Figure 3. The results indicated the spectra of the typical molecular fingerprints of asymmetric phosphate stretching at $1020 (\nu_3)$ and $960 (\nu_1) \text{ cm}^{-1}$ [26].

Table 3 Peak position, Full Width at Half Maximum and mean crystallite size calculated from XRD of all the powder and based on peak at 25.80°

	peak position ($^\circ$)	FWHM ($^\circ$)	mean crystallite size (nm)
HA	25.80	0.40	27.2
SrHA1	25.74	0.47	21.4
SrHA10	25.67	0.50	20.4

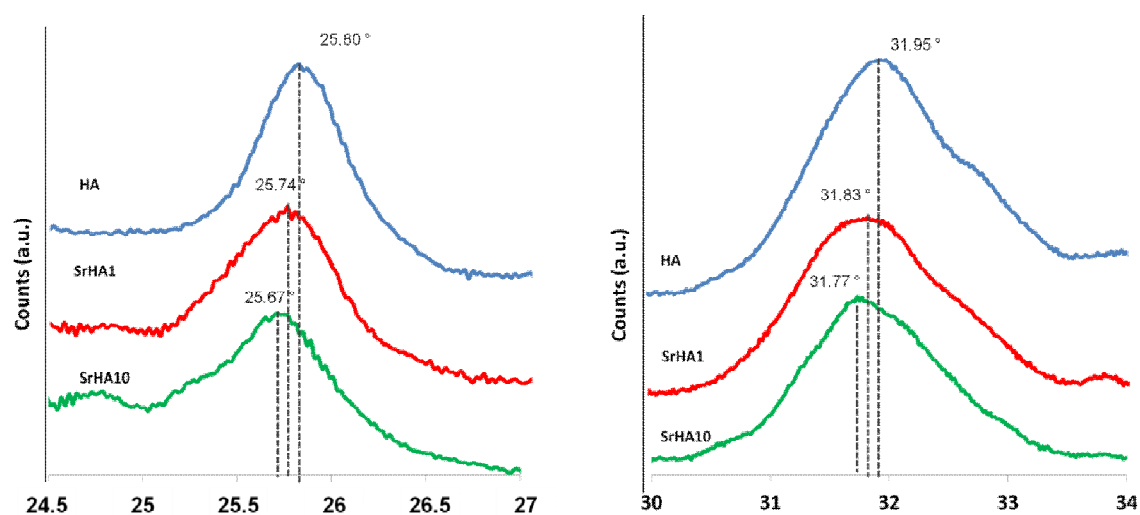


Figure 2 X-Ray Diffraction (XRD) patterns of the synthesized powders. Representative peaks (002 and 112,211) were selected for HA, SrHA1 and SrHA10. Shift of the peak at 25.80° and 31.95° are indicated on the XRD patterns.

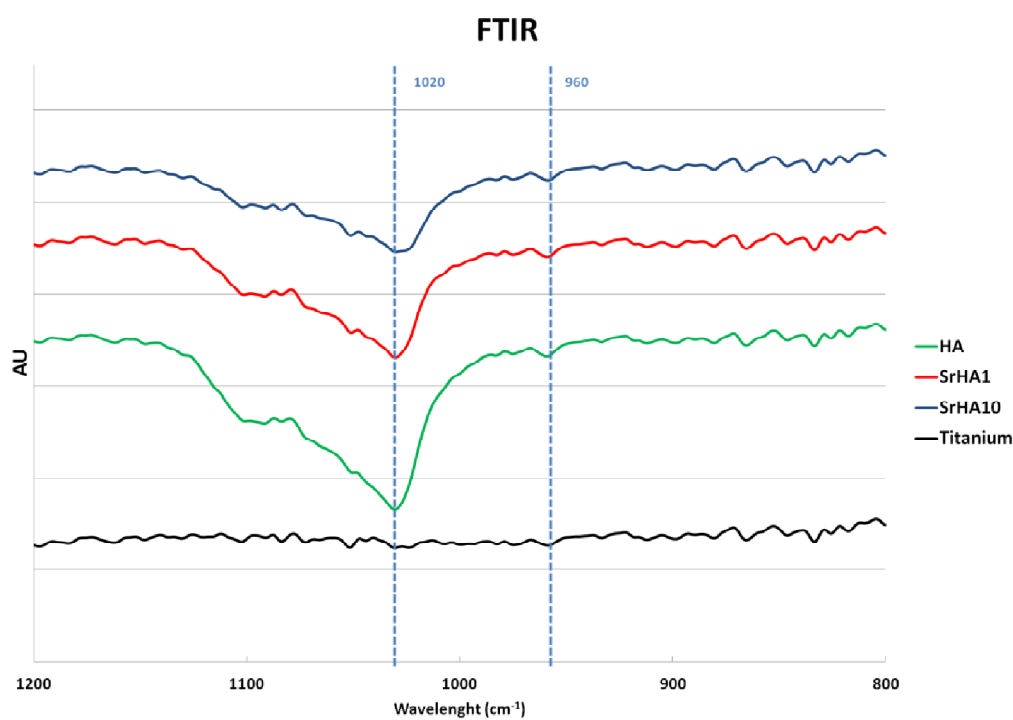


Figure 3 FTIR spectra of coated samples. Disks coated with HA, SrHA1 and SrHA10 were compared with uncoated titanium disk to verify the deposition on the disks. Phosphate stretching bands at 1020 (ν₃) and 960 (ν₁) cm⁻¹ are reported and used as indicator

3.3 In vitro experiment

Cell proliferation, as assessed using DNA-content measurements at different time points during 28 days of cell culture, was observed for all experimental groups (Figure 4). In more detail, DNA-content increased especially for SrHA10 and SrHA1 with the highest values on day 21. For SrHA10, a significantly higher DNA-content ($p < 0.05$) compared to both HA and TCP was observed on day 21.

Figure 5 presents the results for the ALP activity, which are normalized to the DNA content. For all experimental groups, a continuous increase in ALP-activity was observed without significant differences between the experimental groups at individual time points.

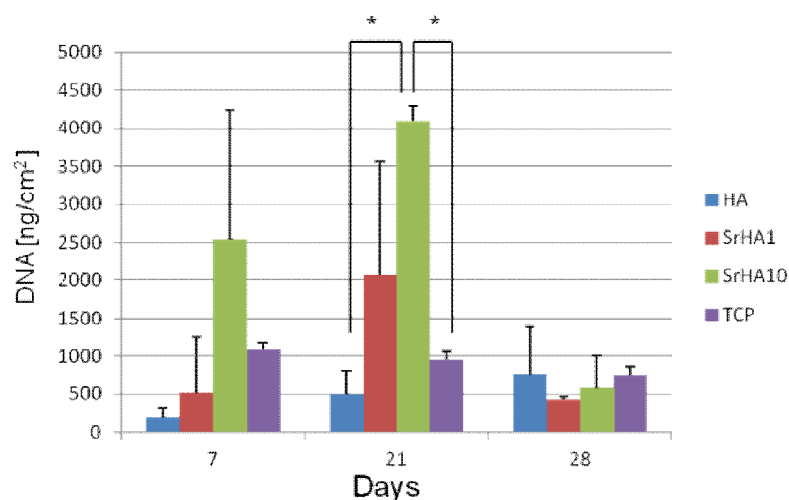


Figure 4 DNA expression of MC3T3 at day 7, 21 and 28. The amount of detected DNA is normalized per surface area. Effect of disks coated with HA, SrHA1 and SrHA10 is compared with cells seeded on tissue culture plastic (TCP). * indicated p value < 0.05

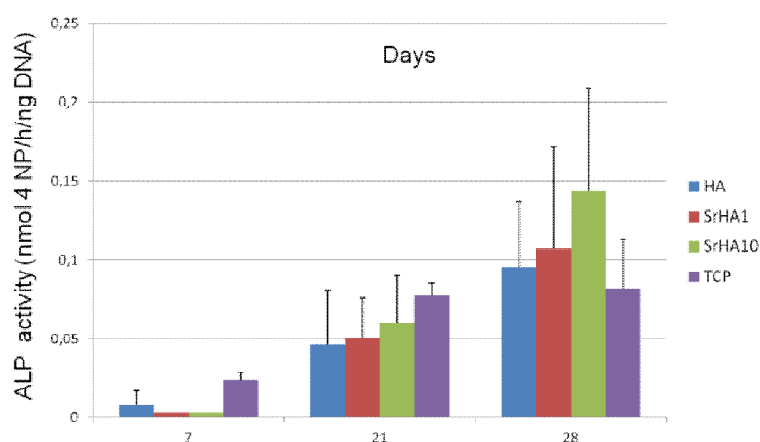
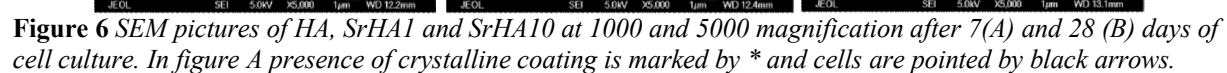


Figure 5. ALP activity quantified at day 7, 14 and 21. Results are normalized to the DNA content to be related to the cell quantity.



4Discussion

The aim of this study was to deposit nano-sized SrHA, with different levels of substitution, on titanium by means of ESD and to evaluate the effect of different amounts of Sr^{2+} -substitution in the coatings on the proliferation and differentiation of osteoblastic cells. We hypothesized that (i) ESD is a feasible method to deposit SrHA on titanium, and that (ii) the level of Sr^{2+} -substitution can modulate osteoblastic cell response in a level-dependent manner. The novelty introduced in this study is the possibility of depositing unaltered single Sr-doped crystals that can maintain all the bioactive properties. The main findings were that ESD can be used to obtain homogenous coatings for SrHA and that Sr^{2+} -substitution can increase the proliferation of osteoblastic cells.

Synthesized powders were analyzed with ICP to reveal the successful incorporation of strontium in the crystalline lattice. ICP offered a chemical analysis of the composition of the obtained powder with results corroborating earlier work[27]. The level of substitution was comparable to the w/w ratio of strontium added during precipitation, confirming the suitability of the method used to synthesize the powders. The unit cell of stoichiometric crystalline hydroxyapatite hosts 10 cations arranged in two non-equivalent positions: four at the M(1) site aligned in the column, each surrounded by nine oxygen atoms, and six at the M(2) site arranged at the apices of distributed equilateral triangles, each surrounded by seven oxygen atoms[28, 29]. For low levels of Sr substitution, due to the change in the crystal lattice, Sr^{2+} tends to replace Ca^{2+} at the M(I) sites. This preferred substitution sites reduce the efficacy of substitution to 50% due to the deformed crystal lattice that also favors PO_4^{4-} and induce a change in the stoichiometric value [30].

The parameters set for deposition were obtained from previous performed studies using nano-sized HA[21, 23]. It was noticed during the coating procedure that SrHA10 deposition required a higher voltage (14kV) to obtain a stable jet-cone. The reason for an increased

voltage could be related to the dispersion of the nano crystals in the precursor suspension. The quality of coating is related to the formation of a dripping effect[31]. The dripping effect can be limited or stopped by increasing the voltage[32] and therefore a reduced conductivity caused by crystals agglomeration could explain the required increased voltage for the deposition of SrHA.

The morphological characterization of the coatings demonstrated complete and homogeneous coverage for all experimental coatings. SEM investigation confirmed the reduced stability of the cone jet during deposition of SrHA. In fact, the presence of micro agglomerations was observed with increasing levels of Sr substitution. A similar effect, concerning formation of agglomeration on the surface during ESD, was previously reported[21] and related to the effect of nozzle-to-substrate distance. As distance is affecting the flying time and increases the evaporation of the medium during the deposition process, a reduced dispersion of nano particles can result in agglomeration in the precursor suspension and effect the coating as observed in this study. The agglomeration effect, therefore, can be due to the ratio of SrHA particles and droplet size. The FTIR spectrum of the surface and particularly the typical shape of the wavelength at 1020 cm^{-1} were used as fingerprints of calcium phosphate. HA, SrHA1 and SrHA10 showed a common pattern that was compared to non-coated disks to assure the presence of coatings prior to the in vitro experiment. Analysis of the coated surfaces, performed by XRD, confirmed the change in the mean crystallite size due to the presence of strontium as doping element[33] after deposition. According to the literature[30], the reduction of the crystallite size is related to the percentage of substitution. Therefore, ESD is not affecting the strontium content as indicated by the analysis performed with XRD of the peak at 25.80° crystallite sizes were measured.

DNA content, related to the number of cells present on the experimental disks, was increased for cells seeded on Sr^{2+} -doped hydroxyapatite already at day 7. A significant increase in cell

proliferation, compared to TCP and HA, was observed for SrHA10 at day 21. The amount of DNA detected on TCP decreased during the evaluated time points, reaching its minimum at day 28. The tendency of the control group is important to attribute variation in DNA content to the coatings. The amount of DNA, normalized per cm^2 , indicates that Sr^{2+} substitution is relevant to cause an increase in cell proliferation. The data collected are in accordance with results reported earlier[27] on the effect of Sr^{2+} -doped coatings on osteoblast cells. Sr^{2+} -doped coatings, deposited with ESD, are effective in controlling the osteoblast proliferation response; in accordance to the relative Sr^{2+} substitution percentage, SrHA1 induced a tendency to increase cell proliferation and SrHA10 significantly increased cell proliferation.

ALP activity was used as an early indicator of osteogenic differentiation[7]. In this experiment, differentiation was not significantly modified by the presence of strontium at any of the time points. The increased ALP expression at the late stage, in all the groups, is related to the transition from proliferation to differentiation. In fact, MC3T3 cells after the proliferation period (16-18 days) seemed to enter their differentiation phase as reported in the literature[34, 35]. Sr^{2+} -doped coatings impacted osteoblast behavior increasing the proliferation rate in case of SrHA10, but leaving the differentiation phase unaltered at a later stage.

The observation of coated disks during the in vitro test showed the presence of a cellular layer onto the coated surfaces. At an early time point (day 7), HA was partially covered by cells and the possibility to detect the coating layer, in areas without cells, indicated that HA coating is relatively stable. It is relevant to mention that SrHA1 and SrHA10, showed a total coverage at day 7.

A SR-doped HA-based coating associated with adsorption of therapeutic drugs can be the starting point for development of coatings able to target different aspects in patients affected by different pathological requirements. For instance, an important class of anti-osteoporotic

drugs, i.e. bisphosphonates, are known for their effect on osteoclastic cells and the affinity for CaP [36]. A Sr^{2+} -doped coating with adsorbed bisphosphonate could be an instructive approach able to control enhance osteoblast activity and suppress osteoclast activity to favor bone formation. A bioinorganic based material enriched with bioactive biomolecules is an appealing material to exploit the full potential of ESD to obtain therapeutic coatings.

5 Conclusions

This study demonstrated that ESD is an effective method to deposit nano-sized SrHA without altering the structure of synthesized materials after deposition. Strontium was confirmed to be a powerful bioinorganic tool to control osteoblast fate. The percentage of substitution played a role in increasing cell proliferation. ESD proved to be a possible deposition method that conserves the integrity of the nano crystals and the characteristics of Sr-doped hydroxyapatite.

References

1. Bosco, R., et al., *Instructive coatings for biological guidance of bone implants*. Surface and Coatings Technology, (0).
2. LeGeros, R.Z., *Properties of osteoconductive biomaterials: calcium phosphates*. Clinical orthopaedics and related research, 2002. **395**: p. 81-98.
3. Wei, M., et al., *Solution ripening of hydroxyapatite nanoparticles: Effects on electrophoretic deposition*. Journal of biomedical materials research, 1999. **45**(1): p. 11-19.
4. Ishizawa, H. and M. Ogino, *Formation and characterization of anodic titanium oxide films containing Ca and P*. Journal of biomedical materials research, 1995. **29**(1): p. 65-72.
5. Chiesa, R., et al., *Osteointegration of titanium and its alloys by anodic spark deposition and other electrochemical techniques: a review*. Journal of applied biomaterials & biomechanics: JABB, 2003. **1**(2): p. 91.
6. Bigi, A., et al., *Nanocrystalline hydroxyapatite coatings on titanium: a new fast biomimetic method*. Biomaterials, 2005. **26**(19): p. 4085-4089.
7. Habibovic, P. and J. Barralet, *Bioinorganics and biomaterials: bone repair*. Acta Biomaterialia, 2011. **7**(8): p. 3013-3026.
8. Bigi, A., et al., *Chemical and structural characterization of the mineral phase from cortical and trabecular bone*. Journal of inorganic biochemistry, 1997. **68**(1): p. 45-51.
9. Dahl, S., et al., *Incorporation and distribution of strontium in bone*. Bone, 2001. **28**(4): p. 446-453.
10. Canalis, E., et al., *The divalent strontium salt S12911 enhances bone cell replication and bone formation in vitro*. Bone, 1996. **18**(6): p. 517-523.
11. Landi, E., et al., *Sr-substituted hydroxyapatites for osteoporotic bone replacement*. Acta Biomaterialia, 2007. **3**(6): p. 961-969.
12. Li, Z., et al., *Chemical composition, crystal size and lattice structural changes after incorporation of strontium into biomimetic apatite*. Biomaterials, 2007. **28**(7): p. 1452-1460.
13. Pereiro, I., et al., *Pulsed laser deposition of strontium-substituted hydroxyapatite coatings*. Applied Surface Science, 2012. **258**(23): p. 9192-9197.
14. Xue, W., et al., *Preparation and cell-materials interactions of plasma sprayed strontium-containing hydroxyapatite coating*. Surface and Coatings Technology, 2007. **201**(8): p. 4685-4693.
15. Oliveira, A., R. Reis, and P. Li, *Strontium-substituted apatite coating grown on Ti6Al4V substrate through biomimetic synthesis*. Journal of Biomedical Materials Research Part B: Applied Biomaterials, 2007. **83**(1): p. 258-265.
16. Bosco, R., et al., *Surface Engineering for Bone Implants: A Trend from Passive to Active Surfaces*. Coatings, 2012. **2**(3): p. 95-119.
17. Nijhuis, A.W., S.C. Leeuwenburgh, and J.A. Jansen, *Wet-Chemical Deposition of Functional Coatings for Bone Implantology*. Macromolecular bioscience, 2010. **10**(11): p. 1316-1329.
18. Leeuwenburgh, S.C.G., et al., *Influence of precursor solution parameters on chemical properties of calcium phosphate coatings prepared using Electrostatic Spray Deposition (ESD)*. Biomaterials, 2004. **25**(4): p. 641-649.
19. Morozov, V.N. and T.Y. Morozova, *Electrospray deposition as a method for mass fabrication of mono-and multicomponent microarrays of biological and biologically active substances*. Analytical chemistry, 1999. **71**(15): p. 3110-3117.
20. Leeuwenburgh, S.C.G., et al., *Deposition of calcium phosphate coatings with defined chemical properties using the electrostatic spray deposition technique*. Journal of the European Ceramic Society, 2006. **26**(4-5): p. 487-493.
21. Iafisco, M., et al., *Electrostatic Spray Deposition of Biomimetic Nanocrystalline Apatite Coatings onto Titanium*. Advanced Engineering Materials. **14**(3): p. B13-B20.
22. de Jonge, L.T., et al., *Electrosprayed Enzyme Coatings as Bioinspired Alternatives to Bioceramic Coatings for Orthopedic and Oral Implants*. Advanced Functional Materials, 2009. **19**(5): p. 755-762.

23. Alghamdi, H.S., et al., *Biological response to titanium implants coated with nanocrystals calcium phosphate or type I collagen in a dog model*. Clinical Oral Implants Research: p. n/a-n/a.
24. de Jonge, L.T., et al., *The osteogenic effect of electrosprayed nanoscale collagen/calcium phosphate coatings on titanium*. Biomaterials. **31**(9): p. 2461-2469.
25. de Jonge, L.T., et al., *In vitro responses to electrosprayed alkaline phosphatase/calcium phosphate composite coatings*. Acta Biomaterialia, 2009. **5**(7): p. 2773-2782.
26. Rehman, I. and W. Bonfield, *Characterization of hydroxyapatite and carbonated apatite by photo acoustic FTIR spectroscopy*. Journal of Materials Science: Materials in Medicine, 1997. **8**(1): p. 1-4.
27. Capuccini, C., et al., *Strontium-substituted hydroxyapatite coatings synthesized by pulsed-laser deposition: in vitro osteoblast and osteoclast response*. Acta Biomaterialia, 2008. **4**(6): p. 1885-1893.
28. MI, K. and Y. RA, *Crystal structure of hydroxyapatite*. Nature, 1964. **204**: p. 1050-1052.
29. Elliott, J.C., *Structure and chemistry of the apatites and other calcium orthophosphates*. Vol. 4. 1994: Elsevier Amsterdam.
30. Bigi, A., et al., *Strontium-substituted hydroxyapatite nanocrystals*. Inorganica Chimica Acta, 2007. **360**(3): p. 1009-1016.
31. Jaworek, A. and A.T. Sobczyk, *Electrospraying route to nanotechnology: An overview*. Journal of Electrostatics, 2008. **66**(3-4): p. 197-219.
32. Cloupeau, M. and B. Prunet-Foch, *Electrostatic spraying of liquids: main functioning modes*. Journal of Electrostatics, 1990. **25**(2): p. 165-184.
33. Li, Z.Y., et al., *Chemical composition, crystal size and lattice structural changes after incorporation of strontium into biomimetic apatite*. Biomaterials, 2007. **28**(7): p. 1452-1460.
34. Quarles, L.D., et al., *Distinct proliferative and differentiated stages of murine MC3T3-E1 cells in culture: An in vitro model of osteoblast development*. Journal of Bone and Mineral Research, 1992. **7**(6): p. 683-692.
35. Gadaleta, S., et al., *Fourier transform infrared spectroscopy of the solution-mediated conversion of amorphous calcium phosphate to hydroxyapatite: new correlations between X-ray diffraction and infrared data*. Calcified tissue international, 1996. **58**(1): p. 9-16.
36. Rogers, M.J., et al., *Biochemical and molecular mechanisms of action of bisphosphonates*. Bone, 2011. **49**(1): p. 34-41.

Chapter VIII

Summary and address to the aims

Chapter I

Synthetic inorganic and organic materials have been extensively investigated in the field of bone regeneration in an attempt to mimic the composition and structure of the extracellular matrix (ECM) of bone tissue with the ultimate aim of generating suitable synthetic bone substitute materials and modifying the surface of bone implants. For load-bearing applications, bone implants are generally made of a bioinert metal with appropriate mechanical properties and a modified surface (i.e. roughened, coated or a combination thereof), to enhance the surface biocompatibility and osteoconductivity. Currently, biomaterials research is evolving from the use of bioinert and biologically passive implants toward interactive implants that stimulate tissue regeneration. Therefore, surface physico-chemical properties of bone implants need to be optimal and capable to biologically instruct and stimulate the regeneration of bone tissue.

In view of the aforementioned statements, the general aim of the research described in this thesis was to investigate the potential of coating modifications for bone implant surfaces. Various surface modification approaches, in the field of load-bearing bone implants, were explored with emphasis on the use of inorganic and organic coating compounds. Bioinspired approaches were primarily investigated and coatings that actively participate in the biological processes that occur upon implantation. In order to obtain a deeper comprehension and conceptualization of the state-of-the-art, the first chapter of this thesis describes surface modifications that can be helpful to achieve desired tissue responses in healthy as well as compromised conditions.

Chapter II

Chapter II provides an analysis of recent trends and strategies in surface engineering that are currently investigated to improve the biological performance of bone implants in terms of

functionality and biological efficacy. Bone is a connective tissue composed of an organic collagenous matrix, a fine dispersion of reinforcing inorganic (calcium phosphate) nanocrystals, and bone-forming and -degrading cells. These different components have a synergistic and hierarchical structure that renders bone tissue properties unique in terms of hardness, flexibility and regenerative capacity. Metallic and polymeric materials offer mechanical strength and/or resilience, which are required to simulate bone tissue in load-bearing applications in terms of maximum load, bending and fatigue strength. Nevertheless, the interaction between devices and the surrounding tissue at the implant interface is essential for success or failure of implants. In that respect, coatings can be applied to facilitate the process of bone healing and obtain a continuous transition from living tissue to the synthetic implant. Compounds that are inspired by inorganic (e.g. hydroxyapatite crystals) or organic (e.g. collagen, extracellular matrix components, enzymes) components of bone tissue, are the most obvious candidates for application as implant coating to improve the performance of bone implants. Electrospray deposition (ESD) has emerged as a coating method able to be applied for a wide range of materials, preserving the control offered by physical deposition methods and the capacity of preserving the integrity of the material used.

Chapter III

Titanium and its alloys are widely used to manufacture orthopaedic and dental implants due to their excellent mechanical properties and corrosion resistance. However, these materials are bioinert and the best way to improve bone implant contact and their biological properties could be the application of a coating made of nanostructured apatite. In chapter III, the applicability of ESD technique for the deposition of nanostructured uniform apatite coating onto commercially pure cp-Ti substrates at room temperature was evaluated. Hence, poorly crystalline bone-like carbonate-apatite nanocrystals were synthesized and characterized. The apatite suspension suitable for the ESD process in terms of dispersion, aggregation and

stability was set up and several ESD processing parameters such as nozzle to substrate distance, relative humidity in the deposition chamber and deposition time were varied in order to assess the morphological effects. Porous films made of agglomerates of plate-like apatite nanocrystals, measuring approximately 50 nm with morphology and dimensions resembling natural bone apatite mineral were formed. The results showed the feasibility of the ESD technique for the generation of thin apatite coatings with a nanosized surface morphology onto titanium substrates. The ability of these nanocrystals to bind therapeutic agents for bone diseases and the capability of ESD to produce coating at physiological conditions makes this work a first step for the set up of coatings for bone implants based on surface-activated apatite with improved functionality.

Chapter IV

The ultimate goal for surface modifications in bone implants is to achieve biologically active surfaces able to control and trigger specific tissue response, as described earlier in Chapter II. After the application of inorganic nano-sized hydroxyapatite (Chapter III), Chapter IV evaluated the effects of organic compounds, derived from extracellular matrix, involved in tissue mineralization. Alkaline phosphatase (ALP) plays a fundamental role in bone mineralization concurrently with collagen, the main organic components of bones. Electrospray deposition (ESD) was used to coat titanium disks with ALP and collagen at room temperature. To verify potential synergistic effects of ALP and collagen, different conformations of coatings (mixed and layered) were obtained and their mineralization capacity was tested *in vitro*. The mineralization tests indicated the fundamental role of collagen to increase ALP retention. Analyses indicated that the coating conformation has a role: mixed collagen/ALP coatings showed improved ALP retention, enzymatic activity and unique mineralized surface morphology. ESD demonstrated to be a successful method to

deposit organic molecules preserving their properties as indicated by the *in vitro* results. These findings proved the synergistic effect of ALP and collagen in inducing mineralization, offering an intriguing coating constituent for medical devices that aims to trigger surface mineralization.

Chapter V

The integration of bone implants within native bone tissue depends on periprosthetic bone quality, which is severely decreased in osteoporotic patients. In Chapter V, the synthesized and characterized bioinspired hydroxyapatite nanocrystals (nHA), previously investigated in Chapter III, were enriched with alendronate (nHA_{ALE}), a well-known bisphosphonate drug used for anti-osteoporotic treatment. *In vitro* tests were used to evaluate the effects of nHA_{ALE} on osteoclast-like cells and showed that nHA_{ALE} significantly promoted apoptosis of osteoclast-like cells. Additionally, nHA and nHA_{ALE} were successfully deposited on titanium disks via electrospray deposition (ESD) while characterization of the deposited coatings confirmed the presence of alendronate in nHA_{ALE} coatings with a nanoscale thickness of 700 nm. These results indicated that alendronate adsorbed to nano-sized hydroxyapatite crystals has therapeutic potential and can be considered as a coating constituent for orthopaedic and oral implants for osteoporotic patients.

Chapter VI

The prevalence of osteoporosis will further increase within the next decades due to the aging world population, which can affect the bone healing response to dental and orthopaedic implants. Consequently, local drug targeting of peri-implant bone has been proposed as a strategy for the enhancement of bone-implant integration in osteoporotic conditions. In Chapter VI, an established *in vivo* femoral condyle implantation model in osteoporotic and

healthy bone is used to analyze the osteogenic capacity of titanium implants coated with bisphosphonate (BP)-loaded calcium phosphate nanoparticles (nCaP), previously described in Chapter V, under compromised medical conditions in the femoral condyle of rats. After 4 weeks of implantation, peri-implant bone volume (%BV; by micro-CT) and bone area (%BA; by histomorphometry) were significantly increased within a peri-implant region of 500 μm adjacent to surfaces functionalized with BP compared to control implants in osteoporotic and healthy conditions. Furthermore, the deposition of nCaP/BP coatings onto implant surfaces increased bone-to-implant contact (%BIC) compared to non-coated implants in osteoporotic and healthy conditions. The results of real-time PCR revealed similar osteogenic gene expression levels to all implant surfaces at 4-weeks post-implantation. In conclusion, simultaneous targeting of bone formation (by nCaP) and bone resorption (by BP) using nCaP/BP surface coatings represents an effective strategy for improving bone-implant integration, especially in osteoporotic conditions.

Chapter VII

Titanium implants are widely used as implants in orthopaedics and dentistry for load bearing applications. Regardless of their success, there is still great interest in improving these implants in terms of faster bone healing, or applicability in compromised conditions, as previously reported in Chapter VI. An established strategy, indicated in Chapter II, is coating titanium implants with materials that resemble the composition of bone, such as hydroxyapatite (HA). Recently, there has been increasing awareness of the biological role of strontium, indicating that it could lead to a more bioactive implant surface. Strontium is easily introduced as a natural substitute for calcium in HA crystals. Strontium-substituted HA (SrHA) crystals have shown the capacity to enhance the proliferation and differentiation of osteoblastic cells in vitro. Among the various coating deposition methods, electrospray

deposition (ESD) is a technique that allows deposition at low temperatures preserving the crystal structure of nanosized SrHA, as reported in Chapter V and VI. The aim of Chapter VII was to deposit SrHA nanocrystals with different percentages of Sr-substitution (1 and 10%, SrHA1 and SrHA10) using ESD and evaluate their effect on osteoblast proliferation and differentiation *in vitro*. ESD demonstrated to be an effective method to deposit SrHA without altering the structure of synthesized materials after deposition. The effect of SrHA on cell behavior was dependent on its substitution degree as shown by the fact that SrHA10 coated disks increased osteoblastic cell proliferation, whereas SrHA1 coated disks did not. Chapter VII showed the possibility to use ESD for the deposition of bioinorganic compounds such as SrHA and the importance of preserving its bioactive properties.

Closing remarks and future perspectives

In this thesis, research efforts focused on the use of different coatings based on organic, inorganic and composite materials in order to create bioactive surface modifications for bone implantology applications. Different materials and deposition methods have been used in the past decades to overcome the limitation imposed by a foreign body implant. Bone implants evolved from biocompatible to instructive, or bioactive, trying to face different approaches (as illustrated in Chapter II) and targeting different issues that affect implant immobilization. Among all the described and available techniques, electrospray deposition (ESD) was selected to standardize the researches done in this thesis and to maintain the same method for all the material deposited. ESD was selected for its versatility regarding the possibility to deposit different compounds, from inorganic to organic, preserving their structure and integrity.

Calcium phosphate (CaP) coatings remain the most successful approach for inorganic surface modifications for application in bone tissue. Inspired by the composition of bone, hydroxyapatite (HA), a specific stoichiometric and configurational form of CaP, was used in nano-sized crystal form (Chapter III, Chapter V, Chapter VI and Chapter VII) to mimic the bone inorganic structure preserving the nano-sized plate shaped. ESD permitted to enrich nHA adding extra bioactive properties as the possibility to adsorb anti-osteoporotic drugs on the crystal surface (Chapter V and Chapter VI). The role of ESD was instrumental to preserve the effect of nHA that was deposited as a homogenous layer of single nano-sized crystals. The nano-scale dimension of the crystals was a core element to mimic natural bone and to maintain a high crystal surface area onto which alendronate was adsorbed, a potent bisphosphonate used for systemic treatment of osteoporosis, and to obtain a coating able to therapeutically treat the local peri-implant area by impacting the osteoclast behaviour. The potential and applicability of these specific and innovative approaches were investigated first in vitro, evaluating the capacity to induce apoptosis of osteoclasts (Chapter V) and thereafter

verified *in vivo* using a rat-osteoporotic model with implantation of coated implants in the femoral condyle (Chapter VI). The results showed the potential in terms of osteoclast reduction, bone to implant contact and bone volume augmentation induced by implants coated with instructive nHA combined with therapeutic alendronate.

A promising approach for inorganic-based coating is the use of ionic substitution to add bioinorganic properties to the established applications of CaP (Chapter VII). The results showed the possibility to incorporate strontium as a calcium substitute to obtain Sr-doped crystals with new characteristics. In fact, where nHA resembles natural bone inorganic phase, the bioinorganic strontium apatite (SrHA) aimed to introduce an active control over cell behaviour. SrHA was tested as a deposited coating using ESD and with an *in vitro* model using osteoblast cells. The potential of bioinorganic coatings to modulate cellular behaviour was demonstrated, opening a new route for inorganic coatings with multiple specific properties depending on ionic substitution and the physiological efficacy thereof.

Beside inorganic coatings, other approaches were investigated using organic materials inspired by the bone extracellular composition. In particular, the combined effect of collagen and alkaline phosphatase (ALP), in different configurations, was investigated to mimic the acellular mineralization process (Chapter IV). Collagen improved ALP retention as well as the already known mineralization ability of ALP. Further, the configuration of ALP combined with collagen was able to increase the ALP enzyme amount retained on the surface, the quantity of surface mineralization, and affect the morphology of the mineralization. The knowledge acquired performing such experiments was essential to obtain insight into the potential of ESD to deposit organic coating at low temperature as well as the effect of coating configurations to affect its physiological properties. The unique properties of the obtained coatings have great potential for regenerative medicine applications as well as for bone implants coatings.

Although the ESD technique was shown to be a powerful method to deposit coatings to metallic implants, several drawbacks need be solved prior to clinical translation. For coating generation, it is fundamental to use a coating method that is not operator-dependent as ESD. The stability of the deposition requires constant monitoring and it represents a strong limitation to upscale the production. Further research efforts should be invested in methodologies to control the deposition stability, for example using a video acquiring system able to monitor the light scattering of a laser beam passing through the sprayed cone. A software algorithm could modify the voltage applied and maintain the stability of the deposition.

Retention of the coating to the substrate is also a weak point of wet-chemical deposition methods such as ESD, that reduces the applicability of the coating in clinical situations. In view of these limitations, more emphasis should be placed on strategies to obtain a double coating process. Starting from CaP coated implants using physical deposition methods (i.e. RF sputtering or plasma-spray deposition), it would be possible to guarantee a strong adhesion between CaP and the titanium surface. To compensate the lack of bioactive properties of these deposition methods (due to the relatively high temperatures during deposition), ESD can be used to deposit instructive materials. The possibility to deposit a bioactive coating on a CaP-coated surface could overcome the retention limit and start a completely new era for ESD. Lastly, the progress in biomedical research for bone applications will be, in the near future, oriented in obtaining more specific or even patient-related solutions (i.e. personalized health care) that will be based on the presence of organic coatings and resorbable bulk materials. In view of this, coatings will play an increasingly important role and it will change the scope of modifying biomedical implant surfaces: previously it was from biocompatible to bioactive and in future it will be from instructive to therapeutic.

Samenvatting, afsluitende opmerkingen en toekomstperspectief

Hoofdstuk I

Synthetische anorganische en organische materialen zijn uitgebreid onderzocht op het gebied van botregeneratie in een poging om de samenstelling en structuur van de extracellulaire matrix (ECM) van botweefsel na te bootsen met als uiteindelijk doel het vervaardigen van geschikte synthetische botvervangende materialen en modificeren van het oppervlak van botimplantaten. Voor lastdragende toepassingen worden botimplantaten gewoonlijk gemaakt van een bioinert metaal met geschikte mechanische eigenschappen en geoptimaliseerd via een gemodificeerd oppervlak (bijvoorbeeld ruw, gecoat of een combinatie daarvan) dat de biocompatibiliteit en osteoconductiviteit verbetert. Momenteel evolueert biomaterialen onderzoek van het gebruik van bioinerte en biologisch passieve implantaten richting interactieve implantaten die weefselregeneratie te stimuleren. Derhalve moeten de fysisch-chemische eigenschappen van bot implantaten optimaal zijn om biologische instructies te geven en regeneratie van botweefsel te stimuleren.

Ten aanzien van de hiervoor genoemde verklaringen was het algemene doel van het in dit proefschrift beschreven onderzoek om het potentieel van verschillende coating-gebaseerde modificaties voor bot implantaatoppervlakken te onderzoeken. Verschillende oppervlakte modificatie benaderingen op het gebied van lastdragende botimplantaten werden onderzocht met de nadruk op het gebruik van anorganische en organische bestanddelen. Biologisch geïnspireerde benaderingen werden voornamelijk onderzocht evenals coatings die actief deelnemen aan de biologische processen die optreden bij implantatie. Om een beter begrip en beeldvorming van de stand van de techniek te verkrijgen, beschrijft het eerste hoofdstuk van dit proefschrift oppervlakmodificaties die nuttige en gewenste weefselreacties in gezonde en gecompromitteerde omstandigheden kunnen realiseren.

Hoofdstuk II

Hoofdstuk II geeft een analyse van recente trends en strategieën in oppervlakte-engineering die momenteel worden onderzocht om de biologische prestatie van bot implantaten ten aanzien van functionaliteit en biologische effectiviteit te verbeteren. Bot is bindweefsel samengesteld uit een organische collagene matrix, een fijne dispersie van anorganische versterkende (calciumfosfaat) nanokristallen en botvormende en –afbrekende cellen. Deze verschillende componenten hebben een synergetische en hiërarchische structuur die botweefsel eigenschappen uniek maken voor wat betreft hardheid, flexibiliteit en regeneratievermogen. Metalen en polymere materialen bieden mechanische sterkte en/of veerkracht, die botweefsel moeten simuleren tijdens lastdragend gebruik ten aanzien van maximale belasting, buiging en vermoeiingssterkte. Toch is de interactie tussen implantaten en het omringende weefsel aan het implantaat oppervlak essentieel voor het succes of falen van implantaten. In dit verband kunnen coatings worden toegepast om het proces van botgenezing te vergemakkelijken en een continue overgang te verkrijgen van levend weefsel naar het synthetisch implantaat. Bestanddelen die zijn geïnspireerd door anorganische (bijvoorbeeld hydroxyapatiet kristallen) of organische (bijvoorbeeld collageen, extracellulaire matrix componenten, enzymen) componenten van het botweefsel, zijn de meest voor de hand liggende kandidaten voor toepassing als implantaat coating om de prestaties van bot-implantaten te verbeteren. Elektrospray depositie (ESD) heeft zich ontpopt als een coating methode die kan worden toegepast voor een breed scala aan materialen, met behoud van controle via fysieke depositiemethodiek en de integriteit van het gebruikte (coating) materiaal.

Hoofdstuk III

Titaan en titaanlegeringen worden veel gebruikt om orthopedische en tandheelkundige implantaten te vervaardigen vanwege hun uitstekende mechanische eigenschappen en

corrosiebestendigheid. Echter, deze materialen zijn bioinert en de beste manier om bot/implantaat contact en de biologische eigenschappen te verbeteren zou de toepassing van een coating op basis van nanogestructureerde apatiet kunnen zijn. In hoofdstuk III werd daarom de toepasbaarheid van de ESD-techniek voor de depositie van nanogestructureerde, uniforme apatietcoatings op commercieel zuiver cp-Ti substraten bij kamertemperatuur geëvalueerd. Daartoe zijn zwak kristallijne, botachtige carbonaat-apatiet nanokristallen gesynthetiseerd en gekarakteriseerd. De apatiet suspensie geschikt voor ESD ten aanzien van dispersie, aggregatie en stabiliteit werd onderzocht en verschillende ESD procesparameters zoals afstand nozzle/substraat, relatieve vochtigheid in de depositiekamer en depositie tijd werden gevarieerd om de morfologische effecten te bepalen. Poreuze films van agglomeraten van plaatvormige apatiet nanokristallen, met een grootte van ongeveer 50 nm en een morfologie en dimensiesgelijkend op natuurlijk bot mineraal apatiet werden gevormd. De resultaten toonden de haalbaarheid van de ESD techniek voor het genereren van dunne apatiet coatings met een nano-sized oppervlaktetopografie op titanium substraten. Het vermogen van deze nanokristallen om therapeutische middelen te binden ter behandeling van botziekten en de mogelijkheid om met ESD coatings te deponeren onder fysiologische omstandigheden maakt van dit onderzoek een eerste stap in de richting van coatings voor botimplantaten gebaseerd op oppervlakte geactiveerd apatiet met verbeterde functionaliteit.

Hoofdstuk IV

Het uiteindelijke doel voor oppervlaktemodificaties van bot implantaten is om biologisch actieve oppervlakken te verkrijgen die een specifieke weefselrespons kunnen realiseren, zoals eerder beschreven in hoofdstuk II. Na het aanbrengen van anorganisch, nano-sized hydroxyapatiet (hoofdstuk III), werden in hoofdstuk IV de effecten van organische bestanddelen afkomstig van de extracellulaire matrixen betrokken bij

weefselmineralisatieonderzocht. Alkalische fosfatase (ALP) speelt een fundamentele rol in de botmineralisatie gelijktijdig met collageen, de belangrijkste organische componenten van botweefsel. Electrospray deposition (ESD) werd gebruikt voor het coaten van titanium disks met ALP en collageen bij kamertemperatuur. Om potentiële synergetische effecten van ALP en collageen te verifiëren, werden verschillende conformaties van coatings (gemengde en gelaagde) vervaardigd en de mineralisatiecapaciteit werd in vitro getest. De mineralisatie testen toonden een fundamentele rol voor collageen om retentie van ALP te verhogen. Uit analyses bleek dat de coating conformatie tevens een rol heeft: gemengde collageen/ALP coatings hadden een betere ALP-retentie, enzymatische activiteit en een unieke, gemineraliseerde oppervlakt morfologie. ESD heeft hiermee aangetoond een succesvolle methode te zijn om organische moleculen te deponeren met behoud van hun eigenschappen zoals bewezen door de in vitro resultaten. Deze bevindingen bewezen het synergetische effect van ALP en collageen met betrekking tot het induceren van (oppervlakte)mineralisatie, op basis van een intrigerend coatingbestanddeel voor medische hulpmiddelen die beogen oppervlaktemineralisatie te activeren.

Hoofdstuk V

De integratie van botimplantaten in bestaand botweefsel hangt af van de peri-prothetische botkwaliteit, welke sterk is afgenomen bij osteoporose patiënten. In hoofdstuk V, werden biologisch geïnspireerde hydroxyapatiet nanokristallen (nHA) gesynthetiseerd en gekarakteriseerd, welke eerder werden onderzocht in hoofdstuk III, maar nu ook verrijkt met alendronaat (nHAALE), een bekende bisfosfonaat medicijn dat gebruikt wordt voor anti-osteoporose behandeling. In vitro testen werden gebruikt om de effecten van nHAALE op osteoclast-achtige cellen te evalueren en toonden dat nHAALE apoptose van osteoclast-achtige cellen aanzienlijk bevordert. Bovendien werden nHA en nHAALE succesvol afgezet

op titanium disks via electrospray depositie (ESD) en karakterisatie van de afgezette coatings bevestigde de aanwezigheid van alendronaat in nHAALe coatings met een nano-size dikte van 700 nm. Deze resultaten gaven aan dat alendronaat geadsorbeerd op nano-sized hydroxyapatietkristallen therapeutische potentieel heeft en kan worden beschouwd als een coatingbestanddeel voor orthopedische implantaten in osteoporotische patiënten.

Hoofdstuk VI

De prevalentie van osteoporose zal verder stijgen in de komende decennia door de vergrijzende wereldbevolking, waardoor de botgenezingsreactie rondom tandheelkundige en orthopedische implantaten negatief wordt beïnvloed. Bijgevolg is lokale drug targeting van peri-implantaat bot voorgesteld als een strategie voor de verhoging van bot-implantaat integratie in osteoporotische omstandigheden. In hoofdstuk VI, werd een gevestigd in vivo femorale condyle implantatie model gebruikt in osteoporotisch en gezond bot om het osteogene vermogen van titanium implantaten gecoat met bisfosfonaat (BP) geladen calciumfosfaat nanodeeltjes (nCaP; eerder beschreven in hoofdstuk V) te analyseren onder medisch-gecompromitteerde condities in ratten. Na 4 weken implantatie, werd een aanzienlijk verhoogd peri-implantaat botvolume (% BV, door micro-CT) en botoppervlak (% BA; door histomorfometrie) waargenomen binnen een peri-implantaat gebied van 500 μ m voor oppervlakken gefunctionaliseerd met BP vergeleken met controle implantaten in osteoporotische en gezonde condities. Bovendien verhoogde de depositie van nCaP/BP coatings op implantaat oppervlakken het bot/implantaatcontact (BIC%) vergeleken met niet-gecoate implantaten onder osteoporose en gezonde omstandigheden. De resultaten van de real-time PCR toonden gelijke osteogene genexpressieniveaus van weefsel rond alle implantaatoppervlakken op 4 weken na implantatie. Geconcludeerd werd dat gelijktijdige targeting van botvorming (door nCaP) en botresorptie (door BP) via een nCaP/BP coating een

effectieve strategie vertegenwoordigt voor het verbeteren van bot-implantaat integratie, vooral in osteoporotische omstandigheden.

Hoofdstuk VII

Titanium implantaten worden op grote schaal gebruikt in de orthopedie en tandheelkunde voor lastdragende toepassingen. Ongeacht hun succes is er nog steeds grote interesse voor de verbetering deze implantaten ten aanzien van snellere botgenezing of toepasbaarheid in gecompromitteerde condities, zoals eerder beschreven in Hoofdstuk VI. Een gevestigde strategie, vermeld in hoofdstuk II, is het coaten van titanium implantaten met materialen die de samenstelling van het bot nabootsen, zoals hydroxyapatiet (HA). Recentelijk is er sprake van een toenemende bewustwording van de biologische rol van strontium, waarvoor data aangeven dat het zou kunnen bijdragen aan een meer bioactief implantaatoppervlak. Strontium wordt gemakkelijk geïntroduceerd als een substituuut voor natuurlijke calcium in HA kristallen. Strontium-gesubstitueerde HA (SrHA) kristallen toonden het vermogen om de proliferatie en differentiatie van osteoblasten in vitro te versterken. Onder de verschillende coating depositiemethoden, is electrospray depositie (ESD) een techniek die toelaat depositie bij lage temperatuur uit te voeren en de kristalstructuur van nanogrootte SrHA te bewaren, zoals beschreven in hoofdstuk V en VI. Het doel van hoofdstuk VII was om SrHA nanokristallen met verschillende percentages van Sr-substitutie (1 en 10%, SrHA1 en SrHA10) via gebruik van een ESD te vervaardigen en hun effect op de osteoblasten proliferatie en differentiatie in vitro te evalueren. ESD heeft aangetoond een effectieve methode te zijn om SrHA te deponeren zonder de structuur van gesynthetiseerde materialen aan te tasten. Het effect van SrHA op celgedrag bleek afhankelijk van de mate van substitutie, hetgeen duidelijk werd uit het feit dat SrHA10 gecoate schijven de osteoblasten proliferatie verhoogden, terwijl SrHA1 gecoate disks dat niet deden. Hoofdstuk VII toonde de

mogelijkheid om ESD te gebruiken voor de depositie van bio-anorganische bestanddelen zoals SrHA en het belang van het behoud van de bioactieve eigenschappen ervan.

Slotwoord en toekomstperspectieven

In dit proefschrift waren de onderzoeksinspanningen gericht op het gebruik van verschillende coatings op basis van organische, anorganische en composiet materialen om bioactieve oppervlakmodificaties voor bot implantologische toepassingen te creëren. Verschillende materialen en depositie-methoden zijn gebruikt in de afgelopen decennia om de nadelen van de implantatie van een vreemd lichaam implantaat te omzeilen. Botimplantaten zijn daarmee geëvolueerd van biocompatibel tot instructief, of bioactieve, daarmee probeerend verschillende benaderingen het hoofd te bieden (zoals geïllustreerd in hoofdstuk II) en gericht op verschillende problemen die implantaat immobilisatie beïnvloeden. Van alle beschreven en beschikbare technieken werd electrospray depositie (ESD) gekozen om de onderzoeken gedaan in dit proefschrift te standaardiseren en dezelfde werkwijze te handhaven voor al het gecoate materiaal. ESD werd geselecteerd vanwege de veelzijdigheid met betrekking tot de mogelijkheid om verschillende bestanddelen, van anorganische tot organische, met behoud van hun structuur en integriteit te deponeren.

Calciumfosfaat (CaP) coatings blijven de meest succesvolle aanpak voor anorganische oppervlakmodificaties voor toepassingen van implantaten in botweefsel. Geïnspireerd door de samenstelling van botweefsel, werd hydroxyapatiet (HA), een specifieke stoichiometrische en configuratie-vorm van CaP, gebruikt in nano-sized kristalvorm (hoofdstuk III, hoofdstuk V, hoofdstuk VI en hoofdstuk VII) om de anorganische structuur van het bot na te bootsen met behoud van de nano-sized plaatvormige vorm. ESD liet toe om nHA te verrijken waardoor extra bioactieve eigenschappen konden worden toegevoegd, zoals de mogelijkheid om anti-osteoporotische drugs op het kristal oppervlak te adsorberen (hoofdstuk V en hoofdstuk VI).

De rol van ESD was instrumenteel om het effect van nHA dat werd afgezet als een homogene laag van enkele nano-kristallen te behouden. De nanoschaal dimensie van de kristallen was een kernelement om natuurlijk bot na te bootsen en een oppervlak te houden waarop alendronaat kon worden geadsorbeerd, een krachtig bisfosfonaat gebruikt voor systemische behandeling van osteoporose, en een coating voor therapeutische behandelingen te kunnen verkrijgen met invloed op osteoclasten gedrag in het lokale peri-implant gebied. Het potentieel en de toepasbaarheid van deze specifieke en innovatieve benaderingen werden voor het eerst onderzocht in vitro door het evalueren van het vermogen om apoptose van osteoclasten (hoofdstuk V) te induceren en daarna gecontroleerd in vivo met behulp van een rat-osteoporotische model met implantatie van gecoate implantaten in de femorale condyle (hoofdstuk VI). De resultaten toonden het potentieel ten aanzien van vermindering van osteoclasten, bot/implantaat contact en botvolume vergroting veroorzaakt door implantaten gecoat met instructievenHA gecombineerd met therapeutisch alendronaat.

Een veelbelovende aanpak voor anorganische coatings is het gebruik van ion-substitutie om bio-anorganische eigenschappen toe te voegen aan de bestaande toepassingen van CaP (hoofdstuk VII). De resultaten toonden de mogelijkheid om strontium op te nemen als substituut voor calcium en Sr-gedoteerde kristallen met nieuwe eigenschappen te verkrijgen. In feite, waar nHA lijkt op de anorganische fase van natuurlijk bot, was het bio-anorganische strontium apatiet (SrHA) gericht op een actieve controle over het gedrag van cellen te introduceren. SrHA werd getest als een afgezette laag via ESD en middels een in vitro model met osteoblast cellen. Het potentieel van bio-anorganische coatings om celgedrag te moduleren werd aangetoond en opent een nieuwe route voor anorganische coatings met meerdere specifieke eigenschappen afhankelijk van de ion-substitutie en de fysiologische werkzaamheid daarvan.

Naast anorganische coatings werden andere benaderingen onderzocht met behulp van organische materialen geïnspireerd op de samenstelling van de extracellulaire matrix van botweefsel. Met name de combinatie van collageen en alkalische fosfatase (ALP), in verschillende configuraties, werd onderzocht in een a-cellulair mineralisatieproces (hoofdstuk IV). Collageen verbeterde de ALP retentie en het reeds bekende mineralisatie-vermogen van ALP. Verder was de configuratie van ALP gecombineerd met collageen een manier om de ALP enzymhoeveelheid op het oppervlak behouden, de hoeveelheid oppervlakte mineralisatie te verhogen en de morfologie van de mineralisatie te beïnvloeden. De kennis verworven via het uitvoeren van dergelijke experimenten was essentieel om inzicht te krijgen in de mogelijkheden van ESD om organische coatings op lage temperatuur te deponeren, evenals het effect van coating configuraties om invloed op de fysiologische eigenschappen te verkrijgen. De unieke eigenschappen van de verkregen coatings hebben een groot potentieel voor toepassingen binnen de regeneratieve geneeskunde en voor botimplantaat coatings.

Hoewel de ESD techniek een krachtige methode bleek om coatings op metallische implantaten te deponeren, dienen verscheidene nadelen te worden opgelost vooraleer klinische toepassing een feit zal zijn. Voor coating vervaardiging is het van fundamenteel belang voor een coating methode dat deze niet afhankelijk is van de operator. De stabiliteit van de depositie vereist constante monitoring en het vertegenwoordigt een sterke beperking voor het opschalen van de productie. Verdere onderzoeksinspanningen moeten worden gewijdaan methodieken om de afzettingsstabiliteit te controleren, bijvoorbeeld met behulp van een video systeem dat in staat is om de lichtverstrooiing van een laserstraal te bewaken. Een software-algoritme kan de spanning wijzigen en de stabiliteit van de afzetting handhaven. Retentie van de coating aan het substraat is een zwak punt van nat-chemische depositie methoden zoals ESD, dat de toepasbaarheid van de coatings in klinische situaties vermindert.

Gezien deze beperkingen moet meer nadruk komen op strategieën voor dubbele coatings te verwezenlijken. Vanaf CaP gecoate implantaten verkregen middels fysische depositie (bijvoorbeeld RF sputteren of plasma-depositie nevel), zou het mogelijk moeten zijn om een sterke hechting tussen CaP en het titanium oppervlak te garanderen. Om het gebrek aan bioactieve eigenschappen van deze depositiemethoden (vanwege de relatief hoge temperaturen tijdens de depositie) te compenseren, kan ESD worden gebruikt om instructieve materialen te deponeren. De mogelijkheid om een bioactieve coating af te zetten op een CaP-gecoat oppervlak kan het retentie-probleem aanpakken en een compleet nieuw tijdperk starten voor ESD. Ten slotte zal de vooruitgang in het biomedisch onderzoek voor bot-toepassingen in de nabije toekomst gericht zijn op het verkrijgen van meer specifieke of zelfs patiënt-gerelateerde oplossingen (d.w.z. gepersonaliseerde gezondheidszorg), hetgeen zal worden gebaseerd op de aanwezigheid van organische coatings en resorbeerbare bulk materialen. Met het oog hierop zullen coatings een steeds belangrijkere rol spelen en zal het modificeren van biomedische implantaatoppervlakken veranderen: vroeger was dat van biocompatibel naar bioactief, waar het in de toekomst zal zijn.

Acknowledgments

Here we are. The most read chapter of this book. I personally think that if life is divided in chapters, as a book, I would say that the last chapter that I wrote, the one of me in the Netherlands, is absolutely about journeys.

I really think that the last 4 years have been a long journey that I could not face just on my own. Writing this book was like a diary. I could read and remember all the memories I gathered in the last four year. The presence of several people around me is the essence of this long, intense and incredible journey.

First of all, I would like to express my sincere gratitude to my promotor Prof. Jansen. It was a sincere honour being part of your group. Thank you for giving me the chance to explore the World and push my curiosity every day a bit further. You were a laconic but always present guide along all my PhD days. Thank you, John.

Surely my PhD trip could not have been started without you, Jeroen. Among all the people of the department you are certainly the one that I will remember for the longest time. You teased me, you pushed me, you motivated me, you taught me what it means being a supervisor. Despite my chaotic attitude you have been able to channel my skills and to keep me on a track. Among all the people of the department you are probably the happiest that I am done with the PhD. I hope you will tell my adventure in Japan to all the next PhD generations. I'm not kidding, thank you for all the good and the bad moments.

During the last 4 years you inspired me the most, Sander. Now that everything is over I want to sincerely thank you for time and help. You have been the compass that I was checking when I felt lost. Your hieratic attitude and ability to overcome difficulties deeply inspired me. Thank you Sandro Castroleone.

Joop and Frank, thanks for all your comments and suggestions. Your paternal attitude and constant threat during the presentations pushed me to do my best and to control my words. A precious gift that I will carry for long time.

Monique, Vincent, Natasja and Martijn, thank you for being there when I needed. I would like to express my gratitude for your help in the lab but I prefer to remember you for the fantastic chats in the coffee corner. Without you the department would be too boring. I'm missing our coffees.

A job is nothing without colleagues. In four years I met so many of you. Each of you coming from all the corner of the World. I know. I have annoyed you with my constant talks and my questions but I could not resist. You offered me the possibility to explore all the World and dozen of cultures without moving from the lab. Absolutely the best part of my PhD experience.

Ljupcho, Huanan, Arnold, Kemal, Edwin, Floor, Bart, Mati, Manu, Kambiz, Paula, Paulo, JW, Eva, Alexey, Simone, Rosa, Floor, Mani, Reza, Astghik, Cristina, Marco, Tim, Rainoud, Daniel, Claire, Fang, Na, Wanxun, Jinling, Xiangzhen, Wei, Hamdam... I'm sure I'm forgetting to many of you in this list! Thank you all. You have been my life for the last 4 years. I would like to thank each of you one by one.. But that would require an extra book!

Some of you, anyway deserve some extra words.. Floor you are the first on the list, you will be forever my personal perfect example of a Dutch girl. I'm missing our beers more than anything else. You still hold the record for the quickest drinker! Eddie, I'm missing your call in the middle of the night to go out and party.. I know now all that is the old good times... Grandpa Ljupcho, you were the first person that gave me his mobile number in Nijmegen. People pushed us to compete on who could talk more, without finding a winner. I just know that I found a great friend in you.

I did not spend all my time in the lab... If I survived for 4 years is mainly due to the family that adopted me in Nijmegen. Shankar, Helene, Mariam, Nina, Vic, Dani, Daniel, Manu, Antonio and Jordan you know that our lives are bind together. Thanks for all the cappuccinos, the dinners, the beers and the huggies. You cheered me up when I was down, you helped me when I was lost and you were there to exalt my happiness. Neither living 100 lifes I could be able to pay back your love. Grazie.

A special Grazie also to Drs. Cossu and Clara..La mia dottoressa di fiducia e la mia IngozzAmica preferita.

Dopo 200 pagine di inglese è il momento di scrivere apertamente in Italiano. Il mio viaggio in Olanda è stato incredibile. Un po' vacanza, un po' missione, un po' esilio ma soprattutto ricerca. Non la ricerca scientifica ma la ricerca di me stesso.

Per mia fortuna in questo viaggio ho avuto voi altrove ad aspettarmi. Un viaggio non sarebbe tale se non partisse da un punto preciso. Beh questo punto non può che essere la mia famiglia. Papà, mamma, Marta, Sara e Bruno grazie per aver conservato immutato il vostro amore per me nonostante la mia partenza e la mia distanza. Scusatemi per i compleanni, gli aperitivi o tutti i momenti persi. Vi ho conservato nei miei pensieri ogni istante, credetemi. Come sempre della nostra famiglia, sorellina, sei quella che più mi è mancata. Non si offendano gli altri ma per te, Marta, avrò sempre un pensiero in più. Vi voglio bene, vi amo e vi porto sempre con me.

Questo mio viaggio non sarebbe stato lo stesso senza una persona in particolare: Marta.

Marta, tu mi hai accompagnato quando sono partito e mi hai accolto ogni volta che sono rientrato. Mi hai amato e fatto sentire speciale come nessuno ha mai fatto nella mia vita. Sei

stata la paziente Penelope che mi ha atteso per tutti questi anni a casa. Sei il premio più bello che io potessi ottenere alla fine di questo viaggio. Tutto è più bello con te.

Per Fortuna a lenire la vostra assenza ho trovato qualche altro rifugiato quassù in Olanda.. Mammamanu, Zerby e Zinny. Siete stati la mia Eindhoven. Vale e Manu non potrò mai ringraziarvi abbastanza della vostra Amicizia. Grazie per avermi ospitato senza batter ciglio e per avermi sempre fatto sentire un membro della vostra famiglia. Vi voglio un bene disperato. Zinny, capocciona mia, tu addirittura hai una riga tutta per te. Così, tanto per. (dai lo sai che ti voglio bene ma non posso dirtelo altrimenti Albe mi lancia via come.. come ... una catapulta!)

Ed infine voglio ringraziare i vecchi amici. Matteo, V, Jan, Moreno, Giovanni e Andrea. A quanto pare non importa quanto distanti siamo nel Mondo, voi rimanete per me delle certezze inscalfibili. Grazie per aver sopportato ogni mio capriccio. Grazie per esser passati di qui (tranne uno.. : P) a ricordarmi quanto voi siate importanti nella mia vita. Non esiste un pezzo di Mondo interessante senza di voi.

Grazie a tutti davvero.

Thanks to all of you.

Ruggero

List of publications

Chapter I

Instructive coatings for biological guidance of bone implants

R Bosco[#], ERU Edreira[#], JGC Wolke, SCG Leeuwenburgh, JJJP van den Beucken, JA Jansen (*Surface and coating technology*, 2013)

Chapter II

Surface Engineering for Bone Implants: A Trend from Passive to Active Surfaces

R Bosco, JJJP van den Beucken, SCG Leeuwenburgh, JA Jansen (*Coatings*, 2012)

Chapter III

Electrostatic Spray Deposition of Biomimetic Nanocrystalline Apatite Coatings onto Titanium

M Iafisco[#], **R Bosco**[#], SCG Leeuwenburgh, JJJP van den Beucken, JA Jansen, M Prat, N Roveri (*Adv. Eng. Mat* 2012)

Chapter IV

Configurational effects of collagen/ALP coatings on enzyme immobilization and surface mineralization

R Bosco, SCG Leeuwenburgh, JA Jansen, JJJP van den Beucken (*Applied Surface Science*, 2014)

Chapter V

Nano-sized hydroxyapatite crystals functionalized with alendronate as bioactive components for bone implant coatings to decrease osteoclastic activity.

R Bosco, M. Iafisco, A Tampieri, SCG Leeuwenburgh, JA Jansen, JJJP Van Den Beucken (Manuscript submitted)

Chapter VI

Synergistic effects of bisphosphonate and calcium phosphate nanoparticles on peri-implant bone response in osteoporotic rats

HS Alghamdi, **R Bosco**, S. K. Both, M. Iafisco, SCG Leeuwenburgh, JA Jansen, JJJP Van Den Beucken (*Biomaterials*, 2014)

Chapter VII

Electrospray deposition of strontium substituted nano-hydroxyapatite to stimulate the response of osteoblastic cells to titanium implants

R Bosco, M Bianchi, M Iafisco, SCG Leeuwenburgh, JA Jansen, JJJP van den Beucken (Manuscript submitted)

Other publications

Biological response to titanium implants coated with nanocrystals calcium phosphate or type 1 collagen in a dog model

HS Alghamdi, B van Oirschot, **R Bosco**, JJJP den Beucken, AAF Aldosari, S Anil, JA Jansen (Clinical oral implants research, 2012)

Osteogenicity of titanium implants coated with calcium phosphate or collagen type-I in osteoporotic rats

HS Alghamdi, **R Bosco**, JJJP van den Beucken, XF Walboomers, JA Jansen (Biomaterials, 2013)

RANKL delivery from calcium phosphate containing PLGA microspheres

R. Felix Lanao, **R. Bosco**, S.C.G Leeuwenburgh, M. Kersten-Niessen, J. Wolke, J.A Jansen, (*Journal of Biomedical Materials Research Part A*, 2013)



Ruggero Bosco was born on February 25, 1983, in Milan (Italy). In 1997 he attended the Liceo Scientifico Bachelet, in Abbiategrasso and graduated in 2002. In September 2005, he obtained his bachelor degree in biomedical engineering at Politecnico of Milan (Italy), followed by a Master degree in the same institute obtained in April 2009. Since February 2010 he has been employed as a PhD candidate in the department of biomaterials at Radboud University Nijmegen Medical Centre under the supervision of Prof. Jansen and Dr. J. van den Beker. His PhD project was part of BMM, a national project that was connecting several Dutch universities and medical centres. His project focused on the development of innovative coatings for bone applications. On March 2011 and from October to

December 2012, he joined the department of ultra precisefabrication team (coordinator Prof. Yamagata) at RIKEN University (Tokyo, Japan) to further develop his knowledge of electrospray deposition. One of his most fruitful collaboration has been established with Prof. Tampieri and Dr. Iafisco from CNR-ISTEC of Faenza (Italy). The results of his PhD are described in this thesis and are presented as separate publications in scientific journals.

Scientific divulgation has been carried out in form of multiple international conference presentations, among which were: BIOCERAMICS 24 – 2012, Fukuoka, Japan; and MiMe 1st edition - 2013 in Faenza, Italy, where in both the conferences he was awarded as best oral presentation.